ICESS 15th OULU FINLAND

15th International Conference on
Electronic Spectroscopy and Structure

21-25 August 2023 | University of Oulu, Finland

Book of Abstracts

Editors: Satu Ojala, Minna Patanen, Samuli Urpelainen, Joachim Schnadt, Marko Huttula

ISBN 978-952-62-3754-1

UNIVERSITY OF OULU
P.O.BOX 8000
90014 UNIVERSITY OF OULU, FINLAND

MB SCIENTIFIC AB

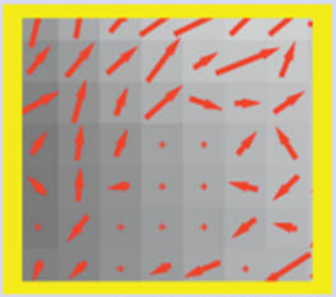

SPIN ARPES
Mapping data

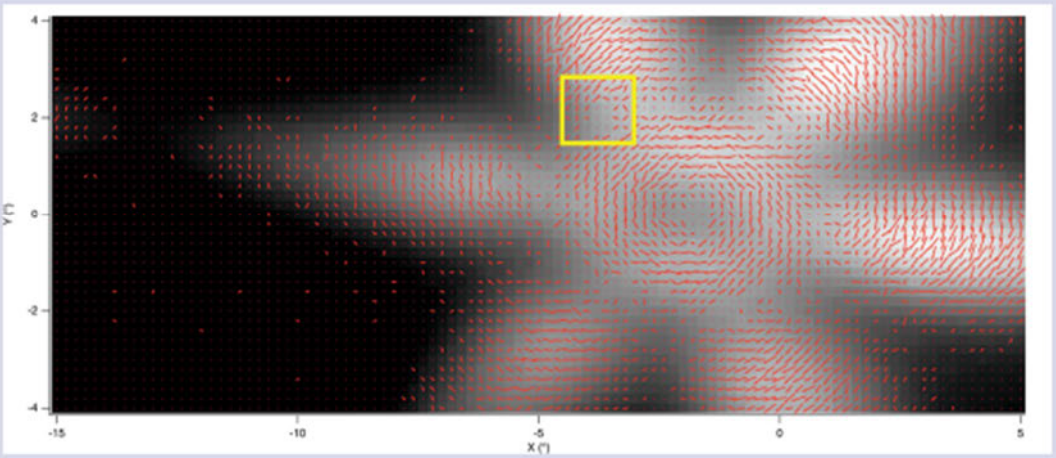

Gives you the result!

Above data was taking by MBS A1 analyser(A1_#0039) and MBS Spin Manipulator together with Focus Ferrum detector at CASSIOPEE beamline at SOLEIL synchrotron.

We challenging every day to develop and produce best possible instruments for the advanced research. MB Scientific AB is a Swedish company who produces photoelectron spectroscopy instruments & systems. Our state of the art ARPES system MBS A1SYS gives you an opportunity for world leading research.

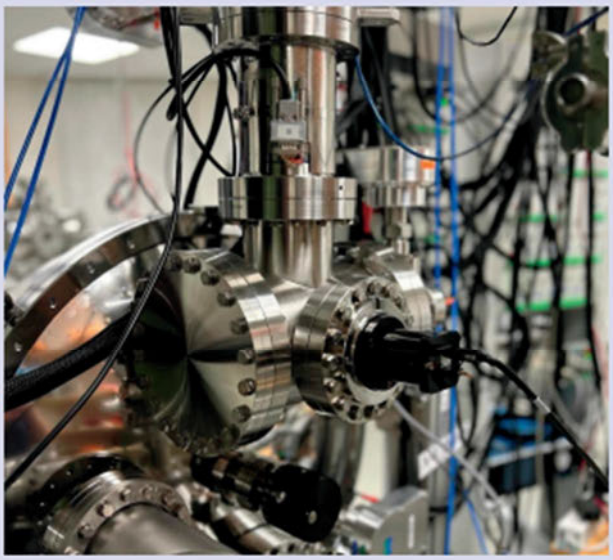

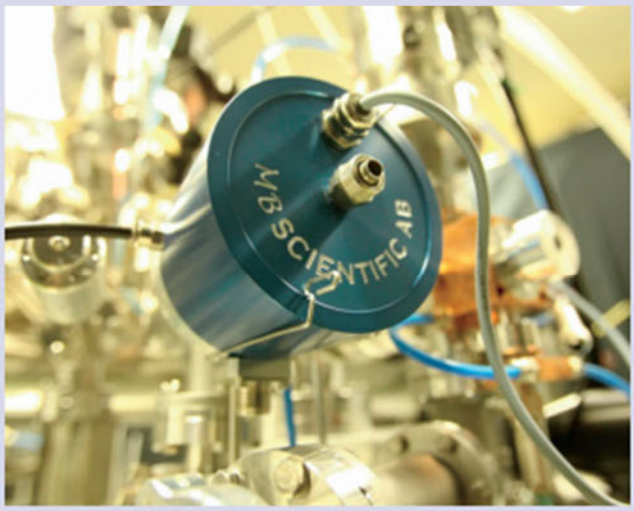

MBS

Fålhagsleden 61, 753 23,
Uppsala, Sweden
Tel +46 18 29 09 60
email: info@mbscientific.se
home page: mbscientific.se

scientaomicron

Accelerating Materials Innovation

1 000+
Installations

6 000+
Publications

200+
Staff

Nobel Prize Technologies Supporting Science and Industry

Scienta Omicron is a leading innovator in Surface Science and Nanotechnology. Supporting more than 85 technologies including **Scanning Probe Microscopy**, **Thin Film Deposition** and **Electron Spectroscopy**.
Our mission is your scientific success!

At our technology centres in Uppsala, Sweden and Taunusstein, Germany we develop and produce high-tech research instruments that are sold and serviced from our four regional hubs in USA, China, Japan and Germany.

www.scientaomicron.com
info@scientaomicron.com

Time-of-Flight Momentum Microscope

with Spin Imaging Option

Momentum Microscopy and Spectroscopy System for
Extraction of ARPES Spectra from Small Sample Real Space Areas

- Images the Full Emission Hemisphere ($2\pi K^2$) k-space
- L-He cooled Sample Stage <15 K - 400 K (<9 k shown)
- Momentum Resolution <0,01 $Å^{-1}$
- Energy Resolution <20 meV (17 meV shown)
- k-space out of Selectable Real Space <1 m
- Upgradable for Parallel Spin Imaging

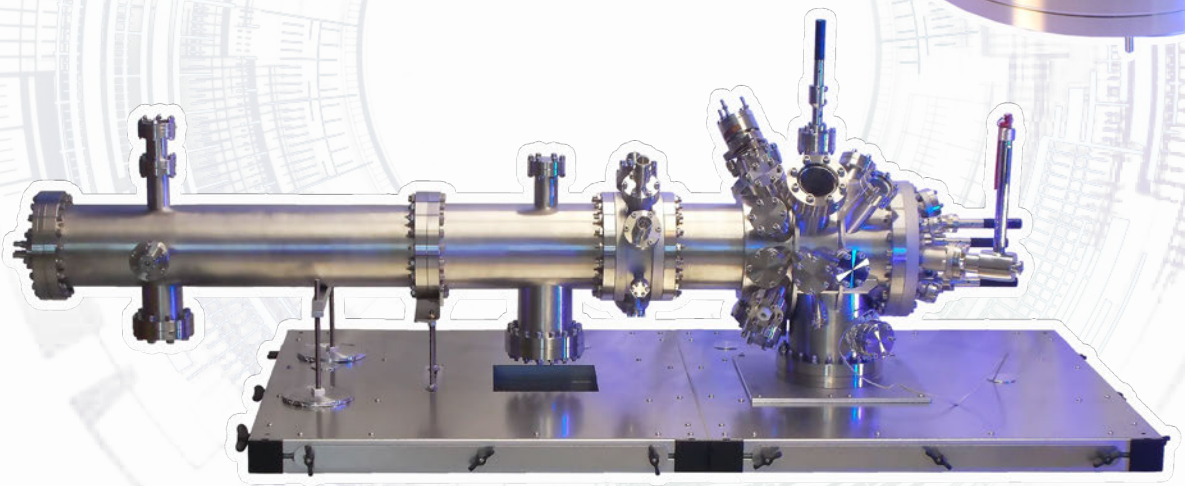

IDEAL FOR

- TIME RESOLVED ARPES
- TIME RESOLVED DARKFIELD MICROSCOPY
- DYNAMIC SPIN IMAGING

SURFACE CONCEPT

Detector Systems | Time Measurement Systems | High Voltage Supplies | Fast Analog Electronics

www.surface-concept.de | info@surface-concept.de | +49 6131 62716 0

YOUR **SURFACE SCIENCE** PARTNER

PREVAC

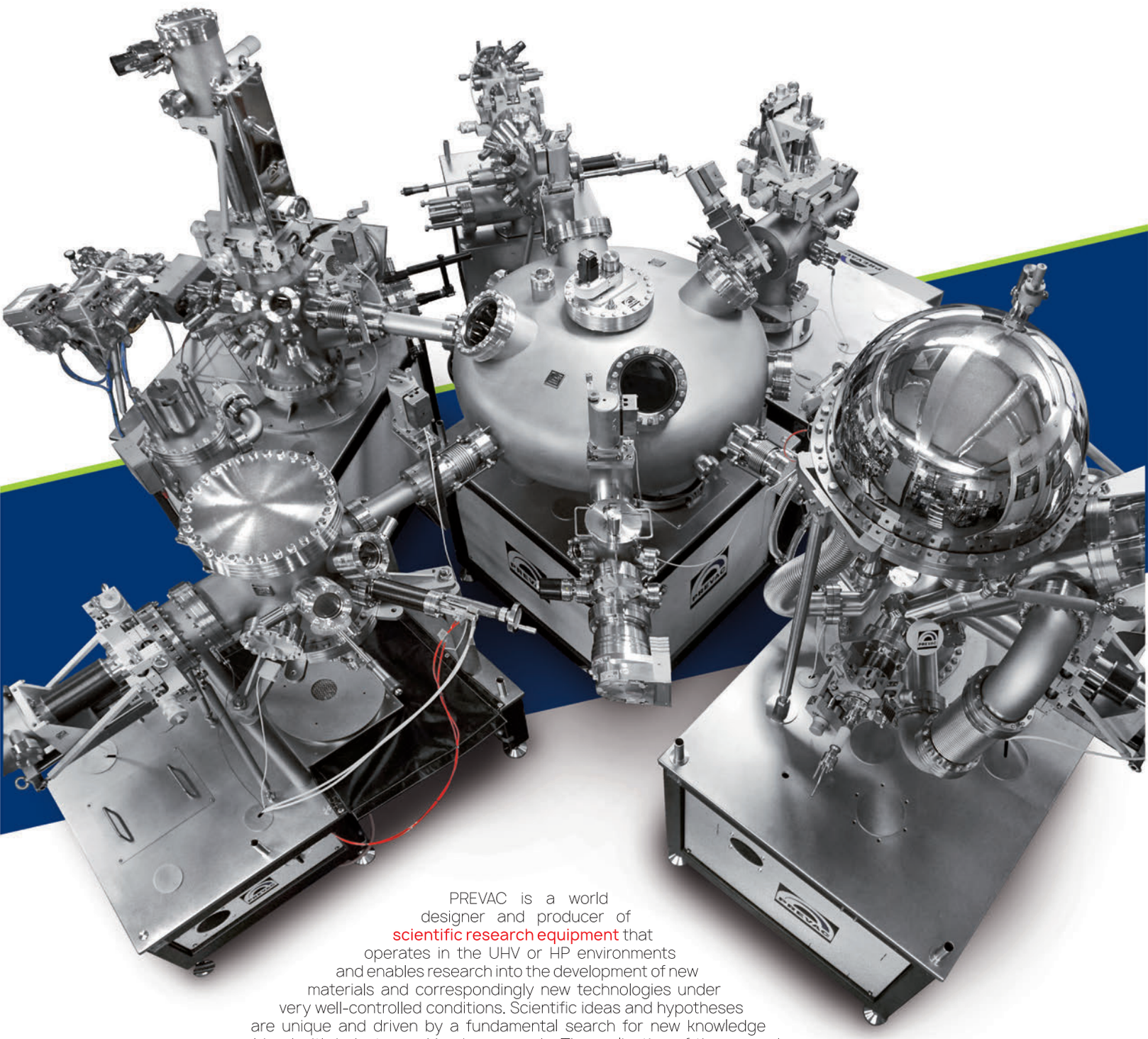

PREVAC is a world designer and producer of scientific research equipment that operates in the UHV or HP environments and enables research into the development of new materials and correspondingly new technologies under very well-controlled conditions. Scientific ideas and hypotheses are unique and driven by a fundamental search for new knowledge combined with industry and business needs. The realisation of these needs requires unique technological solutions. The scope of design, manufacture and sales activities includes electronics, precision mechanical assemblies and motion devices, software and advanced process control and measurement for science and industry.

+48 32 459 2000 prevac@prevac.eu

prevac.eu

Journal of Electron Spectroscopy and Related Phenomena

The *Journal of Electron Spectroscopy and Related Phenomena* publishes experimental, theoretical and applied work in the field of **electron spectroscopy** and **electronic structure**, involving techniques which use **high energy photons** (>10 eV) or **electrons** as probes or detected particles in the investigation.

The journal encourages contributions in the general area of atomic, molecular, ionic, liquid and solid state spectroscopy carried out using electron impact, synchrotron radiation (including free electron lasers) and short wavelength lasers. Papers using photoemission and other techniques, in which synchrotron radiation, free electron lasers, laboratory lasers or other sources of ionizing radiation, combined with electron velocity analysis are especially welcome. The materials properties addressed include characterization of ground and excited state properties as well as time resolved electron dynamics.

The individual techniques of electron spectroscopy include photoelectron spectroscopy of both outer and inner shells; inverse photoemission; spin-polarised photoemission; time resolved 2-photon photoemission, resonant and non-resonant Auger spectroscopy including ion neutralization studies; edge techniques (EXAFS, NEXAFS,...) , resonant and non-resonant inelastic X-ray scattering (RIXS), spectro-microscopy, high resolution electron energy loss spectroscopy; electron scattering and resonance electron capture; electron spectroscopy in conjunction with microscopy; penning ionization spectroscopy including scanning tunneling spectroscopy; theoretical treatments of the photoemission, X-ray emission, Auger, energy loss and Penning ionization processes. Contributions on instrumentation and technique development, data acquisition - analysis - quantification are also welcome.

Subject areas covered include spectroscopic characterization of materials and processes concerning:
- surfaces, interfaces, and thin films;
- atomic and molecular physics, clusters;
- semiconductor physics and chemistry;
- materials for photovoltaics;
- materials science including: metal surfaces, nanoparticles, ceramics, strongly correlated systems, polymers, biomaterials and other organic films;
- catalysis

Editors:

Contents

Welcome to ICESS 15th

Welcome to the 15th ICESS conference! Finally, after five years of waiting it is our pleasure to welcome you - the whole international community – to Oulu, Finland. The scientific program built in collaboration with international advisory board (IAB) covers widely the areas of research and surely engages plenty of discussions and ideas for future collaborations. Great thanks for participating and making the event possible! Let us all make the event pleasant respecting the diversity and committing to strengthening the international community of ICESS.

Welcome to Oulu!

ICESS local committee:

Marko Huttula, chair

Minna Patanen, program committee

Samuli Urpelainen, Satu Ojala, local organization

The Co-Chairs

Professor **Marko Huttula**, University of Oulu, Finland
Professor **Joachim Schnadt**, Lund University, Sweden
Associate Professor **Minna Patanen**, University of Oulu, Finland

The Local Organization Committee

Adjunct Professor **Samuli Urpelainen** (Chair)
Professor **Marko Huttula**
Management assistant **Marjut Saastamoinen**
M.Sc. **Onni Veteläinen**
Doctor **Juho Keskinen**
Adjunct Professor **Satu Ojala**
Doctor **Esa-Ville Immonen**

The International Advisory Board

Professor **Nobuhiro Kosugi**, Institute for Molecular Science (IMS), and Institute of materials Structure Science (IMSS), Japan (Chair)
Doctor **Zahid Hussain**, Advanced Light Source, LBNL, USA (Vice Chair)
Professor **Chris F. McConville**, University of Warwick, UK
Professor **Andrei G. Kochur**, Rostov State University of Transport Communication, Russia
Professor **Wolfgang Werner**, Technical University of Wien, Austria
Professor **Marc Simon**, Sorbonne University, France
Professor **Wolfgang Eberhardt**, Deutsches Elektronen-Synchrotron, Center for Free-Electron Laser Science, Germany
Professor **Hubert Ebert**, Ludwig-Maximilians-Universität München, Germany
Professor **Claus M. Schneider**, Forschungszentrum Jülich, Germany
Doctor **Serguei Molodtsov**, European XFEL, Germany
Doctor **Andrea Locatelli**, Elettra Sincrotrone Trieste, Italy
Professor **Maria Carmen-Asensio**, Madrid Institute of Materials Science of the Spanish Research Council, Spain
Professor **Maria Novella Piancastelli**, Uppsala University, Sweden
Professor **Juerg Osterwalder**, Physik-Institut Universität Zürich, Switzerland
Professor **Mark S. Golden**, University of Amsterdam, Netherlands
Professor **Zhi Liu**, ShanghaiTech University, China
Professor **Dipankar Das Sarma**, Indian Institute of Science, India
Professor **Hiroshi Daimon**, Nara Institute of Science and Technology, Japan
Doctor **Toyohiko Kinoshita**, SPring-8, Japan
Professor **Akiyoshi Hishikawa**, Nagoya University, Japan
Professor **Han Woong Yeom**, Institute of Basic Science and POSTTECH, South Korea
Professor **Di-Jing Huang**, National Synchrotron Radiation Research Center, Taiwan

Professor **Arnaldo Naves de Brito**, University of Campinas, Brazil
Professor **Alexander Moewes**, University of Saskatchewan, Canada
Professor **Kevin E. Smith**, Boston University, USA
Doctor **Peter D. Johnson**, Brookhaven National Laboratory, USA

The International Program Committee

Professor **Bongjin Simon Mun**, Gwangju Institute of Science and Technology, Korea
Assistant professor **Cheng-Tien Chiang**, National Taiwan University, Taiwan
Professor **Hans-Peter Steinrück**, Friedrich-Alexander-Universität, Germany
Professor **Hiroki Wadati**, University of Hyogo, Japan
Assistant Professor **Matteo Mitrano**, Harvard University, USA
Professor **Milan Radovic**, Paul Scherrer Institute, Switzerland
Doctor **Sung-Kwan Mo**, Advanced Light Source, USA
Professor **Tomohiro Matsushita**, Nara Institute of Science and Technology, Japan
Doctor **Vladimir Strocov**, Paul Scherrer Institute, Switzerland
Professor **Xingjiang Zhou**, Chinese Academy of Sciences, China
Professor **Yuhai Jiang**, ShanghaiTech University, China
Professor **Wei Cao**, University of Oulu, Finland

ICESS 15th conference programme

MONDAY 21st of August 2023

Public Lecture

Wolfgang Eberhardt: Designing the Energy System of the Future

Plenary talks

Hyunjung Kim: X-ray free electron studies of ultrafast structural dynamics and phase transformation

Linda Young: Probing chemical processes in water

Parallel Session: Atomic, molecular and optical physics

Oksana Plekan: Probing molecular dynamics of uracil by time-resolved X-ray photoelectron spectroscopy

Catmarna Küstner-Wetekam: Quantification of interatomic Coulombic decay efficiency after inner-shell photoionization of krypton clusters

Geraldine Feraud: Indirect X-ray photodesorption from ices

Abhishek Verma: Experimental study of second step Auger decay in Kr after core 1s excitation

Parallel Session: Spin & Magnetism

Bum Joon Kim: Quantum Spin Nematic Phase in a Square-lattice Iridate

Mohammed Qahosh: Establishing fundamentals of ARPES spin textures with the model material $PtTe_2$

Kenta Amemiya: Determination of anisotropic magnetic moments at the interface by means of depth-resolved x-ray magnetic circular dichroism

Markus Donath: Tamm and Shockley surface states at Re(0001): two paradigmatically different types of states mixed by spin-orbit interaction

Parallel Session: Dynamics, FEL, HHG

Valerie Blanchet: Dynamical interplay between molecular chirality and electrons

Victor Kimberg: Photoelectron recoil-induced rotation: Cohen-Fano and multichannel interference effects

David Reis: Using x-ray FELs to imagine strong-field optical processes

Andreas Lindblad: Hard X-ray core-hole clock spectroscopy and charge transfer processes

Parallel Session: Material & Surface Science

Shuyun Zhou: Floquet engineering of a model semiconducto

Alice Kunin: Direct visualization of charge transfer and hybridized excitons in twisted $MoSe_2/WS_2$ bilayers

Regina Dittmann: Uncovering switching and failure mechanisms of redox-based memristive devices by in-situ spectroscopy

Olena Tkach: Circular Dichroism in Hard X-ray Photoelectron Diffraction Observed by Time-of-Flight Momentum Microscopy

Tuesday 22nd of August 2023

Plenary talks

Takeshi Kondo: Fascinating electronic structures of exotic magnets revealed by ARPES

Di-Jing Huang: Elementary excitations of quantum materials probed with high-resolution RIXS

Parallel Session: Materials science methods

Antonija Grubišić-Čabo: Kinetic In-situ Synthesis (KISS) technique of large-area 2D materials exfoliation

Tuomas Alatarvas: Application of In-situ High Temperature Environmental Scanning Electron Microscopy for Characterising Non-metallic Inclusions within Steel

Constantin Wansorra: Are calculated partial photoionization cross sections good enough for (HAX)PES applications

Alessandro Ruocco: Transmission through Graphene of Electrons in the 30 - 900 eV Range

Parallel Session: RIXS

Yoshihisa Harada: Soft X-ray Emission Spectroscopy of Water at Interfaces

Wanli Yang: RIXS of high-energy battery electrodes: novel states in highly oxidized transition metal oxides

Régis Decker: Using X-ray emission spectroscopy to measure the electron-phonon scattering rates in the demagnetization transient state of ferromagnets

Faris Gel'mukhanov: Young's double slit interference in resonant Auger/X-ray scattering and the Bohr's complementary: new results

Wednesday 23rd of August 2023

Plenary talks

Thomas Pfeifer: Spectroscopy and control of electronic structure in atoms and molecules with intense laser fields from atto-to-femtoseconds, and beyond

Simone Techert: Water-Splitting Catalysts in Real Time and During Operation

Parallel Session: Correlated systems and superconductors

Dong-Lai Feng: Strong electron-boson interactions in oxide superconductors and magnetic materials

Kyoko Ishizaka: Micro-focused ARPES study on 2D transition-metal dichalcogenides

Marco Caputo: Proximity-Induced Novel Ferromagnetism and Metallicity in $NdNiO_3$ Heterostructure

Francesco Rosa: Infinite-Layer Nickelate Superconductors Studied with Resonant Inelastic X-ray Scattering

Parallel Session: Ambient & In-situ spectroscopy

Hendrik Bluhm: Investigation of Liquid-Vapor Interfaces Using Photoelectron Spectroscopy

Andrey Shavorskiy: Event-averaged time-resolved APXPS with chemical perturbations: studying gas/solid processes with a microsecond time resolution

Esko Kokkonen: Using Ambient Pressure XPS to study ALD in real-time

Henri Pauna: Applied physics in the steel industry – optical emission spectroscopy as a method for advanced process control

Thursday 24th of August 2023

Plenary talks

Michael Odelius: Photodissociation of ironpentacarbonyl - $Fe(CO)_5$ - from initial bursts of CO release to branching pathways in solution

Patrick Rinke: ARTIST: Artificial Intelligence for Spectroscopy

Parallel Session: HAXPES

Tatiana Marchenko: Hard X-ray Photoelectron Spectroscopy probing photoionisation dynamics

Aki Pulkkinen: Theoretical description of soft and hard x-ray photoemission spectroscopy using the one-step model of photoemission

Ibrahima Gueye: Probing Halide Ion Transport and Metal Corrosion Process in Halide Perovskite Solar Cells via In Operando Hard X-ray Photoelectron Spectroscopy

Fredrik O.L. Johansson: Resonant Auger spectroscopy on solid xenon on Au, Ag, and Cu substrates

Parallel Session: Liquids and chemistry

Arnaldo Naves de Brito: Insights into the Molecular Composition of Ethanol-Water Liquid Mixtures through Electron Spectroscopy

Robert Temperton: Oxidation of transition metal complexes in solution by resonant X-ray spectroscopy and operando electrochemistry

Lukás Tomaník: Aqueous-phase photoemission for chemical analysis

Nour El Houda Azzouza: Study of the electronic structure of iron metal complexes in aqueous solution by X-ray spectroscopies

Parallel Session: Spectromicroscopy & microspectroscopy

Stephen Urquhart: Exploring Phase in Soft X-ray Spectroptychography

Adam Hitchcock: In-situ spectromicroscopy studies of Cu catalysed CO_2 electroreduction by soft X-ray STXM and spectro-ptychography

Koichi Hayashi: Applications of X-ray/neutron holography to semiconductor defect evaluations

Lukasz Plucinski: Photoemission study of twisted monolayers and bilayers of WSe_2 on graphite substrates

Parallel Session Theory

Nađa Došlić: Efficient simulation of photoelectron spectra with trajectory surface hopping

Assa Sasikala Devi (Presenter Matti Alatalo): First Principles Calculations of the Optical Response of $LiNiO_2$ – a promising cathode material in Cobalt free Lithium ion batteries

Yao Wang: Ultrafast Control of Entanglement Enabled by Time-Resolved RIXS

Sneha Verma: Quantification on Uncertainty in Deep Learning Neural Network while Predicting X-ray Absorption Spectra

Friday 25th of August 2023

Plenary talks

Gerd Schönhense: HAXPES with Full-Field k-Imaging with Time-of-Flight Recording

Tomohiro Matsushita: Photoelectron holography with atomic resolution

Parallel Session: Environmental molecular science

Markus Ammann: Molecular Environmental Surface Science

Noelle Walsh: Opportunities for gas-phase, liquid-phase and aerosol research at MAX IV

Raimund Feifel: Abiotic molecular oxygen production - ionic pathway from SO_2

Rainer Pärna: VUV-induced fragmentation and electronic structure of phenoxy herbicides

Parallel Session: Chuck Fadley Memorial

Hiroshi Daimon: Progress of atomic-resolution holography and new analyzer CoDELMA

Michel van Hove: Memories of the 1990s and 2000s

John J. Rehr: Rehr-Albers approach to Photoelectron Diffraction

Eli Rotenberg: In Operando Measurements on Complex Materials Explored With nanoARPES

Slavomir Nemsak: Photoelectron spectroscopy modalities for studying complex materials

ORAL COMMUNICATIONS

Monday 21st of August, 2023

Designing the Energy System of the Future

Wolfgang Eberhardt
DESY-CFEL, Notkestr. 85, 22607 Hamburg, Germany
wolfgang.eberhardt@desy.de

Keywords: energy transformation, climate change, pollution control

The transformation of the energy system to a clean, stable, affordable, and sustainable system is a major challenge of the 21st century in the world. Presently, we are on a non-sustainable path that poses the danger of major climate changes and creates massive pollution in our cities and countries. This pollution is obvious to anyone who has visited China or India in recent years. Climate change is more difficult to "prove", but the existing collection of data and scientific modeling has been generally accepted as clear evidence that climate change is a reality and presents a serious challenge for our civilization.

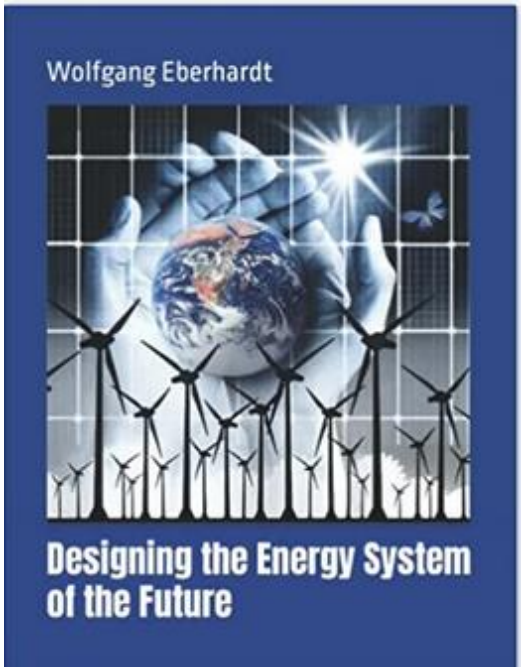

Since the overwhelming accord of the Paris agreement, there is a general consensus, that our energy system needs to be changed from the current fossil fuel base to more sustainable system, largely based upon renewable energies. We have to be very careful to come up with a balanced approach that takes not only the environmental concerns into account, but also accommodates an increased standard of living and a healthy economy---all of which while the population of the earth continues to rise. In view of the total scale of the energy system, this is, however, more easily said than actually done and there is no 'quick fix'. It requires a clear vision, long term strategy, and persistence.

Politicians are quick in getting into a bidding war as far as promising to reduce carbon emissions over the coming decades, without specifying how this is going to be achieved. When it comes to actual measures and implementation of policies, this is falling short of the formulated goals and very often not coherent. The population is threatened by the proposal of measures limiting travel and personal freedom, including dietary restrictions. Misconceptions and "half- truths" are spreading around in social networks and even in the media. In addition, there are large commercial interests at stake, since this transition challenges the business model of most of the current operators in the field. The energy transition involves major policy changes and accordingly there are intense lobbying efforts ongoing to influence these policy changes.

Upon closer inspection of the available data, we derive the limit of CO_2 emissions tolerable upon which the atmospheric CO_2 content actually will start to decline. This is considered to be a first and essential step in the 'war against climate change'. Presently the world is not on a path to accomplish this at any foreseeable time.

The measures needed to achieve this limit by 2050 will be outlined. [1]. We can design an energy system, largely based upon renewable energies and electric power, which satisfies the demands for transportation, industry, and buildings in the society of the future, despite of the worldwide growing population. This system is affordable, and also allows for economic growth without sacrificing our standard of living. In large parts of the underdeveloped world the conditions will even be improved. Once the implementation has made some progress, this will stop and reverse the effects of global warming and climate change, while simultaneously resulting in a massive reduction of pollution. This energy system of the future ensures a largely improved health for ourselves and our planet.

References

1. W. Eberhardt, *'Designing the Energy System of the Future'*, ISBN 979845872873-7, Amazon Direct Publishing (2021)

X-ray free electron studies of ultrafast structural dynamics and phase transformation

Hyunjung Kim

Center for Ultrafast Phase Transformation and Department of Physics, Sogang University, Seoul 04107, Korea

**Contact: hkim@sogang.ac.kr*

Keywords: x-ray free electron laser, ultrafast dynamics, phase transformation, time-resolved scattering

Recent advances in ultrafast science with X-ray free electron laser (XFEL) sources open up many research opportunities in scientific areas. These advances currently enable, e.g., sensitive probing of structural dynamics in materials on the femtosecond time scales of atomic motion, element-specific probing of electronic structure and charge dynamics on the electronic motion time scale, and powerful new approaches for exploring the coupling between electronic and atomic structural dynamics. Pump-probe techniques (i.e., the combination of an ultrafast optical laser pump and an X-ray free-electron laser as the probe) are ideal for understanding the interaction/coupling between the charge, spin, and structural dynamics. It provides direct information on the structural dynamics related to heterogeneity and fluctuations of atoms and charge carriers spanning the atomic scale to the mesoscale and their coupling in complex material systems.

In my talk, I present the recent results of expectation of band inversion related topological phase transition in Bi_2Se_3 followed by carrier-induced contraction and vibration modes [1], the crystalline-amorphous phase transformation of a phase change material [2], time-resolved in situ structural response of zeolites during catalysis [3], and ultrafast polaronic distortion observed in perovskite oxide nanoparticles [4]. I will discuss perspective of new fundamental understanding and insights of materials, which will direct the tailoring of material properties in various complex material systems and ultimately to next-generation materials design.

This research was supported by the National Research Foundation of Korea (NRF-2021R1A3B1077076).

1. S. Kim, et.al., Ultrafast Carrier−Lattice Interactions and Interlayer Modulations of Bi2Se3 by X ray Free-Electron Laser Diffraction, *Nano Lett*.,21,8554-8562 (2021).
2. S. Kim, et.al., Ultrafast Laser induced Ultrafast Amorphization and Re-crystallization of Phase-Change Materials (in preparation)
3. J. Kang, et.al., Time-resolved *in situ* visualization of the structural response of zeolites during catalysis, *Nat. Commun.* **11**, 5901 (2020).
4. S. Ha, et. al., Ultrafast polaronic distortion in perovskite oxide nanoparticles, (in preparation)

Probing chemical processes in water

Linda Young[1,2,*]

1 Chemical Sciences and Engineering Division, Argonne National Laboratory, Lemont, Illinois, USA
2 Department of Physics and James Franck Institute, The University of Chicago, Chicago, Illinois, USA
**Contact: young@anl.gov*

Keywords: ultrafast x-ray spectroscopy, XFEL, dynamics, radiolysis

An understanding of chemical reactions following ionization in aqueous systems forms the basis for radiation chemistry and biology [1]. Ionization initially creates a quasi-free electron and a water radical cation (H_2O^+). The quasi-free electron is implicated in radiation damage of DNA and after solvent relaxation on the few-picosecond timescale the hydrated electron $e^-_{(aq)}$ remains as a potent reducing agent. Its ionization partner, H_2O^+, rapidly undergoes proton transfer to form the hydroxyl radical (OH) which is a powerful oxidizing agent responsible for corrosion in nuclear reactors and cellular damage. Our knowledge of radiation-induced chemical reactions in pure water is rather complete for timescales longer than a few picoseconds as a result of pulse radiolysis experiments with visible-UV and ESR probes, but an understanding of the dynamics on the femtosecond timescale is just now emerging due in part to the entry of ultrafast x-ray probes where clear absorption signatures of both the hole states (H_2O^+, OH) and the solvated electron $e^-_{(aq)}$ have been recently established. Of fundamental interest is the localization timescale for the hole and the mechanism for cavity formation around $e^-_{(aq)}$. Of applied interest is radiolysis in complex chemical and biological systems where ionization is initiated by a high-energy particle (β,γ) producing energetic primary electrons followed by inelastic processes that yield damaging low-energy electrons and reactive radical species.

Tunable ultrafast x rays can dissect the radiolysis process. That is, x-ray pump/x-ray probe methods can systematically either peel electrons from valence, or, eject them from core orbitals and follow the ensuing dynamics on a site-specific basis. Our initial study on pure liquid water used femtosecond laser pump/x-ray probe methods to track dynamics after ionization from the *outermost valence orbital*. That study established prominent x-ray absorption and resonant inelastic scattering signatures of the hydroxyl radical that allowed observation of the ultrafast ~50 fs proton transfer reaction $H_2O^+ + H_2O \longrightarrow OH + H_3O^+$ [2,3]. Continuing to dissect the radiolysis of pure water, we study ionization of the *entire valence band* using an attosecond x-ray pump/x-ray probe scheme with microjoule-level tunable, two-color x-ray pulses from LCLS (Fig. 1). As the first attosecond x-ray pump/x-ray probe transient absorption study in condensed phase, it is imperative to establish the nature of the observed response on sub-femtosecond timescales. Gas-phase theory [4] extended to include the effects of electron collisions and multichannel coherences demonstrates that sub-femtosecond transient-absorption snapshots are meaningful. Multireference restricted-active-space configuration-interaction calculations on a tetrahedrally coordinated water cluster reproduce the observed signal at sub-femtosecond pump/probe delay times. These studies enable observation of the real time electron dynamics that initiate radiolytic chemical reactions.

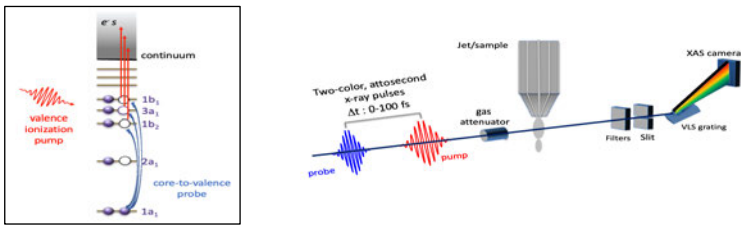

Figure 1. Attosecond x-ray pump/x-ray probe transient absorption in liquid water.

1. E. Alizadeh & L. Sanche, Precursors of Solvated Electrons in Radiobiological Physics and Chemistry, *Chem. Rev.* **112**, 5578−5602 (2012).
2. Z.-H. Loh *et al*., Observation of the fastest chemical processes in the radiolysis of water, *Science* **367**, 179-182 (2020).
3. L. Kjellsson *et al.,* Resonant Inelastic X-Ray Scattering Reveals Hidden Local Transitions of the Aqueous OH Radical, *Phys. Rev. Lett.* **124**, 236001(2020).
4. R. Santra *et al*., Theory of attosecond transient absorption spectroscopy of strong-field-generated ions, *Phys. Rev. A* **83**, 033405 (2011).

Acknowledgements: This work was supported by the US Department of Energy, Office of Science, Basic Energy Sciences, Chemical Sciences, Geosciences, and Biosciences Division and the IDREAM EFRC.

Probing molecular dynamics of uracil by time-resolved X-ray photoelectron spectroscopy

Oksana Plekan

Elettra Sincrotrone Trieste, Area Science Park, 34149 Basovizza, Trieste, Italy
oksana.plekan@elettra.eu

Keywords: nucleobases, photodynamics, time-resolved X-ray photoemission spectroscopy (TR-XPS)

In the last decades, comprehensive efforts have been applied to understand the photodynamics of the canonical nucleobases. DNA and RNA when absorbing ultraviolet (UV) radiation, tend to eliminate the resulting electronic excitation by internal conversion on the picosecond (ps) or even the femtosecond (fs) time scale. The absorbed electronic energy is converted to heat, and is no longer available for harmful chemical reactions. The availability of this ultrafast "safe" de-excitation pathway turns out to depend exquisitely on molecular structure. Remarkably, DNA and RNA are generally short-lived in the excited state, and thus have nearly ideal UV-resistant properties.

Like all other nucleobases, uracil (see Fig. 1(a)) absorbs photons strongly at a wavelength of 267 nm and exhibits an ultrafast relaxation mechanism with experimentally observed relaxation times between 50 fs and 2.4 ps [1 (see Table 3)]. Two of the lowest excited states are involved in the photoinduced dynamics of uracil: the first nπ* dark state (labelled S_1) and the first ππ* bright state (labelled S_2) (see Fig. 1 (b)). In agreement with many previous computational studies S_1 can be described as arising from the excitation from the lone pairs of the C4-O8 carbonyl group to the π* orbital, and is dipole forbidden. The lowest energy bright excited state S_2 corresponds instead to the dipole-allowed, ππ* transition. For the relaxation mechanism of uracil, there is an open issue about whether the nπ* state S_1 is accessible when the bright ππ* state S_2 is selectively excited.

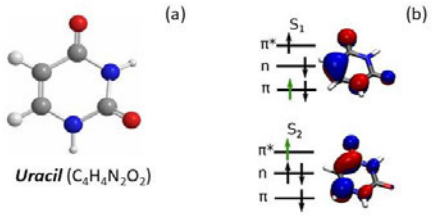

Figure 1: (a) Schematic drawing of uracil. (b) Two excited states (S_1 and S_2) of uracil.

Despite the fact that the photodynamics of uracil has been explored extensively by various spectroscopic techniques, time-resolved studies where a UV-pulse (or pump) is used for promoting the system to a valence electronically excited state, and an X-ray pulse (probe) is used for further excitation or ionization a core electron are still rare. In the present work, time-resolved X-ray photoemission spectroscopy at the C, N, and O K-edges was applied to probe excited states of uracil as well as to gain direct chemical information about their dynamics. We observe the S_2 state and dynamics of its decay to the S_1 state on a 50 fs time scale. Spectra are in good agreement with static theoretical calculations of the spectra [2], with the clearest effects being visible in O 1s spectra.

[1] M. Richter, S. Mai, P. Marquetand and L. Gonzalez, Ultrafast intersystem crossing dynamics in uracil unravelled by *ab initio* molecular dynamics. *Phys. Chem. Chem. Phys.,* **16**, 24423-24436 (2014).
[2] M. L. Vidal, A. I. Krylov and S. Coriani. Dyson orbitals within the fc-CVS-EOM-CCSD framework: theory and application to X-ray photoelectron spectroscopy of ground and excited states. *Phys.Chem.Chem.Phys*. **22**, 3744- 3747 (2020).

Quantification of interatomic Coulombic decay efficiency after inner-shell photoionization of krypton clusters

Catmarna Küstner-Wetekam[1,*], Lutz Marder[1], Dana Bloß[1], Nils Kiefer[1], Uwe Hergenhahn[2], Arno Ehresmann[1], Přemysl Kolorenč[3] and Andreas Hans[1]

1 Institute of Physics and CINSaT, University of Kassel, Kassel, Germany
2 Fritz-Haber-Institute of the Max-Planck Society, Berlin, Germany
3 Institute of Theoretical Physics, Charles University, Prague, Czech Republic

**Contact: c.kuestner-wetekam@uni-kassel.de*

Keywords: multi-coincident electron spectroscopy, interatomic processes

After the theoretical prediction of interatomic Coulombic (ICD) decay in 1997 [1] an ever-growing field of theoretical and experimental research on interatomic and intermolecular energy- and charge-transfer processes opened [2]. Non-local decay processes such as ICD are nowadays believed to be ubiquitous relaxation pathways for electronically excited species in an environment. To understand the processes at play in more complex and biologically relevant samples, it is necessary to study these in prototype systems like weakly-bound van der Waals clusters.

This work focuses on the specific case of ICD following inner-shell ionization, called core-level ICD. While in an isolated atom an inner-shell vacancy often decays locally via Auger decay, leaving the atom in a one-site dicationic state, the situation changes for atoms in a cluster. After inner-shell ionization the vacancy is still filled by an outer-valence electron of the same atom; the excess energy can then either autoionize the atom in a local Auger decay or be transferred to a neutral neighboring atom, ionizing it, and thereby leaving the system in a two-site dicationic state. This results in the appearance of a new spectroscopic feature at a higher electron kinetic energy as the corresponding Auger line.

With core-level ICD being a direct competitor to local Auger decay, it is possible to quantify this non-local process using multi-coincident electron spectroscopy [3, 4]. Auger electron spectroscopy is a frequently used method to investigate the decay of core-hole states in atoms and thereby analyzing the structure of a sample. In a cluster, the binding energy of an electron depends on its immediate environment, enabling site-dependent studies of the ICD process. The excited ion has a different number of nearest neighbors and therefore a different environment depending on its position within the cluster.

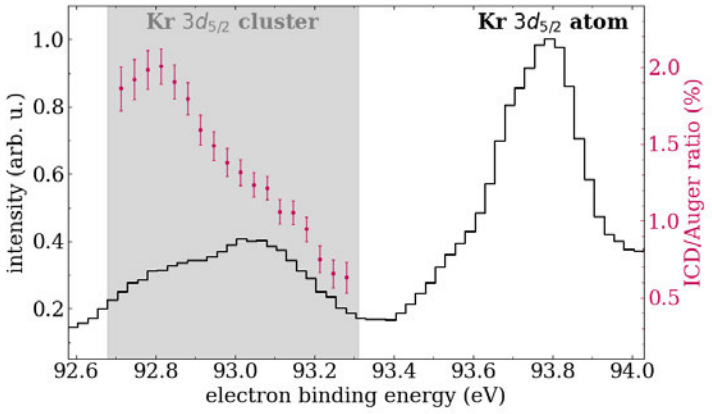

Figure 1: Spectrum of the Kr $3d_{5/2}$ photoelectron measured in coincidence with Auger or core-level ICD electrons for atoms and clusters in a partially condensed cluster jet. The pink dots depict counts of the ICD electron signal divided by the counts of the competing Auger electron signal as a function of the photoelectron binding energy in percent.

1. L. Cederbaum, J. Zobeley, F. Tarantelli, et al., Giant Intermolecular Decay and Fragmentation of Clusters, *Physical Review Letters* **79**, 4778 (1997).
2. T. Jahnke, U. Hergenhahn, B. Winter, et al., Interatomic and Intermolecular Coulombic Decay, *Chemical Reviews* **120**, 11295–11369 (2020).
3. A. Hans, C. Küstner-Wetekam, Ph. Schmidt, et al., Core-level interatomic Coulombic Decay in van der Waals clusters, *Chemical Review Research* **2**, 012022(R) (2020).
4. C. Küstner-Wetekam, L. Marder, D. Bloß et al., Experimental quantification of site-specific efficiency of Interatomic Coulombic Decay after inner shell ionization, communications physics **6**, 50 (2023).

Indirect X-ray photodesorption from ices

R. Basalgète[1], G. Féraud[1], D. Torres-Díaz[1,2], A. Lafosse[2], L. Amiaud[2], P. Jeseck[1], L. Philippe[1], X. Michaut[1], J-H. Fillion[1], and M. Bertin[1]

1 Sorbonne Université, Observatoire de Paris, Université PSL, CNRS, LERMA, F-75005, Paris, France
2 Univ. Paris Saclay, CNRS, ISMO, 91405 Orsay, France

**Contact: geraldine.feraud@sorbonne-universite.fr*

Keywords: X-ray processes, molecular ices, energy transfer, solid-to-gas interface

In the colder parts of the interstellar medium, dust grains are covered with molecular ices composed of H_2O, CO,... Among the many radiation-induced processes that occur in these icy mantles, the ones induced by X-rays may play an important role in star and planet formation regions [1]. In particular, X-rays interacting with interstellar ices can release molecules or radicals into the gas phase, by so-called photodesorption processes, and thus have an important role in the gas phase abundances measured from observations by the most recent telescopes (ALMA, NOEMA). This X-ray induced desorption process is however rarely considered because of a lack of experimental quantitative data and because the processes at play are poorly understood [2-5].

We irradiated ices containing $^{15}N_2$ and ^{13}CO with soft X-rays using the SPICES 2 set-up connected to the SEXTANTS beamline at the SOLEIL synchrotron [6]. The release of ^{13}CO or of $^{15}N_2$ is recorded by mass spectrometry as a function of the incident photon energy near the N (~ 400 eV) and O K-edge (~ 500 eV). Several ices were studied including pure CO ices, pure $^{15}N_2$ ices, and mixed or layered $^{13}CO/^{15}N_2$ ices. Photo-desorption from a layered $^{13}CO/^{15}N_2$ ice reveals an indirect desorption mechanism for which the desorption of ^{13}CO is triggered by the photo-absorption of $^{15}N_2$ at the N-edge. This enables to quantify the relevant depth involved in the indirect desorption process, which is found to be 30 - 40 Monolayers in that case. This value is further related to the energy transport of Auger electrons emitted from the photo-absorbing $^{15}N_2$ molecules that scatter towards the ice surface, inducing the desorption of ^{13}CO. We show that X-ray induced electron stimulated desorption (XESD), mediated by Auger scattering and subsequent secondary electrons, is the dominant process explaining the desorption from the ices studied in this work [6].

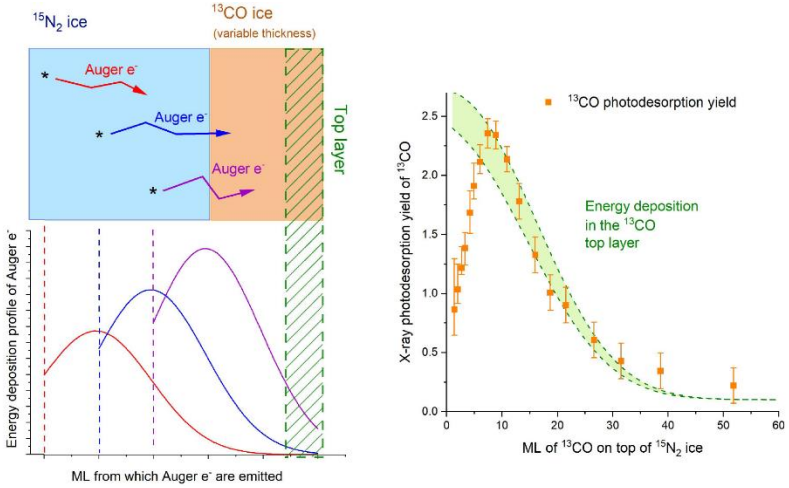

Figure 1: Left: scheme of a simple model to estimate the energy deposited to the top ^{13}CO layer of a layered $^{13}CO/^{15}N_2$ ice by scattering of Auger electrons emitted after photo-absorption by $^{15}N_2$ molecules. Right: in green is displayed the estimation of this energy, compared with the X-ray photodesorption yields of ^{13}CO (orange squares) [7].

1. Walsh, C., Nomura H., Millar T. J., et Aikawa Y. ApJ 747, 2 (2012): 114.
2. Ciaravella,A.; Caro,G. M.; Escobar,A. J.; Cecchi-Pestellini,C.; Giarrusso,S.; Barbera,M.; Collura,A. ApJ 2010, 722, L45–L48.
3. Dupuy, R., M. Bertin, G. Féraud, M. Hassenfratz, X. Michaut, et al. Nat. Astron. 2, 10 (2018): 796-80
4. Basalgète, R.; Dupuy, R.; Féraud, G.; Romanzin, C.; Philippe, L.; Michaut, X.; Michoud, J.; Amiaud, L.; Lafosse, A.; Fillion, J.-H.; Bertin, M. A&A 2021, 647, A35.
5. Basalgète, R.; Dupuy, R.; Féraud, G.; Romanzin, C.; Philippe, L.; Michaut, X.; Michoud, J.; Amiaud, L.; Lafosse, A.; Fillion, J.-H.; Bertin, M. A&A 2021, 647, A36.
6. Basalgète, R.; Torres-Díaz, D.; Lafosse, A.; Amiaud, L.; Féraud, G.; Jeseck, P.; Philippe, L.; Michaut, X.; Fillion, J.-H.; Bertin, M. J. Chem. Phys. 2022, 157 (8), 084308.

Experimental study of second step Auger decay in Kr after core 1s excitation

Abhishek Verma[1,*], Renaud Guillemin[1], Ralph Püttner[2], Shuai Li [3], Dimitris Koulentianos [3], Gilles Doumy [3], Linda Young [3,4], Donald A. Walko [5], Denis Ceolin [6], Maria N. Piancastelli [1,7], Leonid Gerchikov[8], Sergei Sheinerman[9], Stephen H. Southworth [3], John Bozek[6], and Marc Simon[1]

1 Sorbonne Université, CNRS, Laboratoire de Chimie Physique Matière et Rayonnement, F-75005, Paris, France
2 Fachbereich Physik, Freie Universität Berlin, Arnimallee 14, D-14195 Berlin, Germany
3 Chemical Sciences and Engineering Division, Argonne National Laboratory, Lemont, Illinois 60439, USA
4 The James Franck Institute and Department of Physics, The University of Chicago, Chicago, Illinois 60637, USA
5 Advanced Photon Source, Argonne National Laboratory, Lemont, Illinois 60439, USA
6 Synchrotron SOLEIL, l'Orme des Merisiers,Saint-Aubin, F-91192 Gif-sur-Yvette, Cedex, France
7 Department of Physics and Astronomy, Uppsala University, SE-75120 Uppsala, Sweden
8 Department of Physics, Peter the Great St. Petersburg Polytechnic University, 195251 St. Petersburg, Russia
9 Department of Physics, St. Petersburg State Marine Technical University, 190121 St. Petersburg, Russia
[*]Contact: abhishek.verma@sorbonne-universite.fr

Keywords: Auger decay, post-collision interaction, photoelectron recapture

We have studied $L_2M_{4,5}N_{2,3}$ Auger relaxation in krypton after core 1s photoexcitation, in the photon energy range $\pm 10eV$ around the K-edge. The $L_2M_{4,5}N_{2,3}$ Auger spectra are obtained through a two-step relaxation process with fluorescence decay in the first step. Kr is an ideal case for studying the second step of Auger emission processes because the 54% first step relaxation process takes place via fluorescence [1]. The 1s core hole is predominately filled by a 2p electron accompanied by $K\alpha$- radiation. The new vacancy created in the 2p orbital is filled by the Auger decay, which produces fast Auger electrons. The emission of these Auger electrons is delayed relative to the initial photon absorption by the 2p core-hole lifetime and the 1s core-electron lifetime [2].

All electron spectra measurements have been performed in beamline 7-ID at the Advanced Photon Source (APS) with the EW4000 hemispherical electron analyzer. This beamline is suitable to study the inner electron dynamics of heavy atoms because of its wide range of photon energy availability (4.8–32keV).

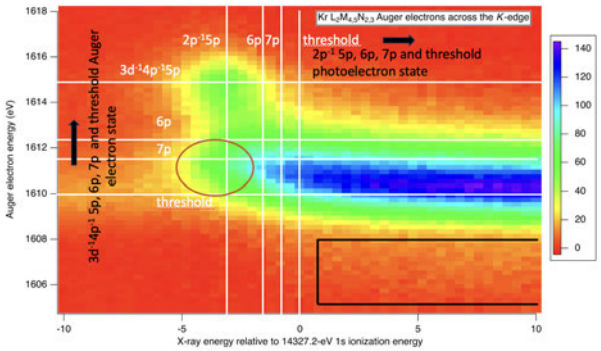

Figure 1: 2D map of $L_2M_{4,5}N_{2,3}$ Auger spectra followed by the $K\alpha$fluorescence decay of $1s^{-1}(n,\varepsilon)p \rightarrow 2p^{-1}(n,\varepsilon)p$.

Above the threshold, the interaction of the photoelectron and the Auger electron takes place at a large distance in the ionic field of Kr. As a consequence, post-collision interaction (PCI) is weaker [3] and we do not observe photoelectron recapture in the 5p and 6p Rydberg states. Below the threshold, the $L_2M_{4,5}N_{2,3}$ Auger emission through the $1s \rightarrow 5p$ resonance excitation leads to the $3d^{-1}4p^{-1}5p$ final state. Using the term values of the Kr $3d_{5/2}np$ and $3d_{3/2}np$ excitations as well as the Z+1 approximation we were able to determine precisely the binding energy of the Rydberg States.

[1] Boudjemia N, Jänkälä K, Püttner R, et al. D Phys Rev A. 101(5):053405. (2020).
[2] Kosugi S, Koike F, Iizawa M, et al., Phys Rev Lett. 124, 183001 (2020).
[3] Li S, Koulentianos D, Southworth SH, et al., Phys Rev A. 106, 023110 (2022).

Quantum Spin Nematic Phase in a Square-lattice Iridate

Bumjoon Kim[1,2,*], Hoon Kim[1,2], Jinkwang Kim[1,2] and Junyoung Kwon[1,2]

1 [1]Department of Physics, Pohang University of Science and Technology, Pohang 37673, South Korea
2 Center for Artificial Low Dimensional Electronic Systems, Institute for Basic Science (IBS), Pohang 37673, South Korea

**Contact: bjkim6@postech.ac.kr*

Keywords: spin nematic, resonant x-ray diffraction, Raman spectroscopy

Spin nematic (SN) is a magnetic analog of classical liquid crystals, a fourth state of matter exhibiting characteristics of both liquid and solid [1, 2]. Particularly intriguing is a valence-bond SN, in which spins are quantum entangled to form a multi-polar order without breaking time-reversal symmetry, but its unambiguous experimental realization remains elusive. In this talk, I will discuss on our recent discovery of a SN phase in the square-lattice iridate Sr_2IrO_4, which approximately realizes a pseudospin one-half Heisenberg antiferromagnet (AF) in the strong spin-orbit coupling limit [3]. Upon cooling, the transition into the SN phase at T_C~263 K is marked by a divergence in the static spin quadrupole susceptibility extracted from our Raman spectra, and concomitant emergence of a collective mode associated with the spontaneous breaking of rotational symmetries. The quadrupolar order persists in the antiferromagnetic (AF) phase below T_N~230 K, and becomes directly observable through its interference with the AF order in resonant x-ray diffraction, which allows us to uniquely determine its spatial structure. Further, we find using resonant inelastic x-ray scattering a complete breakdown of coherent magnon excitations at short-wavelength scales, suggesting a resonating-valence-bond-like quantum entanglement in the AF state. Taken together, our results reveal a quantum order underlying the Neel AF that is widely believed to be intimately connected to the mechanism of high temperature superconductivity.

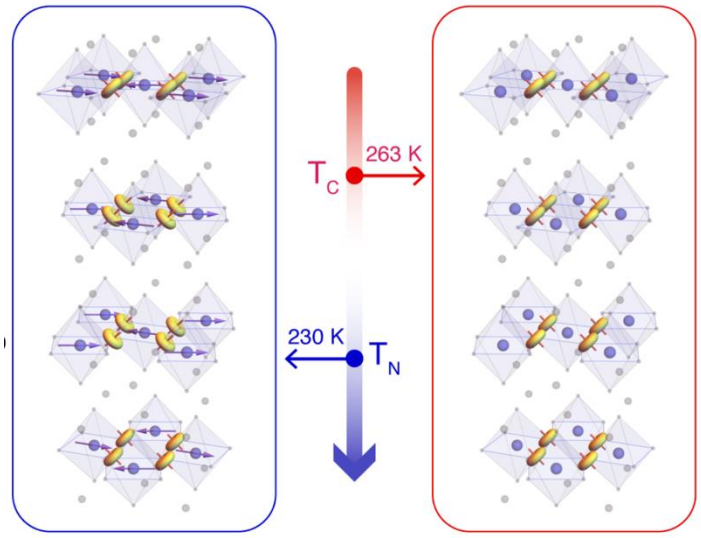

Figure 1**:** A schematic of the Neel AF and SN orders overlaid on the crystal structure of Sr_2IrO_4.

1. M. Blume and Y. Y. Hsieh, J. Appl. Phys. 40, 1249–1249349 (1969).
2. A. F. Andreev and I. A. Grishchuk, Sov. Phys. JETP 60, 267 (1984).
3. J. Bertinshaw, Y. K. Kim, G. Khaliullin, and B. J. Kim, Annu. Rev. Condens. Matter Phys. 10, 315–336 (2019).

Establishing fundamentals of ARPES spin textures with the model material $PtTe_2$

Mohammed Qahosh[1], Gustav Bihlmayer[2], Jakub Schusser[3], Muthu Masilamani[3], Friedrich Reinert[3], Claus M.Schneider[1] and Lukasz Plucinski[1],

1 Peter Grünberg Institut (PGI-6), Forschungszentrum Jülich GmbH, 52428 Jülich, Germany

2 Peter Grünberg Institut (PGI-1) and Institute for Advanced Simulation (IAS-1), Forschungszentrum Jülich and JARA, 52428 Jülich, Germany

3 Experimentelle Physik VII and Würzburg-Dresden Cluster of Excellence ct.qmat,Universität Würzburg, 97074 Würzburg,Germany

Keywords: Spin-ARPES, Spin-texture asymmetry, Surface states, Electronic structure

A novel quantum material $PtTe_2$ is used to establish the connection between spin textures of angle-resolved photoemission spectroscopy (ARPES) and initial state spin textures. $PtTe_2$ has been identified to host type-II bulk Dirac cone [2] and a number of topological surface states [3,4] labeled in our high resolution spin polarized $E(k)$ map Fig.1(a), measured using the *MB Scientific* A1 hemispherical electron analyzer and the exchange-scattering Focus *GmbH* FERRUM spin detector.

The crystal structure of 1T-$PtTe_2$ is trigonal belonging to the space group 164 ($P\bar{3}m1$), that hosts three mirror planes and exhibits inversion symmetry. Since bulk 1T-$PtTe_2$ is both inversion-symmetric and non-magnetic, no bulk spin-polarized bands are allowed due to the Kramers degeneracy. At the surface, a non-zero spin polarization is expected due to the broken inversion symmetry through the 'hidden spin polarization' phenomenon [5], however, it must obey the mirror and time-reversal symmetries. Experimental maps are analysed by comparison to ab-initio slab calculations and one-step model photoemission simulations.

We measured the dependence of the spin-polarization of the surface states of $PtTe_2$ on the symmetries of the spin-ARPES setup using the unpolarized HeI lamp (21.22eV). This is performed in two geometries, with the reaction plane either parallel to $\bar{K}$-$\bar{\Gamma}$-$\bar{K}$ or $\bar{M}$-$\bar{\Gamma}$-$\bar{M}$ reciprocal directions, i.e. either orthogonal or parallel to one of the crystal mirror planes, Fig.1(b-c) respectively. The measured spin texture is symmetric when the reaction plane is parallel to $\bar{K}$-$\bar{\Gamma}$-$\bar{K}$ Fig.1(a-b). However, we see asymmetries in the spin texture when the reaction plane is parallel to $\bar{M}$-$\bar{\Gamma}$-$\bar{M}$ Fig.1(c). For the surface states, the asymmetries are due to the geometry-induced spin filtering in ARPES [1]. On the other hand, for the bulk states, the effect might be additionally related to the asymmetric initial state dispersions. Our results provide a critical benchmark in establishing relationship between spin-ARPES and initial state spin textures.

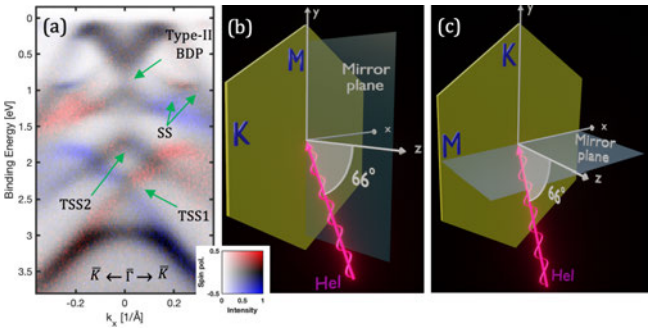

Figure 1: (a) High resolution spin-polarized $E(k)$ map probed using the corresponding geometry (b). Two different experimental geometries; in (b) The reaction plane is parallel to $\bar{K}$-$\bar{\Gamma}$-$\bar{K}$, while in (c) it is parallel to $\bar{M}$-$\bar{\Gamma}$-$\bar{M}$. Topological surface states (TSS), surface states (SS) and bulk Dirac point (BDP) are labeled.

[1] T. Heider et al., Geometry-Induced Spin Filtering in Photoemission Maps from WTe_2 Surface States, *Phys. Rev. Lett* **130**, 146401 (2023).

[2] M. Yan et al., Lorentz-violating type-II Dirac fermions in transition metal dichalcogenide $PtTe_2$, *Nat. Commun* **8**, 257 (2017).

[3] M. Bahramy et al., Ubiquitous formation of bulk Dirac cones and topological surface states from a single orbital manifold in transition-metal dichalcogenides, *Nat. Mater* **17**, 21-28 (2018).

[4] O. Clark et al., Fermiology and Superconductivity of Topological Surface States in $PdTe_2$, *Phys. Rev. Lett* **120**, 156401 (2018).

[5] O. Clark et al., Hidden spin-orbital texture at the $\bar{\Gamma}$-located valence band maximum of a transition metal dichalcogenide semiconductor, *Nat. Commun* **13**, 4147 (2022).

Determination of anisotropic magnetic moments at the interface by means of depth-resolved x-ray magnetic circular dichroism

Kenta Amemiya[1,*] and Kaoruho Sakata[1]

1 Institute of Materials Structure Science, High Energy Accelerator Research Organization, Tsukuba, Japan

**Contact: kenta.amemiya@kek.jp*

Keywords: interface, anisotropic magnetic moments, depth-resolved x-ray magnetic circular dichroism

We have developed a novel experimental method that enables to determine anisotropy in the magnetic moments at the interface of magnetic thin films without thickness-dependent experiment, based on the depth-resolved x-ray magnetic circular dichroism (XMCD) technique, in which the fluorescence soft x rays are collected at different detection angles [1-3]. By combining the depth-resolved XMCD technique with incidence angle-dependent XMCD sum rules, the spin magnetic moment, perpendicular and in-plane orbital magnetic moments, and perpendicular and in-plane magnetic dipole moments are separately estimated at the interface and inner layers. The method has been applied to a Co thin film sandwiched by Au layers, and it was revealed that the perpendicular orbital magnetic moment is significantly larger than the in-plane one at the interface, while the inner Co layers exhibit a small opposite tendency [4].

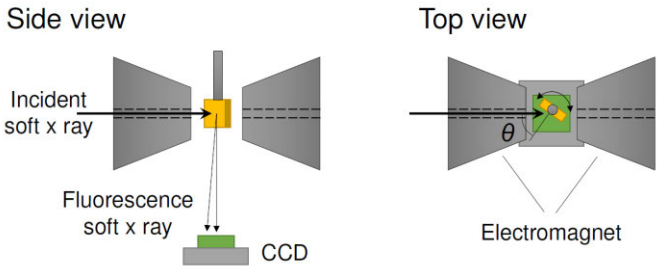

Figure 1: Schematic layout for the fluorescence-yield depth-resolved XMCD measurement under magnetic fields.

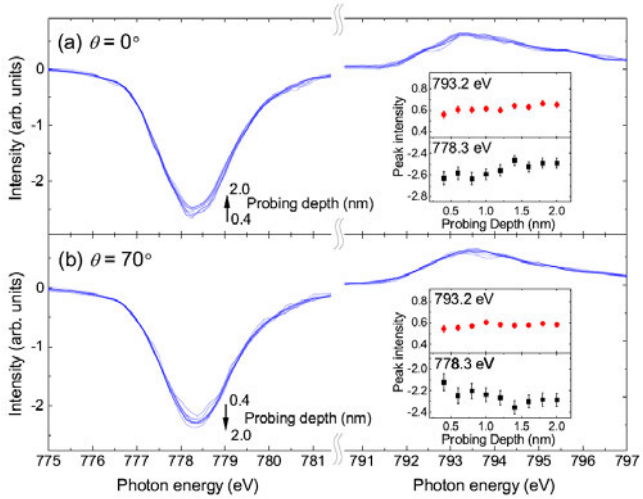

Figure 2: Series of Co L-edge XMCD spectra at different probing depths taken at incidence angles, θ, of 0 and 70°.

1. K. Amemiya, S. Kitagawa, D. Matsumura, T. Ohta, T. Yokoyama, Direct observation of magnetic depth profiles of thin Fe films on Cu(100) and Ni/Cu(100) with the depth-resolved x-ray magnetic circular dichroism, *Appl. Phys. Lett.* **84**, 936 (2004).
2. K. Amemiya, Sub-nm resolution depth profiling of the chemical state and magnetic structure of thin films by a depth-resolved X-ray absorption spectroscopy technique, *Phys. Chem. Chem. Phys.* **14**, 10477 (2012).
3. M. Sakamaki, K. Amemiya, Nanometer-resolution depth-resolved measurement of florescence-yield soft x-ray absorption spectroscopy for FeCo thin film, Rev. Sci. Instrum. **88**, 083901 (2017).
4. K. Amemiya, K. Sakata, Determination of anisotropy in magnetic moments at the interface of Au/Co/Au thin film without a thickness-dependent experiment, *Phys. Rev. B* **106**, 134424 (2022).

Tamm and Shockley surface states at Re(0001): two paradigmatically different types of states mixed by spin-orbit interaction

Markus Donath[1,*], Marcel Holtmann[1], Peter Krüger[2], Koji Miyamoto[3], Taichi Okuda[3], Sven Schemmelmann[1], Fabian Schöttke[1], Pascal J. Grenz[1], Shiv Kumar[3], and Kenya Shimada[3]

1 Physikalisches Institut, University of Münster, Münster, Germany
2 Institut für Festkörpertheorie, University of Münster, Münster, Germany
3 Hiroshima Synchrotron Radiation Center, Hiroshima University, Higashi-Hiroshima, Japan
**Contact: markus.donath@uni-muenster.de*

Keywords: surface states, spin-orbit interaction, spin-resolved (inverse) photoemission

The appearance of surface states is characteristic for semi-infinite crystals caused by the broken symmetry at the surface. Their description for understanding surface properties is a highly noticed and still ongoing research topic in various fields such as electronic surface states and surface states in photonic and phononic crystals. Theoretically, two paradigmatic concepts have been used to describe electronic surface states: Tamm and Shockley states [1,2].

There is a controversy about whether there is a real physical distinction between the two kinds of states. For some authors, the distinction has only historical reasons based on different mathematical approaches. Other authors notice an important distinction. According to Zak [3], the existence of Shockley states is derived for a bulklike potential termination at the surface, while a distortion of the potential in the surface region is essential for the existence of Tamm states. Martin [4] pointed out that Shockley states are "based on a transition in the bulk band structure that is a precursor of modern-day topological insulators." Experimentally, the distinction between Tamm and Shockley states remains to be a challenge.

The Re(0001) surface hosts several types of electronic surface states [5-10]. Our study reveals that Tamm and Shockley states appear in neighboring but qualitatively different energy gaps in the vicinity of the Fermi level [11]. Interestingly, spin-orbit interaction generates a double W-shaped energy vs. $k_{\parallel}$ dispersion by mixing both types of states and lifting their spin degeneracy. As a consequence, the resulting surface bands consist of two electron pockets and one hole pocket, crossing the Fermi level four times. We employ spin- and angle-resolved direct and inverse photoemission to detect the spin-dependent $E(k_{\parallel})$ dispersion of the electron and hole pockets, respectively. In combination with tight-binding model calculations as well as density functional theory including the photoemission process, we develop verifiable criteria to distinguish between the two types of surface states and arrive at a consistent picture of the role of spin-orbit interaction in such a scenario.

1. I. Tamm, *Z. Physik* **76**, 849 (1932).
2. W. Shockley, *Phys. Rev.* **56**, 317 (1939).
3. J. Zak, *Phys. Rev. Lett.* **62**, 2747 (1989).
4. R. M. Martin, *Electronic Structure* (Cambridge University Press, Cambridge, UK, 2020).
5. S. Ouazi, T. Pohlmann, A. Kubetzka, K. von Bergmann, and R. Wiesendanger, *Surf. Sci*. **630**, 280 (2014).
6. A. Urru and A. Dal Corso, *Surf. Sci*. **686**, 22 (2019).
7. H. J. Elmers, J. Regel, T. Mashoff, J. Braun, S. Babenkov, S. Chernov, O. Fedchenko, K. Medjanik, D. Vasilyev, J. Minár, H. Ebert, and G. Schönhense, *Phys. Rev. Research* **2**, 013296 (2020).
8. J. Regel, T. Mashoff, and H. J. Elmers, *Phys. Rev. B* **102**, 115404 (2020).
9. S. Schemmelmann, P. Krüger, F. Schöttke, and M. Donath, *Phys. Rev. B* **104**, 205425 (2021).
10. F. Schöttke, S. Schemmelmann, P. Krüger, and M. Donath, *Phys. Rev. B* **105**, 155419 (2022).
11. M. Holtmann, P. Krüger, K. Miyamoto, T. Okuda, P. J. Grenz, S. Kumar, K. Shimada, and M. Donath, *Phys. Rev. B* **105**, L241412 (2022).

Dynamical interplay between molecular chirality and electrons

V. Blanchet[1], Y. Mairesse[1], B. Pons[1], D. Rajak[1], J. D. Gorfinkiel[13], N. Dudovich[12], B. Fabre[1], A. Comby[1], O. Kneller[12], D. Faccialà[2], M. Devetta[2], S. Beauvarlet[1], N. Besley[3], F. Calegari [4,5], C. Callegari[6], D. Catone[7], E. Cinquanta[2], A. Ciriolo[2], L. Colaizzi[4], M. Coreno[7], G. Crippa[8], G. De Ninno[6,9], M. Di Fraia[6], M. Galli[4,8], G. Garcia[10], M. Negro[2,8], O. Plekan[6], P. P. Geehta[2], K. Prince[6], A. Pusala[8], S. Stagira[2,8], S. Turchini[7], K. Ueda[11], D. You[11], N. Zema[7], L. Nahon[10], I. Powis[3], C. Vozzi[2].

1 - CELIA, Université de Bordeaux-CNRS-CEA, France

2 - Istituto di Fotonica e Nanotecnologie CNR-IFN, Italy

3 - School of Chemistry, University of Nottingham, United Kingdom

4 - Center for Free-Electron Laser Science, DESY, Germany

5 - Hamburg University, Physics Department, Germany

6 - Elettra-Sincrotrone Trieste, Italy

7 - Istituto di Struttura della Materia CNR-ISM, Italy

8 - Politecnico di Milano, Dipartimento di Fisica, Italy

9 - Laboratory of Quantum Optics, University of Nova Gorica, Slovenia

10 - Synchrotron Soleil, France

11 - Institute of Multidisciplinary Research for Advanced Materials, Tohoku University, Japan

12-Weizmann Institute of Science, Israel

13-School of Physical Sciences, The Open University, United Kingdom

**Contact: valerie.blanchet@u-bordeaux.fr*

Keywords: chirality, femtosecond, X-ray FEL, PECD, strong field ionization, attosecond.

By scattering in a chiral molecular potential of pure handedness, photoelectrons exhibit a unique forward-backward antisymmetry in their momenta with respect to the axis of the ionizing elliptical light pulse. Resolving angularly this chiroptical dichroism in the momentum distributions allows to selectively filter out the electrons that are most sensitive to the electronic potential. This fascinating aspect of the light-matter interaction that survives the random distributions of molecular orientations, will be illustrated in various experimental results, such as multiphoton experiments involving pump-probe with local or non-local probes [1-3], and strong laser field experiments [4]. Fenchone is a chiral terpene on which we will present femtosecond dynamics probed by valence or core-level C1s chiral ionization using a Velocity map photoelectron imaging detector [1,2]. This technique is called TR-PECD for Time-Resolved Photoelectron Circular Dichroism. Electrons' chirosensitive scattering can be also manipulated at the attosecond scale with an ionization laser pulse strong enough to compete with the molecular potential [4]. In this tunnel ionization regime, we will show how to identify the electron trajectories the most sensitive to the chiral potential. This technique is called CHILIED, for chiral Laser-Induced Electron Diffraction. Our findings will shed light on the intricate interactions between chirality and electron scattering at ultrafast timescales.

1. Antoine Comby, Samuel Beaulieu, Martial Boggio-Pasqua, Dominique Descamps, Francois L gar , Laurent Nahon, St phane Petit, Bernard Pons, Baptiste Fabre, Yann Mairesse, and Val rie Blanchet, Journal of Physical Chemistry Letters 7, 4514 (2016)
2. D. Faccialà, M. Devetta, S. Beauvarlet, N. Besley, F. Calegari, C. Callegari, D. Catone, E. Cinquanta, A. G. Ciriolo, L. Colaizzi, M. Coreno, G. Crippa, G. de Ninno, M. Di Fraia, M. Galli, G. A. Garcia, Y. Mairesse, M. Negro, O. Plekan, P. Prasannan Geetha, K. C. Prince, A. Pusala, S. Stagira, S. Turchini, K. Ueda, D. You, N. Zema, V. Blanchet, L. Nahon, I. Powis, C. Vozzi, Physical Review X 13, 011044 (2023)
3. Vincent Wanie, Etienne Bloch, Erik P. Månsson, Lorenzo Colaizzi, Sergey Ryabchuk, Krishna Saraswathula, Andrea Trabattoni, Valérie Blanchet, Nadia Ben Amor, Marie-Catherine Heitz, Yann Mairesse, Bernard Pons, Francesca Calegari, https://doi.org/10.48550/arXiv.2301.02002
4. E. Bloch, S. Larroque, S. Rozen, S. Beaulieu, A. Comby, S. Beauvarlet, D. Descamps, B. Fabre, S. Petit, R. Taïeb, A. J. Uzan, V. Blanchet, N. Dudovich, B. Pons, and Y. Mairesse, Physical Review X 11, 041056 (2021)3.

Photoelectron recoil-induced rotation: Cohen-Fano and multichannel interference effects

Victor Kimberg[1,*]

1 Division of Theoretical Chemistry and Biology, KTH Royal Institute of Technology, 10691 Stockholm, Sweden

**Contact: kimberg@kth.se*

Keywords: X-ray pump-probe spectroscopy, XFEL, photoemission, Cohen-Fano interference, rotation

Modern stationary X-ray spectroscopy is unable to resolve rotational structure [1]. In the present study, we propose to use time-resolved two color X-ray pump-probe spectroscopy with picosecond resolution for real-time monitoring of the rotational dynamics induced by the recoil effect [2]. The proposed technique consists of two-steps (Figure 1). The first short pump X-ray pulse ionizes the valence electron, which transfers angular momentum to the molecule. The second time-delayed short probe X-ray pulse resonantly excites a 1s electron to the created valence hole. Due to the recoil-induced angular momentum the molecule rotates and changes the orientation of transition dipole moment of core-excitation with respect to the transition dipole moment of the valence ionization, which results in a temporal modulation of the probe X-ray absorption as function of the delay time between the pulses. An accurate theoretical description is used for analytical discussions and numerical simulations. Our main attention is paid to the following two interference effects that influence the recoil-induced dynamics [3]: (i) Cohen–Fano (CF) two-center interference between partial ionization channels in diatomics and (ii) interference between the recoil-excited rotational levels manifesting as the rotational revival structures in the time-dependent absorption of the probe pulse. The time-dependent x-ray absorption is computed for the heteronuclear CO and homonuclear N_2 molecules as showcases. It is found that the effect of CF interference is comparable with the contribution from independent partial ionization channels, especially for the low photoelectron kinetic energy case. The profile and intensity of the CF interference depend on the phase difference between the individual ionization channels related to the parity of the molecular orbital emitting the photoelectron. This phenomenon provides a sensitive tool for the symmetry analysis of molecular orbitals.

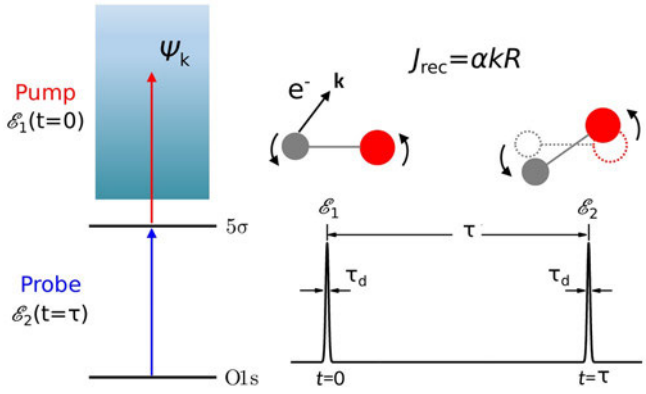

Figure 1: Scheme of the electronic transitions (left panel) in the studied pump-probe process with two time delayed X-ray pulses (right panel).

1. F. Gel'mukhanov, M. Odelius, S.P. Polyutov, A. Föhlisch, & V. Kimberg, *Reviews of Modern Physics*, ***93***, 035001 (2021).
2. J.-C. Liu, N. Ignatova, V. Kimberg, P. Krasnov, A. Föhlisch, M. Simon, & F. Gel'mukhanov, *Physical Chemistry Chemical Physics* **24**, 6627–6638 (2022).
3. J.-C. Liu, J. Wang, N. Ignatova, P. Krasnov, F. Gel'mukhanov, & V. Kimberg, *The Journal of Chemical Physics* **158** (11), 114304 (2023).

Using x-ray FELs to imagine strong-field optical processes

C. Ornelas-Skarin[1,2], T. Bezriadina[3], M. Fuchs[4], S. Ghimire[2], J. B. Hastings[2], N. N. Hua[5]
L. Leroy[5], Q. Nguyen[2], G. de la Peña[2], D. Popova-Gorelova[3], S. Shwartz[6], M. Trigo[2],
T. Sato[2], D. Zhu[2], and D. A. Reis[1,2*]

1 Stanford University, Stanford, CA 94305, USA
2 SLAC National Accelerator Laboratory, Menlo Park, CA 94025, USA
3 University of Hamburg, D-20355 Hamburg, Germany
4 University of Nebraska, Lincoln, NE, 68588, USA
5 Paul Scherrer Institut, 5232 Villigen PSI, Switzerland
6 Bar-Ilan University, Ramat Gan, 5290002, Israel

Contact: dreis@stanford.edu

Keywords: nonlinear optics, high-harmonic generation, x-ray scattering, atomic-scale imaging.

The nonlinear interaction of x-ray and optical photons in crystals produces energy and momentum sidebands on ordinary Bragg diffraction. The resultant x-ray optical wavemixing (XOM) signal depends on the spatial and temporal Fourier components of the induced charges (and thus currents) that would otherwise be invisible due to the long wavelength at optical frequencies[1, 2, 3]. The experimental challenges of measuring XOM stem from its relatively small efficiencies of the signal which is concentrated in an extremely small solid-angle and phase-matching condition about the elastic Bragg peaks, and thus background suppression is key. Here we present preliminary results demonstrating nonlinear XOM in single crystal Si dressed by an intense 1eV optical laser, and discuss plans to extend to the strong-field limit. The experimental setup is shown in Fig 1a. The polarization dependence for the first and second order mixing signal is shown in Fig. 1 (b,c) and was made possible by the extensive background suppression from our custom monochromator and analyzer. In the perturbative limit the second-order mixing (single x-ray and two optical fields) depends on the square of the laser intensity and shows a nontrivial polarization dependence, which we analyze in terms of the microscopic nonlinear optical tensor. Notably, the induced charge density oscillating at twice the optical frequency is forbidden to radiate in the far field due to the inversion symmetry of the crystal, but no such symmetry requirements exist for the microscopic densities. We discuss how XOM could be used to image the microscopic currents responsible for strong-field solid-state high harmonic generation[4, 5].

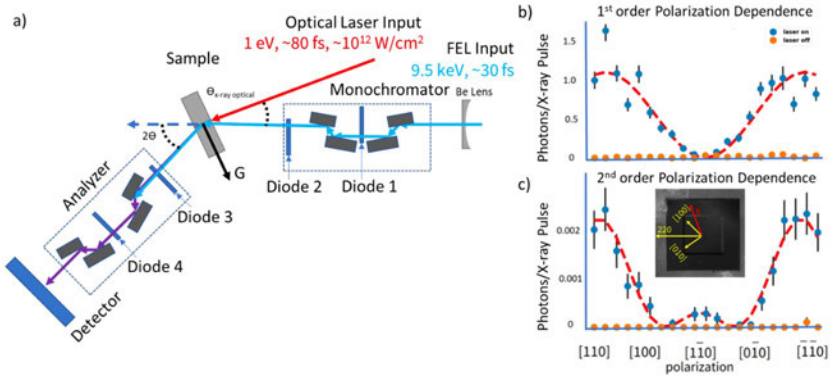

Figure 1: Nonilinear x-ray and optical wave mixing in silicon.

Supported by the US Department of Energy, Office of Science, Office of Basic Energy Sciences, Chemical Sciences, Geosciences, and Biosciences Division through the AMOS program and performed on the LCLS. We thank X. Huang for fabrication and advice on the design of the Si 311 channel cuts, and S. Gerber, H. Lemke, R. Mankowsky, M. Sander and C. Svetina for help with preliminary experiments on SwissFEL.

[1] I. Freund and B. F. Levine. Optically modulated x-ray diffraction. *Phys. Rev. Lett.*, **25**,1241 (1970).
[2] P. Eisenberger and S. McCall. Mixing of x-ray and optical photons. *Phys. Rev. A*, **(3)**,1145 (1971).
[3] T. E. Glover, D. M. Fritz, M. Cammarata, *et al.,* X-ray and optical wave mixing. *Nature*, **488**, 603 (2012).
[4] S. Ghimire and D. A. Reis. High-harmonic generation from solids. *Nat. Phys.*, **15**,10 (2019).
[5] D. Popova-Gorelova, D. A. Reis, and R. Santra. Theory of x-ray scattering from laser-driven electronic systems. *Phys. Rev. B*,**98**, 224302 (2018).

Hard X-ray core-hole clock spectroscopy and charge transfer processes

Fredrik O.L. Johansson[1,2], Ute Cappel[2], Tamara Sloboda[2], Elin Berggren[1], Andreas Lindblad[1]

1 Div. X-ray Photon Science, Dept. Physics and Astronomy, Uppsala University, Box 516, SE-751 20 Uppsala, Sweden

2 Div. of Applied Physical Chemistry, Dept. Chemistry, KTH - Royal Institute of Technology, SE-100 44 Stockholm, Sweden

**Contact: andreas.lindblad@physics.uu.se*

Keywords: Resonant Auger Spectroscopy, hard X-rays, sulfides, polymers

A core-electron (e.g. from S 1s) can be resonantly excited to an unoccupied part of the electronic structure. This core-excited state will decay and the core hole filled by an electron, the excess energy in the system may be carried away by the emission of a valence electron (resonant Auger decay). In the solid state the core-excited electron can tunnel away from the site with the core-hole and the core hole then decays with a normal Auger decay. By measuring the relative intensity of spectral components from the two processes for photon energies close to the resonance we can obtain information about the propensity for the electron in the excited state to tunnel away. This propensity of tunneling depends on the energy landscape surrounding the excited atom which we have been using to charge transfer processes as a function of material structure and material combinations [1-4]. The tunneling process need to occur during the core-hole lifetime (hence ‘’core-hole clock”) so we can infer how fast the process need to be for us to observe it. Depending on excitation energy we get different times which enable us to map the behavior for a system for electrons in the conduction band with small or large excess energies.

In quantum dots (PbS) [1] and polymer heterojunctions [4] the low excess energy part vary depending on composition whereas higher energy excitations have the same tunneling behavior. It turns out that the material compositions that give best macroscopic performance in photovoltaic cells built from these materials also have the swiftest charge transfer times measured via the core-hole clock method.

The transition metal dichalcogenide MoS_2 in single crystal, nano-particle show the same charge transfer behavior whereas in sheets grown on reduced graphene oxide are more structured which is a fingerprint of a barrier for charge transfer between MoS_2 and the graphene sheet[3].

Using the linear polarization of synchrotron light and the anisotropy of SnS_2 crystals we can excite different parts of the conduction band structure selectively[2]. Together with calculations of the orbital projected band structure we demonstrate that we indeed excite different parts of the unoccupied density of states with this method.

I will also present recent experiments we have made on other polymer bulk heterojunctions.

1. T. Sloboda, *et al.* "Unravelling the ultrafast charge dynamics in PbS quantum dots through resonant Auger mapping of the sulfur K-edge." *RSC advances* **12**:49 (2022): 31671-31679.
2. F. O. L. Johansson, *et al.* "Interlayer charge transfer in tin disulphide: Orbital anisotropy and temporal aspects." *Physical Review B* **102**:3 (2020): 035165.
3. F. O. L. Johansson, *et al.* "Tailoring ultra-fast charge transfer in MoS2.", *Physical Chemistry Chemical Physics* **22**:18 (2020): 10335-10342.
4. F.O. L. Johansson, *et al.* "Femtosecond and attosecond electron-transfer dynamics in PCPDTBT: PCBM bulk heterojunctions." *The Journal of Physical Chemistry C* **122**:24 (2018): 12605-12614.

Floquet engineering of a model semiconductor

Shuyun Zhou

Department of Physics, Tsinghua University, Beijing, China

**Contact: syzhou@mail.tsinghua.edu.cn*

Keywords: Floquet engineering, ultrafast time- and angle-resolved photoemission spectroscopy, black phosphorus

Revealing the ultrafast dynamics of quantum materials and further controlling the transient electronic states by ultrashort laser pulses can extend our understanding of the fundamental physics to the nonequilibrium state, with the intriguing possibility to manipulate material properties in the picosecond (ps) to femtosecond (fs) time scale. Time-resolved ARPES (TrARPES) is a powerful tool for capturing the nonequilibrium electronic structures and for investigating possible light-induced new electronic states with energy-, momentum- and time-resolved information. In this talk, I will present our recent progress in developing cutting-edge TrARPES instrumentation, with particular efforts focusing on extending the pump and probe photon energy ranges. I will also present our recent progress on the ultrafast dynamics and Floquet engineering of quantum materials which are made possible by such instrumentation development. In particular, I will discuss the Floquet band engineering of a model semiconductor - black phosphorus - upon near-resonance pumping.

1. "Light-induced emergent phenomena in two-dimensional materials and topological materials", Nature Reviews Physics 4, 33 (2022)
2. "Ultrafast time- and angle-resolved photoemission spectroscopy with widely tunable probe photon energy of 5.3 - 7.0 eV for investigating dynamics of three-dimensional materials", Rev. Sci. Instrum. 93, 013902 (2022)
3. "A newly-designed fs KBBF device for achieving sub-100 fs time resolution for time- and angle-resolved photoemission spectroscopy with a tunable VUV source", Rev. Sci. Instrum. 93, 113910 (2022)
4. "Pseudospin-selective Floquet band engineering in black phosphorus", Nature 614, 75 (2023)

Direct visualization of charge transfer and hybridized excitons in twisted $MoSe_2/WS_2$ bilayers

Alice Kunin[1], Zachary H. Withers[1], Ziling Li[2], Sergii Chernov[1], Jin Bakalis[1], Saba Shalamberidze[1], Alexander Adler[1], Shuyu Cheng[2], Gerd Schönhense[3], Xu Du[1], Roland K. Kawakami[2], Thomas K. Allison[1,*]

1 Stony Brook University, Stony Brook, New York 11794, USA
2 The Ohio State University, Columbus, Ohio 43210, USA
3 Johannes Gutenberg-Universität, Institut für Physik, D-55099 Mainz, Germany
**Contact: thomas.allison@stonybrook.edu*

Keywords: time- and angle-resolved photoemission spectroscopy, excitons, transition metal dichalcogenides

Vertically stacking heterobilayers of transition metal dichalcogenides (TMDs) with a finite twist angle leads to the emergence of new, tunable excitonic properties due to the moiré superlattice that is formed. $MoSe_2/WS_2$ heterobilayers present a unique case among TMD heterobilayers as the conduction band alignment of the two layers is nearly degenerate, leading to hybridization between intralayer and spatially-indirect interlayer excitons. Optical measurements have shown emerging angle- and temperature-dependent features in $MoSe_2/WS_2$ structures proposed to correspond to the formation of hybridized excitons [1, 2], but these momentum-integrated measurements do not allow for the direct observation of electron sharing between the two layers. While small twist angles θ and $60° - \theta$ are expected to lead to strong hybridization due to the overlap of K_{MoSe_2} and K_{WS_2} in momentum space, large angles have been generally implicated to lead to weak interlayer coupling [1]. Recent work has suggested that near 40° twist angle should exhibit a revival of hybridization due to the moiré reciprocal lattice wavevector becoming commensurate with the momentum mismatch of K_{MoSe_2} and K'_{WS_2} [2].

Here, we use a unique, 61 MHz apparatus for time-resolved momentum microscopy [3, 4] to visualize the nature of the charge transfer processes and hybridized exciton dynamics in $MoSe_2/WS_2$ heterobilayers at twist angles of $58.0 \pm 0.3°$ and $40.2 \pm 0.9°$ between 300 and 90 K. In 40.2° twisted $MoSe_2/WS_2$, our measurements resolve the occupation of both of the monolayer Brillouin zones up to few ps timescales (Figure 1). The dynamics suggest that intralayer $MoSe_2$ excitons rather than hybridized excitons ultimately persist at longer timescales. In the 58.0° twisted heterobilayer, we observe the prominent formation of higher energy $K - \Sigma$ excitons in the interior of the Brillouin zone and explore the interplay between these momentum-forbidden dark excitons with the spatially-direct and -indirect $K - K$ excitons.

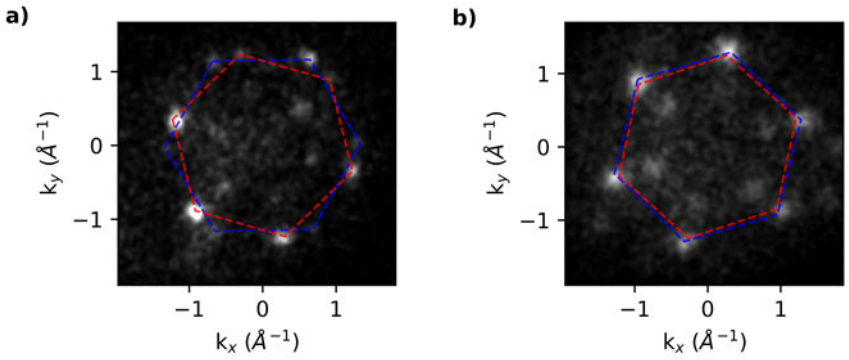

Figure 1: Exciton signal measured at 90K for $MoSe_2/WS_2$ twisted heterobilayers at twist angles of a) 40.2° ($h\nu_{probe}$ = 27.6 eV) and b) 58.0° ($h\nu_{probe}$ = 25.2 eV). Red (blue) dashed lines indicate the $MoSe_2$ (WS_2) Brillouin zone.

[1] E. M. Alexeev et al., Resonantly hybridized excitons in moiré superlattices in van der Waals heterostructures, *Nature* **567**, 81−86 (2019).

[2] L. Zhang et al., Twist-angle dependence of moiré excitons in $WS_2/MoSe_2$ heterobilayers, *Nature Communications* **11**, 5888 (2020).

[3] C. Corder et al., Ultrafast extreme ultraviolet photoemission without space charge, *Structural Dynamics* **5**, 054301 (2018).

[4] A. Kunin et al., Momentum-resolved exciton coupling and valley polarization dynamics in monolayer WS_2, *Physical Review Letters* **130**, 046202 (2023).

Uncovering switching and failure mechanisms of redox-based memristive devices by *in-situ* spectroscopy

Regina Dittmann[1,2*]

1 Peter Grünberg Institut 7, Forschungszentrum Jülich GmbH & JARA-FIT, Germany
2 Faculty of Engineering, Lund University, Sweden
**Contact: r.dittmann@fz-juelich.de*

Keywords: memristive devices, operando spectroscopy, PEEM, HAXPES

Memristive devices have been a hot topic in nanoelectronics for the last two decades in both academia and industry. Originally proposed as non-volatile random access memories, however, based on their large dynamic range in resistance with analog tunability, memristive devices are considered as hardware synapse in neuromorphic circuits. It is generally assumed that voltage-driven oxygen-ion migration and the resulting nanoscale redox processes drive the resistance change in metal oxide based memristive devices. Direct observation of the switching and failure mechanism, however, remain challenging because the net changes of structure, stoichiometry, and valence state during switching are very small and occur primarily at electrode interfaces or within nanoscale filaments. In this talk, we will give an overview about spectroscopic approaches to detect changes of the electronic structure of different types of memristive devices underneath the electrodes or within nanosized filaments.

For non-filamentary manganite-based memristive systems, we employed hard-X-ray spectroscopy to reveal the underlying redox-processes in operando [1]. For filamentary systems, we employed photoemission electron microscopy (PEEM) and complemented it by transmission electron microscopy (TEM) [2]. To overcome the surface sensitivity typically limiting PEEM investigations of memristive devices,we employed photoelectron-transparent graphene top electrodes to attain spectroscopic information from the buried memristive oxide layer [3]. We could thereby determine the position of in-gap states within SrTiO3 filaments by resonant photoemission and use it as input for our calculations of the electronic transport [4]. Quantitative maps of the oxygen vacancy concentration obtained during in situ switching confirm that localized oxygen evolution and reincorporation reactions rather than purely internal movement of oxygen vacancies cause the resistance change. A remarkable agreement between experimental quantification of the redox state and device simulation reveals that changes in oxygen vacancy concentration by a factor of 2 at electrode-oxide interfaces cause a modulation of the effective Schottky barrier and lead to >2 orders of magnitude change in device resistance [3]. Moreover, in-situ PEEM analysis enabled us to identify the microscopic origin of retention failure in SrTiO3 devices and to reveal two different mechanisms for the cycle-to-cycle variability of our devices, namely the change of the shape of the filaments and the movement of filaments during cycling [5].

Based on these studies we could gain a deep understanding of the switching and failure mechanism of the memristive model system SrTiO3. More recently, we could also transfer the developed methodology and knowledge to more industry-relevant systems such Ta2O5 [6].

[1] B. Arndt, F. Borgatti, F. Offi, M. Phillips, P. Parreira, T. Meiners, S. Menzel, K. Skaja, G. Panaccione, D. MacLaren, R.Waser, R. Dittmann, Adv.Funct.Mater. 2017, 1702282

[2] C. Baeumer, C. Schmitz, A. H. H. Ramadan, H. Du, K. Skaja, V. Feyer, P. Mueller, B. Arndt, C. Jia, J. Mayer, R. A. De Souza, C. Michael Schneider, R. Waser, R. Dittmann, Nat. Commun., 2015, 6, 9610

[3] C. Baeumer, C. Schmitz, A. Marchewka, D. N. Mueller, R. Valenta, J. Hackl, N. Raab, S. P. Rogers, M. I. Khan, S. Nemsak, M. Shim, S. Menzel, C. M. Schneider, R. Waser, R. Dittmann, Nat. Commun., 2016, 7, 12398

[4] C. Bäumer, C. Funck, A. Locatelli, T. O. Menteş, F. Genuzio, T. Heisig, F. Hensling, N. Raab, C. M. Schneider, S. Menzel, R. Waser, R. Dittmann, Nano Lett., 2019, 19, 54

[5] C. Baeumer, R. Valenta, C. Schmitz, A. Locatelli, T. O. Menteş, S. P. Rogers, A. Sala, N. Raab, S. Nemsak, M. Shim, C. M. Schneider, S. Menzel, R. Waser, R. Dittmann, ACS Nano, 2017, 11 (7), 6921

[6] T. Heisig, K. Lange, A. Gutsche, K. T. Goß, S.Hambsch, A. Locatelli, T. O. Menteş, F. Genuzio, St. Menzel, R. Dittmann, *Adv. Electron. Mater.* 2100936 (2022)

Circular Dichroism in Hard X-ray Photoelectron Diffraction Observed by Time-of-Flight Momentum Microscopy

O. Tkach[1*], T.-P. Vo[2], O. Fedchenko[1], K. Medjanik[1], Y. Lytvynenko[1], S. Babenkov[1], D. Vasilyev[1], Q. L. Nguyen[3], T. R. F. Peixoto[4], A. Gloskowskii[4], C. Schlueter[4], S. Chernov[4], M. Hoesch[4], D. Kutnyakhov[4], M. Scholz[4], L. Wenthaus[4], N. Wind[4,5], S. Marotzke[4,6], A. Winkelmann[7], K. Rossnagel[4,6], J. Minár[2], H.-J. Elmers[1] and G. Schönhense[1]

1 Inst. Phys., Johannes Gutenberg Univ. Mainz, Germany; 2 Univ. of West Bohemia, Pilsen, Czech Republic;
3 LCLS, SLAC Natl. Accel. Laboratory, Menlo Park, USA; 4 DESY Photon Sci., Hamburg, Germany;
5 Inst. für Exp.physik, Hamburg Univ., Germany; 6 Inst. für Exp. und Angewandte Physik, Kiel Univ., Germany
7 Academic Centre for Materials and Nanotechn., Univ. of Science and Technology, Kraków, Poland
**Contact: tkachole@uni-mainz.de*

Keywords: Photoelectron diffraction, circular dichroism, Kikuchi bands, momentum microscopy

X-ray photoelectron diffraction (XPD) is a powerful technique that provides detailed structural information of solids and thin films, complementing electronic structure measurements. Advances in data processing allow atomic-resolution holography; see a recent review [1]. High-resolution imaging of $k_{||}$-distributions (momentum microscopy) is a new approach to angleresolved photoemission. It provides full-field k_x-k_y XPD patterns with unprecedented acquisition speed and detail [2]. Here, we show that, beyond the pure diffraction information, XPD patterns exhibit a pronounced circular dichroism in angular distribution (CDAD) with asymmetries $A_{CDAD} = (I_{RCP}-I_{LCP}) / (I_{RCP}+I_{LCP})$ up to 80%, together with rapid variations on a small $k_{||}$-scale (0.1 Å^{-1}).

Measurements with circularly polarized X-rays (hν=6 keV and 1.4 keV) for a number of core levels, including Si, Ge, Mo and W, show that core-level CDAD is a general phenomenon, independent of the atomic number [3]. The fine structure in CDAD is more pronounced compared to the corresponding intensity patterns. In addition, they obey the same symmetry rules as found for atomic and molecular species, and valence bands. The CD is antisymmetric with respect to the mirror planes of the crystal, whose signatures are sharp zero lines. Calculations using both the Bloch-wave approach and one-step photoemission reveal the origin of the fine structure, which is the signature of Kikuchi diffraction. To disentangle the roles of photoexcitation and diffraction, XPD has been implemented into the Munich SPRKKR package to unify the one-step model of photoemission and multiple scattering theory. Experimental and theoretical results for several core levels are discussed and compared.

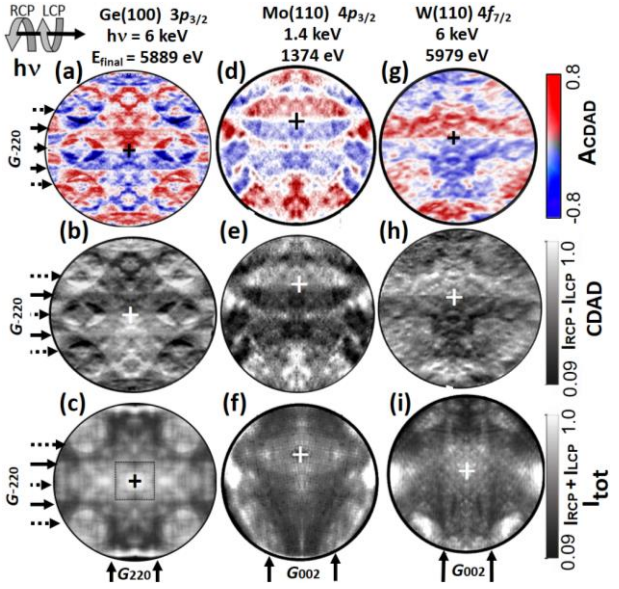

Figure 1: CDAD asymmetry (top row), difference I_{RCP} -I_{LCP} (center) and intensity $I_{RCP}+I_{LCP}$ (bottom) for Ge 3*p*, Mo 4*p* and W 4*f*. Left and right circularly polarized X-rays (RCP, LCP) arrive in from the left. (a-c, g-i) were recorded with hard X-rays of hν= 6 keV and (d-f) with soft X-rays at hν=1.4 keV. CDAD asymmetry and difference are strongly structured, with A_{CDAD} reaching up to +/-80% (see scale bar). Intensity patterns (bottom row) are dominated by Kikuchi bands and show weaker contrast. The main bands are marked by arrows on the left and at the bottom, indicating the corresponding reciprocal lattice vectors $\boldsymbol{G}_{hkl}$. Solid and dotted arrows for band edges and centers, respectively

1. T. Matsushita et al., Reconstruction Algorithm for Atomic-Resolution Holography, *J.Phys.Soc.Jpn*. **87**, 061002 (2018)
2. O. Fedchenko et al., Structure Analysis using Time-of-Flight Momentum Microscopy with Hard X-rays: Status and Prospects, *J. Phys. Soc. Jpn*. **91**, 091006 (2022)
3. O. Tkach et al., Circular Dichroism in Hard X-ray Photoelectron Diffraction, *Ultramicroscopy* (2023) in print.

Tuesday 22st of August, 2023

Fascinating electronic structures of exotic magnets revealed by ARPES

Takeshi Kondo

The Institute for Solid State Physics, The University of Tokyo, Japan

**Contact: kondo1215@issp.u-tokyo .ac.jp*

Keywords: ARPES, magnetism, high-T_c superconductivity, topological properties

The electronic states of magnetic materials are inextricably tied to electron correlations that manifest many-body problems and can exhibit properties that are theoretically unpredictable or even beyond. Antiferromagnetic high-temperature superconductivity, magnetic Weyl states, the devil's staircase, and magnetic skyrmion are good examples, being based on electronic states in which conduction electrons and magnetic moments are strongly coupled. These features of exotic magnetism have become central themes in condensed matter physics because of their high potential toward applications of quantum technology revolutionizing future societies.

As magnetism develops in solids, band folding and splitting occur in electronic structures. This is a naive and simple expectation, that also can be obtained by basic band calculations. In real materials, however, various anomalous features emerge in electronic structures associated with exotic properties, such as heavy quasiparticles emerging via the coupling of electrons with magnetic excitations, the energy gap due to superconductivity coexisting with magnetic orders, and the pseudogap states caused by magnetic and orbital frustrations. These seemingly complex properties can be sorted out through a detailed examination of single-particle spectra obtained by angle-resolved photoemission spectroscopy (ARPES). In this talk, I will introduce anomalous, fascinating electronic structures of several exotic magnets revealed by the state-of-art ARPES.

Firstly, I will introduce our recent ARPES results of multi-layered cuprates $Ba_2Ca_{n-1}CunO_{2n}(F,O)_2$ realizing antiferromagnetic high-T_c superconductivity. These compounds have clean thus ideal CuO_2 planes in their inner layers [3]; hence, they allow one to reveal the phase diagram intrinsic for cuprates without disorder which had not been unveiled. A particular focus is the formation of small Fermi pockets in the doped Mott-states, which had been theoretically predicted from the early age of cuprates research, yet have been experimentally recognized. By investigating the extremely clean CuO_2 planes, we found such small Fermi surface pockets to be indeed generated [1]. We also found that the *d*-wave superconducting gap opens along the pocket, thus the superconductivity and antiferromagnetic order coexist in the same CuO_2 sheet. Our data further indicate that the superconductivity can occur without contribution from the states near the antinodal region, which are shared by other competing excitations such as the charge density wave and pseudogap states. These findings will have significant implications for understanding the superconductivity and puzzling Fermi arc phenomena.

As the second topic, I will discuss the most complex magnetic phenomenon, the so-called “devil’s staircase”. For it, CeSb is the most famous material, where a number of the distinct phases with long-periodic magnet structures sequentially appear below the Néel temperature. An evolution of the low-energy electronic structure going through the devil’s staircase is of special interest, yet it has been elusive. Our bulk-sensitive ARPES measurements have successfully revealed the devil’s staircase transition of the electronic structures [2]. We further found a novel electron-boson coupling that renormalizes the Sb 5*p* band generating a pronounced kink structure at very low energy due to excitations of the 4*f* orbitals with a quadrupole crystal electric field [3]. It generates a novel sort of quasiparticle called "multipole polaron", consisting of a mobile electron dressed by a cloud of the quadrupole crys-tal-electric-field polarization. The electron-boson coupling is extremely strong and exhibits anomalous step-like enhancement during the devil's staircase transition with temperature.

Thirdly, I will present the bulk electrical structures of the Ce monopnictide series (CeP, CeAs, CeSb, and CeBi), and construct the topological phase diagram. In particular, we demonstrate the topological phase transition from a trivial to a nontrivial regime in moving from CeP to CeBi which occurs due to the band inversion with an increase in the spin-orbit coupling [4]. Our thorough observations uncover the detailed electronic properties of the fascinating series of materials.

1. S. Kunisada et al., *Science* **369**, 833 (2020).
2. K. Kuroda et al., *Nature Communications* **11**, (2020).
3. Y. Arai et al., *Nature Materials* **21**, 410 (2022).
4. K. Kuroda et al., *Physical Review Letters* **120**, 086402 (2018).

Elementary excitations of quantum materials probed with high-resolution RIXS

Di-Jing Huang*
National Synchrotron Radiation Research Center, Hsinchu, Taiwan
**Contact: djhuang@nsrrc.org.tw*

Keywords: quantum materials, superconducting cuprate, RIXS, elementary excitation

Recent advancements in synchrotron radiation instrumentation have enabled high-resolution resonant inelastic X-ray scattering (RIXS) to become a powerful technique for probing elementary excitations with momentum resolution and providing direct information about the dynamics arising from fluctuations of spin, charge, and orbital degrees of freedom. This talk will begin with a review of the davances in high-resolution RIXS instrumnetation [1], followed by discussions of recent examples of RIXS studies on quantum materials such as cuprate superconductors [2, 3], spin-orbit materials [4], and Hund's metals.

The superconductivity of cuprates has remained a mystery since its discovery decades ago. Above the superconducting transition temperature (T_c) in cuprate superconductors, various physical quantities show an enigmatic electronic excitation gap called a pseudogap. The mechanisms of the pseudogap formation and the superconductivity itself are core issues of high-T_c superconductivity. The pseudogap and strange-metal phases observed in cuprates above T_c are puzzling. One approach to resolving this puzzle is based on the scenario of quantum phase transition, which is driven by non-thermal fluctuations at absolute zero temperature, playing a crucial role in shaping the phase diagram of high-temperature cuprate superconductors. Understanding the pseudogap and the strange-metal phases might hinge on the influence of quantum criticality at finite temperatures. Recently, charge-density waves (CDW) have garnered renewed interest as an important order parameter in these materials. We investigated the doping-dependent high-resolution RIXS of $La_{2-x}Sr_xCuO_4$ to unravel the quantum fluctuations of CDW. Our findings provide the spectroscopic signature of quantum critical scaling in cuprates, in which the pseudogap and strange-metal phases correspond to the renormalized classical and the quantum critical scaling regimes, respectively.

In addition, electron quasiparticles play a crucial role in simplifying the description of many-body physics in solids with surprising success. However, conventional Landau's Fermi-liquid and quasiparticle theories for high-temperature superconducting cuprates have received skepticism from various angles. Whether the framework of electron fractionalization captures the essential physics of the pseudogap and superconducting phases of cuprates is still an open issue. In this talk, we will show that excitonic excitation of optimally doped $Bi_2Sr_2CaCu_2O_{8+\delta}$ with energy far above the superconducting-gap energy scale, about 1 eV or higher, is unusually enhanced by the onset of superconductivity. Our findings prove the involvement of such high-energy excitons in superconductivity. Therefore, the observed enhancement in the spectral weight of excitons imposes a crucial constraint on theories for the pseudogap and superconducting mechanisms.

If time permits, this talk will also include recent RIXS studies on spin-orbit materials and Hund's metals.

[1] A. Singh et al., J. Synchrotron Radiat. **28**, 977 (2021).
[2] H. Y. Huang et al., Phys. Rev. **X** 11, 04138 (2021).
[3] A. Singh, Nat. Commun. **13**, 7906 (2022).
[4] H. Y. Huang et al., npj Quantum Materials **7**, 33 (2022).

Kinetic *In-situ* Synthesis (KISS) technique of large-area 2D materials exfoliation

Antonija Grubišić-Čabo[1,*], Matteo Michiardi[2,3], Charlotte E. Sanders[4], Marco Bianichi[5], Davide Curcio[5], Dibya Phuyal[6], Magnus H. Berntsen[6], Qinda Guo[6], Maciej Dendzik[6]

1 Zernike Institute for Advanced Materials, University of Groningen, Groningen, The Netherlands
2 Quantum Matter Institute, University of British Columbia, Vancouver, Canada
3 Department of Physics and Astronomy, University of British Columbia, Vancouver, Canada
4 Central Laser Facility, STFC Rutherford Appleton Laboratory, Harwell, United Kingdom
5 School of Physics and Astronomy, Aarhus University, Aarhus, Denmark
6 Department of Applied Physics, KTH Royal Institute of Technology, Stockholm, Sweden *Contact: *a.grubisic-cabo@rug.nl*

Keywords: 2D materials, UHV exfoliation, band structure, ARPES

Two-dimensional (2D) materials provide an extremely rich platform to investigate novel quantum phenomena and to design nanostructures with desired functionalities [1]. Some of the key techniques employed in studies of 2D materials, such as photoemission spectroscopy, have stringent requirements for the quality, sample size and cleanliness of the surface. Fulfilling these conditions using a standard mechanical exfoliation in a glove box is often problematic.

Here, we present a novel method for in situ exfoliation of 2D materials performed directly in ultra-high vacuum, which yields large flakes of excellent crystallinity and purity [2]. In our experiments, multiple semiconducting and metallic transition metal dichalcogenides were exfoliated onto Au, Ag and Ge substrates, showing the versatility of the technique, and characterised by angle resolved photoemission spectroscopy.

Importantly, the proposed method is straightforward, simple, and does not require any specialised equipment. This technique is ideally suited for the electronic structure research of air-sensitive 2D materials since the sample preparation process happens entirely in ultra-high vacuum.

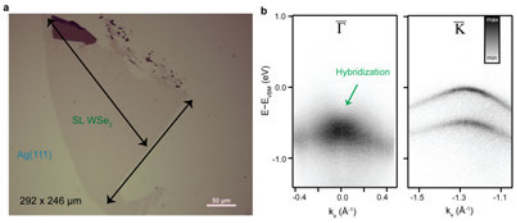

Figure 1: An example of KISS exfoliated flake of WS_2 on Ag(111). a) Optical microscopy image and b) bandstructure around $\bar{\Gamma}$ (left) and $\bar{K}$ point (right).

[1] M. Zheng, Y. Xiao, J. Liu, K. Yang and L. Fu, Exploring Two-Dimensional Materials toward the Next-Generation Circuits: From Monomer Design to Assembly Control *Chemical Reviews* 118, **13**, 6236–6296 (2018).

[2] A. Grubišić-Čabo, M. Michiardi, C.E. Sanders, M. Bianchi, D. Curcio, D. Phuyal, M.H. Berntsen, Q.Guo and M. Dendzik, *In-situ* exfoliation method of large-area 2D materials, *Advanced Science* **In press**, doi: 10.1002/advs.202301243 (2023), arXiv: 2209.15030.

Application of In-situ High Temperature Environmental Scanning Electron Microscopy for Characterising Non-metallic Inclusions within Steel

Tuomas Alatarvas[1], Renaud Podor[2], Eetu-Pekka Heikkinen[1], Qifeng Shu[1] and Harishchandra Singh[3,*]

1 Process Metallurgy Research Unit, Centre for Advanced Steels Research, University of Oulu, Finland
2 ICSM, Univ Montpellier, CEA, CNRS, ENSCM, Marcoule, France
3 Nano and Molecular Systems Research Unit, Centre for Advanced Steels Research, University of Oulu, Finland
**Contact: harishchandra.singh@oulu.fi*

Keywords: in-situ high temperature scanning electron microscopy, non-metallic inclusions, steel

Non-metallic inclusions (NMIs) are inevitably present in all steel products. Typically NMIs comprise of oxide, sulphide and nitride phases. The composition, size, and shape of NMIs affect various properties of the produced steel, such as ductility, fatigue and corrosion resistance. Primary NMIs form during the molten steel processing stages as a result of deoxidation reactions, such as Al_2O_3 in Al-deoxidised steels. Modification of NMIs in molten steel may take place for instance with calcium treatment, transforming Al_2O_3 into calcium aluminates. Further NMI reactions occur during solidification of steel, driven by decreasing temperature and elemental enrichment in the molten steel. Therefore, most of the reactions involving NMIs take place during molten steel processing or during solidification. However, the solid-state reactions, occurring during heat treatments or hot rolling of steel, have gained increasing attention for controlling the NMI size and composition in the final product.

In this study, High Temperature Environmental Scanning Electron Microscope (HT-ESEM) [1] is used for an in-situ observation of calcium aluminate complex, CaS, $MgAl_2O_4$–CaS, MnS and TiN type NMIs in steels at 800°C and 900°C for varying holding times. Backscattered electron imaging was used for observing visual morphological variations in NMIs, accompanied with elemental mapping with Energy Dispersive X-Ray Spectrometry (EDS), where interaction between the primary electron beam and the sample remains was limited to a low volume (approx. $0.05\mu m^3$).

Figure 1 presents backscattered electron images of a CaS–$MgAl_2O_4$ with minor TiN contents before and after 30-minute high-vacuum experiment at 800°C, demonstrating the potential of HT-ESEM for high-temperature NMI imaging and analyses. Chemical reactions, void formation and steel flowing on the NMI surface was observed. HT-ESEM driven thermodynamic calculations were carried out with FactSage 8.2 software to estimate the NMI reactions with the residual atmosphere in the sample chamber during experiments. The modelled data provide insights into the interpretation of the experimental data.

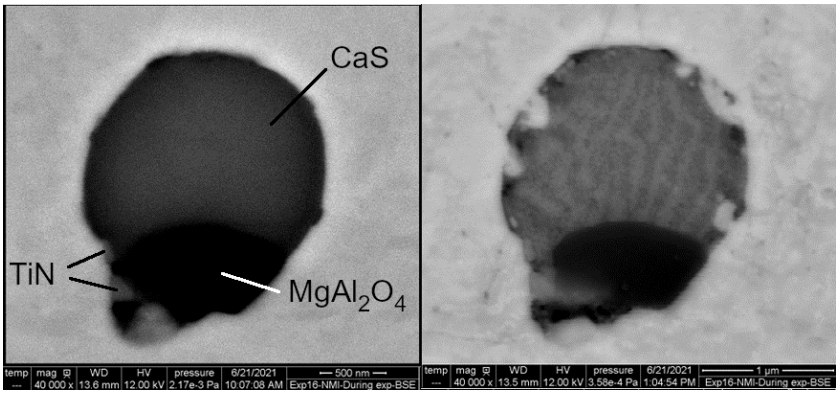

Figure 1: Backscattered electron images of a CaS–$MgAl_2O_4$ NMI before and after experiment at 800°C.

1. R. Podor, G. I. Nkou Bouala, J. Ravaux, J. Lautru, N. Clavier, Working with the ESEM at high temperature, Materials Characterization **151**, 15-26 (2019).

Are calculated partial photoionization cross sections good enough for (HAX)PES applications?

Constantin Wansorra[1,*], Dirk Hauschild[1,2,3], Ralph Steininger[1], Clemens Heske[1,2,3] and Lothar Weinhardt[1,2,3]

1 Institute for Photon Science and Synchrotron Radiation (IPS), Karlsruhe Institute of Technology (KIT), Eggenstein-Leopoldshafen, Germany

2 Institute for Chemical Technology and Polymer Chemistry (ITCP), Karlsruhe Institute of Technology (KIT), Karlsruhe, Germany

3 Department of Chemistry and Biochemistry, University of Nevada, Las Vegas (UNLV), Las Vegas, NV, USA

**Contact: constantin.wansorra@kit.edu*

Keywords: photoionization cross section, HAXPES, depth distribution

Photoelectron spectroscopy (PES) is a powerful technique to analyze the chemical environment and atomic composition of the topmost atomic layers of a material. The depth at which information can be gained in this process is governed by the exponential decay of the signal intensity of the emitted photoelectrons. The characteristic 1/e attenuation length, i.e., the inelastic mean free path (IMFP) of the photoelectrons, is in the region of a few nanometers for laboratory-based excitations. However, by varying the photon energy (e.g., at a synchrotron light source), the IMFP of the photoelectrons can be tuned, for example up to ~16 nm for excitation energies up to 15 keV. This is sometimes exploited to measure the depth distributions of thin-film materials, like thin-film solar cells. If the ratio between different elements is investigated, this approach relies on the accuracy of calculated partial photoionization cross sections (PICs) [e.g., 1-3], which describe the probability that an electron in a certain orbital of an atom is excited by a specific photon energy. The PIC strongly depends on the excitation energy and varies several orders of magnitude in the commonly used excitation energy range (see Figure 1). This raises the question: to what extent can the calculated values be trusted and what deviations can be expected at different energies?

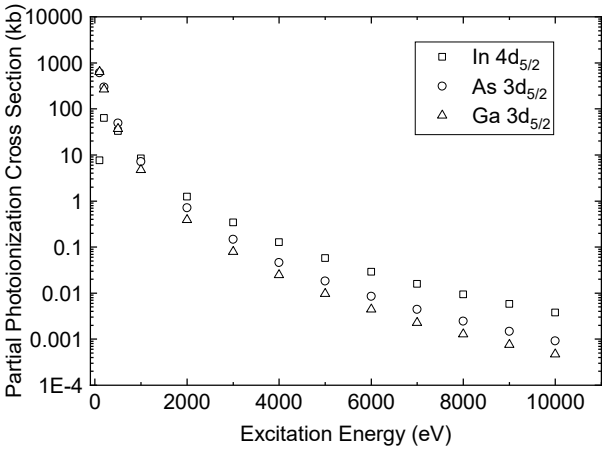

Figure 1: Calculated partial photoionization cross sections of As $3d_{5/2}$, Ga $3d_{5/2}$, and In $4d_{5/2}$ orbitals, derived for the measurement geometry at the X-SPEC beamline, KIT Light Source. (based on [2,3])

In this contribution, we compare calculated values of As 3d, Ga 3d, and In 4d PICs (based on [2,3]) with carefully measured data and discuss the accuracy of the theoretical values for a broad energy range. For this purpose, GaAs and InAs wafers were cleaved in an ultra-high vacuum chamber and subsequently measured at the X-SPEC beamline [4] at the KIT Light Source, using excitation energies from 70 to 10,000 eV. Potential systematic errors and measurement uncertainties are discussed.

1. J. J. Yeh, I. Lindau, *Atomic Data and Nuclear Data Tables* **32**, 1–155 (1985).
2. M. B. Trzhaskovskaya, I. V. Nefedov, V. G. Yarzhemsky, *Atomic Data and Nuclear Data Tables* **77**, 97–159 (2001).
3. M. B. Trzhaskovskaya, V. G. Yarzhemsky, *Atomic Data and Nuclear Data Tables* **119**, 99–175 (2018).
4. L. Weinhardt et al., *Journal of Synchrotron Radiation* **28**, 609–617 (2021).

Transmission through Graphene of Electrons in the 30 - 900 eV Range

Alice Apponi[1], Domenica Convertino[2], Neeraj Mishra[2,3], Camilla Coletti[2,3], Mauro Iodice[4], Franco Frasconi[5], Federico Pilo[5], Gianluca Cavoto[6], Alessandro Ruocco[1,*]

1 Università degli Studi Roma Tre and INFN Sezione di Roma Tre, Via della Vasca Navale 84, 00146 Rome, Italy

2 Center for Nanotechnology Innovation @NEST, Istituto Italiano di Tecnologia, Pisa, Italy

3 Graphene Labs, Istituto italiano di tecnologia, Via Morego 30, I-16163 Genova, Italy

4 INFN Sezione di Roma Tre, Via della Vasca Navale 84, 00146 Rome, Italy

5 INFN Sezione di Pisa, Edificio C, Largo B. Pontecorvo, 3 - 56127 Pisa, Italy

6 Sapienza Università di Roma e INFN Sezione di Roma, Piazzale Aldo Moro 2, 00185 Rome, Italy

**Contact: alessandro.ruocco@uniroma3.it*

Keywords: suspended graphene, electron transmission, electron spectroscopy, π-plasmon excitation.

The transparency, and the attenuation length [1], of graphene and multilayer graphene for low-energy electrons (below 1 keV) is a topic of great interest also for their possible application to the development of electronic devices and novel detectors for particle physics. The investigation of such materials requires a specific approach different from those developed for 3D materials [2]. As a matter of fact, below 25 eV the graphene mean free path does not follow the so-called universal curve [3].

In this presentation we report on the transmission of low-energy electrons (in the 30 to 900 eV energy range) through mono-layer graphene suspended on transmission electron microscopy (TEM) grid. Polycrystalline graphene was grown on copper via chemical vapor deposition (CVD) and transferred onto the TEM grid by a PMMA-assisted wet transfer at the CNI@NEST of Pisa. The sample has been then mapped by using micro-Raman spectroscopy in order to check the quality of graphene. A high-temperature annealing in vacuum have been performed in order to remove PMMA residues from the graphene. Scanning electron microscopy (SEM) allowed to estimate the graphene coverage and the TEM grid geometrical transmission.

The custom-made monochromatic electron gun of the LASEC laboratory at Università Roma Tre has been employed to perform the transmission measurements. The electron beam has tuneable energy in the 30 -900 eV range with a resolution of 45 meV and a very good current stability. We measured the transmission of graphene suspended on the grid as a function of the electron energy with currents in the 200 pA range. The experimental apparatus allows to measure with a Faraday cup either the electron gun emitted current or the current transmitted through the graphene, as shown in figure 1. Thus, the transmission is obtained as the ratio of these two measured values.

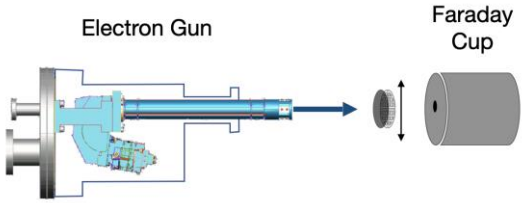

Figure 1: Scheme of the current measurement through the graphene on TEM grid.

Furthermore, we performed spectroscopy with both X-ray photoemission (XPS) and electron energy loss (EELS) on the single-layer graphene and a tri-layer graphene for comparison. Through the first technique we measured the C1s signal to evaluate the graphene quality and, it has been found, that the main contribution to the line shape is sp^2 signal. The plasmon excitation has been measured through EELS. For the tri-layer graphene we observed the π-plasmon at 6.5 eV, while a second excitation appears at lower energy losses in the case of the monolayer. All these spectroscopic results are the footprint of a good-quality suspended graphene.

1. A. Jablonski and C. J. Powell, Surface Science Reports 47, 33 (2002).
2. M. Xu, D. Fujita, J. Gao, and N. Hanagata, ACS Nano 4, 2937 (2010).
3. D. Geelen, J. Jobst, E.E. Krasovskii, S.J. van der Molen, R.M. Tromp, Phys. Rev. Lett. **123** 86802 (2019).

Soft X-ray Emission Spectroscopy of Water at Interfaces

Yoshihisa Harada[1,*]

1 Institute for Solid State Physics, The University of Tokyo, Chiba, Japan

**Contact: harada@issp.u-tokyo.ac.jp*

Keywords: interfacial water, hydrogen bonding, X-ray emission spectroscopy

X-ray emission spectroscopy (XES) of water has attracted attention for more than two decades since it is extremely sensitive to the hydrogen-bonded structure of liquid water and the hydration structure of solutes [1-3]. XES can selectively observe the chemical states of certain specific element by tuning the excitation energy to the absorption peak of a particular functional group. The first report of synchrotron XES experiments on bulk liquid water was made at the beginning of this century [1]. Our understanding of how the XES spectral profile reflects the hydrogen bonding of water has greatly improved after more than two decades of debate.

In this paper, Three XES studies on "unique" water molecules at various materials interfaces are presented, which have not yet been theoretically interpreted, but have provided interesting insights into the function of materials. **Figure 1a** shows the structure of water confined in an electrolyte polymer [4]. A poly(2-(methacryloyloxy)ethyl trimethylammonium chloride) (PMTAC) brush, which represents high-density polymer chains, is well suited to study the interaction between water and polymers as well as confinement of water by the polymer brush. The results indicate the confined water has tetrahedrally coordinated hydrogen bonds with a uniform distortion like high pressure ice. This should be linked to control the antifouling and lubricating functions of polyelectrolyte brushes. The second case shows a link between the function of water treatment membranes and the hydrogen bond of water (**Figure 1b**) [5]. The self-assembled liquid crystalline membrane with uniformly sized pores of 0.6 nm has outstanding selectivity for ion permeation. However, ions with larger effective size and charge are more permeable, which cannot be explained by simple molecular sieving effect or charge interactions. XES of liquid water confined in the pores demonstrated that hydrogen-bonded structure of the confined water is very similar to that of the hydration water of the ion with high permeability, indicating that the high permeability is realized when the hydration water surrounding the ion is stable in the pore. The last example is nano-meter sized ultrafine water droplet deposited on hydrophilic/hydrophobic surfaces (**Figure 1c**). The obtained time evolution of the accumulated XES signal implied the presence of OH^- species which were not observed in deposited water by humidification with a regular humidifier. We will discuss a possible mechanism of the generation of ionic species by deposition of ultrafine water clusters and its role on the moisturizing effect.

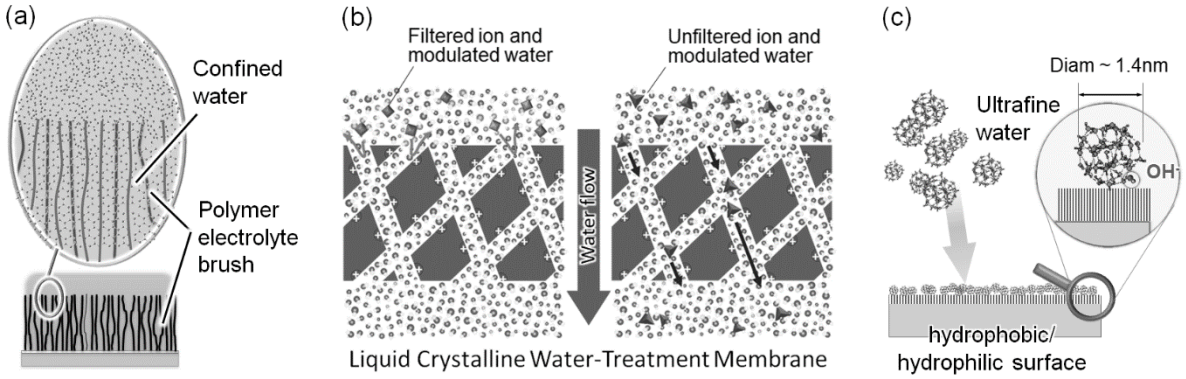

Figure 1: Interfacial water for XES studies (a) Water encapsulated in a polymer electrolyte brush, (b) Water in the nanopore of a self-assembled liquid crystalline membrane, (c) Nanometer sized ultrafine water deposited on a surface.

1. J.-H. Guo *et al.*, X-Ray Emission Spectroscopy of Hydrogen Bonding and Electronic Structure of Liquid Water, *Phys. Rev.Lett.* **89**, 137402 (2002).
2. T. Fransson *et al.*, X-ray and Electron Spectroscopy of Water, *Chem. Rev.* **116**, 7551 (2016).
3. Z. Yin *et al.*, Cationic and Anionic Impact on the Electronic Structure of Liquid Water. *J. Phys. Chem. Lett.* **8**, 3759 (2017).
4. K. Yamazoe *et al.*, Enhancement of the Hydrogen-Bonding Network of Water Confined in a Polyelectrolyte Brush, *Langmuir* **33**, 3954 (2017).
5. R. Watanabe *et al.*, Ion Selectivity of Water Molecules in Subnanoporous Liquid-Crystalline Water-Treatment Membranes: A Structural Study of Hydrogen Bonding, *Angew. Chem. Int. Ed.* **59**, 23461 (2020).

RIXS of high-energy battery electrodes: novel states in highly oxidized transition metal oxides

Wanli Yang[1]

1 Advanced Light Source, Lawrence Berkeley National Laboratory, Berkeley, California, 94720 USA

**Contact: wlyang@lbl.gov*

Keywords: high-energy batteries, oxygen redox reaction, Resonant X-ray Inelastic Scattering.

Modern energy applications, especially electric vehicles, rely on battery systems that are yet to achieve the desired energy density. A major issue for improving battery energy density is the emergence of various detrimental effects when a battery operates at high-energy, i.e., high-voltage, conditions. This provides the opportunities for soft X-ray RIXS as a powerful characterization technique to reveal the relevant fundamental physics and functional chemistry in battery materials.

This presentation first demonstrates RIXS capabilities in clarifying the confusions in conventional wisdom on transition metal-based battery electrodes the high-voltage range [1]. We argue that, regardless of the chemical composition, the high-energy operation spontaneously triggers a highly oxidized oxide state in the battery cathode [2-3]. Such a highly oxidized transition-metal oxide is a complex system, in which conventional ionic crystal models fail and a significant amount of oxygen activities are involved in the electrochemical operations, the so-called oxygen redox reaction. However, the behavior of the oxygen redox reaction strongly depends on the transition metal configurations [4], indicating a highly correlated metal-oxygen system that requires advanced characterizations like RIXS and theory to uncover its intrinsic nature.

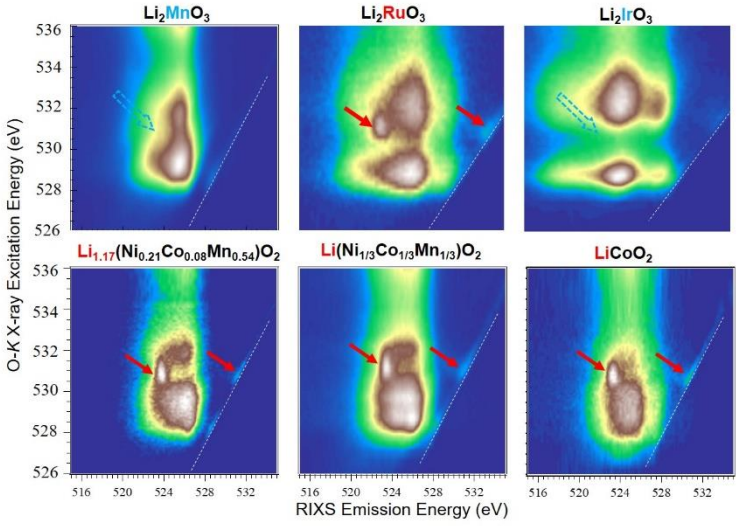

Figure 1: Oxygen K-edge RIXS maps of a series of comparative oxide-based battery cathodes. All the electrodes have been charged to high voltage, i.e., fully oxidized. The appearance of oxidized oxygen feature in the RIXS maps, as indicated by the red arrows, do not rely on the structure or Li contents; however, is strongly affected by transition metal configurations [3-4].

1. J. Wu et al., Science Advances 6, eaaw3871 (2020)
2. G.-H, Lee et al., Angew Chem Int Ed 59, 8681 (2021)
3. Z. Zhuo et al., Joule 5, 975 (2021)
4. Z. Zhuo et al., ACS Energy Letters 6, 3417 (2021)

Using X-ray emission spectroscopy to measure the electron-phonon scattering rates in the demagnetization transient state of ferromagnets

Régis Decker[1,*], Artur Born[1,2], Kari Ruotsalainen[1], Karl Bauer[1], Robby Büchner[1,2], Robert Haverkamp[1,2], Stefan Neppl[1], Christian Stråhlman[1], Annette Pietzsch[1], Alexander Föhlisch[1,2]

[1] *Institute Methods and Instrumentation for Synchrotron Radiation Research PS-ISRR, Helmholtz-Zentrum Berlin, Germany*

[2] *Institute of Physics and Astronomy, Potsdam University, Germany*

**Contact: regis.decker@helmholtz-berlin.de*

Keywords: X-ray emission spectroscopy, ultrafast demagnetization, electron-phonon scattering

The experimental determination of microscopic processes in magnetic systems is important to better understand their macroscopic properties like the ultrafast demagnetization [1]. In crystalline ferromagnets, one of the main microscopic mechanisms of spin relaxation is the electron-phonon driven spin-flip, or Elliott-Yafet, scattering [2-4]. Therefore, the experimental determination of the electron-phonon scattering rate in solids is of first importance in order to better understand the demagnetization mechanisms. However, while most effort has been dedicated to the measurement of the demagnetization time using pump-probe experiments, experimental studies of the underlying microscopic mechanisms are still scarce.

To measure the spin-flip scattering rate, we exploit the stringent atomic symmetry selection rules of X-ray Emission Spectroscopy (XES) and observe the quantifiable change in the decay peak intensities in spectra when changing the temperature, *i.e.* when changing the phonon population. We show a reduction of the decay peak intensity for the Ni model system and its absence in the diamagnetic Cu case [5]. In FeNi alloys, this approach evidences a thresholding of the Elliott-Yafet mechanism by the intra- and intersublattice exchange energies [6]. In Gd, where the magnetic moment is held by the *5d* and the *4f* electrons, we evidence an Elliott-Yafet mechanism for the itinerant *5d* electrons and its absence for the localized *4f* electrons [7].

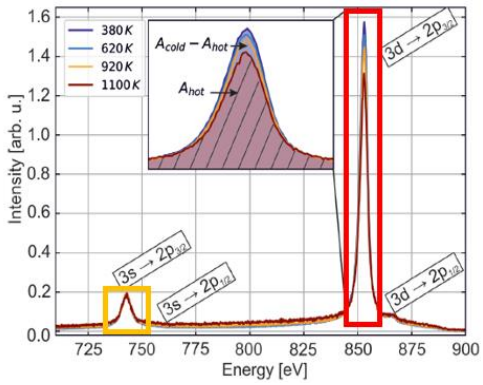

Figure 1: Temperature-dependent L-edge X-ray emission spectra of nickel [5].

1. E. Beaurepaire *et al.*, Ultrafast spin dynamics in ferromagnetic nickel, *Phys. Rev. Lett.* **76**, 4250 (1996).
2. B. Koopmans *et al.*, Explaining the paradoxical diversity of ultrafast laser-induced demagnetization, *Nat. Mater.* **9**, 259 (2009).
3. R.J. Elliott, Theory of the effect of spin-orbit coupling on magnetic resonance in some semiconductors, *Phys. Rev.* **96**, 266 (1954).
4. Y. Yafet in Solid State Physics. Vol 14 (Eds Seitz, F. Turnbull, D.) (1963)
5. R. Decker *et al.*, Measuring the atomic spin-flip scattering rate by x-ray emission spectroscopy, *Sci. Rep.* **9**, 8977 (2019).
6. A. Born *et al.*, Thresholding of the Elliott-Yafet spin-flip scattering in multi-sublattice magnets by the respective exchange energies, *Sci. Rep.* **11**, 1883 (2021).
7. R. Decker *et al*., Spin-lattice angular momentum transfer of localized and valence electrons in the demagnetization transient state of gadolinium, *Appl. Phys. Lett.* **119**, 152403 (2021).

Young's double slit interference in resonant Auger/X-ray scattering and the Bohr's complementary: new results

Johan Chau Söderström (johan.soderstrom@physics.uu.se), Anirudha Ghosh (anirudha.ghosh@maxiv.lu.se), Ludvig Kjellsson (ludvig.kjellsson@maxiv.lu.se), Victor Ekholm (victor.ekholm@maxiv.lu.se), Takashi Tokushima (takashi.tokushima@maxiv.lu.se), Conny Såthe (conny.sathe@maxiv.lu.se), Nicholas Velasquez (nicolas.velasquez@sorbonne-universite.fr), Marc Simon (marc.simon@sorbonne-universite.fr), Olle Björneholm (olle.bjorneholm@physics.uu.se), Arnaldo Naves de Brito (arnaldo.naves@gmail.com), Michael Odelius (odelius@fysik.su.se), Jicai Liu (50901891@ncepu.edu.cn), Victor Kimberg (kimberg@kth.se), Marcus Agåker (marcus.agaker@physics.uu.se), Jan-Erik Rubensson (jan-erik.rubensson@physics.uu.se), and Faris Gel'mukhanov[1*],

1 Royal Institute of Technology, Theoretical Chemistry and Biology, Roslagstullsbacken 15, S-10691 Stockholm, Sweden

**Contact: faris@kth.se*

Keywords: YDSE, resonant Auger scattering (RAS), RIXS, which path information

The key feature of quantum mechanics is the interference which nicely demonstrated by seminal optical Young's double slit experiment (YDSE) with macroscopic slits. Two factors, small size of core-orbitals and rather large bond length comparable with the wave length of Auger electron or X-ray photon, makes the resonant Auger scattering (RAS) and RIXS nice tools to study the YDSE interference with microscopic molecular slits. Contrary to RAS, RIXS allows to observe the YDSE pattern studying the symmetry forbidden scattering channels. The YDSE interference opens the symmetry forbidden gerade→ ungerade RIXS channel [1]. It has often been assumed that the observed parity selectivity constitutes a general rule in the sub-keV region [2, 3]. In contrast, we observe violation of the parity selection rules in the RIXS spectra of the oxygen molecule excited on the $1\pi_g$ resonance. We exploit the capabilities of the new Veritas beamline at MAX IV to measure high-quality RIXS spectra of O_2 and observe the characteristic YDSE pattern, while simultaneously varying the scattering angle. The intensity ratio between parity forbidden $1\pi_u^{-1}1\pi_g^1$ and allowed $3\sigma_g^{-1}1\pi_g^1$ final states is measured accurately as a function of scattering angle, and the results are well described with a theory, where the crucial parameter is the phase difference in the scattering at the two atomic centers of the molecule. The earlier RAS [4] and current RIXS experiments with O_2 allow us to analyse and quantify the Bohr's complementarity principle for such a pair of complementary properties which cannot be observed simultaneously, namely, maximum visibility of the YDSE pattern and which path information.

[1] F. Gel'mukhanov, M. Odelius, S. P. Polyutov, A. Föhlisch, and V. Kimberg, *Rev. Mod. Phys.* **93**, 035001 (2021).

[2] P. Glans, K. Gunnelin, P. Skytt, J.-H. Guo, N. Wassdahl, J. Nordgren, H. Ågren, F. Kh. Gel'mukhanov, T. Warwick, and E. Rotenberg *Phys. Rev. Lett.* **76**, 2448 (1996).

[3] F. Hennies, A. Pietzsch, M. Berglund, A. Föhlisch, T. Schmitt, V. Strocov, H. O. Karlsson, J. Andersson, and J.-E. Rubensson, *Phys. Rev. Lett.* **104**, 193002 (2010).

[4] X.J. Liu, Q. Miao, F. Gel'mukhanov, M. Patanen, O. Travnikova, C. Nicolas, H. Ågren, K. Ueda, and C. Miron, *Nature Photonics* **9**, 4120 (2015).

Wednesday 22st of August, 2023

Spectroscopy and control of electronic structure in atoms and molecules with intense laser fields from atto-to-femtoseconds, and beyond

Thomas Pfeifer

Max-Planck-Institut für Kernphysik, Heidelberg

Electrons are not only the lightest (known) fundamental particles, they are also responsible for virtually anything visible to us from tiny objects under the microscope to the screen or paper we just look at, all the way and far out into the universe. Interactions with electrons also hold atoms together in molecules and electron motion is at the heart of any chemical reaction on earth, our bodies and in outer space. Observing, understanding, and directing electron motion on a fundamental level is thus a core topic in physics and chemistry alike, with substantial impact and relevance to other fields of science and technology.

An ongoing world-wide revolution of high-frequency (XUV and x-ray) light-source development keeps unlocking our access to such electron motion, down to their natural time scale of attoseconds by using intense-laser-driven high-order harmonic generation (HHG). Moreover, the extreme intensity available at free-electron lasers (FELs) allows not only the observation of fundamental quantum dynamics in atoms and molecules, but to actively steer their motion on the fundamental electronic level.

Here in this talk, I will highlight a few examples of our continuing science mission towards building a bottom-up understanding of electron dynamics, starting at the level of isolated atoms featuring only a nucleus and two (correlated) electrons (e.g. in Helium), and working our way up into multi-electron atoms (e.g. neon) and polyatomic molecules (e.g. CH_2I_2 and SF_6).

Our experimental aim is to obtain the most complete picture of such fundamental light-matter interaction processes from low to high intensity by extracting multidimensional observables. These include the spectroscopic detection of photons, ions and electrons in coincidence.

The results from these experiments not only shed new light on fundamental (intense-)light-matter interaction processes, which are generally at work also in large-scale systems, but also provide new technological tools for pulse characterization, to further optimize the light sources themselves. One exemplary long-term dream of this development is the 3D-printer on the atomic level: The writing of custom molecular structures and supramolecular assemblies by the full spatio-temporal control over the electromagnetic spectrum, coherently provided at high intensity from the infrared into the x-ray domain. Another vision is atomic-scale quantum computing programmed by intense femto-to-attosecond-shaped light fields.

Water-Splitting Catalysts in Real Time and During Operation

Simone Techert[1*]

1 Deutsches Elektronen-Synchrotron DESY, Hamburg Germany
2 Institute for X-ray Physics, Goettingen University,Goettingen, Germany
**Contact: simone.techert@desy.de*

Keywords: ultrafast, time-resolved X-ray science, Free-electron lasers, synchrotrons, catalysis

Water splitting is intensively studied for sustainable and effective energy storage in green / alternative energy harvesting-storage-release cycles. In this talk I will present our recent developments for combining liquid jet microtechnology with different types of soft X-ray spectroscopy at high-flux X-ray sources (linear collider or storage ring based), developed for studying the oxygen evolution reaction (OER). We are particularly interested in *in-situ, operando* and ultrafast time-resolved multidimensional photon-in / photon-out techniques, such as resonant inelastic X-ray scattering (RIXS) at high-repetition-frequency X-ray sources - synchrotrons and Free-electron lasers.

The pilot catalytic systems we use are perovskites having the general structure ABO_3 with lanthanides or group II elements at the A sites and transition metals at the B sites. Depending on the chemical substitutions of ABO_3, their catalytic activity for OER can be tuned by varying the composition – even overcoming the scaling law which normally describes the (thermodynamic) limits of OER catalytic activity. I will present our different *in-situ* and time-resolved (optical and) RIXS studies of the manganese L-edge and oxygen K-edge of perovskites during OER of these catalysts.

We have developed various X-ray spectroscopy approaches like transmission-, reflection- zone plate-, and grating-based emission spectroscopy techniques. Combined with tunable incident X-ray energies, we yield complementary information about changing (inverse) X-ray absorption features of the perovskites, allowing us to deduce element- and oxidation-state-specific chemical monitoring of the catalyst.

Adding liquid jet technology, we monitor element- and oxidation-state-specific interactions of the catalyst with water adsorbate during OER. By comparing the different technical spectroscopy approaches combined with high-repetition-frequency experiments at synchrotrons and Free-electron lasers, we conclude that the combination of liquid jet with low-resolution zone-plate-based X-ray spectroscopy is sufficient for element- and oxidation-state-specific chemical monitoring during OER and easy to handle.

For an in-depth study of OER mechanisms, however, including the characterization of catalyst-water adsorbate in terms of their charge transfer properties and especially valence intermediates formed during OER, high-resolution (grating) spectroscopy tools resolving even vibronic couplings, combined with liquid jets bear bigger potential since they allow resolution of otherwise-overlapping X-ray spectroscopy transitions.

Common for all of these experimental approaches is the conclusion that without the versatile developments of liquid jets and liquid beam technologies, elaborate experiments such as high-repetition experiments at high-flux X-ray sources (like synchrotrons or free-electron lasers) would hardly be possible. Such experiments allow sample refreshment for every single X-ray shot for repetition frequencies of up to 5 MHz, so that it is possible (a) to study X-ray-radiation-sensitive samples and also (b) to utilize novel types of flux-hungry X-ray spectroscopy tools like photon-in / photon-out X-ray spectroscopy to study the OER.

1. T. Reuss, S. Sreekantan Nair Lalithambika, C. David, F. Doring, C. Jooss, M. Risch, S. Techert, Advancements in Liquid Jet Technology and X-ray Spectroscopy for Understanding Energy Conversion Materials during Operation, *Acc. Chem. Res.* **56**, 203-214 (2023).
2. J. Schlappa et al., The Heisenberg RIXS Instrument at SCS, European XFEL - Ultrafast Spectroscopy at the Limit of Energy and Time Resolution, EuropeanXFEL User Meeting (2023).
3. L. Le Guyader et al., Beam-splitting Off-axis Zone Plate for Photon Shot-noise Limited MHz Transient Absorption Spectroscopy with the DSSC Detector at the Spectroscopy and Coherent Scattering Instrument at the European XFEL, *J. Synchr.Rad.* **30***,* 284-300 (2023).
4. P. Busse, et al., Probing the surface of La0.6Sr0.4MnO3 in water vapor by in-situ RIXS: Interpretation of the fluorescence yields*, J. Phys. Chem. C* **124** 7893 (2020).
5. Z. Yin, et al., A Highly Efficient Soft X-ray Spectrometer Based on Reflection Zone Plate for Resonant Inelastic X-ray Scattering Measurements, *Opt. Expr.* 25 (10), 10984 (2017).
6. F. Marschall et al., Transmission Zone Plates as Analyzers for Efficient Parallel 2D RIXS-mapping, *Nat. Sci. Rep.* 7(1)*,* 8849-8857 (2017).
7. Z. Yin et al., Cationic and Anionic Impact on the Electronic Structure of Liquid Water, *J. Phys. Chem. Lett.* **8**, 3759-3764 (2017).

Strong electron-boson interactions in oxide superconductors and magnetic materials

Donglai Feng

1 National Synchrotron Radiation Laboratory, University of Science and Technology of China, Hefei, China

**Contact: dlfeng@ustc.edu.cn*

Keywords: angle resolved photoemission spectroscopy, magnetism, superconductivity

Electron-boson interactions play vital roles in determining the ground states and properties of solids. Angle-resolved photoemission spectroscopy (ARPES) could probe how the electron-boson interactions affect band dispersion and spectral lineshape, thus revealing their roles in solids. In this talk, I will showcase a few examples.

We find that electron-phonon interactions is enhanced by long-range electron-electron correlations in (Ba,K)BiO_3, explaining its high superconducting transition temperature [1]. Moreover, with PLD-grown $LiTi_2O_4$ thin films, we are able to obtain the band structure of this spinel-structured superconductor for the first time, and find that the anisotropic and strong electron-phonon interactions causes its high superconducting transition temperature.

In *a*-$LaAlO_3$/$KTaO_3$ interfactial supercondutors, we find that the strengh of electron-phonon interactions depends on the crystalline orientation of $KTaO_3$ substrate, which is in line with the orientation dependency of its superconductivity [2].

In (Ba,K)Mn_2As_2, we find that its electron-antiferromagnetic magnon interactions cause strong band renormalization and alter the density of states (DOS) at the Fermi energy. When the DOS surpasses Stoner's criterion, it becomes an itinerant weak ferromagnet [3].

1. C. H. P. Wen et al., Unveiling the Superconducting Mechanism of $Ba_{0.51}K_{0.49}BiO_3$, *Phys. Rev. Lett.* **121**, 117002 (2018).
2. X. Chen et al., Orientation-dependent electron-phonon coupling in interfacial superconductors $LaAlO_3$/$KTaO_3$, arXiv:2301.13488 (2023)
3. T. L. Yu, et al., Strong Band Renormalization and Emergent Ferromagnetism induced by Electron-Antiferromagtic-Magnon Coupling, *Nat. Commun.* **13** : 6560 (2022).

Micro-focused ARPES study on 2D transition-metal dichalcogenides

Kyoko Ishizaka

Quantum-Phase Electronics Center & Department of Applied Physics, The University of Tokyo, Tokyo, Japan

Center for Emergent Matter Science, RIKEN, Wako, Japan

**Contact: ishizaka@ap.t.u-tokyo.ac.jp*

Keywords: angle-resolved photoelectron spectroscopy (ARPES), micro-beam, 2D materials

There has been increasing interest in the atomically thin two-dimensional materials. When a crystal becomes thinner and thinner to the atomic level, peculiar phenomena discretely depending on its layer-numbers (*n*) start to appear. The symmetry and wave functions strongly reflect the layer-numbers and stacking order, which brings us a potential of realizing new properties and functions that is unexpected in either bulk or simple monolayer.

Multilayer WTe_2 is one such example exhibiting unique n-dependent insulator-metal transition, ferroelectricity and non-linear transport properties related to the Berry-curvature dipole. In this talk, I will introduce about the investigation of the electronic band dispersions in multilayer WTe_2, by performing laser-based micro-focused angle-resolved photoelectron spectroscopy (laser μARPES) on exfoliated-flakes that are strictly sorted by *n* and encapsulated by graphene [1]. We observed the insulator-semimetal transition occurring between 2 and 3-layers, as well as the 30-70 meV spin-splitting of valence bands manifesting in even *n* as a signature of stronger structural asymmetry due to the staggered stacking [2]. Our result fully demonstrates the possibility of the large energy-scale band and spin manipulation through the finite *n* stacking procedure.

1. S. Masubuchi et al., Sci. Rep. 12, 10936/1-7 (2022).
2. M. Sakano et al., Phys. Rev. Research 4, 023247/1-7 (2022).

Proximity-Induced Novel Ferromagnetism and Metallicity in $NdNiO_3$ Heterostructure

Marco Caputo[1,2*], Zoran Ristic[2,3,4], Rajendra S. Dhaka[2,3,5], Tanmoy Das[6], Eduardo B. Guedes[2], Anna Zakharova[2], Cinthia Piamonteze[2], and Milan Radovic[2]

1 MAX IV Laboratory, Lund University, PO Box 118, Lund 22100, Sweden

2 Photon Science Division, Paul Scherrer Institute, Villigen CH-5232, Switzerland

3 Institute of Condensed Matter Physics, Ecole Polytechnique F d rale de Lausanne (EPFL), Lausanne CH-1015, Switzerland

4 Vinca Institute of Nuclear Sciences, University of Belgrade, P.O.Box 522, Belgrade 11000, Serbia

5 Department of Physics, Indian Institute of Technology Delhi, Hauz Khas, New Delhi 110016, India

6 Department of Physics, Indian Institute of Science, Bangalore 560012, India

**Contact: marco.caputo@maxiv.lu.se*

Keywords: magnetic coupling, metal–insulator transition, proximity effect

Rare-earth nickelate ($RENiO_3$) show a wide variety of physical properties [1, 2]. Among those, an intriguing RE-temperature phase diagram show the occurrence of metal-insulator (MIT) and paramagnetic-antiferromagnetic transitions [3]. For RE=Nd ($NdNiO_3$ - NNO) the electronic and magnetic phase transition occur at the same temperature, indicating an intimate relation between electronic structure and magnetic ordering, and suggesting that is possible to act on one to modify the other.

Growing thin NNO films on different substrates allows for fine tuning of different properties, using, for instance, strain, charge transfer, or proximity effect. We use this last effect to induce ferromagnetism in thin films of NNO grown on ferromagnetic $La_{0.67}Sr_{0.33}MnO_3$ (LSMO), as confirmed by X-ray Magnetic Circular Dichroism (XMCD). The new ferromagnetic phase shows an unexpected electronic behavior, with suppressed MIT and persistent conductivity. Temperature-dependent Angle Resolved Photoemission Spectroscopy (ARPES) confirm a finite density of states at the Fermi level down to the lowest attainable temperature, but without any visible change in the Fermi surface topology. Momentum-resolved density fluctuation calculation (MRDF) permits us to link the new ferromagnetic state with the absence of MIT: introducing a ferromagnetic coupling between the Nickel centers our model prevents any gap opening at zero temperature.

This work demonstrate that it is possible to create a new ferromagnetic order in nickelates, and that the ferromagnetic ordering prevent the occurrence of the typical MIT in this class of materials.

1. M. Imada, A. Fujimori, Y.Tokura, *Rev.Mod.Phys.* **70**, 1039 (1998).
2. H. Y. Hwang, Y. Iwasa, M. Kawasaki, B. Keimer, N. Nagaosa, Y. Tokura, *Nat. Mater.* **11**, 103 (2012).
3. P. Zubko, S. Gariglio, M. Gabay, P. Ghosez, J.-M. Triscone, *Annu.Rev. Condens. Matter Phys.* **2**, 141 (2011).

Infinite-layer nickelate superconductors studied with Resonant Inelastic X-ray Scattering

Francesco Rosa (*Politecnico di Milano, Italy*), Leonardo Martinelli (*Politecnico di Milano, Italy*), Guillaume Krieger (*CNRS-IPCMS, Strasbourg, France*), Marco Moretti (*Politecnico di Milano, Italy*), Riccardo Arpaia (*Chalmers University of Technology, Göteborg, Sweden*), Maciej Fidrysiak (*Jagiellonian University, Kraków, Poland*), Nicholas Brookes (*ESRF, Grenoble, France*), Lucio Braicovich (*Politecnico di Milano, Italy*) (*ESRF, Grenoble, France*), Marco Salluzzo (*CNR-SPIN, Napoli, Italy*), Daniele Preziosi (*CNRS-IPCMS, Strasbourg, France*), Giacomo Ghiringhelli (*Politecnico di Milano, Italy*) (*CNR/SPIN, Italy*)

Keywords: nickelates, cuprates, RIXS, magnetism

During the quest for high-T superconductors, nickelates came to the spotlight in 2019, when they were effectively proved as superconductive with a Tc about one order of magnitude lower than cuprates. Nickelates show a strong affinity, both structural and electronic, with copper compounds: they share the same TM-O_2 square lattice planar structure, enhancing the interaction among electrons belonging to the TM *3d* and O *2p* states. In cuprates, the long-range AF order of the parent compound is destroyed upon hole-doping, while the superconducting phase sets in. The same competing mechanism between magnetism and SC may also affect nickelates, but in this case long-range AF order for the ground state of parent compounds has still to be reported. As an alternative, an Anderson-Kondo-like ground state was recently proposed [1] for the $RNiO_2$ class, elicited by the hybridization between 2D Ni *3d* and 3D Nd *5d* states.

RIXS has proved to be a powerful technique for the investigation of such materials. In a recent experiment, we focused on the low-energy excitation (few hundreds meV, typical of spin excitations in cuprates) in RIXS spectra of different Sr- doped $NdNiO_2$ samples. With polarization-resolved analysis, we were able 1) to disentangle such peak from the underlying charge continuum, and 2) to prove its spin-flip nature. Also, it comes as an analogy to the paramagnon peak previously observed in cuprates [2], although the latter is seen at nearly double energies than in nickelates (~400 meV). The analogies and differences to cuprates are analyzed with an original Hubbard-based theoretical model, used to fit the magnetic spectra. Our model seems to correctly predict the different observed behaviors of the paramagnon: in nickelates its energy and intensity seem to decrease with hole doping, while in cuprates they are almost constant. Such behavior, recently reported by Lu et al. [3] is confirmed by our experiment also in these cases where the spin peak is very broad, as it happens for more disordered samples.

1. Hepting, Matthias, et al. Electronic structure of the parent compound of superconducting infinite-layer nickelates." *Nature materials* 19.4 (2020): 381.

2. Peng, Y. Y., Huang, E. W., Fumagalli, R., Minola, M., Wang, Y., Sun, X., ... & Ghiringhelli, G. (2018). Dispersion, damping, and intensity of spin excitations in the monolayer (Bi, Pb) 2 (Sr, La) 2 CuO 6+ δ cuprate superconductor family. *Physical Review B*, *98*, 144507.

3. Lu, H., Rossi, M., Nag, A., Osada, M., Li, D. F., Lee, K., ... & Lee, W. S. (2021). Magnetic excitations in infinite-layer nickelates. *Science*, *373*, 213.

Investigation of Liquid-Vapor Interfaces Using Photoelectron Spectroscopy

Hendrik Bluhm
Fritz Haber Institute of the Max Planck Society, Berlin, Germany
Contact: bluhm@fhi.mpg.de

Keywords: liquid-vapor interface, X-ray photoelectron spectroscopy, aqueous solutions, surfactants

Aqueous solution-vapor interfaces govern important phenomena in the environment and atmosphere, including the uptake and release of trace gases by aerosols and CO_2 sequestration by the oceans. A detailed understanding of these processes requires the investigation of liquid-vapor interfaces with chemical sensitivity and interface specificity. [1,2] This talk will discuss opportunities and challenges for investigations of liquid-vapor interfaces using X-ray photoelectron spectroscopy and describe some recent experiments that have focused on the propensity of certain ions and the role of surfactants at the liquid/vapor interface. The talk will also discuss the utilization of photoelectron angular distributions for the investigation of the depth of solvation of surfactants at the interface. [3-5]

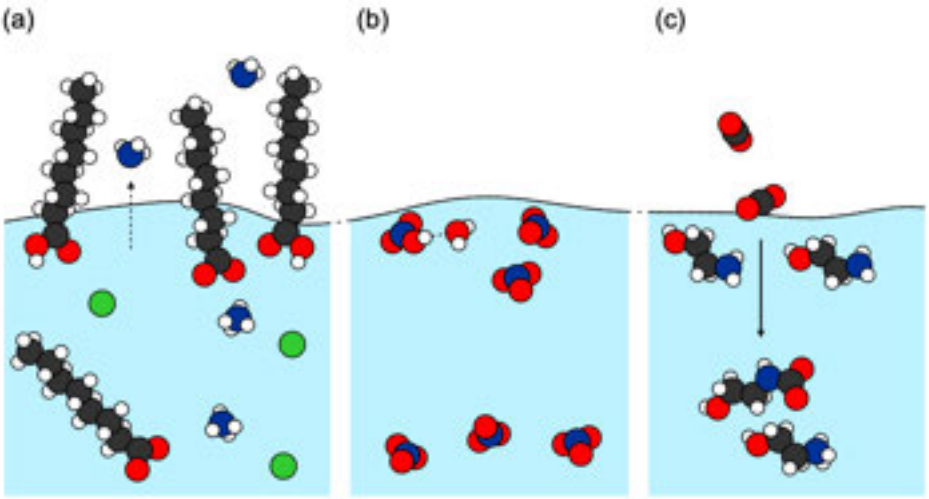

Figure 1: Examples for processes at liquid-vapor interfaces that can be investigated using XPS. (a) Protonation state of surfactants in the presence of gas phase species and ions. (b) Dissociation of acids at the interface and in the bulk. (c) Reaction of gas phase species with dissolved ions. Figure adapted from Ref. 1.

1. R. Dupuy, C. Richter, B. Winter, G. Meijer, R. Schlögl, H. Bluhm, *Core level photoelectron spectroscopy of heterogeneous reactions at liquid-vapor interfaces: Current status, challenges, and prospects*, J. Chem. Phys. **154**, 060901 (2021).
2. C. Richter, R. Dupuy, H. Bluhm, *Investigation of liquid-vapor interfaces with APXPS*, in: A.R. Head, B. Eren, S. Nemšak (Eds.) Ambient Pressure Spectroscopy in Complex Chemical Environments, ACS Symposium Series, Vol. **1396**, 39-66 (2021).
3. R. Dupuy, J. Filser, C. Richter, R. Seidel, F. Trinter, T. Buttersack, C. Nicolas, J. Bozek, U. Hergenhahn, H. Oberhofer, B. Winter, K. Reuter, H. Bluhm, *Photoelectron angular distributions as sensitive probes of surfactant layer structure at the liquid-vapor interface*, Phys. Chem. Chem. Phys. **24**, 4796-4808 (2022).
4. R. Dupuy, C. Richter, T. Buttersack, F. Trinter, S. Thürmer, B. Winter, H. Bluhm, *Core-level photoelectron angular distributions at the liquid-vapor interface*, Acc. Chem. Res. **56**, 215-223 (2023).
5. R. Dupuy, J. Filser, C. Richter, T. Buttersack, F. Trinter, S. Gholami, R. Seidel, C. Nicolas, J. Bozek, D. Egger, H. Oberhofer, S. Thürmer, U. Hergenhahn, K. Reuter, B. Winter, H. Bluhm, *Ångstrom depth-resolution with chemical specificity at the liquid-vapor interface*, Phys. Rev. Lett. **130**, 156901 (2023).

Event-averaged time-resolved APXPS with chemical perturbations: studying gas/solid processes with a microsecond time resolution

Weijia Wang[1], Giulio D'Acunto[2], Virginia Boix de la Cruz[2], Mattia Scardamaglia[1], Suyun Zhu[1], Robert H. Temperton[1], Joachim Schnadt[1,2], Jan Knudsen[1,2], and Andrey Shavorskiy[1]

1 MAX IV Laboratory, Lund University, Lund, 221 00, Sweden

2 Division of Synchrotron Radiation, Department of Physics, Lund University, Lund, 221 00, Sweden

**Contact: andrey.shavorskiy@maxiv.lu.se*

Keywords: APXPS, time-resolved spectroscopy, catalysis

Chemical transformations occurring at the interfaces between gases and solids are the driving forces responsible for multiple industry- and research-relevant processes such as heterogeneous catalysis, gas sensing, and thin film growth. These processes are dynamic by nature, with various steps occurring at different time scales. To obtain a complete picture of surface reactions, one has to study their time evolution using time-sensitive experimental techniques. Recently at MAX IV, we have developed an event-averaging time-resolved Ambient Pressure X-ray Photoelectron Spectroscopy (APXPS) based on chemical perturbations for observing dynamic processes with micro- to millisecond time resolution. The method makes use of the rapid change in the gas pressure/composition as a perturbation that drives the system away from its equilibrium [1,2]. In the experiment, a sharp gradient in chemical potential is created by modulating the gas composition over the catalyst via mass flow controllers or a fast valve. Such gas pulse has internal pressure in the mbar range and a rising edge of a few hundred microseconds. A gated detector based on a fast camera is synchronized with the valve operation to measure X-ray photoemission spectra with up to 40 µs time resolution. We will present several experiments characterizing the setup's performance, including the CO oxidation reaction over Pt (111) (Figure 1) to demonstrate the capability of the setup to correlate the gas phase composition with that of the surface during the transient supply of CO gas into an O_2 stream [1]. These experiments demonstrate that under CO pressure modulation conditions, the system remains active (i.e. producing CO2) at temperatures below the CO lift-off temperature (that is inactive under the flow conditions) [3].

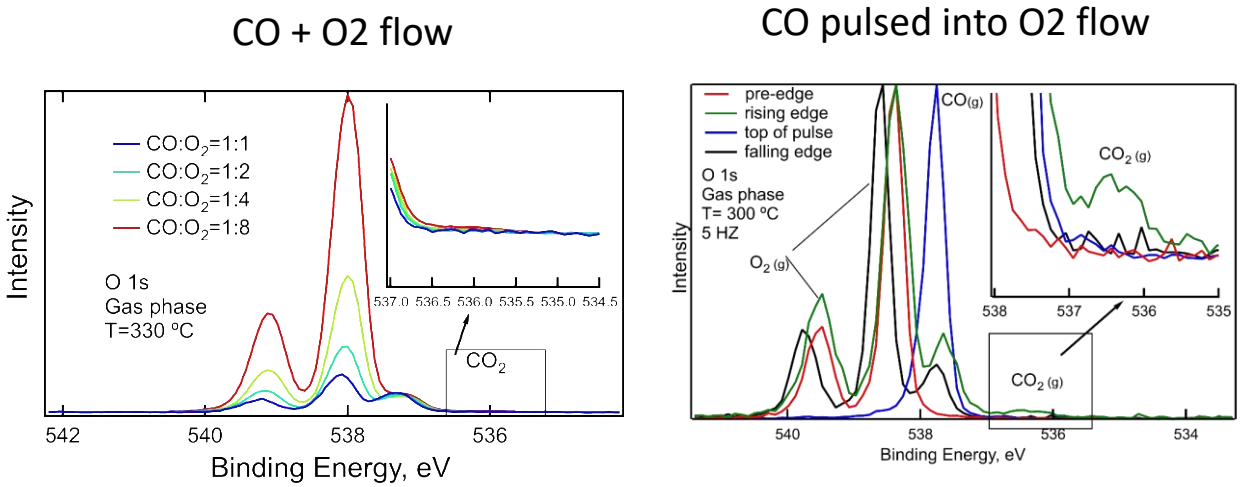

Figure 1: O 1s gas-phase spectra measured above Pt(111) sample under the flow (left) and pulsed (right) conditions. The production of CO_2 is clearly visible under the pulsed (modulated) conditions at the rising edge of the CO pulse (right, green curve).

1. A. Shavorskiy et al. ACS Applied Materials & Interfaces 2021 13 (40), 47629-47641.
2. J. Knudsen et al. Nat Commun 12, 6117 (2021).
3. W.Wang et al. in preparation

Using Ambient Pressure XPS to study ALD in real-time

Esko Kokkonen[1,*], Rosemary Jones[2] and Joachim Schnadt[1,2]

1 MAX IV Laboratory, Lund University, Lund, Sweden

2 Division of Synchrotron Radiation Physics, Department of Physics, Lund University, Lund, Sweden

**Contact: esko.kokkonen@maxiv.lu.se*

Keywords: ALD, APXPS, time-resolved XPS

In the recent years, ambient pressure X-ray photoelectron spectroscopy (APXPS) has become more popular tool to study various processes within the Atomic Layer Deposition (ALD) technique. One reason for the increased popularity is the prevalence of various APXPS setups, which have become widely available at both university-based laboratories and at synchrotron facilities. Here, we will introduce one such setup located at the SPECIES beamline at the MAX IV Laboratory in Lund, Sweden. [1-4]

The beamline is well suited for studies of many different systems as it covers a wide photon energy range from 30 to 1500 eV. This enables studying most core levels with XPS using surface sensitive energies and also focusing on valence band studies due to the availability of low photon energies at high photon flux. The APXPS endstation offers a wide range of equipment for sample characterization and preparation with the main instrument being an ambient pressure X-ray photoelectron energy analyzer capable of high energy and time resolution. [5]

The ALD setup is a dedicated ambient pressure cell installed on the endstation. The cell allows for monitoring the layer growth with XPS in real time, thus enabling *in situ* and *operando* experiments, which can reveal new information on the details of the chemical reactions affecting the layer growth dynamics. The cell has been optimized for realistic gas flow dynamics with the intention of creating a laminar-like flow across the surface of the substrate. Two different mass spectrometers can also be used (one installed in the pre-lense chamber of the spectrometer and another on the outlet line of the cell) at the same time as XPS, which allow to detect and gas phase byproducts produced during the half-cycle reactions. The cell can be operated up to 20 mbar pressure and the substrate can be heated with a resistive heater up to 400 °C. Many different precursors can be mounted on the system thanks to versatile gas system, which also includes programmable pneumatic valves allowing automatic pulsing of the half-cycles. The gas tubing can be also heated both inside and outside of the vacuum chambers.

Here, we will give some example research carried out with the instrument. The research highlights the obtainable results focusing on the initial ALD reactions that occur within the first few half-cycles. The processes and chemical reactions occurring during the early stages of ALD are very important for the quality and properties of the final created film, and thus it is of high interest to understand them correctly and with high detail. The information obtained with these can also reveal how the early stages could demand a different type of pulsing scheme than the rest of the film deposition. Here, we will focus on the deposition of TiO_2 on Si substrate [1] and the deposition of Pt metal film on Si. In both cases, the time-resolved XPS details changes on the surface, which change slowly as the first half-cycle is ongoing.

References:

1. Kokkonen, E., *et al.* Rev. Sci. Instrum. 93.1, 013905 (2022)
2. D'Acunto, Giulio, *et al.* ACS Appl. Electron. Mater. 2.12, 3915-3922 (2020)
3. D'Acunto, Giulio, *et al.* Faraday Discuss. 236, 71-85 (2022)
4. D'Acunto, Giulio, *et al.* J. Phys. Chem. C 126.29 12210-12221 (2022)
5. Kokkonen, Esko, *et al.* J. Synch. Rad. 28.2, 588-601 (2021)

Applied physics in the steel industry – optical emission spectroscopy as a method for advanced process control

Henri Pauna[1,*], Timo Fabritius[1], and Marko Huttula[2]

1 Process Metallurgy Research Unit, P.O. Box 4300, FI-90014, University of Oulu, Finland
2 Nano and Molecular Systems Research Unit, P.O. Box 3000, FI-90014, University of Oulu, Finland
**Contact: henri.pauna@oulu.fi*

Keywords: optical emission spectroscopy, steel industry, process control, plasma, flame

The steel industry accounts for approximately 7 % of all the global CO_2 emissions, where majority of these emissions are caused by carbon-based reduction of iron ores and fossil-based fuels. Due to the significant share of the CO_2 emissions related to the steel industry, a transition toward environmentally sustainable steelmaking has a key role in reaching the climate neutrality and the goals of the Paris Agreement. Overall, this means a staggering 90% reduction in the carbon intensity of the steel production by 2050 [1]. In addition to using pristine iron ore as the raw material, recycled steel scrap can be used to produce steel. This is done with electricity-based steelmaking in electric arc furnaces (EAFs) with refinement at ladle furnaces (LFs), accounting to approximately 40 % of European steelmaking. As such, the EAF route results into approximately 77 % lower CO_2 emissions when compared to the carbon-based reduction of iron ores [2]. However, there is one caveat: since the demand for steel can be expected to increase and the scrap quality to decrease in the following decades, the scrap-based steelmaking route is not enough to keep up with the demand. To make the sustainable steelmaking a reality, novel steelmaking technologies are required, and the existing processes must be optimized further to bring down the carbon footprint and increase the efficiency.

To this end, the research at the process metallurgy research unit has focused on two aspects: optimization of existing processes, and both monitoring and controlling novel steelmaking technologies. The common factor has been the usage of optical emission spectroscopy (OES) as the basis for this novel analysis. The existing processes include, e.g., slag composition, molten bath temperature, and radiative heat transfer analyses for EAFs and LFs together with H_2-burner optimization. Via European collaboration within the past few years, the research on novel steelmaking technology, hydrogen plasma smelting reduction (HPSR), has been initiated with ambitious targets to optimize and characterize the process. An example of a lab-scale HPSR arc and OES spectrum is presented in Figure 1.

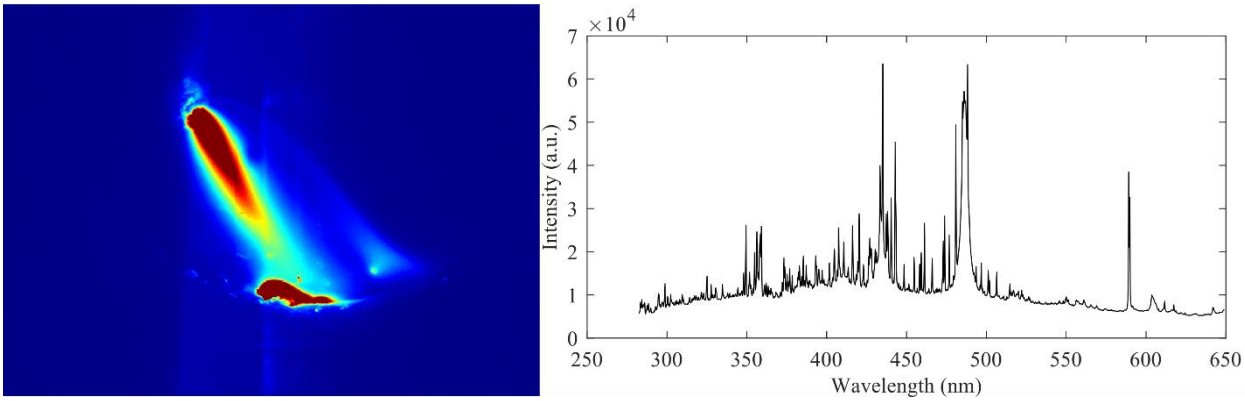

Figure 1: Lab-scale HPSR arc and corresponding OES spectrum.

The presentation covers process metallurgy research unit's work and international collaboration toward OES characterization and process control for in the steel industry. General overview of the applicability of the OES as a method in industrial environment and highlights of the recent research and results that have been achieved will be presented with examples from laboratory, pilot-scale, and industrial demonstrations.

1. M. Pei, A. Regnell, and O. Wijk, "Toward a Fossil Free Future with HYBRIT: Development of Iron and Steelmaking Technology", Metals, vol. 10, no. 7, 972, 2020.
2. H.-J. Odenthal, "Review on Modeling and Simulation of the Electric Arc Furnace (EAF)," Steel Research International, vol. 89, no. 1, 1700098, 2017.

Thursday 22st of August, 2023

Photodissociation of ironpentacarbonyl - $Fe(CO)_5$ - from initial bursts of CO release to branching pathways in solution

Ambar Banerjee[1,2], Michael R. Coates[1], Markus Kowalewski[1], Hampus Wikmark[2], Raphael Jay[2], Philippe Wernet[2], Michael Odelius[1] *1 Department of Physics, StockholmsUniversity, Stockholm, Sweden*
2 Department of Physics and Astronomy, Uppsala Universitet, Uppsala, Sweden
**Contact: odelius@fysik.su.se*

Keywords: Metal complexes, Excited state dynamics, Molecular dynamics simulations, Quantum chemistry

Excited state molecular dynamics simulations of the initial non-adiabatic transitions after photoexcitation of ironpentacarbonyl reveal an intricate ultra-fast dissociation process [1]. The ultrafast nuclear dynamics and non-adiabatic transitions are analyzed in terms of the shapes potential energy surfaces and crossings between manifolds of states with different character. We conclude that the coupled electron-nuclear dynamics involving metal-to-ligand charge-transfer excitations and dissociative metal-centered excited states results in a gradual transition from coherent bond oscillatory motion to reoccurring bursts of carbonmonoxide release.

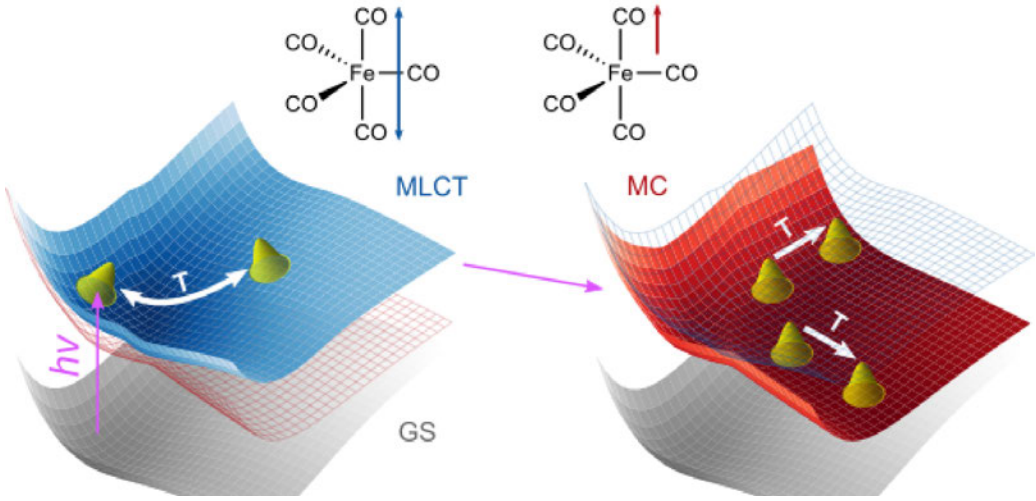

Figure 1: Surface hopping from oscillations in bound states results in bursts of carbonmonoxide [1].

These initial events set the stage for the sequential CO release in gas phase and complex path-ways in ethanol solution as previously observed experimentally in X-ray photoelectron spectroscopy (XPS) [2] and iron L-edge resonant inelastic X-ray scattering (RIXS) [3]. Theoretical simulations of gas phase XPS and solution RIXS spectra based on multi-configurational quantum chemistry allow for kinetic modeling of the processes on different time-scales. The impact and challenges for explicit dynamical modelling of time-resolved X-ray spectra of these and related systems are discussed.

[1] A. Banerjee, M. R. Coates, M. Kowalewski, H. Wikmark, R. M. Jay, P. Wernet, M. Odelius, Photoinduced bond oscillations in ironpentacarbonyl give delayed synchronous bursts of carbonmonoxide release, *Nature Communications* **13**, 1337 (2022).

[2] P. Wernet, T. Leitner, I. Josesfsson, T. Mazza, P. S. Miedema, H. Schröder, M. Beye, K. Kunnus, S. Schreck, P. Radcliffe, S. Düsterer, M. Meyer, M. Odelius, A. Föhlisch, Communication: Direct evidence for sequential dissociation of gas-phase $Fe(CO)_5$ via a singlet pathway upon excitation at 266 nm, *Journal of Chemical Physics* **146**, 211103 (2017).

[3] P. Wernet, K. Kunnus, I. Josefsson, I. Rajkovic, W. Quevedo, M. Beye, S. Schreck, S. Grübel, M. Scholz, D. Nordlund, W. Zhang, R. W. Hartsock, W. F. Schlotter, J. J. Turner, B. Kennedy, F. Hennies, F. M. F. de Groot, K. J. Gaffney, S. Techert, M. Odelius, A. Föhlisch, Orbital-specific mapping of the ligand exchange dynamics of $Fe(CO)_5$ in solution, *Nature* **520**, 78–81 (2015).

ARTIST: Artificial Intelligence for Spectroscopy

Patrick Rinke

Department of Applied Physics, Aalto University, Helsinki, Finland

**Contact: patrick.rinke@aalto.fi*

Keywords: artificial intelligence, machine learning, photoemission spectroscopy, NMR spectroscopy

Spectroscopy is a fundamental tool in molecular and materials research, characterization and discovery. It has consequently become a major objective of artificial intelligence (AI) development but has not received as much attention in the latest machine-learning boom as other experimental or computational techniques. AI for spectroscopy pursues two parallel goals (figure 1) [1]: spectra prediction (typical in computational studies) and property inference (typical in experimental approaches). Successful AI spectra predictions allow us to cut down on the time and resources behind computational or experimental spectroscopy. Trained on available input (e.g., atomic structure or materials attributes) and output (e.g., spectra or spectroscopic quantities) pairs, the AI model can make output predictions for new input instantaneously, without further resource requirements. In property inference tasks, data input and output are reversed to echo spectroscopic applications. AI models predict materials structure and properties from spectral input or classify the inputs into different categories.

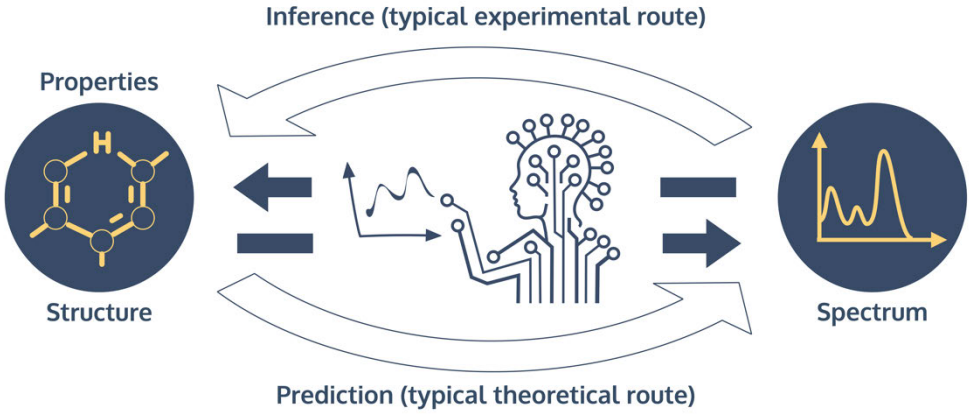

Figure 1: AI in spectroscopy paradigm - AI facilitates the two main tasks in spectroscopy: 1) property and structure inference and 2) spectra prediction. Figure adapted from Ref. 1.

For computational data [2], I will demonstrate that AI models can predict ionization energies and spectra of organic molecules from their atomic structure alone [3,4]. We trained kernel ridge regression and neural network models on quantum mechanically computed molecule-property pairs. The molecules are represented by simple, easily attainable numerical descriptors based on nuclear charges and cartesian coordinates. The complexity of the molecular descriptor and the diversity of the data sets turn out to be crucial for the learning success [3]. Our best AI models predict ionization energies within 0.2 eV and excitation spectra with 97% accuracy surpassing typical measurement uncertainties.

For inference, I will illustrate how we correlate the properties of biopolymers with nuclear magnetic resonance (NMR) spectroscopy. We extracted lignin from birch wood and characterized it with 2D NRM spectroscopy [5]. Using the 2D NRM spectra as input, our AI model infers lignin properties like the antioxidant activity directly from the spectra. We trace the predictions back to NRM peaks to link the antioxidant activity to structural features of lignin encoded in the spectra.

1. H. J. Kulik, P. Rinke, *et al*., Roadmap on machine learning in electronic structure, *Electro. Struct.* **4**, 023004 (2022).
2. A. Stuke, P. Rinke, *et. al.*, Atomic structures and orbital energies of 61,489 crystal-forming organic molecules, *Sci. Data* **7**, 58 (2020).
3. A. Stuke, P. Rinke, *et al*., Chemical diversity in molecular orbital energy predictions with kernel ridge regression, *J. Chem. Phys.* **150**, 204121 (2019).
4. K. Ghosh, P. Rinke, *et al.*, Deep Learning Spectroscopy: Neural Networks for Molecular Excitation Spectra, *Adv. Sci.* **6**, 1801367 (2019).
5. J. Löfgren, P. Rinke, *et al.*, Machine Learning Optimization of Lignin Properties in Green Biorefineries, *ACS Sustainable Chem. Eng.* **10**, 9469 (2022).

Hard X-ray Photoelectron Spectroscopy probing photoionisation dynamics

Tatiana Marchenko

Laboratoire de Chimie Physique-Matière et Rayonnement, CNRS, Sorbonne Université, Paris, France

Contact: tatiana.marchenko@sorbonne-universite.fr

Keywords: Auger spectroscopy, conjugated polymers, post-collision interaction, charge transfer

Along with the rapid development of the laser and XFEL technology allowing for time-resolved studies, a remarkable progress in the synchrotron technology provides nowadays a wealth of information on the relaxation mechanisms of core-exited systems through high energy-resolution electron and X-ray spectroscopy [1]. In this talk I will discuss several applications of Auger spectroscopy in sulfur-containing organic gas-phase molecules and solid-state polymers, providing access to the processes occurring on the time scale determined by the lifetime of the S 1s core hole $\tau \approx 1$ fs.

In the first example, we use Auger spectroscopy to explore post-collision interaction in gas-phase thiophene in comparison to solid thiophene-based polymers: polythiophene (PT) and poly(3-hexylthiophene-2,5-diyl), also known as P3HT. Following S K-shell ionisation, the Coulomb interaction between the photoelectron, the Auger electron and the residual doubly-charged ion results in distortion and energy shift of the photoelectron and Auger electron spectral lines. We discover that this effect is amplified in solid polymers compared to gas-phase molecules due to modification of post-collision interaction by the polarisation screening and photoelectron scattering in the condensed medium [2].

The second example demonstrates a novel application of resonant Auger spectroscopy as a probe of conjugation and hyperconjugation effects in core-excited aromatic molecules [3]. We show that the changes of electronic structure of thiophene and thiazole, occurring in the process of resonant sulfur K-shell excitation and Auger decay, affect the stabilisation energy resulting from π-conjugation and hyperconjugation and reverse the energy order of the first two core-excited states. This effect is absent in thiolane, the saturated analogue of thiophene. The discovered sensitivity of resonant Auger spectroscopy to conjugation effects is equally applicable to larger conjugated systems such as polymers.

In the third example, we apply resonant Auger spectroscopy to explore charge transfer in thiophene-based PT and P3HT polymers upon resonant excitation at the S K-edge. In polymer powders the electron may only be delocalised along the polymer chain (intra-chain mechanism), while in polymer films the delocalisation path can be two-fold: intra-chain and/or inter-chain (between polymer chains). Our results reveal the signature of charge transfer in P3HT polymer films as well as in PT powder, which points towards the dominance of intra-chain charge transfer mechanism occurring on few-femtosecond time scale. Theoretical analysis of the dynamic processes, using methods based on density functional theory and molecular dynamics simulations, confirms this hypothesis.

1. M. N. Piancastelli, T. Marchenko, R. Guillemin, L. Journel, O. Travnikova, I. Ismail and M. Simon, Hard x-ray spectroscopy and dynamics of isolated atoms and molecules: a review, *Rep. Prog. Phys.* **83**, 016401 (2020)
2. N. Velasquez, O. Travnikova, R. Guillemin, I. Ismail, L. Journel, J. B. Martins, D. Koulentianos, D. Céolin, L. Fillaud, M. L. M. Rocco, R. Püttner, M. N. Piancastelli, M. Simon, S. Sheinerman, L. Gerchikov and T. Marchenko, Generalization of the post-collision interaction effect from gas-phase to solid-state systems demonstrated in thiophene and its polymer, *Phys. Rev. Research* **5**, 013048 (2023)
3. J. B. Martins, C. E. Vieira de Moura, G. Goldsztejn, O. Travnikova, R. Guillemin, I. Ismail, L. Journel, D. Koulentianos, M. Barbatti, A. Lago, D. Céolin, M. L. Rocco, R. Püttner, M. N. Piancastelli, M. Simon and T. Marchenko, Electron delocalisation in conjugated sulfur heterocycles probed by resonant Auger spectroscopy, *Phys. Chem. Chem. Phys.* **24**, 8477-8487 (2022)

Theoretical description of soft and hard x-ray photoemission spectroscopy using the one-step model of photoemission

Aki Pulkkinen[1,*], Ján Minár[1]
1 New Technologies Research Centre, University of West Bohemia, Plzeň, Czech Republic
**Contact: apulkkin@ntc.zcu.cz*

Keywords: photoemission spectroscopy, one-step model, KKR method

Photoemission spectroscopies are unique in the sense that they offer a direct way to study the electronic structure of materials. However, the experimental conditions, such as the energy, polarization and direction of the photon or the surface termination of the sample, introduce effects that can complicate the interpretation of the experimental data. Theoretical modeling of the photoemission process, from the photoexcitation of the electron to the escape of the photoelectron to the vacuum, is crucial for understanding the contribution of various effects to the photoemission signal.

Early theoretical models treated the photoexcitation, photoelectron transport to the surface, and its escape to the vacuum as separate processeses in the three-step model of photoemission [1]. However, splitting the process into three steps is a crude approximation that neglects self-energy corrections, which are needed e.g. for a proper treatment of surface effects.

In the one-step model of photoemission [2] the photoemission is treated as a single process, and the finite lifetimes of the initial and final states are taken into account by an imaginary part of the potential. The one-step model is implemented within the spin polarized relativistic Korringa-Kohn-Rostoker (SPR-KKR) package [3], which solves the electronic structure of materials using the multiple scattering Green's function method. The package is capable of modeling the photoemission spectra including dichroism, and treating thermal fluctuations via the Debye model, random alloys within the coherent potential approximation (CPA), and electron correlation effects via the dynamical mean field theory (DMFT) [4].

The basis of the one-step model in modeling x-ray photoemission spectroscopy (XPS), x-ray photoelectron diffraction (XPD), and angle-resolved soft- and hard x-ray photoemission spectroscopy (SX-ARPES and HARPES) will be discussed along with applications [5].

[1] C. N. Berglund & W. E. Spicer, *Physical Review* **136**, A1030 (1964)

[2] J. B. Pendry, Theory of photoemission, *Surface Science* **57**, 679–705 (1976).

[3] H. Ebert, D. Ködderitzsch & J. Minár, Calculating condensed matter properties using the KKR-Green's function method—recent developments and applications, *Reports on Progress in Physics* **74**, 096501 (2011).

[4] J. Braun, J. Minár & H. Ebert, Correlation, temperature and disorder: Recent developments in the one-step description of angle-resolved photoemission, *Physics Reports* **740**, 1–34 (2018).

[5] A. Pulkkinen, G. Kremer, V. N. Strocov, F. Weber, J. Minár & C. Monney, Revealing electronic correlation effects in YNi_2B_2C using photoemission spectroscopy, *in preparation*.

Probing Halide Ion Transport and Metal Corrosion Process in Halide Perovskite Solar Cells via In *Operando* Hard X-ray Photoelectron Spectroscopy

Ibrahima Gueye[1,a], Yasuhiro Shirai[2], Takahiro Nagata[2], Takashi Tsuchiya[2], Dhruba B. Khadka[2], Masatoshi Yanagida[2], Okkyun Seo[1], Kenjiro Miyano[2], Osami Sakata[1,b]

[1] Center for Synchrotron Radiation Research, Japan Synchrotron Radiation Research Institute (JASRI), 1-1-1 Kouto, Sayo, Hyogo 679-5198, Japan.
[2] National Institute for Materials Science (NIMS), 1-1 Namiki, Tsukuba, Ibaraki 305-0044, Japan.
[a)] Electronic mail: ibrahima.gueye@spring8.or.jp ; [b)] Electronic mail: sakata.osami@spring8.or.jp
Keywords: Perovskite solar cells, ion diffusion, photoelectron spectroscopy, synchrotron, operando, bulk, and buried interfaces

In the last decade, organic-inorganic halide perovskite solar cells (HaPSCs) have undergone rapid development, achieving a current power conversion efficiency of nearly 26%, which is comparable to that of the best silicon solar cells. [1]. Besides their exceptionally high efficiency, HaPSCs have shown tremendous potential as a low-cost photovoltaic (PV) technology for the next generation which makes them a desirable candidate for future uptake in the PV market. Although perovskite materials have shown promising optoelectronic features when used as active layers in HaPSCs, their long-term commercial viability is still hindered by the instability of their physicochemical and functional properties under operating conditions. From that, there is still a need for more systematic research efforts to uncover the intricate dynamics underlying their stability even though significant progress has been made in the understanding and improvement of HaPSC performances. Ionic transport, leading to irreversible degradation, has been identified as a critical factor that seriously impedes the long-term stability and performance of HaPSCs. During prolonged operation, ionic compounds can easily self-release from the solar cells, inducing numerous defects in the HaP layer that serve as nonradiative recombination centers. These remaining defects are also sensitive to moisture and oxygen, which accelerate device decomposition. However, there is still debate regarding the types of mobile species and the dynamic behavior of these species. In this regard, identifying and profiling the ions and molecular fragments produced during the lifespan and degradation of HaPSCs is crucial [2]. Here we report an advanced *operando* synchrotron hard X-ray photoelectron spectroscopy (HAXPES) investigation of the dynamic behavior of iodide species in a $MAPbI_{3-x}Cl_x$ (HaP) solar cell under an applied bias [Figure. 1 (*left*)] [3].

The performance and stability of stacked Au/Ag/AZO/PCBM/HaP/NiO/ITO/glass structures, where AZO, PCBM, NiO, and ITO represent Al-doped zinc oxide, phenyl-C61-butyric acid methyl ester, nickel oxide, and indium tin oxide, respectively, were evaluated. Without an ITO barrier layer between Ag and AZO, experimental core-level analysis under an applied bias voltage revealed that the migration of iodide (I^-) ions from HaP to adjacent electron and hole transport layers require a threshold voltage above the open-circuit voltage (V_{OC}) [Figure. 1 (*right top*)]. The study also found that the diffusion of I^- in AZO/PCBM over time is unidirectional and follows a concentration gradient. The irreversibility of I^- transport leads to its absorption by the Ag layer, forming a harmful silver iodide (AgI) compound. Additionally, this work demonstrated that the deposition of an ITO layer between Ag and AZO as an ion diffusion barrier layer effectively restrains the formation of AgI, thereby improving the stability and performance of HaPSCs [Figure. 1 (*right bottom*)]. These findings provide new insights to distinguish various degradation mechanisms and enhance the stability and performance of HaPSCs.

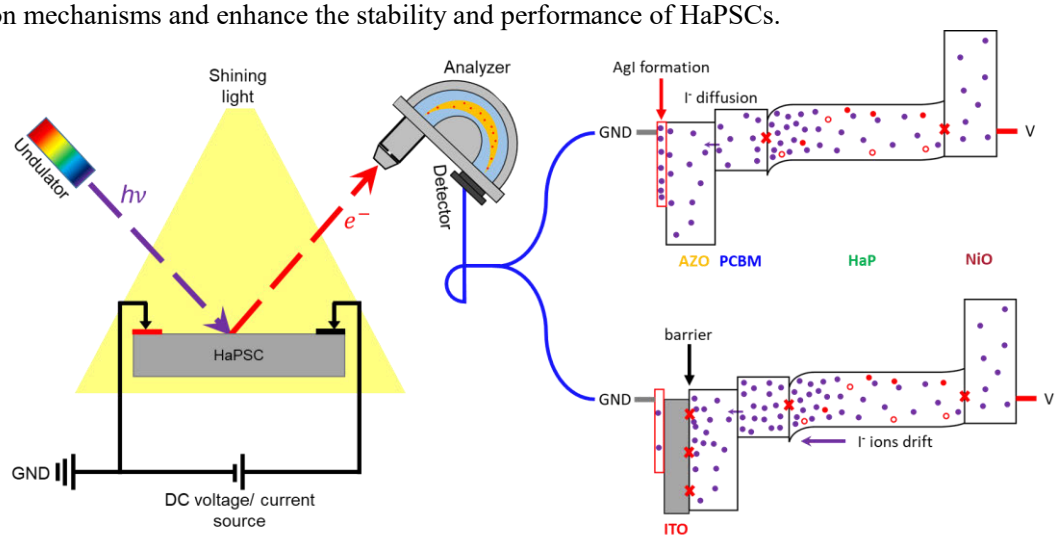

Figure 1: (Left) Simplified operando HAXPES analysis setup under bias voltage based on synchrotron X-rays; (Right) Schematic representative energy band diagram model of samples under 0V reverse and room light: (top) without and (bottom) with ITO barrier layer between Ag and AZO.

1. Best solar cell efficiency chart; https://www.nrel.gov/pv/cell-efficiency.html (Accessed March 06, 2023).
2. Gueye et al., *ACS Appl. Mater. Interfaces* 2021, 13, 42, 50481-50490.
3. Gueye et al., *ACS Chem. Mater.* 2023, 35, 5, 1948-1960.

Resonant Auger spectroscopy on solid xenon on Au, Ag, and Cu substrates

Fredrik O.L. Johansson[1,2,*], Elin Berggren[3], Lucas M. Cornetta[3,4], Denis Céolin[5], Mattis Fondell[6], Hans Ågren[3] and Andreas Lindblad[3]

[1]*Division of Applied Physical Chemistry, Department of Chemistry, KTH Royal Institute of Technology, SE-100 44 Stockholm, Sweden*

[2]*Sorbonne Université, CNRS, Institut des NanoSciences de Paris, INSP, F-75005, Paris, France*

[3]*Division of X-ray Photon Science, Department of Physics and Astronomy, Uppsala University, Box 516, SE-751 20 Uppsala, Sweden*

[4]*Department of Applied Physics, Gleb Wataghin Institute of Physics, State University of Campinas, Campinas, Brazil*

[5]*Synchrotron SOLEIL, l'Orme des Merisiers, Saint-Aubin,Boîte Postale 48, 91192 Gif-sur-Yvette Cedex, France*

[6]*Institute Methods and Instrumentation for Synchrotron Radiation Research PS-ISRR, Helmholtz-Zentrum Berlin für Materialien und Energie, Albert-Einstein-Straße 15, 12489, Berlin, Germany*

**Contact: fjson@kth.se*

Keywords: Resonant Auger, HAXPES, Core Hole Clock

An investigation of the radiationless decay of core excited Xe atoms (Xe $2p_{3/2}\rightarrow nd$ ($n\geq5$) absorption) in the region of Xe $L_3M_{4,5}M_{4,5}$ Auger electron kinetic energies, has been performed for Xe adsorbed on Cu, Ag and Au metal substrates. [1] By doing so, we differentiate between contributions from coherent and incoherent decay channels of the core excited state that build up the X-ray absorption cross section [2].

The intensity distribution of the decay channels is different compared with Xe in the gas-phase [3,4] with no post-collision interaction shifts in the incoherent decay channel for the condensed system is observed within the energy range recorded. Charge transfer of the core excited electron occurs within tens of attoseconds in all studied systems for excitation energies approaching the ionization threshold of the condensed system, whereas charge transfer times are substrate dependent for lower excitation energies, with distinct difference for Au compared with Ag and Cu, which show similar dynamics.

The determination of partial yields in the decay channels allows for observation of a decay channel present in the Xe/Cu and Xe/Ag systems but not in the case of Xe/Au. This extra decay channel is seen on the high kinetic energy side of the incoherent Auger line. Theoretical calculations allow us to interpret this channel as emanating from varying amount of ground state hybridization between Xe and the substrates. This impacts the energy of the Auger final states enabling an identification of these states as system specific features in the experimental data.

1. FOL. Johansson, E. Berggren, LM. Cornetta, D Céolin, M Fondell, H Ågren and A Lindblad, Physical Review A, 107, 032802 (2023)
2. N. Mårtensson, M. Weinelt, O. Karis, M. Magnuson, N. Wassdahl, A. Nilsson, J. Stöhr, and M. Samant, Applied Physics A: Materials Science & Processing 65 (1997)
3. R. K. Kushawaha, K. Jänkälä, T. Marchenko, G. Goldsztejn, R. Guillemin, L. Journel, D. Céolin, J. P. Rueff, A. F. Lago, R. Püttner, M. N. Piancastelli, and M. Simon, Physical Review A, 92, 013427 (2015)
4. G. B. Armen, S. H. Southworth, J. C. Levin, U. Arp, T. LeBrun, and M. A. MacDonald Physical Review A, 56, 2, (1997)

Insights into solvated nanocrystal molecular surfaces via micro-jet electron spectroscopy

Arnaldo Naves de Brito

Department of Applied Physics, University of Campinas, Campinas, Brazil

Keywords: Electron spectroscopy, micro-jet, surface composition

In this talk, we present a combined cylindrical micro-jet photoelectron spectroscopy (cMJ-PES) and theoretical simulations to study the interface of perovskite nano-crystals[1]. These crystals hold great promise for low-cost and efficient solar cells. However, due to contamination and radiation damage in conventional X-ray spectroscopic methods, understanding the atomic surface composition and chemical properties is a significant challenge. We have developed a groundbreaking approach using cylindrical cMJ-PES to overcome these obstacles. This methodology enables us to accurately analyze and compare the surface atomic composition of different diluted nanocrystals. By studying two $CsPbBr_3$ nanocrystals synthesized using different methods, we have discovered that improved stability is associated with the absence of Cs and Br substitution. We have also determined the ratio between Br/Cs and Pb/Cs signals in spectroscopy, considering contributions from layers beneath the surface.

Additionally, we have complemented our research with quantum mechanics calculations, which have allowed us to predict that even smaller nanocrystals (less than 1 nm) have the potential to exhibit even more excellent stability. These findings provide a solid foundation for developing nanocrystals with enhanced properties. If time allows, we plan to discuss insights into the hydrogen bonding and surface composition of ethanol-water mixtures [2,3,4].

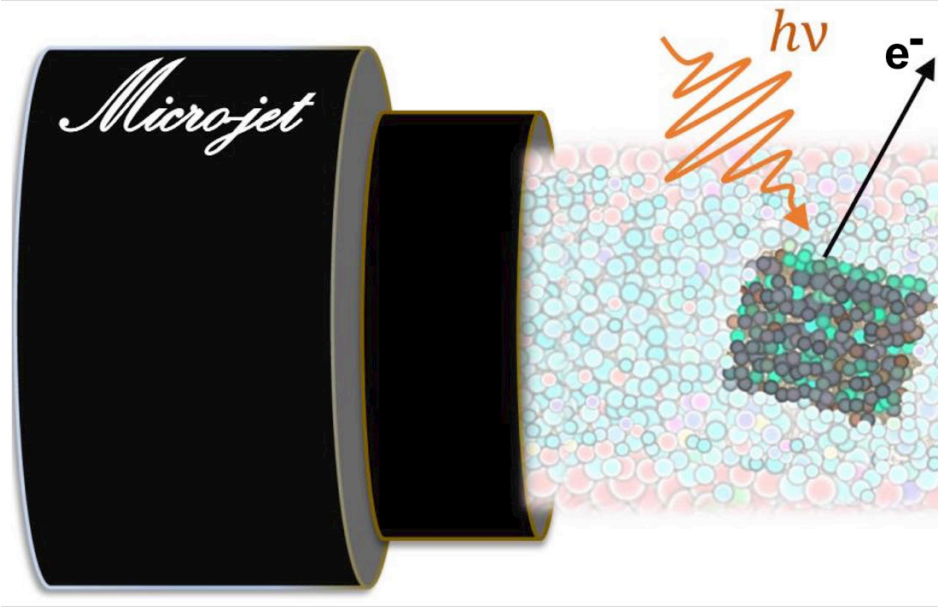

1. Pinheiro, J.; Cornetta, L.; Bonato, L.; Gallo, T.; Zagonel, L. F.; Safadi, Bill; Bjõrneholm, Olle; Walsh, N.; Öhrwall, G.; Nogueira, A. F.; Naves de Brito, A. Atomic-scale probe of lead-halide perovskites nanocrystals surface by micro-jet X-ray photoelectron spectroscopy Sub to ACS Energy Letter **2023,** *00*, 0000.

Ågren, H.; Björneholm, O.; Öhrwall, G.; Carravetta, V.; de Brito, A. N. Ethanol in Aqueous Solution Studied by Microjet Photoelectron Spectroscopy and Theory. *Acc. Chem. Res.* **2022,** *55*, 3080-3087.

2. Marinho, R. R. T.; Walz, M.-M.; Ekholm, V.; Öhrwall, G.; Björneholm, O.; Naves de Brito, A. Ethanol Solvation in Water Studied on a Molecular Scale by Photoelectron Spectroscopy. *J. Phys. Chem. B* **2017,** *121*, 7916-7923.

3. Carravetta, V.; Gomes, A. H. d. A.; Marinho, R. d. R. T.; Öhrwall, G.; Ågren, H.; Björneholm, O.; de Brito, A. N. An Atomistic Explanation of the Ethanol–Water Azeotrope. *Phys. Chem. Chem. Phys.* **2022,** *24*, 26037-26045.

4. Kirschner, J.; Gomes, A. H. A.; Marinho, R. R. T.; Björneholm, O.; Ågren, H.; Carravetta, V.; Ottosson, N.; Brito, A. N. d.; Bakker, H. J. The Molecular Structure of the Surface of Water–Ethanol Mixtures. *Phys. Chem. Chem. Phys.* **2021,** *23*, 11568-11578.

Oxidation of transition metal complexes in solution by resonant X-ray spectroscopy and operando electrochemistry

Robert Temperton[1*], Robert Seidel[2], Andrey Shavorskiy[1], Joachim Schnadt[1], Jens Uhlig[3] and Petter Persson[3]

1 MAX IV Laboratory, Lund University, Lund, Sweden
2 Helmholtz-Zentrum Berlin für Materialien und Energie, Berlin, Germany
3 Department of Chemistry, Lund University, Lund, Sweden
**Contact: robert.temperton@maxiv.lu.se*

Keywords: organometallic, electrochemistry, liquid-jet, photoelectron spectroscopy

The tunable electronic structure properties of organometallic complexes underpin their suitability for charge-transfer applications, such as light harvesting or catalysis. Specifically, the properties of a complex under reduction or oxidation conditions are critical to their performance in devices, including where the redox processes are photo-induced or driven electrochemically. Here we present two methods, based around photoelectron spectroscopy, for measuring the electronic structure properties of organometallic complexes in solution:

Resonant photoelectron spectroscopy (RPES) is a powerful probe of electronic structure. In RPES, the energy of incident X-ray photons is tuned to match core-valence excitations to create a core-excited state. The resulting Auger-like decay processes from this excited state can include an autoionization mechanism (referred to as participant decay) whereby one valence electron fills the core-hole and another is ejected leaving the sample in an oxidized final state. Photoelectron spectroscopy measurements of these ejected electrons can therefore provide a probe of the complex in a photo-oxidized final state. This can provide a direct measurement of fundamental electronic properties, such as the metal-ligand interactions that underpin the photophysical properties of a complex.[1] Here we present liquid-microjet measurements of $Fe^{II/III}(CN)_6$ in aqueous solution, where RPES measurements at the Fe L_3 absorption edge provided a site specific probe of the metal center of the complex. We discuss spin-coupling processes that can occur at the metal center of the open-shell Fe^{III} version of the complex, where following the autoionization of $Fe^{III}(CN)_6$, we observe a dramatic 4x propensity towards the a higher energy singlet final state compared to the lowest lying triplet final states.[2]

Operando photoelectron spectroscopy. We present how the "dip-and-pull" technique (Figure 1) can be used to electrochemically induce molecular redox reactions in a complex in solution, and measure the resulting change in oxidation state using ambient pressure photoelectron spectroscopy. We show we are able to reduce and then re-oxidize $Fe^{III}(CN)_6$, and observe the oxidation state changes in the Fe 2*p* spectra.[3]

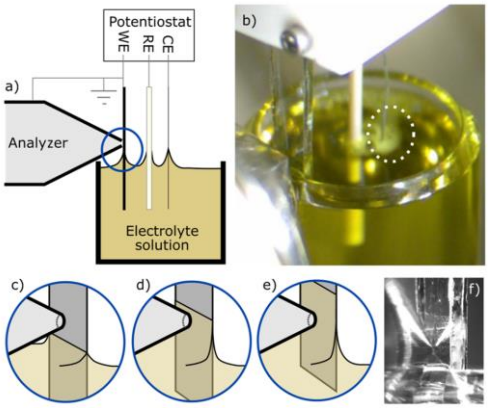

Figure 1: (a) Scheme of the dip-and-pull setup at the HIPPIE beamline (MAX IV Laboratory), where WE, RE, and CE are the working, reference, and counter electrodes, respectively. (b) Photograph of the setup. (c)–(e) Scheme of the dip-and-pull process. The electrodes are first "dipped" [position (c)] before being "pulled" up, with measurements taken while slowly moving between positions shown in (d) and (e). (f) Photograph of the working electrode during measurements.

1. R. Temperton et al., "Resonant X-ray photo-oxidation of light-harvesting iron (II/III) N-heterocyclic carbene complexes," Sci. Rep. **11**(1), 1–14 (2021).
2. R. Temperton, W. Quevedo, R. Seidel, J. Uhlig, J. Schnadt, and P. Persson, "Spin propensity in resonant photoemission of transition metal complexes," Phys. Rev. Res. **3**(3), 033030 (2021).
3. R. Temperton et al. "Dip-and-pull ambient pressure photoelectron spectroscopy as a spectroelectrochemistry tool for probing molecular redox processes," J. Chem. Phys. 157(24), 244701 (2022).

Aqueous-phase photoemission for chemical analysis

Lukáš Tomaník[1],* Bernd Winter[2], and Petr Slavíček[1]

1 Department of Physical Chemistry, University of Chemistry and Technology, Prague, Czech Republic

2 Department of Molecular Physics, Fritz Haber Institute of the Max Planck Society, Berlin, Germany

**Contact: tomanikl@vscht.cz*

Keywords: liquid-jet photoelectron spectroscopy, photoemission, *ab initio* modeling, aqueous phase

Photoemission from aqueous systems can be systematically studied thanks to a progress in photoelectron spectroscopy over the past twenty years. The novel technique called liquid-jet photoelectron spectroscopy (LJ-PES) [1–2] enabled probing of the electronic structure of aqueous-phase molecules. Consequently, even completely new electronic relaxation processes were observed in liquids. [3–4]

I will demonstrate the broad applicability and potential of LJ-PES to probe the chemical state of various systems using several of our studies with a combined experimental-theoretical approach. Particularly, (i) site-specific probing of acid-base chemistry will be introduced for the glucose molecule. It has five hydroxyl groups (–OH) in its cyclic form that could, in principle, deprotonate, and we demonstrate that we can unequivocally assign the deprotonation center, as introduced in Figure 1. (ii) The unraveling of structured solute-solvent interactions using LJ-PES is shown on the indole molecule, the structural motif being part of important biomolecules such as tryptophan. (iii) Probing of Mg^{2+} interactions with adenosine triphosphate (ATP) in the aqueous solution is explored. Here we utilize not only primary photoionization but also a secondary relaxation process called intermolecular coulombic decay (ICD). (iv) Extended possibilities to specifically probe acid-base states are also demonstrated for double deprotonation, as we show on ascorbic acid (vitamin C).

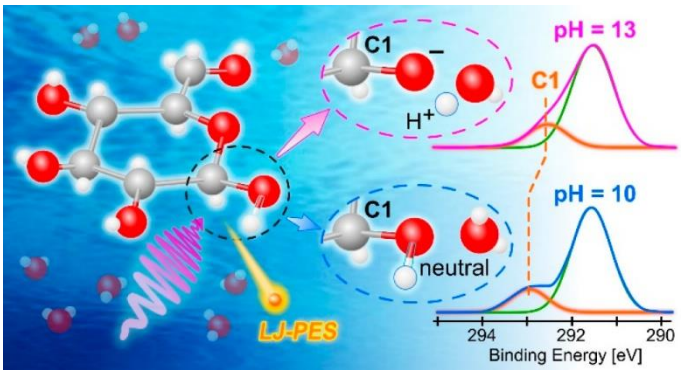

Figure 1: The schematics of applying LJ-PES to probe acid-base chemistry of aqueous-phase glucose. [5]

Ab initio modeling accompanies all the included studies to interpret the data. The pragmatic approach exhibiting an excellent price-performance ratio is used. It is based on neglecting the outgoing electron in the description of ionization, the method often called sudden ionization approximation, and a thrifty description of solvation using a hybrid explicit/implicit model.

The support from the Czech Science Foundation, project no. 21-26601X (EXPRO) is gratefully acknowledged.

1. R. Signorell, B. Winter, Photoionization of the aqueous phase: clusters, droplets and liquid jets, *Physical Chemistry Chemical Physics* **24**, 13438– 13460 (2022).
2. B. Winter, Photoemission from Liquid Aqueous Solutions, *Chemical Reviews* **106**, 1176–1211 (2006).
3. T. Jahnke, U. Hergenhahn, B. Winter, R. D rner, U. Fr hling, P. V. Demekhin, K. Gokhberg, L. S. Cederbaum, A. Ehresmann, A. Knie, A. Dreuw, Interatomic and Intermolecular Coulombic Decay, *Chemical Reviews* **120**, 11295−11369 (2020).
4. I. Unger, R. Seidel, S. Th rmer, M. N. Pohl, E. F. Aziz, L. S. Cederbaum, E. Muchová, P. Slavíček, B. Winter, N. V. Kryzhevoi, Observation of electron-transfer-mediated decay in aqueous solution, *Nature Chemistry* **9**, 708–714 (2017).
5. S. Malerz, K. Mudryk, L. Tomaník, D. Stemer, U. Hergenhahn, T. Buttersack, F. Trinter, R. Seidel, W. Quevedo, C. Goy, I. Wilkinson, S. Th rmer, P. Slavíček, B. Winter, Following in Emil Fischer's Footsteps: A Site-Selective Probe of Glucose Acid–Base Chemistry, *The Journal of Physical Chemistry A* **125**, 6881–6892 (2021).

Study of the electronic structure of iron metal complexes in aqueous solution by X-ray spectroscopies

Nour El Houda AZZOUZA[1,2], Loïc JOURNEL[1], Denis CEOLIN[2]

1 Sorbonne Université, CNRS, UMR 7614, Laboratoire de Chimie Physique-Matière et Rayonnement, 4 Place Jussieu, F-75005 Paris, France

2 Synchrotron SOLEIL, L'Orme des Merisiers, Saint-Aubin, F-91192 Gif-sur-Yvette Cedex, France

**Contact: houda.azzouza@sorbonne-universite.fr*

Keywords: HAXPES, liquid microjet, metal complexes.

Metal complexes are versatile and find applications in chemistry and biology. This is for instance the case for iron complexes which act as redox centers in metalloproteins such as hemoglobin. Their properties depend on their chemical environment, notably the interactions between the metallic center and the ligands, as well as the complex's interaction with the solvent [1].

A detailed description of their electronic structure allows a better understanding of the processes in which they are involved. In this context, X-ray photoemission spectroscopy (XPS) is a powerful technique for their study. It provides valuable information about metal-ligand interactions and is highly sensitive to different types of ligands and coordination environments [2]. Numerous investigations [3-5] have focused on the electronic structure of iron complexes, however there are very few photoemission results for these systems diluted in aqueous solution.

We present XPS spectra of aqueous potassium ferrous $[Fe(II)(CN)_6]^{4-}$ and ferric $[Fe(III)(CN)_6]^{3-}$ hexacyanide complexes. These two complexes have the same octahedral geometry and differ only in their charge state $2^+/3^+$ respectively. The experiments were conducted at the GALAXIES beamline of SOLEIL [6] using a liquid microjet adapted to the high kinetic energy photoemission spectrometer (HAXPES) [7].

The photoemission spectra were recorded at the iron 1s, 2p, and 3p edges, as well as at the carbon and nitrogen 1s edges. Our results revealed that the change in oxidation states leads to their large modification. Specifically the C 1s and N 1s spectra exhibit satellite structures for Fe(II), which are absent in Fe(III). The Fe(III) $2p_{3/2}$ spectrum exhibits a high binding energy shoulder that is not present in Fe(II), interpretated as a charge transfer from ligand to the metal.

This study reveals significant differences between the two complexes due to the charge state of the metallic center. This emphasizes the importance of studying metal complexes in solution to gain a comprehensive understanding of their behavior and properties.

1. R. Golnak et al., Sci. Rep., 2016, 6, 24659.
2. A. Cano et al., J. Inorg. Chem., 2019, 1724.
3. R. K. Hocking et al., J. Am. Chem. Soc. 2006, 128, 32, 10442-10451.
4. T. Yamashita et al., Appl. S. Sci., 2008, 54, 8, 2441-2449.
5. M. Ross et al., J. Phys. Chem., 2018, 122, 19, 5075–5086.
6. J. P. Rueff et al., J. Synch. Rad., 2015, 22(1), 175-179.
7. D. Ceolin et al., J. Electron Spectrosc. Relat. Phenom., 2013, 190 part B: 188–192.

Exploring Phase in Soft X-ray Spectroptychography

Joseph Stitsky[1], Jian Wang[1,2] and Stephen Urquhart[1,*]

1 Chemistry, University of Saskatchewan, Saskatoon, Canada
2 Canadian Light Source, University of Saskatchewan, Saskatoon, Canada
**Contact: stephen.urquhart@usask.ca*

Keywords: X-ray microscopy, ptychography, spectromicroscopy, chemical microanalysis

X-ray spectroptychography is an emerging chemical microanalysis method that builds upon well-established synchrotron X-ray microscopy and spectromicroscopy techniques, with added spatial resolution from ptychography. In ptychography, a coherent beam is scanned across the sample to create a dataset of overlapping diffraction patterns, which are processed with an iterative reconstruction algorithm to yield amplitude and phase information for the sample and X-ray probe.[1] When combined with near edge X-ray absorption fine structure (NEXAFS) ptychography – or spectroptychography[2] – can provide chemical microanalysis at higher spatial resolutions than that provided with conventional X-ray optics.

NEXAFS spectroscopy – from the amplitude signal of spectroptychography – has a direct chemical interpretation and is widely used for microanalysis of materials. Ptychography allows us to access the 'phase' spectrum, which has a tantalizing variation with chemistry. In some cases, phase may have a greater or perhaps a different sensitivity; however, the relationship with 'chemistry' is much less direct and more difficult to rationalize. This chemical sensitivity is illustrated in Figure 1, where amplitude (a) and phase (b) images highlight different contrast for an ensemble of Fe_2O_3 nanoparticles, and where amplitude and phase spectra(c) show distinct differences.

This presentation will discuss our work to explore chemistry and chemical microanalysis through soft X-ray spectroptychography, and exploration of the chemical sensitivity of phase.

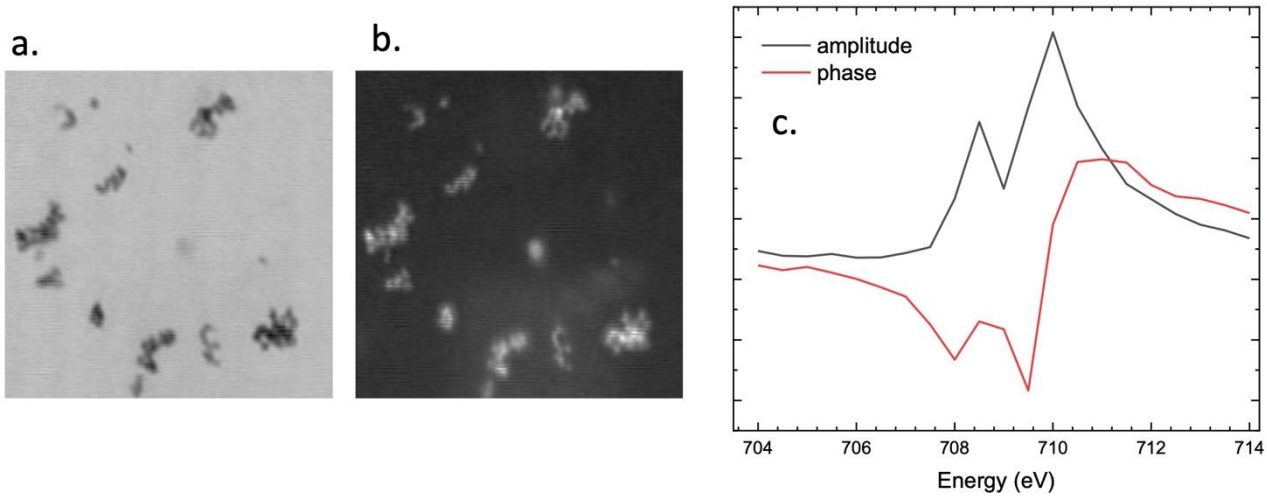

Figure 1 Spectroptychography of 30 nm diameter Fe_2O_3 nanoparticles; Amplitude (a) and Phase (b) ptychography images (2.1 x 2.1 micron), recorded at 710.0 eV. (c) Absorption (optical density) and phase Fe L_3 spectra, obtained from this sample.[2]

1. F. Pfeiffer, Nat. Photonics 2018, 12, 9–17.
2. S.G. Urquhart, ACS Omega 2022, 7, 11521–11529.

In-situ spectromicroscopy studies of Cu catalysed CO_2 electroreduction by soft X-ray STXM and spectro-ptychography

Adam P. Hitchcock,[1*] Chunyang Zhang,[1,2] Haytham Eraky[1] and Drew Higgins[2]

1 Dept. of Chemistry & Chemical Biology, McMaster University, Hamilton, ON, Canada

*2 Dept. of Chemical Engineering,, McMaster University, Hamilton, ON, Canada *Contact: aph@mcmaster.ca*

Keywords: STXM, ptychography, electro-catalysis, *in-situ* liquid flow electrochemical reactor

At present there is a major effort worldwide to develop and optimize catalysts for electrochemical reduction of CO_2 (CO_2R) [1]. Powered by renewable electricity, CO_2R has the potential, not only to consume CO_2, but also produce useful chemical products. Cu-based CO_2R electrocatalysts can produce valuable multi-carbon products like ethanol and ethylene, but yields and selectivity are not yet optimized [2]. The morphology and chemical composition of Cu catalysts change during the reaction, which means pre- / post-reaction *ex-situ* studies are of limited value. *in-situ* characterization methods that enable control of the local reaction conditi-ons and applied electrochemical potentials can provide mechanistic insights into CO_2R processes.

Soft X-ray scanning transmission microscopy (STXM) is a powerful tool for nanoscale materials analysis. Ptychography (scanning coherent diffraction imaging), which can be measured using soft X-ray STXMs equipped with a post specimen X-ray camera, provides better spatial resolution (~10 nm, as opposed to ~30 nm for conventional STXM). Recently we have developed a STXM/ptychography *in-situ* device with controlled electrolyte flow, rapid electrolyte exchange, and full electrochemical control in a classical 3-electrode configuration (Fig.1a,b) [3]. This device has been used for soft X-ray STXM [4] and ptychography [5] studies of Cu catalysed CO_2 electroreduction. STXM results (Fig. 1c) show that, mixed Cu(0)/Cu(I) nanoparticles generated by *in-situ* electro-deposition, are reduced to Cu metal at +0.2 V_{RHE} more positive potential than the onset of CO_2R, showing that the active catalyst is metallic Cu during the CO_2R process at −0.6 V_{RHE} [4]. *In-situ* spectro-ptychography studies, at significantly improved spatial resolution, tracked reduction of the initial mixed-oxidation state of a single Cu nanoparticle to metallic Cu as a function of potential and detected CO_2R reaction-induced modifications of the shape of the particle [5].

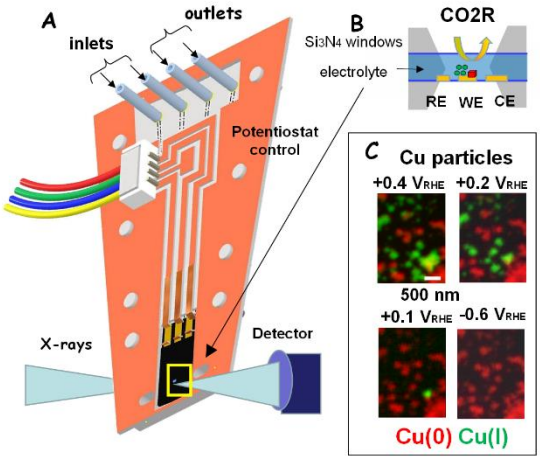

Figure 1. (a, b) Flow electrochemical *in-situ* device for *in-situ* STXM and ptychography studies. (c) Maps of oxidation states of Cu catalyst particles at different potentials. CO_2R starts at −0.4 V_{RHE}

1. De Luna, P. et al. What would it take for renewably powered electrosynthesis to displace petrochemical processes ? *Science* **364**, p.eaav3506 (2019).
2 T.C. Chou, et al. Controlling the oxidation state of the Cu electrode and reaction intermediates for electrochemical CO_2 reduction to ethylene. *J. American Chemical Society* **142**, 2857-2867 (2020).
3. C. Zhang, et al. *In-situ* STXM Characterization of Cu/Cu_2O Electrocatalysts for CO_2 Reduction, *AIP Conference Proceedings* (2023) in press
4. C. Zhang, et al. *In-situ* Studies of Copper-based CO_2 Reduction Electrocatalysts by Scanning Transmission X-ray Microscopy, *Nature Catalysis* (2023) submitted.
5. C. Zhang, et al. Copper CO_2-Reduction Electrocatalysts studied by *In-situ* Soft X-ray Spectro-Ptychography, Nature Communication, in review. ChemRxiv. Cambridge: Cambridge Open Engage; 2023

Applications of X-ray/neutron holography to semiconductor defect evaluations

Koichi Hayashi*

Department of Physical Science and Engineering, Nagoya Institute of Technology, Nagoya, Japan
**Contact: khayashi@nitech.ac.jp*

Keywords: semiconductor, defect, local structure, X-ray fluorescence holography, neutron holography

It is very important to evaluate the state of defects in semiconductors for the further development of electronic devices. However, details of their local structures can be hardly determined by conventional methods. For this reason, we have developed atomic-resolution holography, such as X-ray fluorescence holography (XFH) and neutron holography (NH).[1] The atomic resolution holography can observe 3D local structures around specific elements. In particular, since we have worked on X-ray fluorescence holography for a quarter of a century, it has been applied to many materials to clear the roles of detects.

In the presentation, first I will introduce the XFH application to defects in CdTe, which is used in solar cells. Compared to the Si solar cell, the energy cost for production of a CdTe solar cell is lower, and therefore it is widely used in the world. However, its disadvantage is the small conversion efficiency, which is a serious issue of the CdTe solar cell. Although As dopant has been used for producing hole, it has long believed that some As atoms form harmful defects, that capture holes. To clear this problem, we measured As Kα XFH holograms from As-doped CdTe singles crystal. The reconstructed atomic images showed local structures around As substituting for both Te and As sites, which are termed As_{Te} and As_{Cd}, respectively. The As_{Cd} produces electrons. Furthermore, by the combination with density functional theory (DFT) calculation, we found that the some As_{Cd} was accompanied with Cd vacancy (V_{Cd}). The activation energy of hole generation from the As_{Cd}-V_{Cd} defect complex is as high as 240 meV. [2]

Next, I will introduce the application of neutron holography to B-doped SiC. This material has recently attracted much interest for its LED applications. Boron highly emits prompt γ-rays after absorbing neutrons. The γ-rays can be used equivalently to X-ray fluorescence in XFH. The polytype of mother SiC crystal is 6H, in which there are six different crystallographic sites. It has been believed that different occupied sites have different impurity levels. 3D atomic images from neutron hologram revealed both silicon and carbon substitutions. To determine boron locations more accurately, we calculated holograms with varying occupancies of six different sites, and fit image intensities with those obtained from experimental holograms by the steepest descent method. Eventually, we found that B-atoms were selectively located at the Si- and C-cubic site layer.[3]

We believe that these results provide important clues for improving the effective active sites in semiconductors.

1. K. Hayashi and P. Korecki, J. Phys. Soc. Jpn. 87, 061003 (2018).
2. A. Nagaoka, et al., J. Am. Chem. Soc. 145, 9191 (2023).
3. K. Hayashi, M. Lederer, Y.Fukumoto, M. Goto, Y. Yamamoto, N. Happo, M. Harada, Y. Inamura, K. Oikawa, K. Ohoyama ,and P. Wellmann, Appl. Phys. Lett.120, 132101 (2022).

Photoemission study of twisted monolayers and bilayers of WSe_2 on graphite substrates

B. Parashar[1,2], L. Rathmann[3], H.-J. Kim[4], I. Cojocariu[1], A. Bostwick[5], C. Jozwiak[5], E. Rotenberg[5], J. Avila[6], P. Dudin[6], V. Feyer[1], C. Stampfer[3], B. Beschoten[3], G. Bihlmayer[4], C. M. Schneider[1], and L. Plucinski[1,*]

1 Peter Grünberg Institut (PGI-6), Forschungszentrum Jülich GmbH, 52428 Jülich, Germany

2 Fakultät für Physik, Universität Duisburg-Essen, 47048 Duisburg, Germany

3 2nd Institute of Physics and JARA-FIT, RWTH Aachen University, 52074 Aachen, Germany

4 Peter Grünberg Institute (PGI-1), Forschungszentrum Jülich GmbH, 52425 Jülich, Germany

5 Advanced Light Source, Lawrence Berkeley Nat. Laboratory, One Cyclotron Road, Berkeley, California 94720, USA

6 Synchrotron-SOLEIL, Université Paris-Saclay, Saint-Aubin, BP48, F91192 Gif sur Yvette, France

**Contact: l.plucinski@fz-juelich.de*

Keywords: angle-resolved photoelectron spectroscopy (ARPES), micro-ARPES

Using microfocused angle-resolved photoemission spectroscopy we investigated exfoliated microstructures containing regions of single-layer (SL) and bilayer (BL) WSe_2 on graphite substrates at different twist angles between SL WSe_2 and graphite and within the BL WSe_2 [1], with the results from the one of the microflake structures shown in Fig. 1(a-c). We investigated two twisted BL WSe_2 at twist angles ~28° and ~10° and found no evidence of hybridization gaps at the interlayer band-crossing points, that could be signatures of the moire physics and precursors of the flat bands at smaller twist angles. Similarly, no such gaps were found for SL WSe_2/graphite. Experimental results are complemented by theoretical density functional theory calculations, which suggest that a formation of hybridization gaps in the WSe_2/graphene (which approximates the experimental WSe_2/graphite system) sensitively depends on the WSe_2 band character at the crossing point with the graphene Dirac band. Fermi level electrons emitted from the graphite are sharply focused near their K_{gr} points in the Brillouin zone, and, when passing through the WSe_2, get diffracted to form band replicas readily observed in experimental Fermi surface maps from twisted SL WSe_2/graphite, with the result from another microsctructure shown in Fig. 1(d). Previously Ulstrup et al. [2] have measured analogue, although less sharp, band replicas in the reversed graphene/WSe_2 interface.

This work paves the way for designing future experiments on twisted TMDC bilayers at smaller twist angles, which would enable imaging their fascinating predicted properties such as topologically nontrivial flat bands.

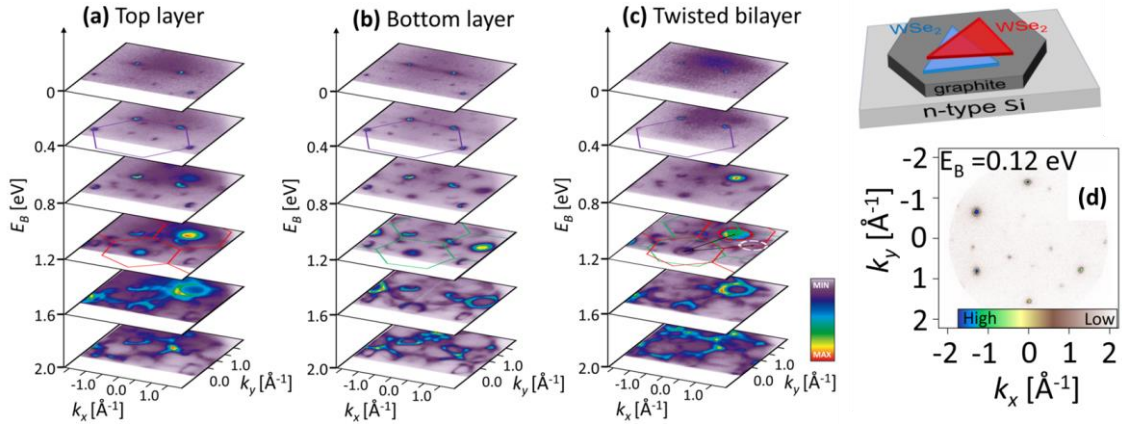

Figure 1: ARPES spectra from WSe_2 SLs and BL from twisted bilayer WSe_2 (twist angle ~28°) on graphite substrate. (a), (b) Show maps from top and bottom SLs, and (c) from the BL. Right top corner shows the schematic diagram of the sample. (d) Fermi surface maps of another monolayer WSe_2/graphite microstructure, showing the main *K* points of graphite, as well as multiple copies related the diffraction of the electrons through the WSe_2 monolayer.

1. B. Parashar, L. Rathmann, H.-J. Kim, I. Cojocariu, A. Bostwick, C. Jozwiak, E. Rotenberg, J. Avila, P. Dudin, V. Feyer, C. Stampfer, B. Beschoten, G. Bihlmayer, C. M. Schneider, and L. Plucinski, Photoemission study of twisted monolayers and bilayers of WSe_2 on graphite substrates, Phys. Rev. Lett. 130, 146401 (2023), https://doi.org/10.1103/PhysRevMaterials.7.044004
2. S. Ulstrup, R. J. Koch, S. Singh, K. M. McCreary, B. T. Jonker, J. T. Robinson, C. Jozwiak, E. Rotenberg, A. Bostwick, J. Katoch, and J. A. Miwa, Direct observation of minibands in a twisted graphene/WS_2 bilayer, Sci. Adv. 6, eaay6104 (2020), https://doi.org/10.1126/sciadv.aay6104

Efficient simulation of photoelectron spectra with trajectory surface hopping

Tomislav Piteša[1] and Nađa Došlić[1,*]

1 Ruđer Bošković Institute, Zagreb, Croatia

**Contact: nadja.doslic@irb.hr*

Keywords: adiabatic to diabatic transformation, time-resolved photoelectron spectroscopy cyclohexadiene

Trajectory surface hopping (TSH) methods are routinely applied to study ultrafast photo-induced processes in organic and biomolecules. In TSH, nuclear trajectories are propagated classically on a single Born-Oppenheimer surface, whereas hops between electronic states are dictated by a stochastic algorithm. As TSH methods are usually implemented on-the-fly, they bypass the main limitations of quantum nuclear dynamics - the requirement for precalculated global potential energy surfaces and the exponential scaling of computational costs with the number of nuclear degrees of freedom. However, it is not straightforward to assess the accuracy of TSH simulations [1,2]. The comparison with fully quantized methods is made difficult because quantum calculations are run in the basis of diabatic states, while TSH simulations are performed in the adiabatic basis. A possible approach would be to compute the diabatic populations in TSH simulations. In the first part of this talk, I'll discuss algorithmic and computational challenges encountered when computing diabatic populations in TSH simulations.

In recent years, TSH simulations are increasingly used as a basis for computational spectroscopy. Specifically, the implementation of efficient methods for the computation of photoelectron spectroscopy observables and the development of trajectory-based protocols for the simulation of photoelectron spectroscopy signals [3] allowed us to monitor the excited-state dynamics with unprecedented efficiency. Here I'll present a protocol for simulating and interpreting time-resolved photoionization spectra and selected applications to systems of current interest. [4,5]

1. W. Xie *et al*. Assessing the performance of trajectory surface hopping methods: Ultrafast internal conversion in pyrazine, *J. Chem. Phys.* **150**, 154119 (2019)
2. J. Coonjobeeharry *et al.* Mixed-quantum-classical or fully-quantized dynamics? A unified code to compare methods, *Philos. Trans. Royal Soc. A* **380**, 20200386 (2022)
3. M. F. Gelin *et al.* Ab Initio Surface-Hopping Simulation of Femtosecond Transient-Absorption Pump–Probe Signals of Nonadiabatic Excited-State Dynamics Using the Doorway–Window Representation, *J. Chem. Theory Comput.* **17**, 2394–2408 (2021)
4. T. Piteša *et al.* Combined Surface-Hopping, Dyson Orbital, and B-Spline Approach for the Computation of Time-Resolved Photoelectron Spectroscopy Signals: The Internal Conversion in Pyrazine, *J. Chem. Theory Comput.* **17**, 5098-5109 (2021)
5. O. Travnikova *et al.* Photochemical Ring-Opening Reaction of 1,3-Cyclohexadiene: Identifying the True Reactive State, *J. Am. Chem. Soc.* **144**, 21878–21886 (2022)

First Principles Calculations of the Optical Response of $LiNiO_2$ – a promising cathode material in Cobalt free Lithium ion batteries

S. Assa Aravindh[1*], V. Kothalawala[2], J. Nokelainen[3], M. Alatalo[1], B. Barbiellini[2], Tao Hu[4], Ulla Lassi[1b], K. Suzuki[4], H. Sakurai[4] and Arun Bansil[3]

1 Nano and Molecular Systems Research Unit, University of Oulu, Finland
1b Research Unit of Sustainable Chemistry, University of Oulu, Finland
2 Department of Physics, School of Engineering Science, LUT University, 53851 Lappeenranta, Finland
3 Department of Physics, Northeastern University, Boston, MA 02115, USA
4 Graduate School of Science and Technology, Gunma University, Kiryu 376-8515, Gunma, Japan

**Contact: Assa.Sasikaladevi@oulu.fi*

Keywords: $LiNiO_2$, DFT, Cathode material, Optical properties, Electronic structure, RIXS

With the current focus on clean energy, demand for more efficient batteries with greater capacity and lighter weight is inevitable and lithium-ion batteries (LIBs) are promising due to their higher power and energy densities [1]. Therefore, interest has been growing in electrode materials as well such as LiNiO2, (LNO) as an environmentally friendly cathode material, which offers higher discharge capacity and lower cost compared to other conventional materials [2]. However, stability concerns exist and it is important to understand the interplay between the structural, electronic, and optical properties of LNO for efficient battery performance. Therefore, we investigate the LNO ground state in-depth by using density functional theory (DFT) based first-principles simulations, employing different approximations such as generalized gradient approximation (GGA) and strongly-constrained-and-appropriately-normed (SCAN) exchange-correlation functionals, along with computations using the DFT+U scheme [3], in order to capture the strong correlation effects in LNO. Optical properties of LNO are computed, including the dielectric function, refractive index (Fig1), and the absorption coefficient. We also compute the energy loss function, which is related to the resonant inelastic X-ray scattering (RIXS) cross Section, and compare with available experimental results, to understand the redox reactions that can occur at the LNO cathodes. The computed refractive index (3.56) and energy loss function is consistent with RIXS experiments and displays a maximum related to the electronic states responsible for the redox potential of the LNO cathode.

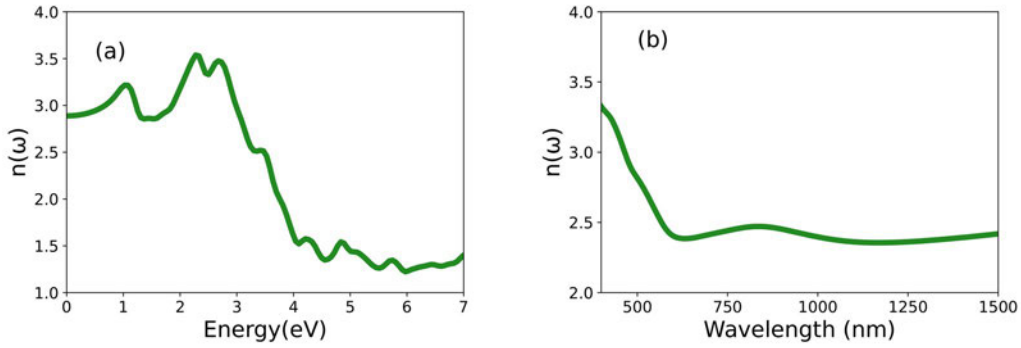

Figure 1: The Computed refractive index of LNO as a function of (a) energy and (b) wavelength.

1. D. Larcher, J. Tarascon, Towards greener and more sustainable batteries for electrical energy storage, *Nat. Chem.*,**7**, 19–29 (2015).
2. Y. Kim, W. M. Seong, A. Manthiram, Cobalt-free, high-nickel layered oxide cathodes for lithium-ion batteries: Progress, challenges, and perspectives, *Energy Storage Mater.*, **34,** 250–259 (2021).
3. V.I. Anisimov, J. Zaanen, J, O. K. Andersen, Band theory and Mott insulators: Hubbard U instead of Stoner I, *Phys. Rev. B*,***44,*** 943–954 (1991).

Ultrafast Control of Entanglement Enabled by Time-Resolved RIXS

Yao Wang
[1] *Department of Physics and Astronomy, Clemson University*

The rapidly evolving quantum science calls for precise and predictive control of collective electronic properties beyond the classical realm. Among various control knobs, an ultrafast laser pump is a promising approach due to its rich degrees of freedom. Together with the laser's capability of influencing electronic structure comes the necessity to track the instantaneous status of a time-dependent nonequilibrium material. Novel pump-probe spectral techniques play a critical role in bridging experiments and theory and quantifying the nonequilibrium state of materials.

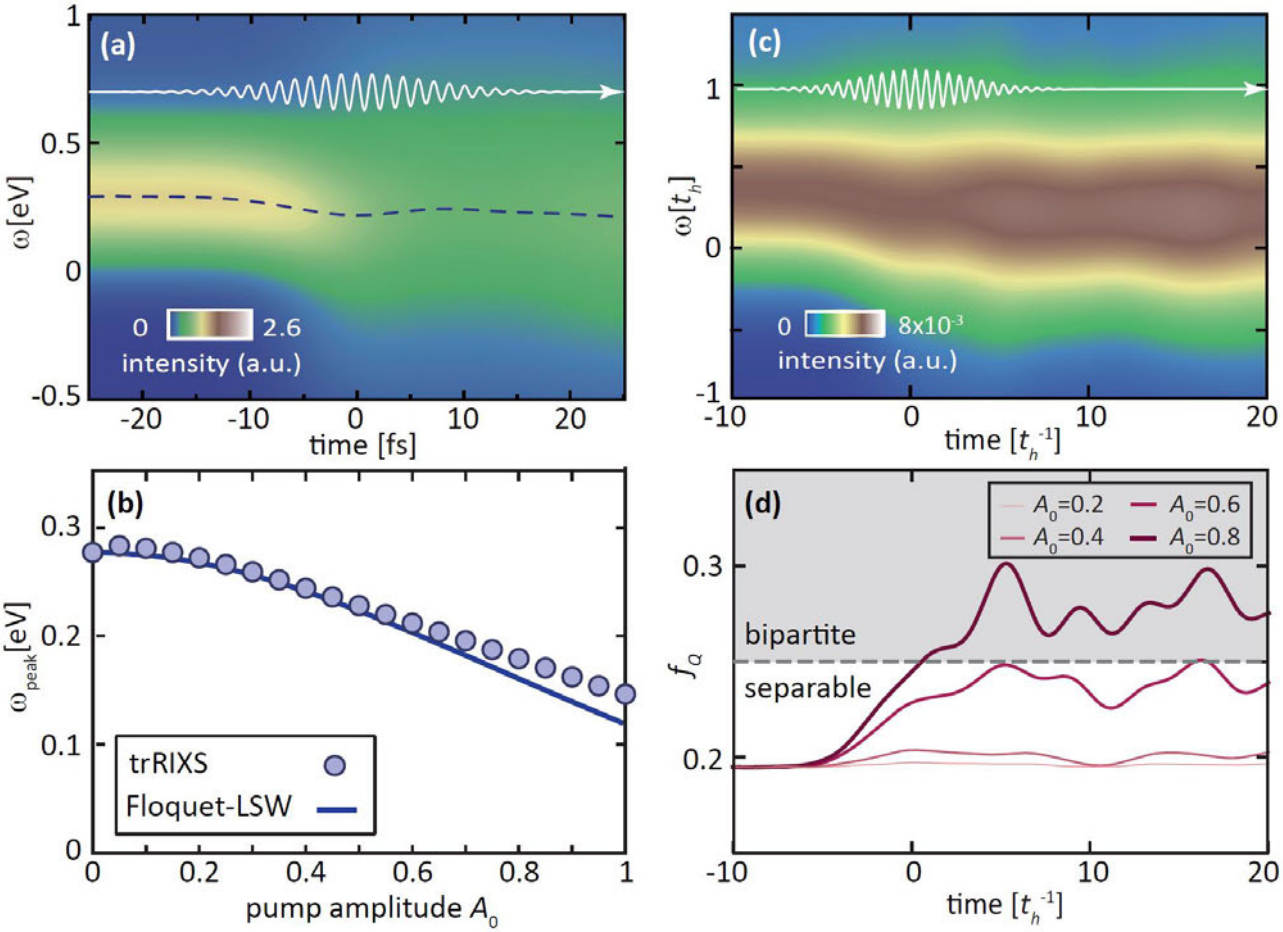

Fig. 1. (a)*: Collective spin excitations measured by trRIXS in a 2D doped Mott insulator, reflecting the light-induced softening of paramagnons. The dashed line tracks the evolution of the peak position in time, following the pump pulse (white line).* ***(b)*** *The comparison of the transient paramagnon energy (circles) at the center of pump pulse with the Floquet-linear-spin wave theory (solid line).* ***(c)*** *The trRIXS measurement of a quarterly filled 1D cuprate chain.* ***(d)*** *Dynamics of quantum Fisher information revealed from trRIXS, witnessing a bipartite-entangled state induced by laser.*

In this talk, I will discuss the application of time-resolved resonant inelastic x-ray scattering (trRIXS) in magnetic materials [see Fig.1(a)]. By comparing the trRIXS for antiferromagnetic materials, we find that the instantaneous paramagnon excitations can be manipulated by pulsed laser in a predictive manner, following the Floquet theory in the center of the pulse [see Fig.1(b)]. Such a Floquet engineering works only at doped Mott insulators without long-range order, while the trRIXS study of an undoped Mott insulator violates the Floquet approximation. Leveraging the light-engineered magnetic excitations, we further study the nonequilibrium dynamics of a 1D cuprate chain [see Fig.1(c)]. Through a self-consistent iteration, trRIXS can probe the transient entanglement of wavefunctions in nonequilibrium materials via the quantum Fisher information. Via this approach, we reveal the possibility of enhancing entanglement in a cuprate chain using an ultrafast laser pulse [see Fig.1(d)].

References

[1] M. Mitrano, Y. Wang. *Communications Physics* **3**, 184 (2020).
[2] Y. Wang, Y. Chen, T.P. Devereaux, B. Moritz, and M. Mitrano, *Communications Physics* **4**, 212 (2021)
[3] J. Hales, U. Bajpai, T. Liu, D.R. Baykusheva, M. Li, M. Mitrano, and Y. Wang, Nature Communications in press (2022)

Quantification of Uncertainty in Deep Learning Neural Network while Predicting X-ray Absorption Spectra

Sneha Verma[1] and Thomas Penfold[1]
[1]Chemistry–School of Natural and Environmental Sciences, Newcastle University, Newcastle Upon Tyne NE1 7RU, United Kingdom
Sneha.verma@newcastle.ac.uk, tom.penfold@ncl.ac.uk

The local atomic and electronic structure around an absorbing atom has been extensively studied using X-ray absorption near-edge structure (XANES) spectra [1]. Yet, because the underlying theory is so intricate, quantitative interpretation can be complicated and time-consuming. Recently, we created XANESNET [2, 3], a deep neural network that can only predict the spectrum intensities of the transition metal complexes represented in a feature vector of weighted atom-centered symmetry functions (wACSF). Yet, this brings up an important question: *Is there a way to evaluate the accuracy of the forecasts made by XANESNET?*

In this investigation, we expand this approach to assess the uncertainties associated with the forecasts generated by these models. To determine the degree of uncertainty in the X-ray absorption spectra of third row transition metal complexes, we use the deep ensembles and Bootstrap resampling techniques. A substantial association between the expected uncertainty and the mean square error between the actual and anticipated spectra serves as evidence of the effectiveness of the generated models. We also add convolutional neural networks and autoencoders to the XANESNET model, which was originally a multi-layer perceptron, and evaluate the benefits and drawbacks of each model's performance.

Keywords: X-ray spectroscopy; deep neural networks; uncertainty and error; transition metals; ensemble; bootstrapping; uncertainty prediction.

References

1. Guda, A. A., Guda, S. A., Martini, A., Kravtsova, A. N., Algasov, A., Bugaev, A., Kubrin, S. P., Guda, L.V., Šot, P., Van Bokhoven, J. A. and Copéret, C., 2021. *Understanding X-ray absorption spectra by means of descriptors and machine learning algorithms.* Npj Computational Materials, 7(1), pp.1-13.
2. Penfold, T. J. and Rankine, C. D., 2022. *A deep neural network for valence-to-core X-ray emission spectroscopy*. Molecular Physics, p.e2123406.
3. Rankine, C. D. and Penfold, T. J., 2022. *Accurate, affordable, and generalizable machine learning simulations of transition metal x-ray absorption spectra using the XANESNET deep neural network*. The Journal of Chemical Physics, 156(16), p.164102.

Friday 22st of August, 2023

HAXPES with Full-Field *k*-Imaging plus Time-of-Flight Recording

Gerd Schönhense

Johannes-Gutenberg University, Institute of Physics, 55128 Mainz, Germany
Contact: schoenhe@uni-mainz.de

Keywords: Hard-X-ray photoemission, photoelectron diffraction, momentum microscopy, HARPES

Full-field imaging of transversal momentum distributions (k_x,k_y), also termed momentum microscopy (MM), has proven to be a powerful method for electronic structure analysis. When combined with time-of-flight (ToF) recording, it enables rapid three-dimensional mapping of the topology of Fermi surfaces, Fermi velocity and identification of electron and hole pockets [1]. The third momentum coordinate, k_z in the 4D data array I(E_B,***k***) is accessed through a variation of photon energy.

Angular-resolved photoelectron spectroscopy in the hard-X-ray range (HARPES) suffers from decreasing photoemission cross sections alongside with increased thermal diffuse scattering [2]. With increasing photon energy, the high recording speed of ToF-MM effectively counteracts the unfavorable trend of the signal-to-background ratio. Hard-X-ray photoelectron diffraction (HXPD) patterns in *k*-space representation (k_x,k_y) can be recorded with unprecedented speed, an example is shown in Fig. 1(a). Moreover, parallel recording of large *k*-fields-of-view comprising up to tens of Brillouin zones gives access to the perpendicular momentum component, k_z, without scanning photon energy. At such high photon energies (here 5.3 keV) the HARPES transition leads to a quasi-free-electron-like final state band with the final-state momentum k_f defining a sphere (energy conservation). This sphere intersects periodic *k*-space, paved with Brillouin zones (BZ), which in turn leads to a variation of k_z across the field-of-view, as illustrated in Fig. 1(b,c). Due to momentum conservation the sphere centre is displaced from the origin *k*=(0,0,0) by the vector of the photon momentum k_{hv}. Fig. 1(d) shows 3D views of constant-energy maps of the spectral density of electronic states at the indicated binding energies. The experiment probed the temperature dependence of isoenergetic surfaces and band dispersions for $YbRh_2Si_2$, revealing changes of the electronic states at temperatures much higher than T_{Kondo}; details in [3].

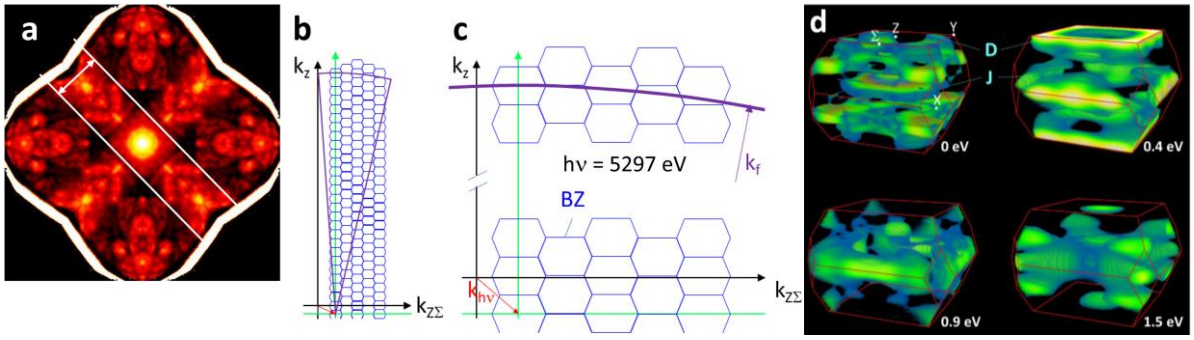

Figure 1: (a) Full-field HXPD pattern of the Yb 4*f* level in the Kondo system $YbRh_2Si_2$ at a photon energy of 5.3 keV. In the *k*-space image, the Kikuchi bandwidth (as marked) directly gives the corresponding reciprocal lattice vector, here $\boldsymbol{G}_{110} = 3.1\text{Å}^{-1}$. (b,c) k_x,k_z-scheme of a valence-band transition into a quasi-free-electron-like final state; plots are to scale for the $YbRh_2Si_2$ structure. (d) Three-dimensional representation of the measured spectral density of states at four indicated binding energies (0 eV is the Fermi surface), recorded at 20 K and hν = 5297 eV (adapted from [3]).

High-energy ToF-MM leverages all other strongholds of HARPES, such as band mapping through protective capping layers [4], probing buried interfaces, or measuring true bulk-magnetic properties with an imaging spin filter; cf. [3] and refs. therein. The full-field imaging approach provides information on the nature of the photoemission final state (Pendry's multiple-scattering description) with an unprecedented richness in details. In particular, the recently-discovered circular dichroism in core-level HXPD patterns bears additional information that goes beyond the classical information content of XPD experiments ([5]; O. Tkach et al., and T.-P. Vo et al., this conf.). Projects funded by BMBF and DFG.

1. K. Medjanik et al., Direct 3D Mapping of the Fermi Surface and Fermi Velocity, *Nature Materials* **16**, 615 (2017)
2. A. X. Gray et al., Probing bulk electronic structure with hard X-ray ARPES, *Nature Materials* **10**, 759 (2011)
3. G. Schönhense and H.-J. Elmers, Spin- and time-resolved photoelectron spectroscopy and diffraction studies using time-of-flight momentum microscopes, *J. Vacuum Sci. Technol.* A **40,** 020802 (2022)
4. H.-J. Elmers et al., Néel vector induced manipulation of valence states in Mn_2Au, *ACS Nano* **14**, 17554 (2020)
5. O. Tkach et al., Circular Dichroism in Hard X-ray Photoelectron Diffraction, *Ultramicroscopy* 113750 (2023)

Photoelectron holography with atomic resolution

Tomohiro Matsushita[1]
1 Graduate school of Science and Technology, Nara Institute of Science and Technology, Nara, Japan
**Contact: t-matusita@ms.naist.jp*

Keywords: photoelectron holography, atomic resolution holography, atomic arrangement, dopant, impurity

In 2022, there was a rapid development of AI technologies such as ChatGPT, which is expected to significantly change our way of life. Additionally, there has been a rapid increase in research exploring the application of data science in materials science. By the way, doping is a very important technique for developing functional materials. By adding impurities (dopants) to a mother crystal, it is possible to modify its properties. The atomic arrangement of dopants is important, but for a long time, there was no way to observe their three-dimensional (3D) atomic arrangement. Our research group has revealed that atomic-resolution holography is the optimal method for measuring the 3D atomic arrangement of dopants. There are multiple methods of atomic-resolution holography, such as photoelectron holography (PEH), x-ray fluorescence holography (XFH), and neutron holography (NH). Figure 1(a) shows the principle of photoelectron holography. When excited light is irradiated, photoelectrons are emitted from the dopant. The photoelectron is scattered by surrounding atoms and forms an interference pattern. Although this angular distribution is known as photoelectron diffraction, the pattern measuring a large solid angle can be regarded as a hologram that records the 3D atomic arrangement. We developed a new retarding field analyzer for this measurement [1] (Fig. 1(b)). By designing the electrodes, we achieved simultaneous energy resolution $E/\Delta E$ of about 2000, angular resolution $d\theta$ of about 0.5°, and a wide solid angle of ±50°. Figure 1(c) shows the raw measurement image. I also developed simulation software for the holograms as shown in Fig. 1(d). In addition, I constructed a theory for reconstructing the 3D atomic arrangement from a single-energy photoelectron hologram using quantum scattering theory and sparse modeling, which is used in data science [2]. By using the new analyzer and the new theory, we have succeeded in investigating atomic arrangements of dopants in crystals for each valence using the chemical shift of core-levels[3, 4]. We are also advancing the application of atomic imaging at interfaces[5] as shown in Fig. 1(e). We are also developing not only PEH but also XFH and NH. In the future, atomic-resolution holography will become important measurement technique.

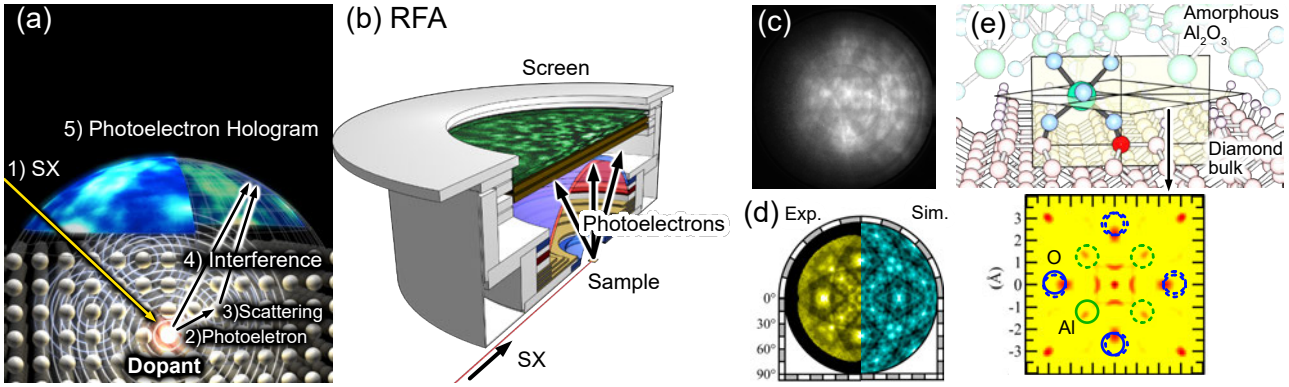

Figure 1: (a) Principle of photoelectron holography. (b) Retarding field analyzer (RFA). (c) Raw observed image of RFA. (Diamond E_k=700eV). (d) Holograms of experiment and simulation. (e) Reconstructed atomic image from a PEH of a defect between H-terminated diamond and Al_2O_3 isolation layer and atomic structural model.

[1] T. Muro, T. Matsushita, et al., J. Synchrotron Rad., **28**, 1669 (2021); Rev. Sci. Instrum., **88**, 123106 (2017).
[2] T. Matsushita, et al., J. Phys. Soc. Jpn., **87**, 061002 (2018).
[3] K. Tsutsui, T. Matsushita, et al., Nano Lett., **17**, 7533 (2017).
[4] T. Yokoya, T. Matsushita, et al., Nano Lett., **19**, 5915 (2019).
[5] M. Fujii, T. Matsushita, et al., Nano Lett., **23**, 1189 (2023).

Molecular Environmental Surface Science

Markus Ammann[1,*], Thorsten Bartels-Rausch[1] and Luca Artiglia[1,2]

1 Laboratory of Atmospheric Chemistry, Paul Scherrer Institut, Villigen, Switzerland
2 Laboratory of Sustainable Chemistry, Paul Scherrer Institut, Villigen, Switzerland
**Contact: markus.ammann@psi.ch*

Keywords: X-ray photoelectron spectroscopy, ambient pressure, aerosol particles, atmospheric chemistry

X-ray photoelectron spectroscopy (XPS) of typically core atomic electronic levels provides chemical and electronic structure information and electron yield near edge X-ray absorption fine structure (NEXAFS) spectroscopy gives insight into the structure of the local molecular environment. The low inelastic mean free path of electrons in the nanometer range enables sensitivity for the condensed matter – gas interfacial region. The development of ambient pressure electron analyzers has offered tremendous opportunities for molecular understanding of environmentally relevant aqueous solution surfaces, ice surfaces, and mineral oxides, all in presence or absence of reactive trace gases and in or out of equilibrium with water vapor [1,2].

Examples will be presented for a variety of relevant substrates, environmental conditions and experimental settings. Electron yield O K-edge NEXAFS spectroscopy can be used to address the hydrogen bonding structure at interfaces. We have used this technique to probe the quasi-liquid layer at the surface of ice in presence of trace gases [3]. In analogous ways, this allows to address questions of water ordering on mineral oxides [4] or aqueous solutions in presence of surfactants [5]. In turn, ambient pressure XPS has been used to directly measure the surface excess, the orientation and the degree of dissociation (for acids) or protonation (for bases) [6] on either of solid or liquid substrates. Furthermore, the development of a flexible and inert dosing system to the sample environment allows the admission of reactive gases to ice [3], mineral oxides and liquid water. For the latter, the example of oxidation of bromide by ozone will be presented, for which the rate limiting reaction intermediate could be identified at the water surface [7].

1. Orlando, F.; Waldner, A.; Bartels-Rausch, T.; Birrer, M.; Kato, S.; Lee, M.-T.; Proff, C.; Huthwelker, T.; Kleibert, A.; Bokhoven, J.; et al. The Environmental Photochemistry of Oxide Surfaces and the Nature of Frozen Salt Solutions: A New in Situ XPS Approach. *Topics in Catalysis,* **59**, 591-604, DOI: 10.1007/s11244-015-0515-5 (2016).
2. Ammann, M.; Artiglia, L. Solvation, Surface Propensity, and Chemical Reactions of Solutes at Atmospheric Liquid–Vapor Interfaces. *Accounts of Chemical Research,* **55**, 3641-3651, DOI: 10.1021/acs.accounts.2c00604 (2023).
3. Kong, X.; Waldner, A.; Orlando, F.; Artiglia, L.; Huthwelker, T.; Ammann, M.; Bartels-Rausch, T. Coexistence of Physisorbed and Solvated HCl at Warm Ice Surfaces. *The Journal of Physical Chemistry Letters*, **8**, 4757-4762. DOI: 10.1021/acs.jpclett.7b01573 (2017).
4. Orlando, F.; Artiglia, L.; Yang, H.; Kong, X.; Roy, K.; Waldner, A.; Chen, S.; Bartels-Rausch, T.; Ammann, M. Disordered Adsorbed Water Layers on TiO2 Nanoparticles under Subsaturated Humidity Conditions at 235 K. The *Journal of Physical Chemistry Letters*, **10**, 7433-7438, DOI: 10.1021/acs.jpclett.9b02779 (2019).
5. Yang, H.; Gladich, I.; Boucly, A.; Artiglia, L.; Ammann, M. Orcinol and resorcinol induce local ordering of water molecules near the liquid–vapor interface. *Environmental Science: Atmospheres*, **2**, 1277-1291, DOI: 10.1039/D2EA00015F (2022).
6. Lee, M.-T.; Orlando, F.; Artiglia, L.; Chen, S.; Ammann, M. Chemical Composition and Properties of the Liquid–Vapor Interface of Aqueous C1 to C4 Monofunctional Acid and Alcohol Solutions. *The Journal of Physical Chemistry A*, **120**, 9749-9758, DOI: 10.1021/acs.jpca.6b09261 (2016).
7. Artiglia, L.; Edebeli, J.; Orlando, F.; Chen, S.; Lee, M.-T.; Corral Arroyo, P.; Gilgen, A.; Bartels-Rausch, T.; Kleibert, A.; Vazdar, M.; et al. A surface-stabilized ozonide triggers bromide oxidation at the aqueous solution-vapour interface. *Nature Communications*, **8**, 700. DOI: 10.1038/s41467-017-00823-x (2017).

Opportunities for gas-phase, liquid-phase and aerosol research at MAX IV

N. Walsh[a], V. Ekholm[a], T. Gallo[a,b], A. Kivimäki[a], E. Kokkonen[a], C. Preger[a,c], H. Sa'adeh[a,d], M. Scardamaglia[a], K. Sigfridsson Clauss[a], C. Såthe[a], M. Tchaplyguine[a], G. Öhrwall[a]

[a] *MAX IV Laboratory, Lund University, Lund 22484, Sweden*
[b] *Division of Synchrotron Radiation Research, Lund University, Lund 22363, Sweden*
[c] *Ergonomics and Aerosol Technology, LTH, Lund University, Lund 22363, Sweden*
[d] *Dept. Of Physics, The University of Jordan, Amman 11942, Jordan*

Keywords: AMO, LDM[1], photoelectron spectroscopy, coincidence spectroscopy, liquid jet, aerosols, clusters

Experiments that investigate the interaction of light with molecules, clusters and liquids/aqueous solutions provide an opportunity to characterise the properties of these samples and to gain a deeper understanding of a variety of physical processes that are as yet only partly understood. In addition to this, such research can also contribute to industrial and technological advancement and various challenges related to climate change.

In recent years, MAX IV Laboratory has engaged in several development projects to expand its LDM-equipment repertoire thus ensuring that AMO facilities at the lab can cater to the evolving needs of the international user community. We have a number of LDM-relevant beamlines at MAX IV that deliver photon energies over a broad photon energy range - from 4.5eV to many keV. These beamlines can facilitate different types of gas-phase or liquid phase research experiments using a range of experimental techniques:

Multicoincidence momentum imaging, angle-resolved electron spectroscopy on molecules, clusters, aerosols and liquid jets[2], Time-of-Flight Mass Spectrometry, AP-XPS[3] on liquid jet/laboratory generated nanoparticles, RIXS on liquid jets and gas phase samples, electron energy resolved multi-coincident PEPIPICO[4], Negative Ion Positive Ion Coincidence (NIPICO)[5] and absorption spectroscopy on liquid samples at Balder ($h\nu$ > 2.4keV) are all possible. Amongst the available instrumentation we also offer a number of mobile pieces of equipment that are designed to be used on different beamlines. Examples include the ICE[6] end station (which is reported in a separate poster), liquid jet sample delivery systems and a newly commissioned aerosol source. Ongoing development projects in collaboration with the MAX IV user community include the development of a liquid flat jet setup for XAS and XPS, and TRISS – a new mobile end station for trapped ion research using synchrotron radiation.

[1] LDM – Low Density Matter – relating to AMO/liquid jet research
[2] Also discussed in a poster by A. Kivimäki - *Instrumentation for electron spectroscopy and related research at the FinEstBeAMS beamline at MAX IV Laboratory*
[3] Ambient Pressure X-ray Photoelectron Spectroscopy
[4] Photoelectron Photoion Photoion Coincidence
[5] Also reported in the poster by H. Sa'adeh - *Fragmentation of methanol molecules after valence photoexcitation studied by negative-ion positive-ion coincidence spectroscopy*
[6] Ions in Coincidence with Electrons

Abiotic molecular oxygen production – ionic pathway from SO_2

M. Wallner[1], M. Jarraya[2,3], E. Olsson[1], V. Ideböhn[1], R. J. Squibb[1], S. Ben Yaghlane[3], G. Nyman[4], J.H.D. Eland[5], R. Feifel[1]*, and M. Hochlaf[2]

[1]*University of Gothenburg, Department of Physics, 412 58 Gothenburg, Sweden*

[2]*Université Gustave Eiffel, COSYS/LISIS, 5 Bd Descartes 77454, Champs sur Marne, France*

[3]*Université de Tunis El Manar, Faculté des Sciences de Tunis, Laboratoire de Spectroscopie Atomique, Moléculaire et Applications – LSAMA, 2092, Tunis, Tunisia*

[4]*University of Gothenburg, Department of Chemistry and Molecular Biology, 405 30 Gothenburg, Sweden*

[5]*Oxford University, Department of Chemistry, Physical and Theoretical Chemistry Laboratory, South Parks Road, Oxford OX1 3QZ, United Kingdom*

**Contact: raimund.feifel@physics.gu.se*

Keywords: dissociative double ionisation, molecular oxygen production, multi-particle coincidence

Molecular oxygen, O_2, is vital to life on Earth and possibly also on exoplanets. Although the biogenic processes leading to its accumulation in the Earth's atmosphere are well understood, its abiotic origin is still not fully established. Recently [1], SO_2 has been investigated experimentally by multi-particle coincidence detection using our established TOF-PEPEPIPICO technique where the target species were irradiated by 40.81 eV photons (HeIIα) from a pulsed helium discharge lamp, mimicking an intense component of the solar spectrum and of many stellar spectra. In addition, ion-ion coincidence measurements on SO_2 were carried out at the synchrotron radiation facility BESSY-II where photon energies of several more solar X-ray lines were available to us. We find experimental evidence for electronic-state-selective production of O_2 from SO_2, a chemical constituent of many planetary atmospheres and one which played an important part on Earth in the Great Oxidation Event. This finding is supported by advanced ab initio computations suggesting the following model: The O_2 production involves isomerization of SO_2 by a roaming mechanism (cf. Fig. 1) leading to efficient formation of the O_2^+ ion in form of dissociative double ionisation of SO_2, which can be converted to abiotic O_2, for instance by electron neutralisation. This formation process may contribute significantly to the abundance of O_2 and related ions in planetary atmospheres, such as the Jovian moons Io, Europa and Ganymede. It represents an alternative to and may compete with the well-established abiotic O_2 production pathways via the photodissociation of water vapor by extreme ultraviolet light or the near ultraviolet photochemistry of titanium-(IV)-oxide (titania). We suggest that this sort of ionic pathway for the formation of abiotic O_2 involving multiply-charged molecular ion decomposition may also exist for other atmospheric and planetary molecules.

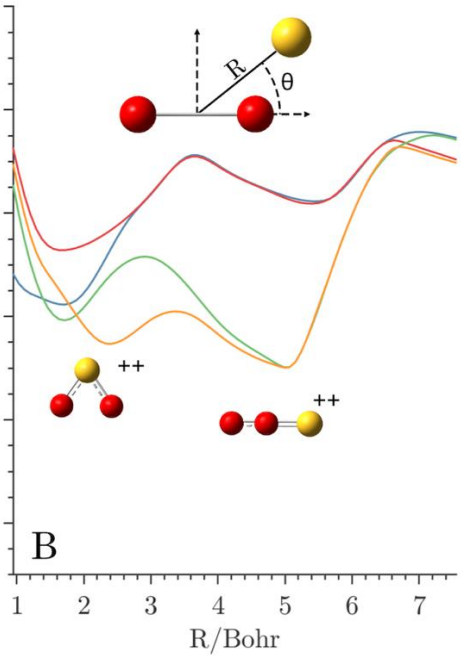

Figure 1: Partial minimal energy path of SO_2, showing the roaming mechanism leading to abiotic production of O_2 [1].

1. M. Wallner *et al.*, Sci. Adv. 8, eabq54303 (2022).

VUV-induced fragmentation and electronic structure of phenoxy herbicides

R. Pärna[1,*], M. Kook[1], A. Kivimäki[2], I. Kuusik[1], A. Tõnisoo[1], V. Kisand[1] and Reisberg[1]

1 Institute of Physics, University of Tartu, W. Ostwaldi 1, EE-50411 Tartu, Estonia
2 MAX IV Laboratory, Lund University, Fotongatan 2, 225 94 Lund, Sweden
**Contact: rainer.parna@ut.ee*

Keywords: electronic structure, fragmentation, herbicides

Pesticides are chemical compounds, which are used to control pests, i.e., insects, weeds, fungus etc. Globally, ~3.5 million tons of pesticides are applied each year [1]. Despite the benefits of pesticides to crop yields and their economic importance, intensive pesticide use raises serious environmental concerns [2]. Pesticides can accumulate in nature and reach surface waters due to repeated applications on soil, spill or disposal [3]. Furthermore, pesticides can reach water bearing-aquifers, thus contaminating ground waters [4].

Very recently, vacuum ultraviolet radiation (VUV) based processes have been demonstrated as an alternative and effective way to carry out both direct and indirect photolysis of pesticides, thus avoiding the disadvantages and complexity of (photo)catalysts or addition of oxidants [5]. Examples of direct and indirect photolysis are pesticide molecule dissociation as an immediate result of photoionization and photolysis reactions with reactive photo-induced species, respectively. However, it is still unclear what are the fragmentation pathways of pesticides under VUV radiation.

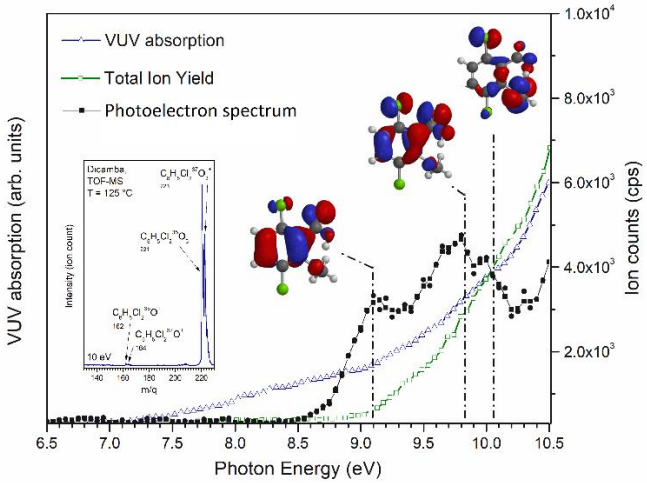

Figure 1: The VUV absorption and Total Ion Yield (TIY) of dicamba ($C_8H_6Cl_2O_3$) measured in the photon energy range of 6.5 and 10.5 eV. The photoelectron spectrum of dicamba is shown together with first three molecular orbitals. The inset is TOF-MS spectrum measured with 10 eV excitation energy.

In this research, the photodegradation processes of phenoxy herbicides induced by VUV were investigated. The focus has been on the relationship between the photofragmentation of gas-phase (free) pesticide molecules and their electronic structures. In this investigation, basic processes governing VUV fragmentation of pesticide molecules have been studied. It was shown that VUV absorption by pesticide molecules is possible at wavelengths longer than 149 nm (the first water VUV absorption maximum) or in a water permeability window (at ~ 137 nm). We did not detect the formation of toxic phenolic compounds using VUV. In the frame of the work, it was also demonstrated that the presence of water plays an important role in the evaporation and decomposition of pesticides.

1. A. Sharma, et al., *SN Applied sciences* **1**, 1446 (2019).
2. V. Silva et al., *Science of the Total Environment* **653**, 1532 (2019).
3. M. Syafrudin, et al., *Int. J. Environ. Res. Public Health* **18**, 468 (2021).
4. R.Z. Marsala et al., *Science of the Total Environment* **736**, 139730 (2020).
5. G. Moussavi et al., *Journal of Photochemistry and Photobiology A: Chemistry* **290**, 86 (2014).

Progress of atomic-resolution holography and new analyzer CoDELMA

Hiroshi Daimon[1,2*], Hiroki Momono[3], Hiroyuki Matsuda[2], Fumihiko Matsui[2], László Tóth[4], Yu Masuda[5], Koichi Moriguchi[5], Keiko Ogai[5], Yusuke Hashimoto[6] and Tomohiro Matsushita[6]

1 Toyota Physical and Chemical Research Institute, Yokomichi, Nagakute, Aichi 480-1192, Japan
2 Institute for Molecular Science, 38 Nishigo-Naka, Myodaiji, Okazaki, Aichi 444-8585, Japan
3 National Institute of Technology, Yonago , Hikona, Yonago, Tottori 683-8502, Japan
4 SciTech Műszer Kft., H-4032 Debrecen, Hungary
5 APCO Ltd., 522-10 Kitano-machi, Hachioji-shi, Tokyo 192-0906 Japan
6 Nara Institute of Science and Technology, 8916-5 Takayama, Ikoma, Nara 630-0192, Japan
**Contact: daimon@ms.naist.jp*

Keywords: photoelectron holography, atomic-resolution holography, display-type analyzer, CoDELMA

Photoelectron diffraction is a powerful technique which can analyze local 3D atomic arrangement around specific atoms. Prof. Charles S. Fadley (Nicknamed Chuck) is the initiator of the photoelectron diffraction. He started the photoelectron diffraction study in Hawaii university and published the first photoelectron diffraction paper in 1978 [1]. The analysis of photoelectron diffraction was made by comparison between the observed angular dependence of the core level photoelectron intensity with the calculated one. In 1990, Chuck moved to ALS (Advanced Light Source) in California and started photoelectron holography study [2]. The photoelectron holography can deduce the local 3D atomic arrangement around specific atoms by converting the 2D angular distribution of core-level photoelectron intensity.

An example of photoelectron hologram is shown in Fig. 1(a), which is the angular distribution of O 1s core-level photoelectrons emitted from W(110)1×1-O surface [3]. It took three days to obtain this hologram at Chuck's laboratory by using laboratory X-ray source and narrow acceptance angle spherical analyzer. The holographic converted atomic arrangement in surface oxygen plane is shown in Fig. 1(b) [4] in white color. The white circles show the expected atomic positions. The accuracy of the atomic position is larger than 0.5 Å and not enough to analyze unknown structure. Figure 1(c) shows the atomic image converted by a recently developed algorism SPEA-L1 [5]. The positions of atomic image (green) and the expected positions (red) show good agreement within 0.1 Å, which is good enough to analyze unknown structure. An effective analyzer CoDELMA (Fig. 2) which can measure a hologram in a short time has been developed recently [6].

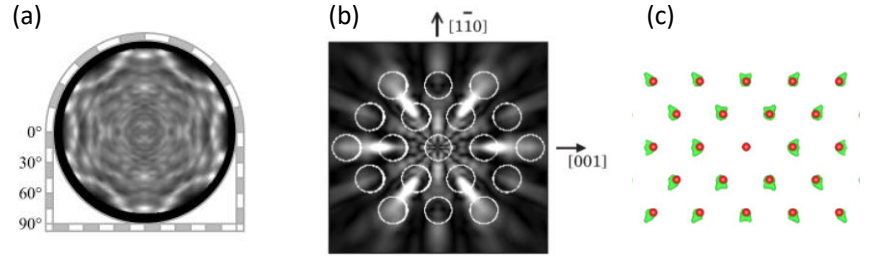

Figure 1: Development of atomic-resolution holography. (a) O 1s hologram [3], (b) reconstructed image by FFT [4], (c) reconstructed image by SPEA-L1 [5].

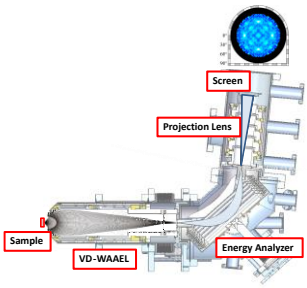

Figure 2: CoDELMA [6]

1. S. Kono, C. S. Fadley, N. F. T. Hall, and Z. Hussain, Azimuthal Anisotropy in Deep Core-Level X-Ray Photoemission from an Adsorbed Atom: Oxygen on Copper(001), *Phys. Rev. Lett.* **41**, 117 (1978).
2. S. Thevuthasan, G. S. Herman, A. P. Kaduwela, R. S. Saiki, Y. J. Kim, W. Niemczura, M. Burger, and C. S. Fadley, Electron emission holography at keV energies: Estimates of accuracy and limitations, *Phys. Rev. Lett.* **67**, 469 (1991).
3. H. Daimon, R. Ynzunza, F.J. Palomares, H. Takagi, C.S. Fadley, Direct structure analysis of W(110)-(1×1)-O by full solid-angle X-ray photoelectron diffraction with chemical-state resolution *Surf. Sci*. **408**, 260 (1998).
4. H. Takagi, H. Daimon, F.J. Palomares, C.S. Fadley, Photoelectron holography analysis of W(110)-(1×1)-O Surface, *Surf. Sci*. **470**, (3) 189 (2001).
5. S. Takeuchi, Y. Hashimoto, H. Daimon, T. Matsushita, High-precision atomic image reconstruction from photoelectron hologram of O on W(110) by SPEA-L1, *J. Electr. Spectr. Relat. Phenom.*, **256**, 147177 (2022).
6. H. Matsuda, H. Momono, L. Tóth, Y. Masuda, K. Moriguchi, K. Ogai, H. Daimon, Compact 2D electron analyzer CoDELMA: Simultaneous wide reciprocal and real space analysis using wide-angle deceleration lens, CMA and projection lens, *J. Electr. Spectr. Relat. Phenom.*, **264,** 147313 (2023).

Memories of the 1990s and 2000s

Michel A. Van Hove
Retired; Chuck Fadley's "most frequent co-author"
Contact: vanhove88@yahoo.com

Keywords: photoelectron diffraction, photoelectron holography

Chuck Fadley and I co-authored 58 papers, including 7 letters and 7 review articles: Chuck called me his most frequent co-author. Our joint work dealt primarily with photoelectron diffraction and photoelectron holography. Related topics included: multi-atom resonant photoemission, resonant x-ray fluorescence holography, circular dichroism, soft x-ray standing wave spectroscopy, and soft x-ray standing wave spectroscopy.

Chuck graciously introduced me to the world of photoelectrons and synchrotron radiation around 1990, when he joined Lawrence Berkeley Laboratory (where I worked since 1978) and the University of California at Davis as Advanced Light Source Professor of Physics. My contribution was mainly the theory of low-energy electron diffraction. We had a highly productive collaboration until I left for Hong Kong in 2005 and turned to modeling large molecules on surfaces and molecular machines.

Rehr-Albers approach to Photoelectron Diffraction

J.J. Rehr[1], A. P Kaduwela[2], R. C. Albers[2], J. J. Kas[1], F. D. Vila[1]

1 Dept. of Physics, University of Washington, Seattle, WA 98195-1560, USA
2 Air Quality Research Center, University of California Davis, Davis, CA 95616, USA
3 Theoretical Division, Los Alamos National Laboratory, Los Alamos, NM 87545, USA
**Contact: jjr@uw.edu*

Keywords: Photoelectron diffraction, Real-space Green's function, multiple-scattering, FEFF

Photoelectron diffraction (PD) refers to the variation of the differential photoemission cross section with energy and direction. This important technique has been extensively developed by C. S. Fadley and collaborators, including both experimental[1] and theoretical advances.[2] The physics of PD is similar to that for x-ray absorption spectroscopy (XAS),[2] and our mutual interest in photoexcitation phenomena led to a fruitful collaboration.[3] The methods differ in that external electron detectors are used for photoemission and external photon detectors for photoabsorption. Both require accurate treatments of the photoelectron states, which can be described by high-order multiples scattering theory. This theory is especially important for local and surface atomic structural determinations. Because of the electron detector and the short-ranged mean-free path of the escaping photoelectron, PD is sensitive to the surface of a material, and has become one of the most important tools in surface-science.

In this talk we briefly review the development of the real-space green's function (RSGF) approach for core-level photoelectron diffraction (PD) based on the Rehr-Albers (RA) scattering-matrix formalism. This development was carried out in collaboration with the Fadley group. The RA method for PD is adapted from that originally developed for x-ray absorption spectra (XAS), e.g., in the FEFF codes,[2] and its separational nature is computationally advantageous. Computational details such as scattering potentials, self-energy effects, Debye-Waller factors, and inelastic losses are also discussed. The code MSCD was based on this development.[4] We also discuss prospects for improving ab initio PD calculations. For additional details, see Ref. 5 and references therein.

1. C. Fadley, M. Van Hove, Z. Hussain, A. Kaduwela, Photoelectron diffraction: new dimensions in space, time, and spin*, J. Elec. Spec. Relat. Phen*, **75,** 273–297 (1995).
2. J. J. Rehr, R. C. Albers, Theoretical approaches to x-ray absorption fine structure, *Rev. Mod. Phys*. **72** 621 (2000).
3. J. M. De Leon, J. Rehr, C. Natoli, C. Fadley, J. Osterwalder, Spherical-wave corrections in photoelectron diffraction, *Phys. Rev. B* **39**, 5632 (1989).
4. Y. Chen, F. G. De Abajo, A. Chass´e, R. Ynzunza, A. Kaduwela, M. Van Hove, C. Fadley, Convergence and reliability of the Rehr-Albers formalism in multiple-scattering calculations of photoelectron diffraction, *Phys. Rev. B* **58**, 13121 (1998).
5. J. J. Rehr, A. P. Kaduwela, R. C. Albers, J. J. Kas, F. D. Vila, Real-space Green's function approach to Photoelectron Diffraction, *J. Elec. Spec. Relat. Phen, **259**,* 147237 (2022).

In Operando Measurements on Complex Materials Explored With nanoARPES

Eli Rotenberg

Advanced Light Source, Lawrence Berkeley National Laboratory, USA

**Contact: erotenberg@lbl.gov*

Keywords: nanoARPES, 2D materials, heterostructures

Angle-resolved photoemission is a premiere technique for measuring the electronic structure of materials, as represented by momentum-resolved electronic bands. Furthermore, with modern high-resolution instrumentation it is possible to access the single-particle spectral function A(k,ω), which gives important information on the renormalization of excited state energies and lifetimes due to many-body interactions and defect scattering.

NanoARPES machines capable of spatially-resolving the ARPES spectrum on the mesoscopic scale are coming online at synchrotrons around the world, with spatial resolution in the range 100-1000nm. Combining these new small probes with arbitrary stacking orders of diverse materials assembled micromechanically, nanoARPES can obtain information on new materials far faster than in the past, when probe sizes limited us to wafer-scale, epitaxially grown heterostructures. Using small x-ray probes, nanoARPES can also study naturally or spontaneously-formed heterogenous materials. Most if not all nanoARPES machines are accessible through proposals to international user facilities, and the community specializing in these experiments is growing rapidly.

Most excitedly, nanoARPES offers the possibility to measure 2D materials and heterostructures at true device scales, and can thus enable for the characterization of materials under in operando conditions. In this talk I will review recent developments and pioneering experiments at the MAESTRO beamline at the Advanced Light Source in Berkeley, CA. These capabilities include the application of external fields (electrical, magnetic, and optical), current, and strain. Prospects for the application of magnetic fields to create a new "MagnetoARPES" technique will be presented.

Photoelectron spectroscopy modalities for studying complex materials

Slavomir Nemsak[1,2]

[1] *Advanced Light Source, Lawrence Berkeley National Laboratory, Berkeley, CA, USA*
[2] *Department of Physics and Asotronomy, University of California, Davis, CA, USA*
**Contact:* snemsak@lbl.gov

Keywords: X-ray photoelectron spectroscopy, angle-resolved photoelectron spectroscopy, standing-wave photoelectron spectroscopy, ambient pressure photoelectron spectroscopy.

X-ray photoelectron spectroscopy (XPS) became a mature go-to technique to characterize electronic and chemical properties of complex materials several decades ago. However, the development of the field is still undergoing along different modalities and modern extensions of the XPS, such as scanning imaging (nano-ARPES), full-field imaging (momentum microscopy), depth and site-resolution (standing-wave excitation), complex environments (ambient pressure and beyond), time-resolved experiments, etc.

In this talk, I will show some examples of standing-wave photoelectron spectroscopy applied to multilayers as well as to single-crystals, both in momentum-resolved [1] and angle-integrated fashion [2]. I will also describe application of standing-wave excitation in ambient pressure photoemission, enabling probing solid/gas and solid/liquid interfaces with high depth precision [3].

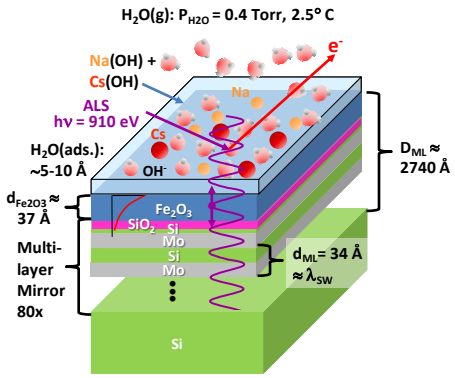

Figure 1: Schematics of standing-wave photoemission experiment studying alkali-ion adsorption on hematite.

1. Nemšák, S., Gehlmann, M., Kuo, CT. et al. Element- and momentum-resolved electronic structure of the dilute magnetic semiconductor manganese doped gallium arsenide. Nat Commun 9, 3306 (2018). https://doi.org/10.1038/s41467-018-05823-z
2. Lu, Q., Martins, H., Kahk, J.M. *et al.* Layer-resolved many-electron interactions in delafossite $PdCoO_2$ from standing-wave photoemission spectroscopy. *Commun Phys* **4**, 143 (2021). https://doi.org/10.1038/s42005-021-00643-y
3. Nemšák, S., Shavorskiy, A., Karslioglu, O. et al. Concentration and chemical-state profiles at heterogeneous interfaces with sub-nm accuracy from standing-wave ambient-pressure photoemission. Nat Commun 5, 5441 (2014). https://doi.org/10.1038/ncomms6441

POSTERS

Posters

1. Morsal Babayan: Low-pressure, isomer-selective kinetic characterization of DME conversion over zeolite by PEPICO
2. Manoj Ghosalya: APXPS Study of Photocatalytic Driven Atomic and Electronic Transformation of Core-Shell Ni@$NiCO_3$/NiO Photocatalyst
3. Miho Kitamura: Development of operando transmission soft x-ray absorption spectroscopy of Li-ion battery structure by x-ray excited optical luminescence
4. Yoshiyuki Ohtsubo: Nano-spintronics beamline with versatile photon polarization at NanoTerasu, a new synchrotron facility at Tohoku, Japan
5. Klemen Bučar: Magnetic bottle electron spectrometer driven by electron pulses
6. Mariusz Pawlak: Accurate potential energy surface for cold collisions of metastable helium with molecular hydrogen
7. Ville Lindblom: Nuclear Dynamics in Cyclopropane
8. Maria Novella Piancastelli: Structural dynamics in multiphoton core ionization of water isotopologues
9. Jan-Erik Rubensson: Imaging Soft X-ray Spectroscopy at the Small Quantum Systems Instrument of the European XFEL
10. Johan Söderström: X-ray absorption and Resonant Inelastic X-ray Scattering from condensed N2
11. Stacey L. Sörensen: Selective C 1s excitation on Auger-Meitner decay in the ESCA molecule
12. Onni Veteläinen: Modeling the fragmentation dynamics and valence photoelectron spectra of aminobenzoic acid
13. **Antti Kivimäki:** Instrumentation for electron spectroscopy and related research at the FinEstBeAMS beamline at MAX IV Laboratory
14. Hanan Sa'adeh: Fragmentation of methanol molecules after valence photoexcitation studied by negative-ion positive-ion coincidence spectroscopy
15. Noelle Walsh: ICE: A versatile Reaction Microscope for molecular/cluster dynamics research at MAX IV Laboratory
16. Rémi Dupuy: Resonant Intermolecular Coulombic Decay (ICD) in solvated ions
17. Jack J. Lin: Measurements of aggregate structures in atmospheric carboxylate solutions using X-ray absorption spectroscopy
18. Kazumasa Okada: Hydration structure of acetone studied by quantitative ultraviolet absorption spectroscopy
19. Chika Sugahara: Electronic structure of water in acetone aqueous solution revealed by liquid-phase soft X-ray absorption spectroscopy
20. Shin-ichiro Ideta: Nodal metallic behavior of underdoped triple-layer cuprate Bi2223
21. Yudai Miyai: Symmetry reduction of the electronic structure in heavily overdoped Pb-Bi2201 observed by Angle-resolved photoemission spectroscopy
22. James Penner-Hahn: Mechanistic insight into vitamin B12 chemistry: Polarized femtosecond x-ray spectroscopy of cobalamins
23. Elin Berggren: Charge Transfer in the BBL:P(g42T-T) Organic Polymer Heterojunction Measured with Core-Hole Clock Spectroscopy
24. Nicolas Velasquez: X-ray induced charge transfer in conjugated polymers by core-hole-clock spectroscopy
25. Trung Phuc Vo: Circular dichroism by core-level angle-resolved photoemission: Application of multiple & single-site scattering theory
26. Yi-Chen Weng: Determination of inelastic mean free path for hard oxide and soft polymers by overlayer method

27. Satoshi Yasuno: Development of hard X-ray photoelectron spectroscopy excited by photon energy up to 30 keV
28. Mohammed Alaoui Mansouri: Unraveling Surface Chemistry through the association of Time-Resolved XPS and Chemometrics: Case studies of Fe_2O_3 powder and DRI pellet
29. Guido Arthur Fabre: $L_{2,3}$ X-ray absorption spectra of transition metal oxides (Mn, Fe, Co): The influence of covalence effects
30. Daisuke Asakura: Soft X-ray absorption studies of nanocomposite $La_{0.6}Sr_{0.4}Co_{0.2}Fe_{0.8}O_{3-\delta}$ / $Ce_{0.9}Gd_{0.1}O_{2-\delta}$ electrode for solid oxide fuel cells
31. Daisuke Asakura: Transition-metal L-edge RIXS and multiplet calculation of cathode materials for Li-ion batteries
32. **Kati Asikainen:** Hematite Clusters on Anatase TiO_2 Surface and Effect of Oxygen Vacancy: A First Principles Study
33. Jonas Erhardt: Mapping the local Berry curvature of a quantum spin Hall insulator by circular dichroism ARPES
34. Sari Granroth: Reducing degradation and preferential sputtering using Ar cluster ion beam: An XPS study of some organic material and thin metal oxide films
35. Robert Haverkamp: Near-isotropic local attosecond charge transfer within the anisotropic puckered layers of black phosphorus
36. Alex Laikhtman: Hydrogen interaction with tungsten disulfide nanoparticles
37. Kyungchan Lee: Electronic structure of few-layer Pb on SiC
38. Bing Liu: Moiré Pattern Formation in Epitaxial Growth on a Covalent Substrate: Sb on InSb(111)A
39. **Ni'matil Mabarroh:** Photoelectron spectroscopy of artificially designed three-dimensional Si{111} facet surfaces on Si(110) and (001) substrates
40. Olga V. Molodtsova: In situ study of multi-phase In nanoparticles self-organized in organic thin film $CuPcF_4$
41. Olga V. Molodtsova: Nobel metal nanoparticles self-organized in organic matrix
42. X. Wang: Unveiling XPS spectra in the web browser using AiiDAlab
43. Alexei Nefedov: Control of dipole assembly into molecular films with photoelectron spectroscopy
44. Juan F. Sánchez-Royo: Origin of optically active color-centers in two-dimensional lead iodide perovskites revealed by photoemission
45. Ragini Sengupta: Chemical and electronic structure of $Fe_xNi_{100-x}(O,OH)_y$ electrocatalysts studied by soft and hard x-ray spectroscopies
46. Harishchandra Singh: Grazing X-ray absorption spectroscopy of 2D MoS_2-Based Memristor Device
47. Harishchandra Singh: Spectromicroscopy for steel and beyond
48. Serguei Soubatch: Momentum-selective orbital hybridization at molecule/metal interfaces
49. Filipp Temerov: Electron Spectroscopy for Hydrogen Future as a Climate Change Solution (H2FUTURE)
50. Hiroto Tomita: Local structural analysis of boron atoms heavily doped in diamond
51. Lothar Weinhardt: Valence band hybridization in sulfides
52. Lingyu Kong: Spatially resolved composition of laboratory-generated atmospheric model aerosol particles investigated with STXM-NEXAFS
53. Francesco Rosa: Infinite-layer nickelate superconductors studied with Resonant Inelastic X-ray Scattering
54. Jun Miyawaki: Construction of Ultrahigh Energy Resolution 2D-RIXS at NanoTerasu
55. Koji Horiba: Nano-ARPES beamline at NanoTerasu
56. Haytham Eraky: Scanning Transmission X-ray Microscopy Studies of MnO_2 / Zn Ion Battery Electrodes
57. Tuomas Mansikkala: Scanning transmission soft X-ray spectromicroscopy of mouse liver and kidney

58. Ekta Rani: Electron transfer path in Ni-Ag-MoS_2 photocatalyst
59. Parisa Talebi: Analysis of Ni chemical environments in MoS_2-Ag-Ni ternary systems via spectromicroscopy
60. Md Thasfiquzzaman: Formation of hydrated magnesium carbonate cement from brucite: A synchrotron radiation based STXM study
61. Zexu Sun: Local atomic structure analysis of F-doped layered perovskite $NaYTiO_4$ by photoelectron holography
62. Hubert Ebert: Theoretical description of X-ray experiments on magnetic materials exposed to an electric field
63. Ji Soo Lim: Interface electronic structure and anomalous magnetotransport properties of $SrIrO_3$ (111) superlattices
64. Lukasz Plucinski: Geometry-Induced Spin Filtering in Spin-ARPES Maps from WTe_2
65. **Fabian Schöttke:** Rashba-split image-potential state
66. Shigenori Ueda: Bulk-sensitive spin-resolved hard X-ray photoemission spectroscopy of half-metallic Co_2MnSi
67. Christopher Deeks: Combining XPS and Other Surface Analysis Techniques for in-situ Analysis

Low-pressure, isomer-selective kinetic characterization of DME conversion over zeolite by PEPICO

Morsal Babayan[1,*], Tomas Cordero-Lanzac[2], Satya Joshi[1], Juan Ignacio Mirena[2], Esko Kokkonen[3], Evgeniy Redekop[2], Samuli Urpelainen[1], Unni Olsbye[2], Marko Huttula[1]

1 Nano and Molecular Systems Research Unit, University of Oulu, Oulu, Finland

2 Department of Chemistry, Centre for Materials Science and Nanotechnology (SMN), University of Oslo, Oslo, Norway

3 MAX IV Laboratory, Lund University, Lund, Sweden

[*]Contact: morsal.babayan@oulu.fi

Keywords: PEPICO, methanol-to-hydrocarbons (MTH), zeolite

The Methanol-To-Hydrocarbons (MTH) process represents a novel approach in the feedstock base industry, aimed at shifting towards sustainable resources. The process involves the conversion of methanol, a C1 feedstock that can be produced from green sources, into hydrocarbons using acid zeolite or zeotype catalysts [1]. However, the reaction that occurs in zeolites yields a complex mixture of multiple isomers and species, which poses challenges for effluent analysis. The conventional gas-phase chromatography (GC) method, typically employed for effluent analysis [2], is often insufficient for separating isomers or detecting highly reactive molecules, especially with increased time resolution. A potential solution to enhance the isomer selectivity and analytical power of mass spectrometry (MS) is to detect ions in coincidence with the emitted photoelectron through the Photoelectron-Photoion Coincidence (PEPICO) method [3].

In this study, the reaction of dimethylether (DME) on a ZSM-5 is investigated using in situ/operando PEPICO at low pressure, which is conducted at the FinEstBeAMS beamline in MAX IV. The reaction between DME and freshly activated zeolite is performed at 1×10^{-6} [mbar] and 375 [°C], while PEPICO was conducted with 40 [eV] photon energy in coincidence with electrons in a binding energy range of approximately 7-17 [eV], leading to single valence ionization. Ions are identified using Time of Flight mass spectrometry, and parent molecules are distinguished from fragments by analyzing the coincidence ion yield photoelectron spectra (CIY-PES) for each cation. ZSM-5 deactivates quickly in an ambient DME flow but remains stable at low pressure. Stable full DME conversion for several hours allows for the accumulation of sufficient statistics for qualitative evaluation.

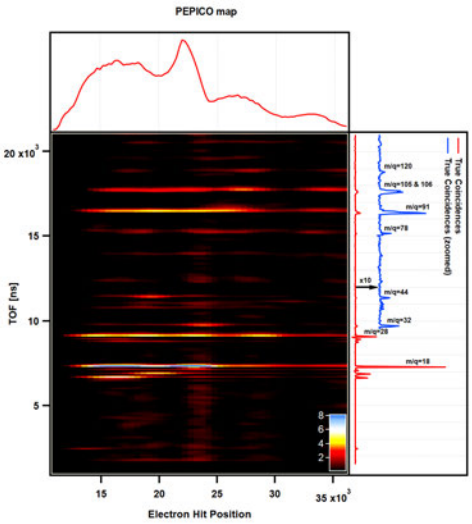

Figure 1: PEPICO map of the effluent stream.

Water, ethylene, methane, benzene, toluene, and various isomers of xylene and trimethylbenzene are detected. While the overall photoelectron spectra for different isomers of xylene are similar, they differ in their first peak related to the ionization channel of $C_8H_{10} + h\nu \rightarrow C_8H_{10}^+ + e^-$. Comparison between the CIY-PES for $C_8H_{10}^+$ cations with reference spectra of xylene isomers reveal that m-xylene is the dominant one in the effluent. Consequently, PEPICO-based effluent analytics is well-suited for systematic, quantitative, isomer-selective kinetic studies of MTH-relevant reactions under well-defined, low-pressure conditions, with minimized interference from secondary and deactivating reactions.

[1] Olsbye et al., Conversion of methanol to hydrocarbons: how zeolite cavity and pore size controls product selectivity, *Angewandte Chemie International Edition* **51**, 5810-5831 (2012).

[2] Bowers et al. Gas-phase ion chromatography: transition metal state selection and carbon cluster formation, *Science* **260**, 1446-1451 (1993).

[3] Hemberger et al., New analytical tools for advanced mechanistic studies in catalysis: photoionization and photoelectron photoion coincidence spectroscopy, *Catalysis Science & Technology* **10**, 1975-1990 (2020).

APXPS Study of Photocatalytic Driven Atomic and Electronic Transformation of Core-Shell Ni@NiCO3/NiO Photocatalyst

Manoj Kumar Ghosalya,[1,] * Harishchandra Singh,[1] Parisa Talebi,[1] Alexander Klyushin,[2] Esko Kokkonen,[2] Marko Huttula[1] Wei Cao[1] and Samuli Urpelainen[1]

1. Nano and Molecular Systems Research Unit, University of Oulu, FIN-90014, Finland.

2. MAX IV Laboratory, Lund University, Box 118, Lund, 22100, Sweden

Contact: manoj.ghosalya@oulu.fi

Keywords: Insitu photocatalysis, APXPS, Solar simulator

Atomic-level understanding of the active sites and transformation mechanisms under realistic conditions is a prerequisite for the rational design of a high-performance photocatalyst. A detailed study of photocatalytic-driven atomic structure and electronic transformation of core-shell Ni@$NiCO_3$/NiO photocatalysts was carried out using ambient pressure X-ray photoelectron spectroscopy under 1 mbar H_2O pressure. Ni@$NiCO_3$/NiO, with a metallic Ni^0 core and mixed $NiCO_3$ and NiO shell, is a visible light active photocatalyst used for water splitting to hydrogen.[1] Many interesting reversible structural and electronic transformations are observed in photocatalysts when subjected to water vapor and solar simulator light (Fig. 1). Solar simulator light under UHV conditions does not affect the photocatalyst's electronic structure. However, under in-situ conditions, APXPS results demonstrate that metallic Ni^0 (catalyst's core) absorbs light and frees up photoelectrons under 1 mbar of water vapor. These excited electrons from Ni^0 are further transferred to $NiCO_3$, where they are utilized to reduce hydrogen ions in the hydrogen evolution reaction (HER). In addition, Ni/NiO interfaces are oxidized to NiOOH when the catalyst is subjected to water vapor and solar simulator light. Furthermore, as a resolute of our study, we outline the carbonate's role and participation in the reaction mechanism, which is rarely investigated in photocatalysis. We also used principal component analysis (PCA) to identify the underlying chemical components contributing to the complex Ni 2p, C1s, and O 1s spectra under operando conditions and justified our data fitting and analysis.

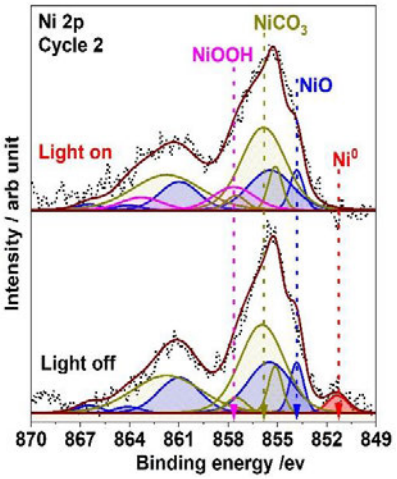

Figure 1: - In-situ XPS measurement of chemical states evolution of nickel during in situ photocatalysis.

[1] Talebi, P., Singh, H., Rani, E., Huttula, M. & Cao, W. Surface plasmon-driven photocatalytic activity of Ni@NiO/Nico 3 core-shell nanostructures. RSC Adv. 11, 2733–2743 (2021).

Development of *operando* transmission soft x-ray absorption spectroscopy of Li-ion battery structure by x-ray excited optical luminescence

Miho Kitamura[1,2,*], Shigeru Kobayashi[3,4], Taro Hitosugi[3,4], and Koji Horiba[1,2]

1 Institute for Advanced Synchrotron Light Source, National Institutes for Quantum Science and Technology (QST), Sendai, Japan

2 Photon Factory, Institute of Materials Structure Science, High Energy Accelerator Research Organization (KEK), Tsukuba, Japan

3 Department of Chemistry, The University of Tokyo, Tokyo, Japan

4 School of Materials and Chemical Technology, Tokyo Institute of Technology, Tokyo, Japan

**Contact: kitamura.miho@qst.go.jp*

Keywords: soft x-ray spectroscopy, x-ray excited optical luminescence, *operando* measurement, Li-ion battery

Soft x-ray absorption spectroscopy (XAS) is an excellent method for the direct observation of electronic states with element selectivity. It allows the observation of valence modulations due to reactions as well as modulations of crystal structure from the ligand field. Therefore, soft XAS is expected to be used to elucidate not only the basic material properties but also the mechanisms of the device operation in the fields of environmental and energy sciences. However, because it is necessary to thin the thickness of the sample due to the short probing depth of soft x-ray, there are barriers to the *operando* observation of changes in electronic states of multilayered device structure under the operation using soft XAS. Thus, an unconventional soft x-ray spectroscopy technique, where the thinning of the sample is not required, and we can directly measure the soft XAS on the actual device structure, is indispensable for *operando* observation of changes of electronic states under the operation.

We proposed an unconventional *operando* soft XAS method that can measure changes in electronic states of device structure under the operation, which is called "transmission x-ray absorption spectroscopy by x-ray excited optical luminescence (Tr-XAS by XEOL)." In this method, a thin film and a device structure are prepared on a fluorescent substrate that emits visible light fluorescence (XEOL) by soft x-ray irradiation. XAS spectra are obtained by measuring XEOL generated from a fluorescent substrate by the transmitted soft x-ray through a thin film and a device [1]. Although this method is a kind of Tr-XAS, it does not require sample thinning, such as removal of the substrate, and soft XAS measurements can be performed on thin films with substrates and multilayered device structures. In addition, the signal intensity of Tr-XAS by XEOL is expected to be several orders of magnitude higher than that of the fluorescence XAS, allowing for faster scanning during the *operando* measurements.

In this presentation, we introduce the results of the developed *operando* Tr-XAS by XEOL of the thin-film all-solid-state Li-ion battery structure fabricated on an Al_2O_3 fluorescent substrate. The continuous valence changes of Co ions between Co^{3+} and Co^{4+} in the cathode electrode ($LiCoO_2$) following the charge-discharge reactions have been clearly observed from Tr-XAS spectra.

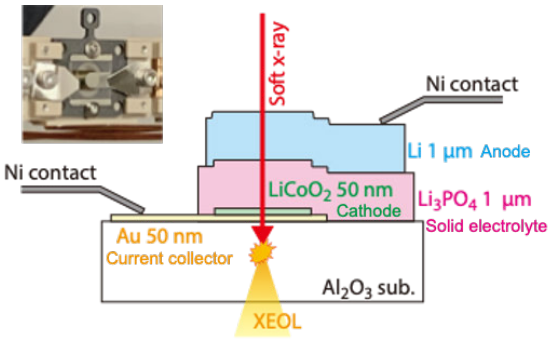

Figure 1: Measured structure of the thin-film all-solid-state Li-ion battery. The inset shows the sample picture of *operando* measurement sample.

1. C. Piamonteze, Y. W. Windsor, S. R. V. Avula, E. Kirk, U. Staub, Soft X-ray absorption of thin films detected using substrate luminescence: a performance analysis, J. Synchrotron Rad. **27**, 1289 (2020).

Nano-spintronics beamline with versatile photon polarization at NanoTerasu, a new synchrotron facility at Tohoku, Japan

Yoshiyuki Ohtsubo[1,*], Miho Kitamura[1], Tetsuro Ueno[2], Hideaki Iwasawa[1], Kohei Yamamoto[1], Jun Miyawaki[1], Koji Horiba[1], Kento Inaba[1], Akane Agui[1], Takeshi Nakatani[1], Nobuhito Inami[1], Kentaro Fujii[1], Tomoyuki Takeuchi[1], Takashi Imazono[1], Hiroaki Kimura[1] and Masamitu Takahasi[1]

1 Institute for Advanced Synchrotron Light Source, National Institutes for Quantum Science and Technology, Sendai, Japan

2 Synchrotron Radiation Research Center, National Institutes for Quantum Science and Technology, Hyogo, Japan

**Contact: y_oh@qst.go.jp*

Keywords: X-ray absorption spectroscopy, X-ray magnetic circular dichroism, spintronics, nanostructure

A new beamline dedicated for microscopic x-ray magnetic circular dichroism (XMCD) and x-ray magnetic linear dichroism (XMLD) is planned as one of the public beamlines in the 3-GeV next-generation synchrotron radiation facility at Tohoku, Japan (NanoTerasu) [1], which is scheduled to start operation in 2024. To investigate variety of magnetic and spintronic materials/elements with high sensitivity, wide range of energies of synchrotron radiations and accurate, versatile control of its polarization are desirable. For this purpose, four segmented APPLE-II type undulators are designed to provide brilliant soft and tender X-rays in 180-3000 eV [2]. It also enables versatile photon polarizations with high-speed polarization switching in ~100 msec. The beamline optics is selected for a highly efficient and precise use of XMCD/XMLD technique balancing high photon flux and energy resolution.

Such photons are used in a series of endstations. One branch is designed to use a monolithic Wolter mirror to balance the high flux of the mirror optics and sub-μm beam size (a geometrical demagnification factor is around 20). Another branch is dedicated for a microscopy setup using Fresnel zone plates with the target spot size around 10 nm. The other sample positions for various other experiments to use the versatile photons from segmented undulators are also reserved [3].

In the presentation, the simulated performance of the segmented undulator, such as the expected photon flux, polarization, and spatial distribution derived from the interference of four undulator segments will be presented. Planned layout of endstations as well as their possible applications for future microscopic XMCD/XMLD studies will be shown together.

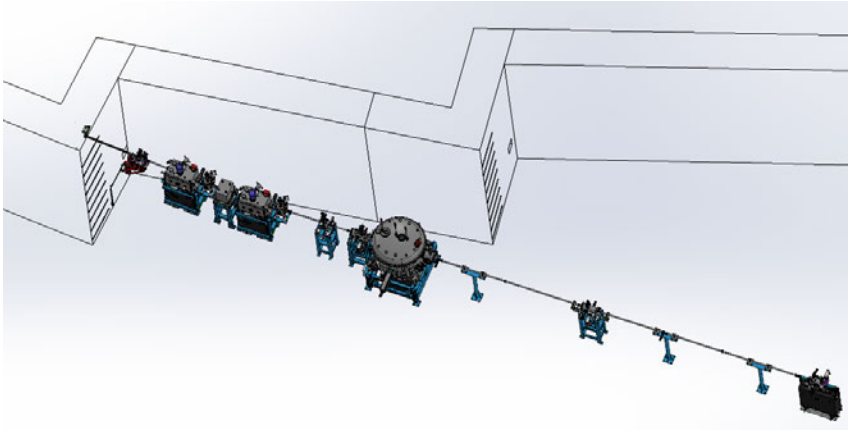

Figure: A 3D overview of the beamline.

1. Design report of NanoTerasu, available at https://www.qst.go.jp/uploaded/attachment/18596.pdf
2. I. Matsuda *et al.*, Segmented Undulator for Extensive Polarization Controls in ≤1 nm-rad Emittance Rings, *e-J. Surf. Sci. Nanotech.* **17**, 41-48 (2019).
3. Y. Ohtsubo *et al.*, Design of nano-spintronics beamline at 3-GeV next-generation synchrotron radiation facility, NanoTerasu, J. Phys.: Conf. Ser. **2380**, 012037 (2022).

Magnetic bottle electron spectrometer driven by electron pulses

Klemen Bučar*, Žiga Barba, and Matjaž Žitnik.
Jožef Stefan Institute, Jamova 39, SI-1001 Ljubljana, Slovenia
**Contact: klemen.bucar@ijs.si*

Keywords: electron TOF spectrometer, electron excitation, electron coincidence measurements

We presented the design, construction, characteristic properties, and first application of a new spectroscopic tool, the *electron-driven magnetic bottle spectrometer*. Similar to the MBES arrangement with the pulsed He lamp, the instrument enables spectroscopic studies in the laboratory where measuring time is not as limited as that at the synchrotron facilities. Apart from accessing the physics of electron scattering by recording the complete electron spectra, the advantage of the electron-driven device with respect to the lamp technique is the possibility to easily switch between different electron-impact energies. The crucial part of the machine is a pulsed nanosecond electron beam that hits a dense gas in the region of a strong magnetic field gradient from where the electrons are collected according to the well-known magnetic bottle principle of operation.
To demonstrate the inital performance of the new instrument, the electron scattering on the argon gas at 800 eV impact energy was studied. While the (e, 2e) coincidence data clearly show all the opened ionization channels, a single-hit distribution of arrival times still hides the weak atomic signal under the background signal. It turns out that BEB theory describes the electron scattering quite precisely, including kinetic energy sharing distribution for electron pairs released in the ioniza- tion of different atomic shells. The theory predicts an enhanced contrast of 3s vs 3p ionization yield when the energy sharing between the scattered and the ejected electron departs from the asymmetric one, as, indeed, observed. Looking at the Auger electron—scattered or ejected electron coincidences—the method based on the BEB theory is devised to estimate the MBES electron detection efficiency over a range of kinetic energies simultaneously. Another way to look at the data is introduced by making histograms of the sum of two, three, and four electron kinetic energies and separate false coincidences by the introduction of the low-kinetic energy cutoff. That way, we were able to isolate the signal of $3p^{-2}$ and $2p^{-1}$ $3p^{-1}$ states and also detect a weak feature that may be due to the Coster-Kronig decay of the 2s hole. The signal of the corresponding $3p^{-3}$ final states involves detection of four electrons from a single atomic event, triggered by the electron scattering.

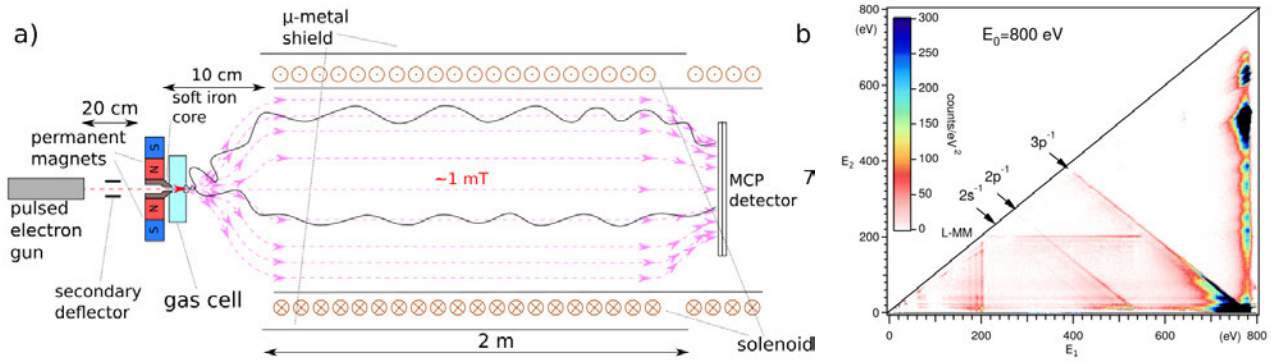

[1] Ž. Barba, K. Bučar, Š. Krušič, M. Žitnik, Magnetic bottle electron spectrometer driven by electron pulses, *Rev Sci Instrum.* **91**(7):073108 (2020). doi:10.1063/5.0012523

Accurate potential energy surface for cold collisions of metastable helium with molecular hydrogen

Mariusz Pawlak[1,*], Piotr S. Żuchowski[2] and Piotr Jankowski[1]

1 Faculty of Chemistry, Nicolaus Copernicus University in Toruń, Gagarina 7, 87-100 Toruń, Poland
2 Faculty of Physics, Astronomy and Informatics, Nicolaus Copernicus University in Toruń, Grudziądzka 5, 87-100 Toruń, Poland
**Contact: teomar@chem.umk.pl*

Keywords: electronic structure calculations, potential energy surface, cold collisions, kinetic isotope effect

We have confirmed the very strong kinetic isotope effect in cold Penning ionization reactions of hydrogen isotopologues with excited metastable helium atoms [1] based on our recently developed high-quality ab initio potential energy surface [2]. We have shown that one fundamental physical phenomenon hidden in the experimental data [3,4] was not recognized, namely the dependence of the interaction of colliding species on the vibrations of the molecule. The proper incorporation of this effect into the interaction potential leads to a remarkable agreement of the theoretical predictions with the experimental findings without a need for any empirical adjustment whatsoever. We have demonstrated that even rigorous calculations at the full CI level of theory within the rigid-rotor approximation may be insufficient to achieve excellent agreement between the theory and experiment at subkelvin temperatures. Thus, for the cases where the highest accuracy is indispensable, one has to take into account the nonrigidity effects of the molecule.

1. M. Pawlak, P. S. Żuchowski, P. Jankowski, Kinetic isotope effect in low-energy collisions between hydrogen isotopologues and metastable helium atoms: Theoretical calculations including the vibrational excitation of the molecule, *J. Chem. Theory Comput.* **17**, 1008-1016 (2021).
2. M. Pawlak, P. S. Żuchowski, N. Moiseyev, P. Jankowski, Evidence of nonrigidity effects in the description of low-energy anisotropic molecular collisions of hydrogen molecules with excited metastable helium atoms, *J. Chem. Theory Comput.* **16**, 2450-2459 (2020).
3. E. Lavert-Ofir, Y. Shagam, A. B. Henson, S. Gersten, J. Kłos, P. S. Żuchowski, J. Narevicius, E. Narevicius, Observation of the isotope effect in sub-kelvin reactions, *Nature Chem.* **6**, 332-335 (2014).
4. A. Klein, Y. Shagam, W. Skomorowski, P. S. Żuchowski, M. Pawlak, L. M. C. Janssen, N. Moiseyev, S. Y. T. van de Meerakker, A. van der Avoird, C. P. Koch, E. Narevicius, Directly probing anisotropy in atom-molecule collisions through quantum scattering resonances, *Nature Phys.* **13**, 35-38 (2017).

Nuclear Dynamics in Cyclopropane

Ville Lindblom[1,*], Stacey Sörensen[1]
1 Department of Physics, Lund University, Lund, Sweden
[*]Contact: ville.lindblom@sljus.lu.se

Keywords: AMO, Inner-Shell Electronic States, Momentum Imaging, Multiparticle Spectroscopy

Three-dimensional electron and ion imaging spectrometry is used to study the evolution of the molecular geometry in gas-phase cyclopropane after inner-shell electron excitation. Cyclopropane is the simplest cyclic hydrocarbon and the high ring strain affects the stability of the molecule. Deformation of the carbon 'ring structure' in cyclopropane can arise due to the Jahn-Teller effect. Dication states serve as "gateway" states [1] which are directly associated with certain fragmentation channels in the molecule. Core-excited states at the C 1s ionization threshold are predicted to exhibit nuclear dynamics which reflect the bonding character of the valence molecular orbitals [2,3]. This study investigates whether trends in fragmentation pathways reflect the nuclear dynamics in the core-excited states of cyclopropane. In other words, if it is possible to control the nuclear dynamics of a molecule by tuning the frequency of the interacting photon.

In an earlier study we showed that the $C_2H_3^+$+CH_3^+(1) and $C_3H_3^+$+H^+ (4) ion pairs indicate ring deformation where one C-C bond is elongated, which can lead to ring opening. The $C_3H_3^+$+H_3^+ (3) pair retains the carbon 'ring' after bond rearrangement, and $C_2H_2^+$+CH_3^+ (5) ion pairs indicate methylene formation after hydrogen migration. The ion pair $C_2H_4^+$+CH_2^+ (2) results from extension of two C-C bonds. The model described in [1] suggests that the nuclear dynamics of the core-excited state influences the propensity of certain fragmentation pathways, specifically the C1s→5e'(σ_{in}*) should promote the fragmentation channels (1) and (4), C1s→2a"$_2$(π*) should promote (3) and (5). Lastly, C1s→2a'$_2$(σ_{ex}*) is expected to increase the intensity of the (2) fragmentation channel.

The fragmentation patterns differ substantially for excitation to different states. This can be in an overview seen in Figure 1. These trends are discussed and analyzed in light of the theoretical predictions. This experiment was carried out at MAX IV Laboratory in Lund, Sweden, at the beamline FlexPES on the experimental end station ICE (Ions in Coincidence with Electrons).

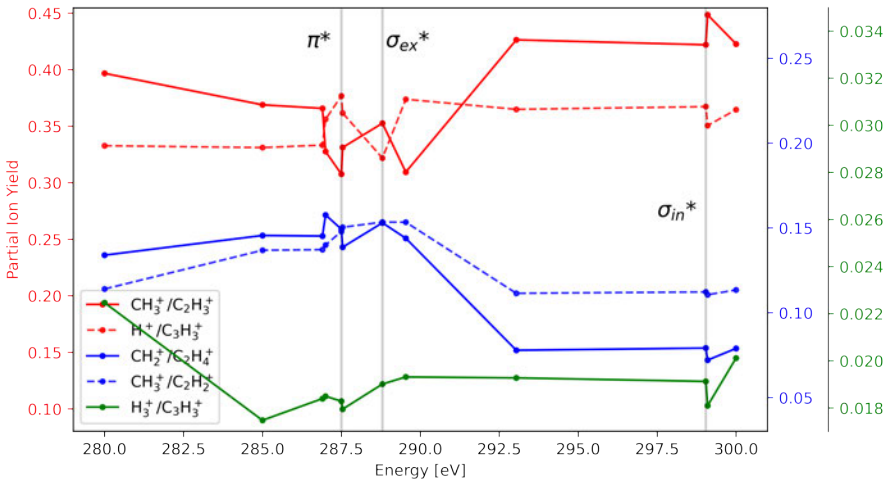

Figure 1: The partial ion yield of a select ion pair combinations.

[1] Oghbaiee, S. et al. (2017), Dissociation of cyclopropane in double ionization continuum, *Phys. Chem. Chem. Phys.*, **19**, pp. 19631-19639. doi:10.1039/C7CP01667K.

[2] Hitchcock, A. P. et al. (1986), Carbon K-shell excitation of gaseous and condensed cyclic hydrocarbons:C_3H_6,C_4H_8,C_5H_8,C_5H_10,C_6H_10,C_6H_12 and C_8H_8, *J. Chem. Phys.* **85**,4849. doi:10.1063/1.451719.

[3] Duflot, D. et al. (2006), *Ab initio* study of core excited cyclopropane, *Chemical Physics* **327**, pp. 518-528. doi:10.1016/j.chemphys.2006.05.027.

Structural dynamics in multiphoton core ionization of water isotopologues

Maria Novella Piancastelli
Sorbonne Université, CNRS, Laboratoire de Chimie Physique-Matière et Rayonnement, Paris, France
Contact: maria-novella.piancastelli@sorbonne-universite.fr

Keywords: multiphoton photoionization, structural dynamics, water core level

The ultrafast structural dynamics of water following inner-shell ionization are a crucial issue in high-energy radiation chemistry in liquid media. We have exposed isolated water isotopologues to a short x-ray pulse from a free-electron laser, the EuXFEL in Hamburg, Germany, and detected momenta of all produced ions in coincidence by a reaction microscope apparatus. We have studied the series H_2O-HDO-D_2O. By combining experimental results and advanced theoretical modelling, we can image dissociation dynamics of individual molecules in unprecedented detail. We reveal and compare significant molecular structural dynamics along the series, such as asymmetric bond elongation and bond-angle opening, leading to two-body or three-body fragmentation on a timescale of a few femtoseconds. Furthermore, by exploiting a novel analysis method, a deep insight into the fragmentation processes in HDO is achieved [1,2].

1. T. Jahnke, R. Guillemin, L. Inhester, S.-K. Son, G. Kastirke, M. Ilchen, J. Rist, D. Trabert, N. Melzer, N. Anders, T. Mazza, R. Boll, A. De Fanis, V. Music, Th. Weber, M. Weller, S. Eckart, K. Fehre, S. Grundmann, A. Hartung, M. Hofmann, C. Janke, M. Kircher, G. Nalin, A. Pier, J. Siebert, N. Strenger,I. Vela-Perez, T. M. Baumann, P. Grychtol, J. Montano,Y. Ovcharenko, N. Rennhack, D. E. Rivas, R. Wagner, P. Ziolkowski, P. Schmidt, T. Marchenko, O. Travnikova, L. Journel, I. Ismail, E. Kukk, J. Niskanen, F. Trinter, C. Vozzi, M. Devetta, S. Stagira, M. Gisselbrecht, A. L. Jäger, X. Li, Y. Malakar, M. Martins, R. Feifel, L. Ph. H. Schmidt, A. Czasch, G. Sansone, D. Rolles, A. Rudenko, R. Moshammer, R. Dörner, M. Meyer, T. Pfeifer, M. S. Schöffler, R. Santra, M. Simon and M. N. Piancastelli, Inner-Shell-Ionization-Induced Femtosecond Structural Dynamics of Water Molecules Imaged at an X-Ray Free-Electron Laser, Phys.Rev.X 11, (2021) 041044.

2. R. Guillemin, L. Inhester, T. Mazza, R. Boll, Th. Weber, S. Eckart, P. Grychtol, N. Rennhack, T. Marchenko, N. Velasquez, O. Travnikova, I. Ismail, J. Niskanen, E. Kukk. F. Trinter, M. Gisselbrecht, R. Feifel, G. Sansone, D. Rolles, M. Martins, M. Meyer, M. Simon, R. Santra, T. Pfeifer, T. Jahnke and M. N. Piancastelli, in manuscript

Imaging Soft X-ray Spectroscopy at the Small Quantum Systems Instrument of the European XFEL

J.-E. Rubensson[1], M. Agåker[1,10], H. Ågren[1], O. Björneholm[1], R. Boll[2], J. Bozek[3], L. Budewig[16,21], S. Cardoch[1], S. Coriani[4], L. Cornetta[1,20], A. De Fanis[2], E. De Santis[1], S. Dold[2], G. Doumy[5], U. Eichmann[6], X. Gong[7], J. Gråsjö[1], I. Ismail[9], L. Kjellsson[10], K. Li[11], E. Lindroth[12], T. Mazza[2], J. Montaño[2], T. Mullins[2], H. Ni[7], J. Nordgren[1], C. Ott[13], Y. Ovcharenko[2], M. Patanen[14], T. Pfeifer[13], M.N. Piancastelli[9], R. Püttner[15], N. Rennhack[2], N. Rohringer[16,21], C. Sánchez-Hanke[8], R. Santra[16,21], C. Såthe[10], P. Schmidt[2], B. Senfftleben[2], M. Simon[9], J.C. Söderström[1], S.-K. Son[16], N. Timneanu[1], M. Togawa[2], K. Ueda[17], S. Usenko[2], H.J. Wörner[18], W. Xu[19],Z. Yin[17], L. Young[5], M. Meyer[2], and T.M. Baumann[2]

[1]Uppsala University, Uppsala, Sweden, [2]European XFEL, Schenefeld, German, [3]Synchrotron Soleil, Gif-sur-Yvette Cedex, France, [4]Technical University of Denmark, Lyngby, Denmark, [5]Argonne National Laboratory, Lemont, USA, [6]Max-Born-Institut, Berlin, Germany, [7]East China Normal University, Shanghai, China, [8]Diamond Light Source, Chilton, United Kingdom, [9]Sorbonne University, Paris, France, [10]MAX IV Laboratory, Lund University, Lund, Sweden, [11]University of Chicago, Chicago, USA, [12]Stockholm University, Stockholm, Sweden, [13]Max-Planck-Institut für Kernphysik, Heidelberg,Germany, [14]University of Oulu, Oulu, Finland, [15]Freie Universität Berlin, Berlin, Germany, [16]Deutsches Elektronen-Synchrotron (DESY), Hamburg, Germany, [17]Tohoku University, Sendai, Japan, [18]ETH Zürich, Zürich, Switzerland, [19]ShanghaiTech University, SHINE, Shanghai, China, [20] University of Campinas, SP, Brazil, [21] Universität Hamburg, Hamburg, Germany

**Contact: jan-erik.rubensson@physics.uu.se*

Keywords: X-ray spectroscopy, free-electron lasers, non-linear phenomena

We present the first measurements with the 1D imaging soft X-ray spectrometer [1], recently installed at the Small Quantum Systems (SQS) instrument [2] of the European XFEL. The imaging capability allows for separation of emission spectra excited along the path of the X-ray incident beam, intended to facilitate investigation of non-linear X-ray-matter interactions in dense gaseous media, and time-resolved pump-probe measurements.

The soft X-ray fluorescence spectra of Ne and Xe show a rich phenomenology with a multitude of emission lines, critically depending on photon energy, fluence, and target density. The dependence on the incident photon energy shows a complex resonant behavior that enables a detailed characterization of the population mechanisms for core excited states in multiply ionized species [3], for Ne including all charge states from Ne^{+} to hydrogen-like Ne^{9+}. Core excited states with lifetimes in the ps-to-ns range are studied with time resolution, and as a function of target density, thereby enabling us to address interactions with the surrounding plasma. Pulse propagation effects become manifest in non-trivial spectral variations along the imaged path of the incident photons.

1. M. Agåker et al., in preparation, (https://indico.desy.de/event/30652/)
2. T. Mazza et al., J. Synchrotron Radiat. **30** (2), 457–467 (2023)
3. L. Budewig, et al., Phys. Rev. A **107**, 013102 (2023)

X-ray absorption and Resonant Inelastic X-ray Scattering from condensed N_2

Johan Söderström[1,*], Marcus Agåker[1], Olle Björneholm[1], Jan-Erik Rubensson[1], Ricardo Marinho[2], Arnaldo Naves de Brito[3], Conny Såthe[4], Marco Caputo[4], Ludvig Kjellson[4], Takashi Tokushima[4], Anirudha Ghosh[4], Victor Ekholm[4]

1. *Department of Physics and Astronomy, Uppsala University, Uppsala, Sweden*
2. *Instituto de Física, Universidade de Brasília, Brasília, DF, Brazil and Instituto de Física, Universidade Federal da Bahia, Salvador, BA, Brazil*
3. *Department of Applied Physics, Institute of Physics "Gleb Wataghin", Campinas University, CEP, 13083859 Campinas SP, Brazil*
4. *MAX IV Laboratory, Lund University, SE-221 00 Lund, Sweden*

**Contact: Johan.Soderstrom@physics.uu.se*

Keywords: XAS, RIXS, condensed N_2, long-lived transient species

Condensed N_2 is a van-der-Waals bonded molecular material with weak intermolecular interaction. Due to its relevance in chemistry in the universe, condensed N_2 has been extensively studied. As an example, it has previously been shown that long-lived excited atomic species are observed in some abundance in condensed N_2 [1] as has the occurrence of N_3^- ions [1, 2]. We here present X-ray studies of condensed N_2 corroborating these claims, as well as suggesting that the N_3^- ions can be formed in a vibrationally excited state.

Our X-ray absorption data (see Fig. 1) shows well-resolved peaks at lower excitation energy as compared to the molecular π* resonance. We attribute these peaks to excitations in both ground state atomic nitrogen as well as in excited atomic species. The associated Resonant Inelastic X-ray Scattering (RIXS) spectra shows energy losses associated with these excitations reveals parts of the excitation process in the atom.

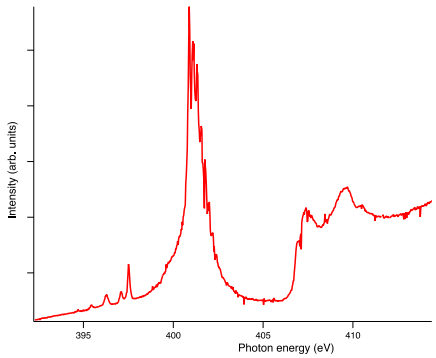

Figure 1. X-ray absorption spectra near the 1s ionization threshold in condensed N_2 showing the well-known π* resonance, and at lower photon energies excitations in atomic nitrogen which is not present in the gas phase. At approximately 1 eV lower photon energy as compared to the *v=0* vibration in the π* resonance a "shoulder" is observed.

Furthermore, at slightly lower excitation energies as compared to the molecular π* resonance we observe a "shoulder", here the RIXS spectra reveals a complicated landscape, see Fig. 2. The RIXS spectra from this region shows clear evidence of formation of N_3^- or N_3 complexes, the RIXS spectra also shows anti-Stokes lines (energy gain) associated with the N_3 molecule/ion. Preliminary analysis indicates that the N_3 molecule/ion are formed predominantly in the *v=3* vibrationally excited state.

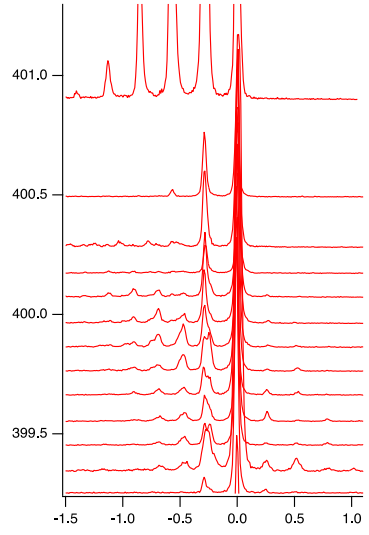

Figure 2. RIXS spectra acquired near the "shoulder" of the π* resonance (the incident photon energy is indicated on the vertical axis and the energy loss/gain on the horizontal axis) showing several energy loss and gain features. These can be attributed to vibrational energy loss in condensed N_2, from N_3 molecules/ions and likely also from NO.

The Rydberg region near the 1s ionization threshold has also been studied with RIXS (not shown here) which shows significantly broadened structures as compare to gas-phase studies of N_2 [3]. This could potentially be understood as the excited electron delocalizing in the N_2 matrix on ultrafast timescales, leading to increased lifetime broadening.

References:

1. Jen-Iu Lo, et al., PNAS, 116(49), 24420–24424 (2019)
2. R. Tian, et al., J. Chem. Phys., 92, 4073–4079 (1988)
3. J.-E. Rubensson, et al., Phys. Rev. Lett. 114, 133001 (2015=

The effect of selective C 1s excitation on Auger-Meitner decay in the ESCA molecule

A.E.A. Fouda[1], V. Lindblom[2], S.H. Southworth[1], G. Doumy[1], L. Cheng[3], P. J. Ho[1], L. Young[1,4], S.L. Sorensen[2]*

1.Chemical Sciences and Engineering Div., Argonne National Laboratory, 9700 S Cass Avenue, Lemont, IL 60439 USA
2. Department of Physics, Lund University, Box 118, 22100 Lund, Sweden
3. Department of Chemistry, Johns Hopkins University, Baltimore, MD, USA
4. Department of Physics and James Franck Institute, The University of Chicago, Chicago, IL 60637, USA
**Contact: stacey.sorensen@sljus.lu.se*

Keywords: site-selective excitation and decay, calculated photoelectron and resonant spectra

The trifluoro ethyl acetate molecule with four carbon 1s peaks in the photoelectron spectrum is a showcase for the chemical shift in electron spectra. While a number of studies have focused on photoionization or Auger-Meitner decay none of these have addressed the valence electrons or the resonant Auger spectra. In a recent paper we analyzed the NEXAFS spectrum of the ESCA molecule via coupled-cluster calculations, and found that these theoretical methods reproduce the spectrum very well and the site of the core electron excitations was assigned [1].

Here we address the question of whether the final states populated after decay of localized core-excited states retain the signature of the site of the original photoexcitation. The excited states decay on the 8-10 fs time scale populating one-hole or two-hole one-particle states. In order to probe the localization of the core hole the transition rates are calculated. The core-excited states were calculated in the previous study [1], but the valence electrons states have not been published in any previous experimental or theoretical studies. EOM-CCSD Dyson orbitals from the CFOUR program [2] were used to describe the bound states in the calculation, and the continuum electron wave function and cross section calculations were performed using the ezDyson software [3,4].

In Fig. 1 the upper panel shows the measured electron yield over the range 285-300 eV, with the most intense transitions arising from the C_{OO} (1s-π*) transition (red bar) and the C_{F3} (1s-π*), C_{F3} (1s-σ*) and C_{F3} (1s-3p) transitions indicated with blue bars [1]. The lower panel shows the Auger-Meitner spectra measured over the entire range. The one-hole final valence states exhibit a linear dispersion of the kinetic energy with increasing photon energy. In the right hand panels the valence electron spectra measured at 120 eV are compared to calculated spectra. The site dependence is discussed based on the calculated valence electron orbitals.

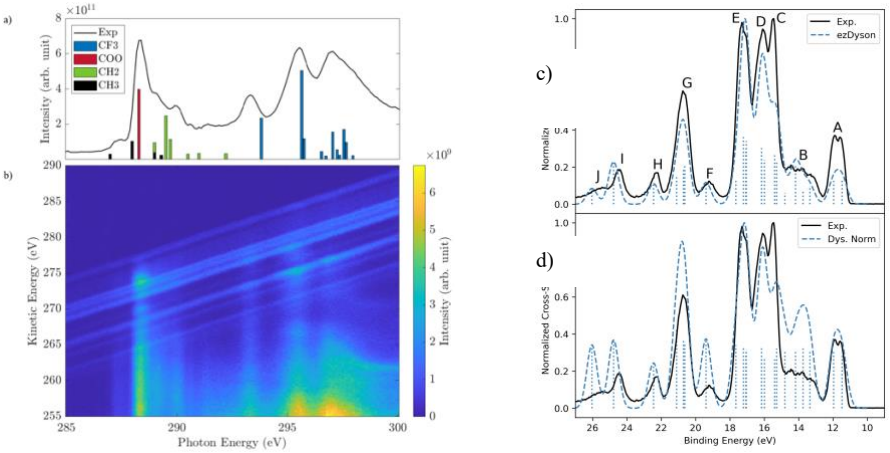

Figure 1: Electron-yield spectrum (a) and 2D Auger map (b) obtained by measuring electron spectra across the resonance range for all four carbon 1s electrons. In the upper panel we show the integrated electron intensity at each photon energy. The red bar indicates the most intense transition for the COO 1s-π*, and the blue bars indicate the energy and oscillator strengths for the C_{F3} transitions. Right panels: Measured and calculated direct valence electron spectra (c) using exDyson (d) Dyson orbital norms for the outgoing photoelectron wave. The valence spectrum was measured at a photon energy of 120 eV. The measurements were carried out at MAX IV at the FlexPES beam line using the gas-phase VG Scienta electron analyzer.

1. S. L. Sorensen, X. Zheng, S. H. Southworth, M. Patanen, E. Kokkonen, B. Oostenrijk, O. Travnikova, T. Marchenko, M. Simon, C. Bostedt, G. Doumy, L. Cheng and L. Young, J. Phys. B, **53** 244011 (2020).
2. D. A. Matthews, L. Cheng, M. E. Harding, F. Lipparini, S. Stopkowicz, T.-C. Jagau, P. G. Szalay, J. Gauss and J. F. Stanton, J. Chem. Phys **152**, 214108 (2020).
3 S. Gozem, A. O. Gunina, T. Ichino, D. L. Osborn, J. F. Stanton and A. I. Krylov, J. Phys. Chem. Lett. **6**, 4532 (2015).
4 S. Gozem and A. I. Krylov, Wiley Interdisciplinary Reviews: Computational Molecular Science, **12** e1546 (2022).

Modeling the fragmentation dynamics and valence photoelectron spectra of aminobenzoic acid

Onni Veteläinen [1,*], Minna Patanen[1], Matti Alatalo[1], Sergio Díaz-Tendero[2]
1 NANOMO, University of Oulu, Oulu, Finland
2 Departamento de Química, Universidad Autónoma de Madrid, Madrid, Spain
[*]Contact: onni.vetelainen@oulu.fi

Keywords: molecular dynamics, hydrogen migration, photoionization, theoretical spectroscopy

The fragmentation of dicationic aminobenzoic acid has been investigated using extended Lagrangian molecular dynamics. The orto-, meta- and para-isomers were considered, including the two rotational isomers for the orto- and meta species. The Franck-Condon approximation was applied and an estimated excess internal energy was randomly distributed among the nuclear degress of freedom at the beginning of each trajectory. This computational approach has been successful in studying hydrogen migration processes in the past [1]. A thousand trajectories were calculated for each isomer and internal energy estimate, and propagated for 250 fs. The formation of hydronium H_3O^+ as a fragmentation product following Auger decay of orto- and meta-aminobenzoic acid was experimentally observed in a previous study [2]. In particular the rate of H_3O^+ production was much higher for the orto-isomer. The molecular dynamics provide a clear mechanism for hydronium production; a combination hydrogen migration, neutral water emission and roaming, and a partial explanation for the production rate discrepancy between the two isomers.

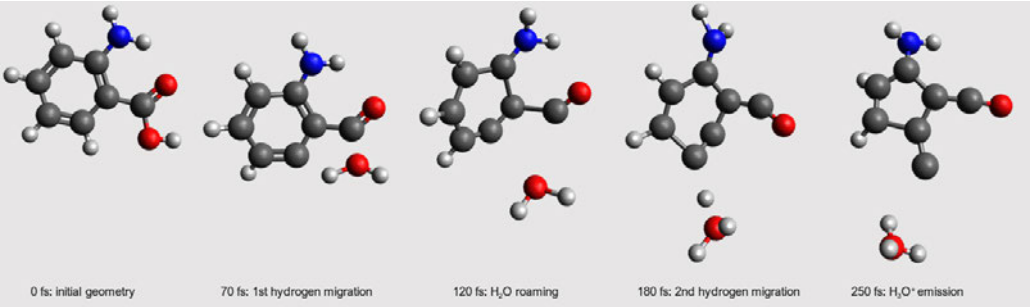

Figure 1: Snapshots of H_3O^+ formation.

Adapting the computational scheme of [3], the vibrationally resolved valence photoelectron spectra was calculated with the time-dependent adiabatic Hessian Frank-Condon method, and fixing the (0-0) transition energy using the vertical ionization potential obtained from an eigenvalue self-consistent GW calculation. Comparison of the theoretical and experimental photoelectron spectra provides insight into the relative abundancies of the rotational isomers.

[1] Kling, N.G., Díaz-Tendero, S., Obaid, R. et al. Time-resolved molecular dynamics of single and double hydrogen migration in ethanol. *Nat Commun* **10**, 2813 (2019).

[2] Abdul Rahman Abid, Onni Veteläinen, Nacer Boudjemia, Eetu Pelimanni, Antti Kivimäki, Matti Alatalo, Marko Huttula, Olle Björneholm, and Minna Patanen, Forming Bonds While Breaking Old Ones: Isomer-Dependent Formation of H3O+ from Aminobenzoic Acid During X-ray-Induced Fragmentation, *The Journal of Physical Chemistry A* **2022**, *127*(6), 1395-1401.

[3] Lukas Gallandi and Thomas Körzdörfer, Long-Range Corrected DFT Meets GW: Vibrationally Resolved Photoelectron Spectra from First Principles, *Journal of Chemical Theory and Computation* **2015**, *11*(11), 5391-5400

Instrumentation for electron spectroscopy and related research at the FinEstBeAMS beamline at MAX IV Laboratory

A. Kivimäki[1,2,*], W. Wang[1], K. Chernenko[1], C. Preger[1,3], T. Käämbre[4,1], A. Ghassami[1], R. Pärna[4], E. Kukk[5], K. Kokko[5], M. Lastusaari[6], M. Valden[7], M. Hirsimäki[7], K. Kooser[4,5], M. Patanen[2], P. Turunen[2], K. Jänkälä[2], S. Urpelainen[2], N. Walsh[1], M. Kirm[4] and M. Huttula[2]

1 MAX IV Laboratory, Lund University, Lund, Sweden
2 Nano and Molecular Systems Research Unit, University of Oulu, Oulu,Finland
3 Ergonomics and Aerosol Technology, Lund University, Lund, Sweden
4 Institute of Physics, University of Tartu, Tartu, Estonia
5 Department of Physics and Astronomy, University of Turku, Turku, Finland
6 Department of Chemistry, University of Turku, Turku, Finland
7 Faculty of Engineering and Natural Sciences, Tampere University, Tampere, Finland
**Contact: antti.kivimaki@maxiv.lu.se*

Keywords: electron spectroscopy, synchrotron radiation, gas-phase research, surface science

FinEstBeAMS has been designed as a multipurpose beamline for spectroscopic studies of materials in different phases using photons in the energy range 4.5-1300 eV. After completion of the ongoing upgrade of the undulator, users will be able to select the polarization of radiation between linear (in horizontal, vertical and inclined directions) and circular (left and right). Electron spectroscopy is practiced at two end stations – Gas-phase end station (GPES) [1] and Solid-state end station (SSES) [2] – which are mounted at two different branches of the beamline. A third end station is used for photoluminescence spectroscopy of inorganic materials, and it shares the same branch with the GPES.

The GPES has been designed especially for photoelectron-photoion coincidence (PEPICO) experiments, in which the kinetic energies of the electrons are analysed [1]. Its main instruments comprise a high-resolution Scienta R4000 hemispherical electron analyser and a momentum imaging ion time-of-flight (TOF) spectrometer, which is equipped with a RoentDek HEX80 delay line detector (DLD). The spectrometers can also be used independently. The ion TOF spectrometer is indeed often removed from the GPES, when large sample delivery systems such as a cluster source or an aerodynamic lens sample delivery system are used in experiments. A second vacuum chamber can be mounted downstream from the GPES for user experiments that cannot be performed with the standard GPES. That possibility has been used for a magnetic bottle electron spectrometer (MBES) and for a negative-ion/positive-ion coincidence setup, which consists of two TOF spectrometers mounted opposite one another. The operation of the MBES requires single-bunch operation, which is typically available for two weeks annually.

The SSES has been designed as a high-throughput instrument with flexible sample preparation options for X-ray photoelectron spectroscopy (XPS), angle-resolved photoemission spectroscopy (ARPES) and X-ray absorption spectroscopy (XAS) [2]. Its main instrument is a SPECS Phoibos 150 R7 electron analyser with a two-dimensional DLD. There are many surface science end stations in the world, but the SSES offers an attractive combination of the wide photon energy range, high photon energy resolution, variable polarization, and a small spot size (~10 x 15 μm^2). Moreover, the SSES is highly automated, and it is protected by programmable logic controller, which makes it very user friendly during on-site operation and allows remote access to the control system from outside MAX IV.

1. K. Kooser et al., Gas-phase endstation of electron, ion and coincidence spectroscopies for diluted samples at the FinEstBeAMS beamline of the MAX IV 1.5 GeV storage ring, *J. Synchrotron Rad.* **27**, 1080–1091 (2020).
2. W. Wang et al., A new user-friendly materials science end station at the FinEstBeAMS beamline of MAX IV, *J. Phys. Conf. Series* **2380**, 012048 (2022).

Fragmentation of methanol molecules after valence photoexcitation studied by negative-ion positive-ion coincidence spectroscopy

Hanan Sa'adeh[1,2*], Antti Kivimäki[2,3], Christian Stråhlman[4], Kevin C Prince[5], and Richard D Thomas[6]

1 Department of Physics, The University of Jordan, Amman 11942, Jordan
2 MAX IV Laboratory, Lund University, Lund 22100, Sweden
3 Nano and Molecular Systems Research Unit, University of Oulu, Oulu 90014, Finland
4 Ma University, Ma 20506, Sweden
5 Elettra Sincrotrone Trieste, Area Science Park, Basovizza, Trieste, Italy
6 Department of Physics, Stockholm University, Stockholm 106 91, Sweden
**Contact: hanan.saadeh@ju.edu.jo*

Keywords: coincidence, negative ions, methanol, valence excitation

One of the main advantages of using negative-ion positive-ion coincidence (NIPICO) spectroscopy is the ability to determine ion-pair appearance energies, rather than just the appearance energy of the negative ion, as it is the case in conventional negative ion spectroscopy. This enhances the understanding of the fragmentation dynamics. In this work, we report results on ionic fragmentation upon valence photoexcitation of the simplest aliphatic alcohol, methanol (CH_3OH, m= 32 u). Methanol is an interesting organic compound; it is an interstellar molecule, a clean energy resource, and the chemical building block for hundreds of everyday products. It also serves as a good candidate for photodissociation studies due to its simple structure.

NIPICO spectra at C 1s and O 1s resonances were previously measured for methanol [1]. To our knowledge, there have been no reports on formation of negative ions in photon-excited methanol molecules in the valence region, which we report in this contribution.

Measurements were performed at the gas-phase end station (GPES) of the FinEstBeAMS beamline [2] in MAX IV Laboratory, Lund, Sweden, using the NIPICO setup where two time-of-flight (TOF) spectrometers are mounted opposite one another: One of these is for positive ions, and the other for negative ions and electrons. We have measured NIPICO spectra at several selected ranges of photon energy in the VUV region, by collecting coincidence signals at each photon energy for one hour. The obtained NIPICO spectra (e.g., Figure 1) revealed the following fragmentation channels (i.e., anion/cation pairs): H^-/H^+ (after 18.8 eV excitation), OH^-/CH_3^+, H^-/CHO^+, H^-/CH_2O^+, and H^-/CH_3O^+.

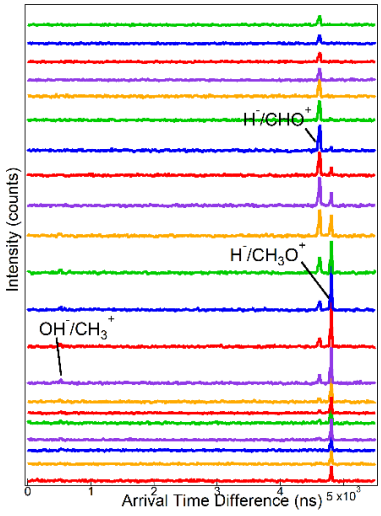

Figure 1: NIPICO spectra of methanol, measured at photon energies 13.0-16.4 eV (from bottom to top). [3]

1. A. Kivimäki, C. Stråhlman, R. Richter, R. Sankari, Fragmentation of methanol molecules after core excitation and core ionization studied by negative-ion/positive-ion coincidence experiments, *J. Phys. Chem. A* **122**, 224-233 (2018).
2. K. Kooser, A. Kivimäki, P. Turunen, R. Pärna, L. Reisberg, M. Kirm, M. Valden, M. Huttula and E. Kukk, Gas-phase endstation of electron, ion and coincidence spectroscopies for diluted samples at the FinEstBeAMS beamline of the MAX IV 1.5 GeV storage ring, *J. Synchrotron Radiat.* **27** 1080-1091 (2020).
3. H. Sa'adeh et al., In preparation.

ICE: A versatile REaction Microscope for molecular/cluster dynamics research at MAX IV Laboratory

N. Walsh[1,*], S. Ganguly[2], B. Oostenrijk[3], G. Michailoudi[4], S. Sörensen[2], M. Gisselbrecht[2], V. Lindblom[2], M. Tchaplyguine[1], G. Öhrwall[1], A. Preobrajenski[1], A. Generalov[1] and J. Adell[1]

1 MAX IV Laboratory, Lund, Sweden
2 Division for synchrotron radiation research, Lund University, Lund, Sweden
3 Struct. Dyn. Chem.Sys., DESY, Hamburg, Germany
4 Nano and Molecular Systems Research Unit, University of Oulu, P.O. Box 3000, 90014 Oulu, Finland

**Contact: noelle.walsh@maxiv.lu.se*

Keywords: multi-coincidence, COLTRIMS, Reaction Microscope, molecular dynamics

Reaction microscopes (REMI's) enable the correlated measurement of the 3-D momentum distributions of electrons and ions produced in a reaction and thus allow kinematically complete studies of fragmentation and photo-induced processes in small quantum systems [1-3]. With relatively high collection efficiency, such spectrometers have proven invaluable within the field of AMO science [3-6].

ICE[1] is a mobile coincidence spectroscopy end station at MAX IV Laboratory, in Lund, Sweden and is available to general users since 2022. The ICE REMI is a versatile instrument that enables multi-coincident electron-ion measurements following photo-excitation of atoms, molecules and clusters [7]. The spectrometer is adjustable in length and in electrostatic field geometry and can be used during either single bunch or multi-bunch delivery. In this contribution, the ICE end station will be presented and the performance of the spectrometer will be demonstrated using various experimental results.

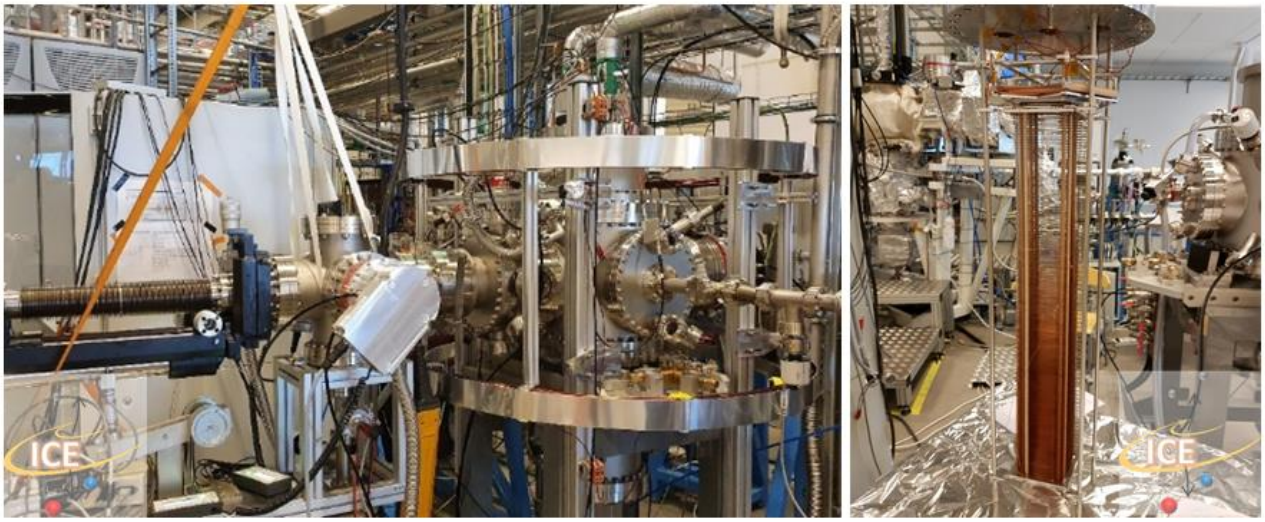

Figure 1: (left) ICE end station with the MAX IV molecular/cluster source; (right) ICE spectrometer

1. J. Ullrich et al., *Reports on Progress in Physics* 66 (2003) 1463.
2. F. Trinter et al., *Molecular Physics* 110 (2012) 1863-1872.
3. H. Schmidt-Böcking, et al., *Ann. Phys.* 533 (2021) 2100134.
4. R. Boll et al., *Nat. Phys*., 18 (2022) 423.
5. S. Grundmann et al., *Science*, 370 (2020) 339.
6. M. Pitzer, *J. Phys. B: At. Mol. Opt. Phys*., 50 (2017) 153001.
7. N. Walsh et al., *In Manuscript*.

[1] Acronym stands for **I**ons in **C**oincidence with **E**lectrons

Resonant Intermolecular Coulombic Decay (ICD) in solvated ions

Rémi Dupuy[1,2,*], Tillmann Buttersack[2], Florian Trinter[2], Clemens Richter[2], Shirin Gholami[2], Olle Björneholm[3], Uwe Hergenhahn[2], Bernd Winter[2], Hendrik Bluhm[2]

1 Sorbonne Université, CNRS, Laboratoire de Chimie Physique - Matière et Rayonnement, LCPMR, F-75005 Paris Cedex 05, France

2 Fritz-Haber-Institut der Max-Planck-Gesellschaft, Faradayweg 4-6, 14195 Berlin, Germany

3 Department of Physics and Astronomy, Uppsala University, Box 516, SE-751 20 Uppsala, Sweden

[*]Contact: remi.dupuy@sorbonne-universite.fr

Keywords: liquids, photoemission spectroscopy, non-local decay

Inner-shell photoionization and photoexcitation, and the ensuing decay processes, form the basis of many spectroscopic techniques. Understanding these phenomena is also of primary importance to understand the interaction of matter with ionizing radiation. In the condensed phase (e.g. in aqueous media, of prime importance in biological contexts, for instance), in addition to the well-known decay pathways observed in the gas phase (Auger decay and fluorescence, mainly), new ones open [1]. These so-called non-local decay processes involve neighbouring species (e.g. the solvation shell in liquids). Typically, in Intermolecular Coulombic Decay (ICD), the neighbouring species is ionized by energy transfer from the primarily ionized species in the course of its electronic relaxation, making it a two-center analog to Auger decay.

These processes have been extensively studied for model cluster systems. It is however also possible to investigate this kind of process directly in liquids, in large part thanks to the liquid microjet photoemission spectroscopy technique. Pioneering [2, 3, 4] and more recent [5] experiments in liquids have been dedicated to "core" ICD, i.e. ICD from deep inner/core shells, which is in competition with Auger decay. This is in contrast with the focus initially put on ICD from more shallow inner-shell holes, where the available energy is below the double-ionization potential of the species that absorbed a photon, making ICD the dominant relaxation pathway.

A much less explored aspect of ICD in liquids so far is resonant ICD, i.e. ICD after a resonant inner/core-shell excitation (and in competition with resonant Auger decay). Resonant ICD in liquids is precisely what will be explored here. Results will be presented for a number of solvated monoatomic ions (K^+, Ca^{2+}, Sc^{3+}, Br^-...). The different flavors of resonant ICD will be detailed, as well as their branching ratios with respect to the Auger decay pathways. The use of ICD in liquids as a new spectroscopic tool, to investigate e.g. ion pairing and the electronic structure of solvation shell molecules, will also be discussed.

[1] T. Jahnke, U. Hergenhahn, B. Winter, R. Dörner, U. Frühling, P. V. Demekhin, K. Gokhberg, L. S. Cederbaum, A. Ehresmann, A. Knie & A. Dreuw; "Interatomic and Intermolecular Coulombic Decay"; Chemical Reviews **120**, pp. 11295–11369 (2020).

[2] W. Pokapanich, H. Bergersen, I. L. Bradeanu, R. R. T. Marinho, A. Lindblad, S. Legendre, A. Rosso, S. Svensson, M. Tchaplyguine, N. V. Kryzhevoi & L. S. Cederbaum; "Auger Electron Spectroscopy as a Probe of the Solution of Aqueous Ions"; Journal of the American Chemical Society **131**, pp. 7264–7271 (2009).

[3] W. Pokapanich, N. V. Kryzhevoi, N. Ottosson, S. Svensson, L. S. Cederbaum, G. Öhrwall & O. Björneholm; "Ionic-Charge Dependence of the Intermolecular Coulombic Decay Time Scale for Aqueous Ions Probed by the Core-Hole Clock"; Journal of the American Chemical Society **133**, pp. 13430–13436 (2011).

[4] P. Slavíček, B. Winter, L. S. Cederbaum & N. V. Kryzhevoi; "Proton-Transfer Mediated Enhancement of Nonlocal Electronic Relaxation Processes in X-ray Irradiated Liquid Water"; Journal of the American Chemical Society **136**, pp. 18170–18176 (2014).

[5] G. Gopakumar, E. Muchová, I. Unger, S. Malerz, F. Trinter, G. Öhrwall, F. Lipparini, B. Mennucci, D. Céolin, C. Caleman, I. Wilkinson, B. Winter, P. Slavíček, U. Hergenhahn & O. Björneholm; "Probing Aqueous Ions with Non-Local Auger Relaxation"; Physical Chemistry Chemical Physics **24**, pp. 8661–8671 (2022).

Measurements of aggregate structures in atmospheric carboxylate solutions using X-ray absorption spectroscopy

Jack J. Lin,[1] Georgia Michailoudi,[2,†] Kamal R. R. Mundoli,[1] Hayato Yuzawa,[3] Hiroshi Iwayama,[4,5] Masanari Nagasaka,[4] Marko Huttula,[2] and Nønne L. Prisle[1,*]

1 Center for Atmospheric Research, University of Oulu, Oulu, Finland

2 Nano and Molecular Systems Research Unit, University of Oulu, Oulu, Finland

3 UVSOR Synchrotron Facility, Institute for Molecular Science, Okazaki, Japan

4 Institute for Molecular Science, Myodaiji, Okazaki, Japan

5 School of Physical Sciences, The Graduate University for Advanced Studies (SOKENDAI), Okazaki, Japan

[†] *Now at: Cooperative Institute for Research in Environmental Sciences, Boulder, USA*

[*] *Contact: nonne.prisle@oulu.fi*

Keywords: aqueous solutions, atmospheric droplets, micelles, X-ray absorption spectroscopy

Many organic compounds found in the atmosphere have the ability to form aggregate structures in aqueous solutions (Tabazadeh, 2005; Pfrang et al., 2017). When these structures form, it affects the reactivity and, therefore, lifetime of these compounds in the atmosphere (Milsom et al., 2021). Their formation also affects the thermodynamics and climate effects of cloud droplets (Malila and Prisle, 2018; Calderón and Prisle, 2021). Neither of these effects are currently not accounted for in current atmospheric models.

The point at which these aggregate structures–known as micelles–form is called the critical micelle concentration (CMC). While there have been many measurements of CMC values, there is still a lot of uncertainty associated with CMC values in the literature. In addition, many measurements do not directly detect the presence of micelles, nor their specific structures and properties, but rather rely on inferring their presence based on changes in solution properties such as conductivity, surface tension, or optical properties (Mukerjee and Mysels, 1971). Many different aggregate structures have been observed in atmospherically relevant systems adding to the complexity of their comprehensive descriptions and impacts on atmospheric processes.

Here, we present measurements on solutions of atmospheric surfactants sodium hexanoate and sodium octanoate, both below and above the CMC, along with reference measurements on pure hexanoic and octanoic acid. Carbon K-edge absorption spectra show clear differences between spectra below and above the CMC. However, how the energies and intensities of individual absorption peaks in the spectra shift with changing solution concentration is not so clear. This points to the complicated phase state of the systems studied and suggests that the process of micellization in atmospheric aqueous systems cannot be encapsulated in a simple parameter.

Calderón, S. M. and Prisle, N. L.: Composition dependent density of ternary aqueous solutions of ionic surfactants and salts, Journal of Atmospheric Chemistry, 78, 1–25, 2021.

Malila, J. and Prisle, N. L.: A Monolayer Partitioning Scheme for Droplets of Surfactant Solutions, Journal of Advances in Modeling Earth Systems, 10, 3233–3251, 2018.

Milsom, A., Squires, A. M., Boswell, J. A., Terrill, N. J., Ward, A. D., and Pfrang, C.: An organic crystalline state in ageing atmospheric aerosol proxies: spatially resolved structural changes in levitated fatty acid particles, Atmospheric Chemistry and Physics, 21, 15 003–15 021, 2021.

Mukerjee, P. and Mysels, K. J.: Critical micelle concentrations of aqueous surfactant systems, NSRDS-NBS, U.S. National Bureau of Standards; for sale by the Supt. of Docs., U.S. Govt. Print. Off., 1971.

Pfrang, C., Rastogi, K., Cabrera-Martinez, E. R., Seddon, A. M., Dicko, C., Labrador, A., Plivelic, T. S., Cowieson, N., and Squires, A. M.: Complex three-dimensional self-assembly in proxies for atmospheric aerosols, Nature Communications, pp. 1–8, 2017.

Tabazadeh, A.: Organic aggregate formation in aerosols and its impact on the physicochemical properties of atmospheric particles, Atmospheric Environment, 39, 5472–5480, 2005.

Hydration structure of acetone studied by quantitative ultraviolet absorption spectroscopy

Kazumasa Okada[1,2,*], Chika Sugahara[1] and Koichi Matsuo[2]

1 Graduate School of Advanced Science and Engineering, Hiroshima University, Higashi-Hiroshima, Japan
2 Hiroshima Synchrotron Radiation Center, Hiroshima University, Higashi-Hiroshima, Japan
**Contact: okadak@hiroshima-u.ac.jp*

Keywords: quantitative ultraviolet spectroscopy, hydration structure, acetone

The electronic structure of molecules is sensitive to the environment around them. In solution, solute–solvent interaction causes a peak shift in ultraviolet absorption spectra, so-called solvatochromic shift [1]. Despite plenty of spectroscopic studies, limited insights have been gained into molecular properties in solutions, mainly due to the broadness of the absorption bands. In infrared/Raman spectroscopy, a spectroscopic analysis called the principal component analysis (PCA) has been developed recently and the PCA without centering is sometimes applied for quantitative discussion of the band property [2]. This study is aimed at seeing whether the method is applicable for the discussion on solvation from a series of ultraviolet absorption spectra.

We choose the acetone aqueous solution as our system because the mixture is considered as a model system to probe the feature of the carbonyl–water interaction as well as is a typical aprotic–protic solvent system. The interaction is a hydrogen-bond type, and an additional weak C–H···OH_2 bond has been reported in a very dilute region [3]. We are therefore focused on the n-π* absorption band which covers from 220 to 320 nm.

The experiments were conducted on the beamline BL-12 of the Hiroshima Synchrotron Radiation Center (HiSOR), Japan. The sample chamber for measurements was purged with the nitrogen gas rather than evacuated for easy access for sample exchange. The sample cell was composed of a holder assembly made of stainless steel and two CaF_2 windows separated by a Teflon spacer ring with a thickness of 200 μm. The sample solutions were prepared by the gravimetrical mixing of acetone with water.

The peak of the n-π* absorption band depends on the molar fraction of acetone (x_A). The peak positions plotted as the open circles in Figure 1 seem to have a slight deviation from a linear line. This infers that a rather complex interaction exists between acetone and water. Also, the spectra shown in Figure 1 have a tail to the shorter wavelength, indicating that the band consists of multiple components. The PCA yields two components for interpreting the measurement spectra. The primary component, having a peak at 270.7 nm, is similar to the spectrum for $x_A = 0.35$. The score of this component almost proportional to x_A suggests that a main hydration structure is the 1:1 complex. The secondary component has a peak at 252.6 nm and a valley at 287.4 nm. The score of this component turns negative for $x_A > 0.35$. This indicates that two other components are included in the acetone solution. In total three different hydration structures exist, with varying fractions of abundance.

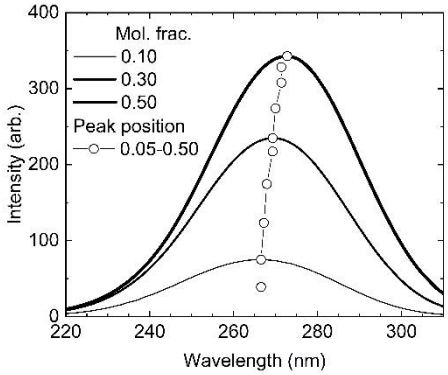

Figure 1: The n-π* absorption band of acetone in aqueous solutions. The open circles indicate the peak positions for samples with the molar fraction of acetone of 0.05–0.50.

1. W. P. Hayes, C. J. Timmons, Solvent and substituent effects on the n → π* absorption bands of some ketones, *Spectrochim. Acta* **21,** 529–541 (1965).
2. T. Hasegawa, Quantitative Infrared Spectroscopy for Understanding of a Condensed Matter, Springer (2017).
3. K. Mizuno, T. Ochi, Y. Shindo, Hydrophobic hydration of acetone probed by nuclear magnetic resonance and infrared: Evidence for the interaction C–H···OH_2, *J. Chem. Phys.* **109,** 9502–9507 (1998).

Electronic structure of water in acetone aqueous solution revealed by liquid-phase soft X-ray absorption spectroscopy

Chika Sugahara[1, *], Hiroshi Iwayama[2,3], Masanari Nagasaka[2,3] and Kazumasa Okada[1]

1 Graduate School of Advanced Science and Engineering, Hiroshima University, Higashi-Hiroshima, Japan
2 Institute for Molecular Science, Okazaki, Japan
3 School of Physical Sciences, The Graduate University for Advanced Studies (SOKENDAI), Okazaki, Japan
**Contact: chika-suga@hiroshima-u.ac.jp*

Keywords: hydration, hydrogen bonds, soft X-ray absorption spectroscopy

Acetone–water binary system is one of the typical aqueous solutions. The mixture has negative excess molar enthalpy in the dilute region [1], indicating an attractive interaction between acetone and water. In the solution, the interaction characterizes water as bulk water or water interacting with acetone, "hydrated water". To determine the electronic structure of hydrated water, we use soft X-ray absorption spectroscopy which offers information on the local atomic environment of a molecular system under study. However, subtle differences in character prevent us from clear distinction from one another without a useful analysis method. We propose a new quantity, called the excess absorption coefficient, for the analysis of the absorption spectra. The quantity allows us to determine the electronic structure of hydrated water.

The experiments were performed on the soft X-ray beamline, BL3U [2] in UVSOR, Japan. The photoabsorption spectra were measured in the oxygen K-edge region, with sample cell windows made of silicon nitride with a thickness of 150 nm. The sample solutions were prepared by mixing acetone with purified water to give molar fraction of acetone, x_A, in the range 0–0.50.

Absorption by hydrated water is determined from the observed spectra in a following manner. Some of the observed X-ray absorption spectra are shown in Fig. 1(a). The peak of water at 534.6 eV shifts to lower energies with x_A. Water changes its character in the solution. To discuss the behavior, we propose a new physicochemical quantity called the excess absorption coefficient, μ^E, defined as

$$\mu^E = \mu - \mu^{id}$$
$$\mu^{id} = (1 - x_A)\mu_W^* + x_A\mu_A^*$$

where μ_W^* and μ_A^* are the absorption coefficients of pure water and pure acetone. The excess absorption coefficient is shown in Fig. 1(b). The behavior of μ^E at 534.6 eV differs from that at 534.0 eV. By the definition of μ^E,the difference is attributed to the component other than bulk water, i.e., hydrated water.

The component of hydrated water is confirmed by the principal component analysis. The component which has a peak at 534.0 eV is analyzed as the secondary component. The change of score with x_A is parallel to that of μ^E at 534.0 eV.

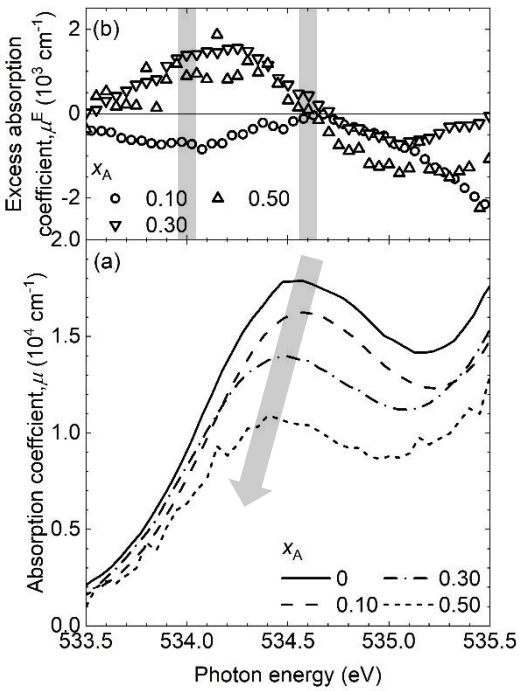

Figure 1: (a) The soft X-ray absorption spectra of liquid water and acetone aqueous solutions measured for a series of molar fractions of acetone, x_A; (b) the dependence of the excess absorption coefficient on x_A.

1. B. Löwen, S. Schulz, Excess molar enthalpies of acetone + water, cyclohexane, methanol, 1-propanol, 2-propanol, 1-butanol and 1-pentanol at 283.15, 298.15, 343.15 and 363.15 K, *Thermochim. Acta* **262**, 69–82 (1995).
2. M. Nagasaka, H. Yuzawa, T. Horigome, N. Kosugi, Reliable absorbance measurement of liquid samples in soft X-ray absorption spectroscopy in transmission mode, *J. Elec. Spec. Rel. Phen.* **224**, 93–99 (2018).

Nodal metallic behavior of underdoped triple-layer cuprate Bi2223

Shin-ichiro Ideta[1,3*], T. Yoshida[2], K. Tanaka[3], W. O. Wang[4], B. Moritz[4], T. P. Devereaux[4], T. K. Lee[5], C. Y. Mou[5], S. Adachi[6], N. Sakaki[6], S. Yamaguchi[6], T. Watanabe[6], T. Noji[7], S. Uchida[8,9], S. Ishida[8], and A. Fujimori[5,9]

1 Hiroshima Synchrotron Radiation Center (HiSOR), Hiroshima University, Higashi-hiroshima, Japan
2 Graduate School of Human and Environmental Studies, Kyoto University, Kyoto, Japan
3 UVSOR-III Synchrotron, Institute for Molecular Science, Aichi, Okazaki, Japan
4 Department of Materials Science and Engineering, Stanford University, Stanford, California, USA
5 Center for Quantum Technology, and Department of Physics, National Tsing Hua University, Hsinchu, Taiwan
6 Graduate School of Science and Technology, Hirosaki University, Hirosaki, Aomori, Japan
7 Department of Applied Physics, Graduate School of Engineering, Tohoku University, Sendai, Miyagi , Japan
8 National Institute of Advanced Industrial Science and Technology, Tsukuba, Ibaraki, Japan
9 Department of Physics, University of Tokyo, Tokyo, Japan

**Contact: idetas@hiroshima-u.ac.jp*

Keywords: electronic structure, high-T_c cuprates, angle-resolved photoemission spectroscopy

The energy gap in the superconducting (SC) and normal (N) states is a key for understanding the microscopic mechanism of high-T_c superconductivity in cuprates. It has been well known that two different representative energy gaps open in the SC and N states, namely, the SC gap and pseudogap (PG), respectively [1,2]. While the origin of the PG has been discussed in relation to superconductivity, it has also been discussed as a phenomenon distinct from superconductivity. Thus, shedding light on its nature would elucidate the mechanism of high-T_c superconductivity. The PG shows almost the same size as that in the SC state at the antinode while it closes near the node, forming disconnected portions of the Fermi surface (FS), so-called, Fermi arcs [3]. In a previous angle-resolved photoemission spectroscopy (ARPES) study [4], heavily underdoped non-superconducting Bi2212 was shown to have the same gap structure as that of the *d*-wave supercondcutor, and was called the "nodal liquid" state. Besides, the Fermi-arc length as a function of T/T^*, where T^* is the pseudogap temperature, was shown to vanish when T/T^* approaches $T = 0$ [5], which means that the "nodal metal" exists as the ground state of the PG phase. On the other hand, a recent high-resolution ARPES study of Bi2212 reported that the point node of the *d*-wave superconductor persists up to a few to several tens K above T_c [6]. Therefore, the ground state of the PG phase still remains highly controvertial.

Triple-layer Bi-based high-T_c cuprate superconductor $Bi_2Sr_2Ca_2Cu_3O_{10+\delta}$ (Bi2223) shows the highest T_c (110 K) among the Bi-based cuprates and has two inequivalent CuO_2 planes with different hole concentrations [7]. Optimally doped Bi2223 has been studied by ARPES, and two FSs were observed corresponding to the outer (OP) and inner (IP) CuO_2 planes. Doping dependence of the electronic structure of Bi2223 is crucial for understanding the mechanism of the highest T_c among Bi-based multilayer cuprates. In this study, we have successfully observed the electronic structure of underdoped, optimally doped, and overdoped Bi2223 by ARPES. Particularly, we found that the *d*-wave gap of 60-80 meV and the point node in the IP band persis well above T_c in the IP band of the underdoped Bi2223. This result indicates that the IP band of underdoped Bi2223 is a nodal liquid in the N states.

1. D. S. Marshall *et al*., Unconventional electronic structure evolution with hole doping in $Bi_2Sr_2CaCu_2O_{8+\delta}$: Angle-resolved photoemission results, *Phys. Rev. Lett*. **76**, 4841 (1996).
2. H. Ding *et al*., Spectroscopic evidence for a pseudogap in the normal state of underdoped high-T_c superconductor, *Nature (London)* **382**, 51 (1996).
3. M. R. Norman *et al*., Modeling the Fermi arc in underdoped cuprates, *Phys. Rev. B* **76**, 174501 (2007).
4. U. Chatterjee *et al*., Observation of a *d*-wave nodal liquid in highly underdoped $Bi_2Sr_2CaCu_2O_{8+\delta}$, *Nat. Phys*. **6**, 99 (2010).
5. A. Kanigel *et al*., Evolution of the pseudogap from Fermi arcs to the nodal liquid, *Nat. Phys*. **2**, 447 (2006).
6. T. Kondo *et al*., Point nodes persisting far beyond T_c in Bi2212, *Nat. Commun*. **6**, 7699 (2015).
7. S. Ideta *et al*., Enhanced superconducting gaps in the trilayer high-temperature $Bi_2Sr_2Ca_2Cu_3O_{10+\delta}$ cuprate superconductor, *Phys. Rev. Lett.* **104**, 227001 (2012).

Symmetry reduction of the electronic structure in heavily overdoped Pb-Bi2201 observed by Angle-resolved photoemission spectroscopy

Yudai Miyai[1*], Tohru Kurosawa[2], Migaku Oda[3], Masashi Arita[4], K. Tanaka[5]
Shinichiro Ideta[5], and Kenya Shimada[5]

1 Graduate School of Science, Hiroshima University, Higashi-Hiroshima, 739-8526, Japan
2 Fuculty of Science and Engineearing, Muroran Institute of Technology, Muroran 050-8585, Japan
3 Department of Physics, Hokkaido University, Sapporo 060-0809, Japan
4 Hiroshima Synchrotron Radiation Center, Higashi-Hiroshima 739-8526, Japan
5 UVSOR-III Synchrotron, Institute for Molecular Science, Okazaki, 444-8585, Japan
**Contact: d220057@hiroshima-u.ac.jp*

Keywords: high-T_C superconductor, cuprate, angle-resolved photoemission spectroscopy

High transition-temperature (T_C) cuprate superconductors have attracted much interest since their discovery in 1986. Recently, symmetry reduction of the electronic structure has been reported in Bi-based cuprate superconductors [1,2]. Similar symmetry reduction or *nematicity* which breaks the four-fold rotational symmetry (C_4) of the underlying lattice has been found in the Fe-based superconductor [3,4]. Although nematicity in electron liquids has attracted much interest, the rotational symmetry breaking in the electronic states for high-T_C cuprate superconductors has not been fully clarified yet.

Here, we have examined the symmetry of the electronic structure in heavily overdoped $(Bi,Pb)_2Sr_2CuO_{6+\delta}$ (Pb-Bi2201) (T_C = 6 K) using high-resolution angle-resolved photoemission spectroscopy (ARPES). Figs. 1(a) and 1(b) show the Fermi surface (FS) obtained by rotating the sample around the two nodal directions on the same cleavage surface taken at $h\nu$=22 eV and T=20 K with the *s*-polarization geometry. We have found the $2k_F$ (k_F: Fermi wavenumber) values for the two nodal directions are different; $2k_F^{(1)} = (7.948 \pm 0.003) \times 10^{-1}$ Å^{-1} (Fig. 1(a)) and $2k_F^{(2)} = (8.340 \pm 0.003) \times 10^{-1}$ Å^{-1} (Fig. 1(b)). The deviation is temperature independent from T = 20 K to 260 K. In addition, we have revealed the energy dependence of the quasiparticle lifetime broadening is also different for these two nodal directions. Our results indicate the C_4 symmetry breaking of the electronic structures in the CuO_2 plane in the heavily overdoped Pb-Bi2201, which may be related to a charge order formation in heavily overdoped Pb-Bi2201 as observed by resonant inelastic X-ray scattering [4], and/or the nematic phase associated with the Pomeranchuk instability as suggested by the Raman scattering measurements on Bi2212 [5].

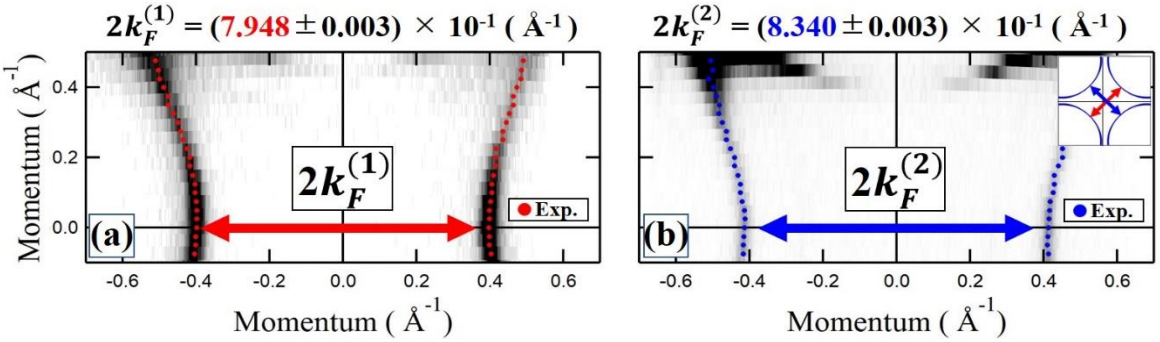

Figure 1: (a), (b) Fermi surface mapping obtained by rotating around the two nodal directions taken at $h\nu$= 22 eV and T = 20 K with the *s*-polarization geometry. Red and blue dots indicate the Fermi surface points determined from the peaks of the momentum distribution curves. We have determined $2k_F$ values ($2k_F^{(1)}$ and $2k_F^{(2)}$) for the two nodal directions as shown in the inset of panel (b).

1. S. Nakata *et al*., *npj Quantum Materials* **6**, 86 (2021).
2. Y. Zheng *et al*., *Scientific Reports* **7**, 8059 (2017).
3. H. C. Xu *et al*., *Physical Review Letters* **117**, 157003 (2016).
4. J-H. Chu *et al*., Science **329**, (2010) 824.
5. Y. Y. Peng *et al*., *Nature Materials* **17**, 697 (2018).
6. N. Auvray *et al., Nature Communications* **10**, 5209 (2019).

Mechanistic insight into vitamin B_{12} chemistry: Polarized femtosecond x-ray spectroscopy of cobalamins

James Penner-Hahn[1,2,*], Taylor McClain[1], Ryan Lamb[2] Alivia Mukherjee[2], Roseanne Sension[2],

1 Program in Biophysics, University of Michigan, Ann Arbor, US
2 Department of Chemistry, University of Michigan, Ann Arbor, US
**Contact: jeph@umich.edu*

Keywords: XANES, X-ray Emission, RIXS, Potential Energy Surface

Vitamin B_{12} is a family of biologically essential cofactors containing a cobalt that is coordinated equatorially to a corrin ring and axially to a variety of possible ligands (see Figure 1).[1] Vitamin B_{12} is essential for life, catalyzing a wide range of both 1- and 2-electron reactivity.[2] In addition, the B_{12} unit has a rich, well-characterized photochemistry which is believed to have direct relevance to its non-photochemical reactivity. This connection has grown stronger with the recent discovery that some organisms use B_{12} as the photosensor for photoactivated transcriptional regulation[3] and the recognition that B_{12}-related chemistry can be used to catalyze organic transformations.[4]

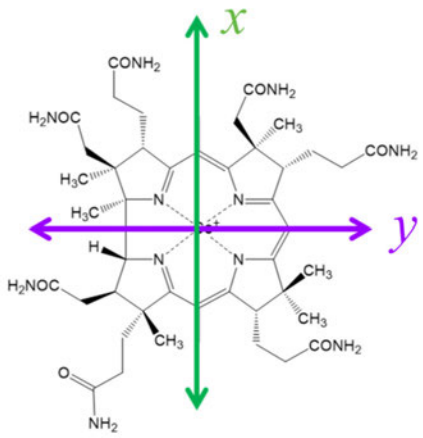

Figure 1: Corrin ring in vitamin B_{12} showing molecular coordinate system. In addition to the tetrapyrrole ligation that is shown, the Co is also coordinated by 2 ligands along the *z* axis: a "lower" benzimidazole ligand and a variable "upper" ligand (e.g., cyanide, water, hydroxide, methyl, or adenosyl)

We have used a combination of ultrafast X-ray absorption and X-ray emission to interrogate the changes in electronic and molecular structure that take place as a function of time following photoexcitation. By adjusting the relative polarization of the UV-visible pump and the X-ray probe beams, we are able to resolve contributions arising from changes along the *x*, *y*, and *z* axes (see Figure 1)[5-6] Taken together, these data allow us to demonstrate that at earliest times the corrin ring undergoes a small expansion, consistent with population of a π^* excited state and that this is followed elongation and/or contraction of the axial ligands, depending on the details of the ligation, consistent with formation of a metal-centered excited state. When combined with steady-state illumination studies, these studies provide important insights into the biological and non-biological reactivity of alkyl-cobalamins.

(1) Banerjee, R., *Chemistry and biochemistry of B12*. Wiley: New York, 1999; p xxii, 921 p.
(2) Marques, H. M., The inorganic chemistry of the cobalt corrinoids – an update. *Journal of Inorganic Biochemistry* **2023,** *242*, 112154.
(3) Padmanabhan, S.; Jost, M.; Drennan, C. L.; Elias-Arnanz, M., A New Facet of Vitamin B-12: Gene Regulation by Cobalamin-Based Photoreceptors. *Annu Rev Biochem* **2017,** *86*, 485-514.
(4) Bam, R.; Pollatos, A. S.; Moser, A. J.; West, J. G., Mild olefin formation via bio-inspired vitamin B-12 photocatalysis. *Chem Sci* **2021,** *12* (5), 1736-1744.
(5) Miller, N. A.; Deb, A.; Alonso-Mori, R.; Glownia, J. M.; Kiefer, L. M.; Konar, A.; Michocki, L. B.; Sikorski, M.; Sofferman, D. L.; Song, S.; Toda, M. J.; Wiley, T. E.; Zhu, D. L.; Kozlowski, P. M.; Kubarych, K. J.; Penner-Hahn, J. E.; Sension, R. J., Ultrafast X-ray Absorption Near Edge Structure Reveals Ballistic Excited State Structural Dynamics. *Journal of Physical Chemistry A* **2018,** *122* (22), 4963-4971.
(6) Sension, R. J.; Chung, T.; Dewan, P.; McClain, T. P.; Lamb, R. M.; Penner-Hahn, J. E., Time-resolved spectroscopy: Advances in understanding the electronic structure and dynamics of cobalamins. In *Methods in Enzymology*, Marsh, E. N. G., Ed. Academic Press: 2022; Vol. 669, pp 303-331.

Charge Transfer in the BBL:P($g_4$2T-T) Organic Polymer Heterojunction Measured with Core-Hole Clock Spectroscopy

Elin Berggren[1], Yi-Chen Weng[1], Qifan Li[2], Chi-Yuan Yang[2], Ute Cappel[3], Fredrik Johansson[3,4], Magnus Berggren[2], Simone Fabiano[2] and Andreas Lindblad[1]

1 X-ray Photon Science, Uppsala University, Uppsala, Sweden
2 Laboratory of Organic Electronics, Linköping University, Norrköping, Sweden
3 Applied Physical Chemistry, Royal Institute of Technology, Stockholm, Sweden
4 Institute des NanoSciences de Paris, Sorbonne University, Paris, France

**Contact: elin.berggren@physics.uu.se*

Keywords: charge transfer, organic polymers, core-hole clock spectroscopy

The conductivity in organic polymer heterojunction devices depends on electron dynamics at interfaces between acceptor and donor moieties. This study explores the electron dynamics at interfaces between the n-type polymer poly(benzimidazo-benzophenanthroline) (BBL) and the p-type polymer bithiophene-thiophene (P($g_4$2T-T)) in organic polymer heterojunctions using Resonant Auger Spectroscopy (RAS). The results indicate that the 50/50 blend of BBL and P($g_4$2T-T) has the highest ordering and the fastest charge transfer time. This finding highlights the importance of chemically specific probes of local charge tunnel propensity for macroscopic conductivity in organic polymer heterojunction devices. To measure the charge transfer times, RAS was employed at the High Kinetic Energy (HIKE) end station at BESSY II [1]. By measuring the Auger electron spectra created upon X-ray absorption in the donor polymer, the different decay paths can be separated where the core-excited electron remain on the atom with the core hole or where it tunneled away. The competitive decay modes of those local and delocalized (charge-transfer) decay processes allowed the charge transfer time to be calculated as a function of excitation energy using the core-hole clock method [2].

The X-ray absorption spectra were also used to compare molecular structure, orientation, and ordering in the polymer heterojunctions. The 50/50 polymer blend had the highest ordering, as inferred from the angular dependence of the X-ray absorption. Derived electron delocalization times (figure 1) were observed in the as/fs regime for all polymer blends, with the fastest charge transfer time in the sample with equal amounts of donor and acceptor polymer.

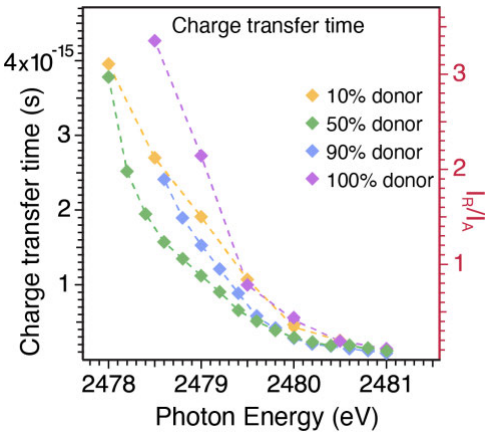

Figure 1: Charge transfer times from the donor polymer in different D-A heterojunctions.

Core-hole clock spectroscopy proved to be a chemically specific probe of the local charge tunnel propensity, which is fundamental for macroscopic conductivity. These findings contribute to the understanding of the electron dynamics at interfaces in organic polymer heterojunctions, which is essential for the development of efficient and sustainable optoelectronic devices.

1. M. Gorgoi *et al*, The high kinetic energy photoelectron spectroscopy facility at BESSY progress and first results, *Nuclear Instruments and Methods in Physics Research A,* **610**, 48-53 (2009).
2. P. A. Brühwiler *et al*, Charge-transfer dynamics studied using resonant core spectroscopies, *Reviews of Modern Physics,* **74**, 703-740 (2002).

X-ray induced charge transfer in conjugated polymers by core-hole-clock spectroscopy

Nicolas Velasquez[1,*], Fernanda B. Nunes[2], Oksana Travnikova[1,3], Iyas Ismail[1,3], Renaud Guillemin[1,3], Loïc Journel[1,3], Jessica B. Martins[1], Denis Céolin[3], Laure Fillaud[4], Maria Luiza M. Rocco[5], Ralph Püttner[6], Kamal Chinnathambi[7], Maria N. Piancastelli[1], Marc Simon[1,3], Michael Odelius[8], Marcella Iannuzzi[2], and Tatiana Marchenko[1,3]

1 *Sorbonne Université, CNRS, LCPMR, F-75005 Paris Cedex 05, France*
2 *Department of Chemistry, University of Zurich, Zurich 8057, Switzerland*
3 *Synchrotron Soleil, L'Orme des Merisiers, Saint-Aubin, F-91192 Gif-sur-Yvette, France*
4 *Sorbonne Université, CNRS, LISE, F-75005 Paris Cedex 05, France*
5 *Instituto de Quimica, Universidade Federal do Rio de Janeiro, Rio de Janeiro, Brazil*
6 *Institut für Experimentalphysik, Freie Universität Berlin, Arnimallee 14, D-14195 Berlin, Germany*
7 *Homi Bhabha National Institute, Training School Complex, Anushakti Nagar, Mumbai, Maharashtra 400094, India*
8 *Department of Physics, Stockholm University, AlbaNova University Center Stockholm 10691, Sweden*
[*] *Contact: nicolas.velasquez@sorbonne-universite.fr*

Keywords: resonant Auger spectroscopy, polymers, charge transfer, electron delocalization

Charge transfer (CT) involving electron and nuclear dynamics is of paramount importance not only in chemistry, but also in biology and materials science. When CT involves complex systems where nuclear and electron dynamics become relevant, X-ray sources, which allow for element-specific core-shell excitation, are essential. In this regard, X-ray spectroscopy enables us to glimpse at ultrafast dynamics processes taking place in molecular ensembles. The core-hole clock spectroscopy (CHCS) method relies on high resolution, monochromatic X-ray radiation to provide an insight into processes with a span shorter than that of the core-hole lifetime [1]. Such processes as core-excitation and decay, in which an X-ray photon or an Auger electron are emitted, occur within the lifetime of a core-excited state, and serve as a probe for dynamics taking place in the molecule on the same time scale. Inducing site-specific electron dynamics through resonant absorption of an X-ray photon and emission of a resonant Auger electron enables us in turn to investigate electron delocalization not only in macro-molecules but also in extended systems in the solid-state. Using the HAXPES end-station at the GALAXIES beamline of the SOLEIL French synchrotron facility, we measured high resolution resonant S*KLL* Auger spectra in the region below the sulfur 1s threshold of the $\pi-$conjugated polymers 1) polythiophene (PT), in powder form (where delocalization is possible *only along* the polymer chain), and 2) P3HT, as a thin-film (where delocalization is possible *both along and between* chains). An earlier investigation on PT in powder form using resonant Auger spectroscopy (RAS), found no evidence of CT [2]. While a following study of PT as a thin-film showed the presence of electron delocalization in resonant Auger spectra in the low femtosecond regime [3]. The prevailing interpretation of the observed dynamics were ascribed to an interaction between polymer chains. Our results using RAS exhibit hallmark features of CT in *both* PT and P3HT (white dashed line region in Fig. 1), indicating a predominant delocalization mechanism along the chain. Our work is in good agreement with theoretical calculations based on real-time time-dependent DFT methods.

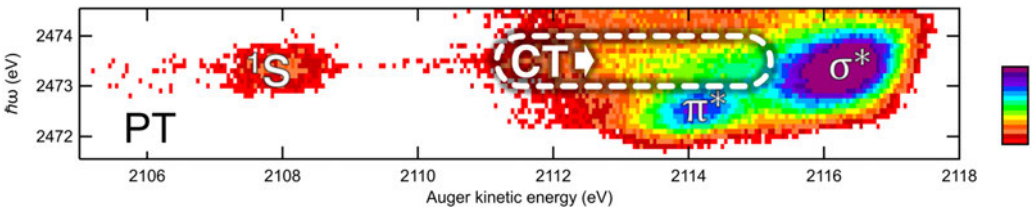

Figure 1: 2D maps of S $KL_{2,3}L_{2,3}$ Auger spectra of PT. White dashed line stadium-shape highlights CT region.

[1] O. Björneholm, et al., Determination of time scales for charge-transfer screening in physisorbed molecules. *Phys. Rev. Lett.*, **68**, 1892–1895 (1992).

[2] H. Sekiguchi, et al., Unoccupied electronic states in poly- thiophene as probed by XAS and RAS: Unoccupied electronic states in polythiophene as probed by XAS, *Surf. Interface Anal.*, **40**, 673-675 (2008).

[3] C. Arantes, et al., Femtosecond Electron Delocalization in Poly(thiophene) Probed by Resonant Auger Spectroscopy, *J. Phys. Chem. C*, **117**, 8208-8213 (2013).

Circular dichroism by core-level angle-resolved photoemission: Application of multiple&single-site scattering theory

T.-P. Vo[1], O. Tkach[2,3], S. Tricot[4], D. Sébilleau[4], A. Winkelmann[5], O. Fedchenko[2], Y. Lytvynenko[2,6], D. Vasilyev[2], H.-J. Elmers[2], G. Schönhense[2], and J. Minár[1,*]

1 New Technologies - Research Centre, Univ. of West Bohemia, 30100 Pilsen, Czech Republic
2 Johannes Gutenberg-Universität, Institut für Physik, 55128 Mainz, Germany
3 Sumy State University, Rymskogo-Korsakova 2, 40007 Sumy, Ukraine
4 Univ Rennes, CNRS, IPR (Institut de Physique de Rennes) - UMR 6251, F-35000, Rennes, France
5 Academic Centre for Materials and Nanotechn., Univ. of Science and Technology, Kraków, Poland
6 Institute of Magnetism of the NAS of Ukraine and MES of Ukraine, 03142 Kyiv, Ukraine
**Contact: jminar@ntc.zcu.cz*

Keywords: photoelectron diffraction, core-level photoemission, circular dichroism, one-step model

Photoelectron diffraction (PED) is a powerful and driving experimental technique for resolving the structure of surfaces with sub-ångstrom resolution. Being able to opt the emitters based on their specific binding energy makes PED widely used for following investigation purposes: crystal structures, bonding geometries of atoms and the local environment of impurity or dopant atoms inside surfaces [1]. Similarly, to angle-resolved photoemission spectroscopy (ARPES), the angular distribution of photoelectrons emitted from a crystal surface is studied. Nevertheless, the physics behind and investigation objective are distinct for two mentioned approaches. The angular distribution of emitted electrons represents the momentum of initial states in ARPES meanwhile it reveals the interference of photoelectron waves from final states in PED. Depending on the utilized photon energies, this tool can be termed either ultraviolet-PED (UPD) or X-ray-PED (XPD). In high energy regime, XPD effects are found in ARPES measurements beside other obstacles (low cross-sections, large photon momentum transfer, non-negligible phonon scattering) [2]. Overall, XPD is not only an advantageous approach but also an unexpected effect [3]. Here, to disentangle these diffraction influences, we present a PED implement for SPRKKR package [4] which makes use of multiple scattering theory and one-step model in photoemission process [5].

In contrast to the other real space implementations of the multiple scattering XPD formalism, here we propose to use k-space implementation based on the layer KKR method. Main advantage of this method is that we can without convergence problems (wrt. the angular momentum and cluster size) address very broad kinetic energy range (20-8000eV). Furthermore, the so-called alloy analogy model [6,7] can be used to simulate XPD at finite temperatures as well as XPD effects observed in the soft and hard X-ray ARPES [8]. For the sake of applications, we have calculated the circular dichroism in angular distributions (CDAD) associated with core-level photoemission of 3d from W(110) and 3p from Ge(100) [9]. Photoelectrons are excited by hard X-rays (6000 eV) with right and left circularly polarized radiation (RCP and LCP, respectively).

1. M. Greif, et al., Photoelectron diffraction in the x-ray and ultraviolet regime: Sn-phthalocyanine on Ag (111), Physical Review B **87**, 085429 (2013).
2. S. Babenkov, et al., High-accuracy bulk electronic bandmapping with eliminated diffraction effects using hard X-ray photoelectron momentum microscopy, Communications Physics **2**, 107 (2019).
3. G. Schönhense, et al., Momentum-transfer model of valence-band photoelectron diffraction, Communications Physics **3**, 45 (2020).
4. H. Ebert, et al., Calculating condensed matter properties using the KKR-Green's function method—recent developments and applications, Reports on Progress in Physics **74**, 096501 (2011).
5. J. Braun, et al., Correlation, temperature and disorder: Recent developments in the one-step description of angle-resolved photoemission. Physics Reports **740**, 1-34 (2018).
6. J. Braun, et al., Exploring the XPS limit in soft and hard x-ray angle-resolved photoemission using a temperature-dependent one-step theory, Physical Review B **88**, 205409 (2013).
7. H. Ebert, et al., Calculating linear-response functions for finite temperatures on the basis of the alloy analogy model, Physical Review B **91**, 165132 (2015).
8. A. X. Gray, et al., Bulk electronic structure of the dilute magnetic semiconductor Ga1− x Mn x As through hard X-ray angle-resolved photoemission, Nature materials **11**, 957-962 (2012).
9. O. Tkach, et al., Circular Dichroism in Hard X-ray Photoelectron Diffraction, Ultramicroscopy (2023), in print.

Determination of inelastic mean free path for hard oxide and soft polymers by overlayer method

Yi-Chen Weng[1,*], Rickard Gauffin[1], Elin Berggren[1], and Andreas Lindblad[1]

1 Physics and Astronomy Department, Uppsala University, Uppsala, Sweden

**Contact: yichen.weng@physic.uu.se*

Keywords: Photoelectron spectroscopy, polymer electrolytes, inelastic mean free path

In recent decades, the safety concerns from the use of flammable liquid electrolytes in Li-ion batteries have motivated the research in the area of solid-state electrolytes. The interfaces between the electrodes and electrolytes plays an important role in the performance of batteries. The X-ray photoelectron spectroscopy (XPS) technique, which can provide surface-sensitive information of the materials, has become a prevalent method for examining interfaces in battery systems. The inelastic mean free path (IMFP) of electrons needs to be known for a material if chemical information from various depths is to be extracted from XPS data [1]. The IMFP dependence on both material and energy needs to be known for this analysis to be accurate.

The overlayer method is a commonly used for the determination of IFMPs which is based on XPS intensity ratio between a known thickness overlayer and the substrate underneath [2, 3]. In this work, this method and both HAXPES (9258 eV, Ga Kα) and XPS (1486 eV, Al Kα) were applied to the SiO_2/Si two-layer system. Atomic force microscopy (AFM) was applied to investigate the surface roughness of SiO_2. Varying thicknesses of SiO_2 on Si substate were measured with different emission angles, and the estimated IMFP was compared with values from literatures. The overlayer method together with AFM analysis were further extended to determine the IMFPs for the polymer material used in organic solar cells, poly(benzimidazobenzophenanthroline) (BBL), and different polymers and polymer electrolytes in solid-state Li-ion batteries. Results on spin-coated BBL on Au/Cr substrates, polymers and polymer electrolytes on Au substrates are presented.

1. Jablonski, Aleksander, and Cedric J. Powell. "Relationships between electron inelastic mean free paths, effective attenuation lengths, and mean escape depths." Journal of Electron Spectroscopy and Related Phenomena 100.1-3 (1999): 137-160.

2. Powell, Cedric J. "Attenuation lengths of low-energy electrons in solids." Surface Science 44.1 (1974): 29-46.

3. Clark, D. T., and H. R. Thomas. "Application of ESCA to polymer chemistry. XVI. Electron mean free paths as a function of kinetic energy in polymeric films determined by means of ESCA." Journal of Polymer Science: Polymer Chemistry Edition 15.12 (1977): 2843-2867.

Development of hard X-ray photoelectron spectroscopy excited by photon energy up to 30 keV

Satoshi Yasuno[1], Okkyun Seo[1], Yasumasa Takagi[1] and Tappei Nishihara[1]

1 Japan Synchrotron Radiation Research Institute, Sayo, Japan

**Contact: yasuno@spring8.or.jp*

Keywords: Hard X-ray photoelectron spectroscopy, HAXPES

Hard X-ray photoelectron spectroscopy (HAXPES) is a powerful tool for investigating the electronic states of the buried interface in a non-destructive manner due to the large probing depth [1,2]. In order to obtain a much larger probing depth than conventional HAXPES, we have developed a high-energy HAXPES (HE-HAXPES) system excited by photon energies up to 30 keV. This system is achieved by combining an applied bias voltage upon the sample with a conventional hemispherical electron energy analyzer.

In this study, we performed the HE-HAXPES experiments using the Si (333) double bounce monochromator (DCM) equipped with an undulator at the BL46XU beamline of SPring-8. We have used the hemispherical electron energy analyzer (R-4000L1-10kV, Scienta Omicron AB) which can operate the range of electron kinetic energy up to 10 keV. In order to retard the photoelectron kinetic energy to less than 10 keV when the incident X-rays are 14 keV or more, we used the pre-retarding techniques, which applied the high voltage source (HERR-20P, Matsusada Precision Inc.) of +5~19.5 kV to the sample. Then, it was necessary to re-calibrate the photoelectron kinetic energy due to applied bias voltage. The kinetic energy shifts were determined by the position of the Fermi edge or the core level peak of an Au plate reference. Figure 1 shows Si 1s spectra of 110-nm-thick SiO_2 film/ n-type crystalline Si-substrate measured by using photon energies from 14 to 30 keV in the 2 keV step. In the spectrum at photon energy of 14 keV, a feeble signal assigned to a bulk-Si substrate is observed around a binding energy of 1840.5 eV. The signal intensities gradually increased with increasing the photon energy and the Si substrate signal is clearly observed at a photon energy of 30 keV. Additionally, from the Si substrate signals with photon energy over 24 keV, the asymmetric shapes with a shoulder appear at the higher binding energy side. It was suggested that these spectral shapes may originate from the upward band bending, namely the depletion layer formed in the Si substrate side at the interface.

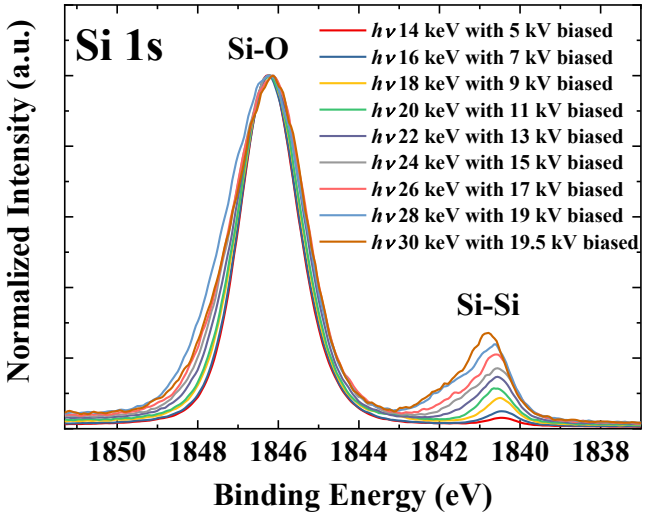

Figure 1: Si 1s spectra of 110-nm-thick SiO_2 film/Si-substrate measured at photon energies from 14 to 30 keV. The photoelectrons emerging from the sample are decelerated to a kinetic energy below 10 keV by the applied bias voltage upon a sample. For example, photoelectrons with an initial kinetic energy of 28 keV are retarded by + 19 kV and detected by the electron analyzer with a residual kinetic energy of 9 keV.

1. K. Kobayashi, Nucl. Instrum. Methods Phys. Res. A. **601**, 32 (2009).
2. K. Kobayashi, M. Yabashi, Y. Takata, T. Tokushima, S. Shin, K. Tamasaku, D. Miwa, T. Ishikawa, H. Nohira, T. Hattori, Y. Sugita, O. Nakatsuka, A. Sakai, and S. Zaima, Appl. Phys. Lett. **83**, 1005 (2003).

Unraveling Surface Chemistry through the association of Time-Resolved XPS and Chemometrics: Case studies of Fe_2O_3 powder and DRI pellet

Mohammed Alaoui Mansouri[1*], Manoj Ghosalya[1], Aidin Heidari[2], Mikko Iljana[2], Anne Hietava[2], Timo Fabritius[2], Marko Huttula[1], Samuli Urpelainen[1]

1 Nano and Molecular Systems Research Unit, University of Oulu, FI-90014, Oulu, Finland
2 Process Metallurgy Research Unit, University of Oulu, FI-90014 Oulu, Finland
**Contact: mohammed.alaouimansouri@oulu.fi*

Keywords: TR-XPS, PCA, MCR-ALS, Fe_2O_3, DRI.

This research work presents a study on the application of Time-Resolved X-ray Photoelectron Spectroscopy (TR-XPS) in conjunction with chemometric techniques, specifically Principal Component Analysis (PCA) and Multivariate Curve Resolution with Alternating Least Squares (MCR-ALS), to investigate the surface chemistry and dynamics of Fe_2O_3 reduction processes. The use of TR-XPS allows for real-time monitoring of chemical changes at the surface of Fe_2O_3 during reduction, providing valuable insights into the reaction mechanisms and kinetics involved [1].

One of the challenges in analyzing TR-XPS data is the presence of overlapping peaks and complex spectral features, which can make accurate quantification and interpretation difficult [2]. Traditional nonlinear fitting methods may struggle with these complexities and result in ambiguous or inaccurate results. However, MCR-ALS, a chemometric approach, can effectively overcome these challenges by extracting pure spectral profiles of individual chemical species and their temporal profiles from the complex and overlapping data [3].

The results obtained from the TR-XPS coupled with MCR-ALS analysis provide a detailed and precise understanding of the surface chemistry changes during the Fe_2O_3 reduction processes as it has been highlighted in Figure 1 in case of the reduction of direct reduced iron (DRI) pellet. This includes identifying and pursuing the formation of various intermediate species and their evolution over time from one spectrum to another, which permit later to establish correlations between surface chemistry and process conditions.

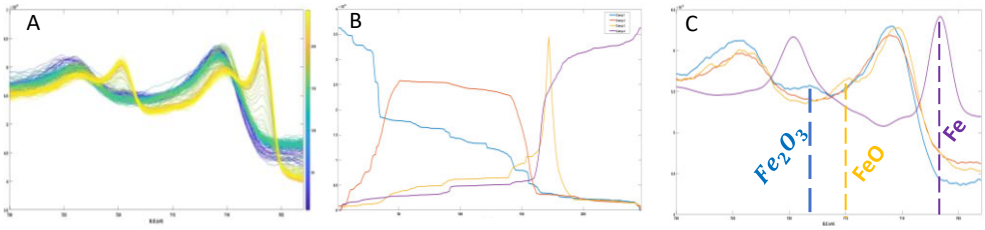

Figure 1: MCR-ALS decomposition of TR-XPS. (A): Raw XPS contains all components, (B): evolution of each component obtained by MCR-ALS during reduction process (Fe_2O_3, Fe_3O_4, FeO and Fe) and (C): Pure spectra of components by MCR-ALS

The integration of MCR-ALS in TR-XPS data analysis not only addresses the fitting issues associated with complex spectral features, but also contributes to a deeper understanding of the underlying chemical changes and their dynamics during Fe_2O_3 reduction. The findings of this study have significant implications for process optimization, material synthesis, and tailoring of material properties for specific applications. This research highlights the potential of combining TR-XPS with chemometric techniques for studying surface chemistry and dynamics of complex systems and opens up new possibilities for advancing our understanding of chemical processes.

[1] J.F. Watts, J. Wolstenholme, An introduction to surface analysis by XPS and AES, John Wiley & Sons, 2019.
[2] V.L. Le, T.J. Kim, Y.D. Kim, D.E. Aspnes, External removal of endpoint-discontinuity artifacts in the reciprocal-space analysis of spectra, Current Applied Physics. 20 (2020) 232–236.
[3] T. Azzouz, R. Tauler, Application of multivariate curve resolution alternating least squares (MCR-ALS) to the quantitative analysis of pharmaceutical and agricultural samples, Talanta. 74 (2008) 1201–1210. https://doi.org/https://doi.org/10.1016/j.talanta.2007.08.024.

$L_{2,3}$ X-ray absorption spectra of transition metal oxides (Mn, Fe, Co): The influence of covalence effects

Guido Arthur Fabre[1,*], Miguel Abbate[1], Rodrigo José Ochekoski Mossanek[1]

1 Departamento de Física, Universidade Federal do Paraná, Caixa Postal 19044, 81531-990 Curitiba, PR, Brazil

[*]Contact: fabre@fisica.ufpr.br

Keywords: XAS, spectra, covalence, electronic configurations

Transition metals (TM) present a plethora of physical properties, which makes their study very interesting for theoretical and experimental purposes. There are several techniques available to study these properties, but we focused on the x-ray absorption spectroscopy (XAS) [1]. This method is based on electronic transitions between core and empty conduction states, which can be very sensitive to the local chemical environment. Therefore, we consider the full multiplet effects on the nominal valence, such as on-site Coulomb, crystal field and spin-orbit interactions of the analyzed compound, for a more complete analysis [2]. Further, we take into account the covalence between different TM and their ligands, which is often mistreated. If not considered correctly, this effect can affect the interpretation of the results. In this work, we analyze the XAS of different transition metal oxides, namely, manganese, iron and cobalt, with different nominal valences of 2+, 3+ and 4+. By using atomic multiplet, ligand and crystal field theories [1, 2, 3], we obtained the ground state energy, 3d band electron count, and the TM 2p XAS spectra of all these systems, considering different number of electronic configurations, which some results are presented below in Figure 1. From the analysis of our results, we found that, to correctly describe the electronic structure of these materials, the required number of electronic configurations are usually greater than one expects from the direct comparison with the experimental data. Also, this effect is heavily dependent on the TM valency. Thus, the covalent effect between transition metal and ligand ions is of great importance to correctly interpret the XAS technique.

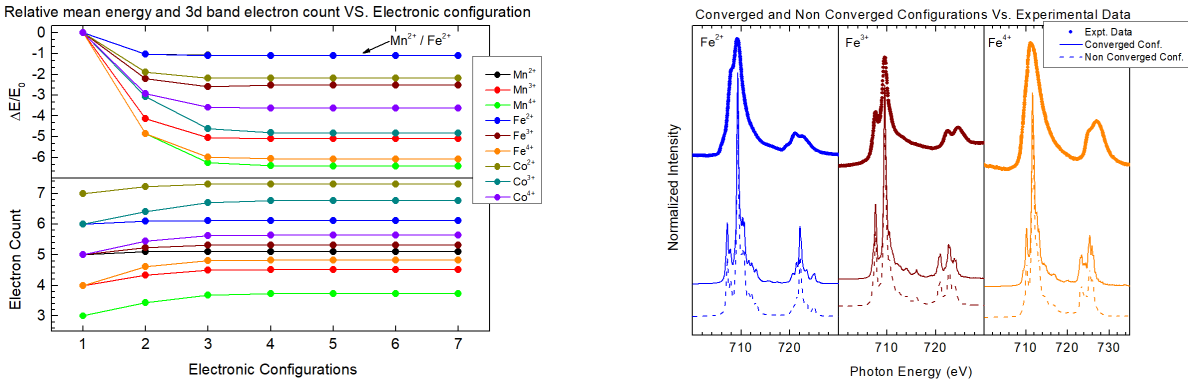

(a) (b)

Figure 1: (a): Evolution of the ground state relative energy and 3d band electron count for each TM studied. (b): Comparison between experimental[4, 5] and theoretical data of iron system.

[1] F. de Groot, A. Kotani, Core Level Spectroscopy of Solids, CRC Press (2008).

[2] Satoru Sugano, Multiplets of Transition-Metal Ions in Crystals, Elsevier (2012).

[3] F. M. F. De Groot, et al, L 2,3 x-ray-absorption edges of d 0 compounds: K+, Ca 2+, Sc 3+, and Ti 4+ in Oh (octahedral) symmetry, *Physical Review B* **41.2**, 928 (1990).

[4] Hiroki Kurata, and Christian Colliex, Electron-energy-loss core-edge structures in manganese oxides, *Physical Review B* **48.4**, 2102 (1993).

[5] Alexander S. Vinogradov, et al, X-ray absorption evidence for the back-donation in iron cyanide complexes, *Surface Review and Letters* **9.01**, 359-364 (2002).

Soft X-ray absorption studies of nanocomposite $La_{0.6}Sr_{0.4}Co_{0.2}Fe_{0.8}O_{3-\delta}$/ $Ce_{0.9}Gd_{0.1}O_{2-\delta}$ electrode for solid oxide fuel cells

Daisuke Asakura[1,2,*], Tomohiro Ishiyama[1], Eiji Hosono[3,2], Katherine Develos-Bagarinao[3], Katsuhiko Yamaji[1], Masaki Kobayashi[4], Miho Kitamura[5,6], Koji Horiba[5,6], and Haruo Kishimoto[3]

1 Research Institute for Energy Conservation, National Institute of Advanced Industrial Science and Technology (AIST), Tsukuba, Japan

2 AIST-UTokyo Advanced Operando Measurement Technology Open Innovation Laboratory, Kashiwa, Japan

3 Global Zero Emission Research Center, AIST, Tsukuba, Japan

4 Center for Spintronics Research Network, The University of Tokyo, Tokyo, Japan

5 Photon Factory, Institute of Materials Structure Science, High Energy Accelerator Research Organization (KEK), Tsukuba, Japan

6 Institute for Advanced Synchrotron Light Source, National Institutes for Quantum Science and Technology (QST), Sendai, Japan

**Contact: daisuke-asakura@aist.go.jp*

Keywords: solid oxide fuel cells, air electrode material, nano composite, soft X-ray absorption

Solid oxide fuel cell (SOFC) is one of the important energy conversion devices in cogeneration system. Decrease of the high operating temperature and improvement of the efficiency of power generation are necessary to further spread SOFCs. To elevate the efficiency, the resistance of the air electrode (cathode) should be reduced. It is known that increase of the triple-phase-boundary (TPB) among the electrodes, electrolyte, and gas phase enhances the cathode reactions. Moreover, construction of a fine TPB structure can reduce the overvoltage because the reaction interphase increases.

Recently, we have developed nanocomposite of $La_{0.6}Sr_{0.4}Co_{0.2}Fe_{0.8}O_{3-\delta}$ (LSCF, an air electrode material) and $Ce_{0.9}Gd_{0.1}O_{2-\delta}$ (GDC, an oxide ion conducting material) by using a pulsed laser deposition (PLD) method [1]. A fine heterostructure at the LSCF/GDC interface has been confirmed. In general, lattice distortion exists at the hetero-interface because of the different lattice constants of two materials. Lee *et al*. have reported that tensile stress in $La_{0.6}Sr_{0.4}CoO_{3-\delta}$ enhances the oxygen desorption/absorption reaction by modulating the electronic structure [2]. The strain effect at the hetero-interface should be a factor of the high activation in our nanocomposite electrode. Thus, we conducted electronic-structure analysis of the LSCF/GDC nanocomposite and LSCF bulk by soft X-ray absorption spectroscopy (XAS) to investigate the strain effect at the interface. Transition-metal *L*-edge XAS is advantageous to understand the 3*d* orbitals. The XAS measurements were performed at BL-2B of the Photon Factory, KEK.

The Co *L*-edge XAS line shape was obviously different between the LSCF/GDC nanocomposite and LSCF bulk. Considering the results of charge-transfer multplet (CTM) calculation [3] and spectra for reference materials [4], the Co *L*-edge XAS spectrum for the nanocomposite is attributed to Co^{2+} state that is much lower than the valence of Co for the bulk sample. The reduction of Co is due to the composite structure, which should be related to the improvement of electrode performance for the nanocomposite. Concerning the Fe *L*-edge XAS measurements, small differences were found between the nanocomposite and LSCF bulk. Analysis using CTM calculation revealed that the difference originated from the crystal-field splitting for the FeO_6 octahedrons. In the presentation, the Co 3*d* and Fe 3*d* electronic structure will be discussed in detail.

1. K. Develos-Bagarinao, T. Ishiyama, H. Kishimoto, H. Shimada, and K. Yamaji, Nanoengineering of cathode layers for solid oxide fuel cells to achieve superior power densities, *Nat. Commun.* **12**, 3979 (2021).
2. D. Lee, R. Jacobs, Y. Jee, A. Seo, C. Sohn, A. V. Ievlev, O. S. Ovchinnikova, K. Huang, D. Morgan, and H. N. Lee, Stretching Epitaxial $La_{0.6}Sr_{0.4}CoO_{3-\delta}$ for Fast Oxygen Reduction, *J. Phys. Chem. C* **121**, 25651-25658 (2017).
3. E. Stavitski and F. M. F. de Groot, The CTM4XAS program for EELS and XAS spectral shape analysis of transition metal L edges, *Micron* **41**, 687-694 (2010).
4. J. van Elp, J. L. Wieland, H. Eskes, P. Kuiper, G. A. Sawatzky, F. M. F. de Groot, and T. S. Turner, Electronic structure of CoO, Li-doped CoO, and $LiCoO_2$, *Phys. Rev. B* **44**, 6090-6103 (1991).

Transition-metal *L*-edge RIXS and multiplet calculation of cathode materials for Li-ion batteries

Daisuke Asakura[1,2,3,*], Eiji Hosono[1,2,3], Yusuke Nanba[1,#], Takaaki Sudayama[1], Hisao Kiuchi[4,5], Hideharu Niwa[4,5,†], Kosuke Yamazoe[4,5], Jun Miyawaki[4,5,‡], Ru-Pan Wang[6,7], Frank M. F. de Groot[6], and Yoshihisa Harada[3,4,5]

1 Research Institute for Energy Conservation, National Institute of Advanced Industrial Science and Technology (AIST), Tsukuba, Japan

2 Global Zero Emission Research Center, AIST, Tsukuba, Japan

3 AIST-UTokyo Advanced Operando Measurement Technology Open Innovation Laboratory, Kashiwa, Japan
4 Institute for Solid State Physics, The University of Tokyo, Kashiwa, Japan

5 Synchrotron Radiation Research Organization, The University of Tokyo, Kashiwa, Japan

6 Debye Institute for Nanomaterials Science, Utrecht University, Utrecht, The Netherlands

7 Department of Physics, University of Hamburg, Hamburg, Germany

 # Present affiliation: Research Initiative for Supra-Materials, Shinshu University, Nagano, Japan

† Present affiliation: Faculty of Pure and Applied Sciences, University of Tsukuba, Tsukuba, Japan

‡ Present affiliation: Institute for Advanced Synchrotron Light Source, National Institutes for Quantum Science and Technology (QST), Sendai, Japan

**Contact: daisuke-asakura@aist.go.jp*

Keywords: Li-ion battery, cathode materials, redox reaction, RIXS

Nowadays Li-ion battery (LIB) is an essential energy-storage device to realize low-carbon society. The performances of LIBs still need to be improved for applications to electric vehicles and large-scale stationary energy storages. Especially, enhancement of the energy density and cyclability for the cathode materials of LIBs is a crucial issue. To develop novel cathode materials, clarification of the redox reaction of prototypical cathode materials such as $LiMn_2O_4$, $LiCoO_2$, and $LiFePO_4$ is of particular importance.

Soft X-ray absorption spectroscopy (XAS) is a powerful tool to investigate the electronic structure of such 3*d* transition-metal (TM) compounds. By using multiplet calculation, the experimental XAS spectra at the TM *L*-edges can be analyzed in detail: not only the valence of TMs, but also electronic-structure parameters (crystal-field splitting, Coulomb interaction of 3*d* electrons, core-hole potential, charge-transfer (CT) energy, etc.) can be determined. Then, resonant inelastic X-ray scattering (RIXS) at the TM *L*-edges in combination with XAS has been attractive recently because of the high state selectivity. The excitation energy dependence of RIXS is helpful to understand each valence in mixed-valence state on the charge/discharge process.

We demonstrate the TM *L*-edge RIXS results of $LiMn_2O_4$, $LiCoO_2$, and $LiFePO_4$ in combination with multiplet calculations [1,2]. The hybridization and CT effect of the O 2*p*-TM 3*d* orbitals are intensively discussed. By analyzing the Mn *L*-edge RIXS spectra for $LiMn_2O_4$, very strong CT effects are found for the Mn^{4+} state, which is much enhanced compared to the Mn^{3+} state. Thus, the redox reaction of Mn^{3+}/Mn^{4+} due to charge/discharge has a strong covalent character with the O 2*p* orbital [1]. The redox reaction of Co^{3+}/Co^{4+} for $LiCoO_2$ is similar to that of $LiMn_2O_4$. In contrast, the redox reaction of Fe^{2+}/Fe^{3+} for $LiFePO_4$ is attributed to an ionic character. The analysis for the Fe *L*-edge RIXS spectra revealed that the hybridization between the Fe 3*d* and O 2*p* orbitals is weak for both Fe^{2+} and Fe^{3+} states [2]. Most likely, the strong covalency in the PO_4 tetrahedron should lower the electron density on the O 2*p* orbital bonded with the Fe 3*d* orbital. In the presentation, we will discuss the relation between the covalent/ionic character and charge-discharge cycle performance in each material.

1. D. Asakura *et al.*, Mn 2p resonant X-ray emission clarifies the redox reaction and charge-transfer effects in $LiMn_2O_4$, *Phys. Chem. Chem. Phys.* **21**, 18363-18369 (2019).
2. D. Asakura *et al.*, Large Charge-Transfer Energy in $LiFePO_4$ Revealed by Full-Multiplet Calculation for the Fe L_3-edge Soft X-ray Emission Spectra, *ChemPhysChem* **19**, 988-992 (2018).

Hematite Clusters on Anatase TiO_2 Surface and Effect of Oxygen Vacancy: A First Principles Study

Kati Asikainen*, Matti Alatalo, Marko Huttula and S. Assa Aravindh

Nano and Molecular Systems Research Unit, University of Oulu, Finland

*Contact: Kati.Asikainen@oulu.fi

Keywords: Photocatalysis, TiO_2, iron oxide clusters, DFT

The search of photocatalytic materials, used in several environmental applications, has become increasingly important during the recent years. The prototype material, TiO_2, has been intensively studied and a lot of attention has been paid to its 3.2 eV band gap, which is too large for visible light absorption, and quick recombination rate. Since TiO_2 is a cheap and abundant material, several methods have been developed to improve its properties. One way to proceed is to combine TiO_2 with other semiconductors with a smaller band gap. One such material is hematite, Fe_2O_3, which has a bulk band gap of 1.9–2.2 eV, and which have been reported to improve photocatalytic properties of TiO_2 [1].

We have performed first principles calculations using the VASP code [2], in order to study the atomic, magnetic and electronic properties of $(Fe_2O_3)_n$ $(n = 1, 2)$ clusters on the anatase $TiO_2(101)$ surface [3]. The choice of a small cluster size was motivated by the earlier experimental study of Fe_2O_3 clusters on the TiO_2 surface [4]. We find that the adsorption of the clusters on the surface is energetically favorable, thus enabling the modification of the surface properties. Due to the adsorption, impurity states arise, narrowing the band gap. We observe a notable electron transfer from the cluster to the surface, attributed to a formation of heterojunction in the heterostructure. Low charge transfer at higher coverage can support the claim that increase in Fe_2O_3 concentration and cluster size can hinder the photoactivity of TiO_2 [4]. Moreover, we investigated the effect of the clusters on hydrogen evolution reaction (HER) of TiO_2, and the results showed enhanced interaction between the heterostructure and hydrogen and HER activity compared to the pristine TiO_2.

We also studied the possibility of altering the properties of the heterostructure by introducing an oxygen vacancy in the heterostructure of TiO_2 and $(Fe_2O_3)_1$. The vacancies are shown to further alter the electronic structure, and also locally affect the magnetic and charge transfer properties of the system. The results show that the oxygen vacancy can be widely used for tuning both the electronic and magnetic properties of the heterostructure of TiO_2 and Fe_2O_3.

[1] A. Hiltunen *et al.* Sustainable Energy Fuels **2**, 2124 (2018); Y-Q. Cao *et al.* Sci. Reports **10**, 13437 (2020); W. Bootluck *et al.*, *J. Environ. Chem. Eng.* **9**, 105660 (2021).
[2] G. Kresse and J. Hafner Phys. Rev. B, **47**, 558 (1993); G. Kresse and J. Hafner Phys. Rev. B, **49** 14251, (1994); G. Kresse and J. Furthmüller Comput. Mat. Sci. **6**, 15 (1996); G. Kresse and J. Furthmüller Phys. Rev. B **54**, 11169 (1996).
[3] K. Asikainen *et al.* arXiv:2301.11034 [cond-mat.mtrl-sci] (2023).
[4] Q. Sun *et al.* J. Hazard. Mater., **229-230**, 224 (2012).

Mapping the local Berry curvature of a quantum spin Hall insulator by circular dichroism ARPES

Jonas Erhardt[1], Cedric Schmitt[1], Matthias Schmitt[1,2], Timur Kim[2], Cephise Cacho[2], Simon Moser[1] and Ralph Claessen[1,*]

1 Physikalisches Institut and Würzburg-Dresden Cluster of Excellence ct.qmat, Universität Würzburg, Würzburg D-97074, Germany

2 Diamond Light Source, Harwell Science and Innovation Campus, Didcot, OX11 0DE, United Kingdom

**Contact: ralph.claessen@physik.uni-wuerzburg.de*

Keywords: ARPES, dichroism, quantum spin Hall insulator, Berry curvature

Indenene, a monolayer of In atoms arranged in a triangular lattice on SiC(0001), has recently been identified as a quantum spin Hall insulator (QSHI) [1]. Its topological character is encoded in a characteristic energy staggering of its orbital angular momentum (OAM) polarized Dirac states that is determined by the competition of spin orbit coupling (SOC) and SiC-induced in-plane inversion symmetry breaking (ISB), see Fig. 1a. This makes indenene an ideal test case for recent claims that circular dichroism in angle-resolved photoelectron spectroscopy (CD-ARPES) gives access to local Berry curvature signatures via the OAM [2]. However, a particular challenge of such experiments is the extraction of the intrinsic OAM-related CD signal, requiring its distinction from final state effects and extrinsic contributions induced by experimental geometry.
Here, I will present a systematic photon energy dependent CD-ARPES study of indenene's Dirac states and use simple geometric considerations to disentangle experimental from OAM induced CD. The resulting OAM sequence (Fig.1 b) confirms indenene to be a QSHI and thus establishes a new approach to experimentally identify the topological character of a 2D quantum material directly from its bulk states.

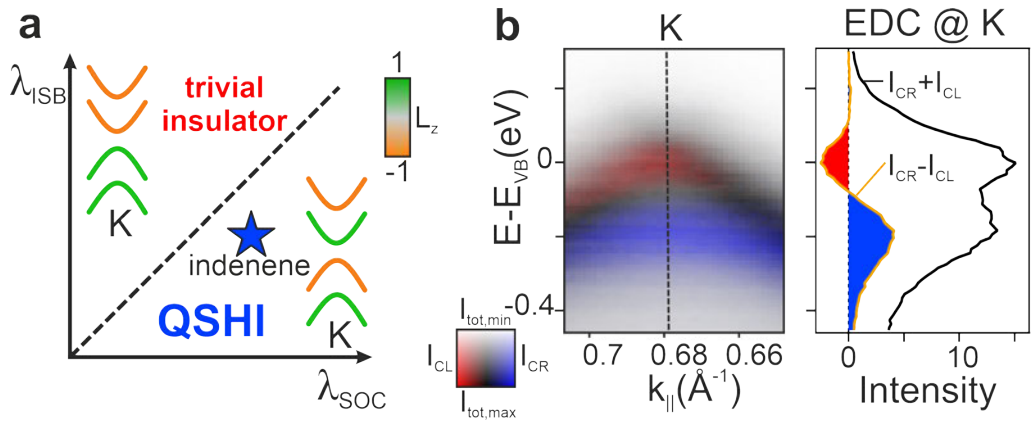

Figure 1: **a** Schematic topological phase diagram of indenene in dependence of SOC (λ_{SOC}) and ISB (λ_{SOC}) terms inducing a distinct L_z energy sequence of the K-point Dirac bands. **b** K-point valence band (VB) CD-ARPES (red, blue) of indenene overlaid with the sum (white, black) of circular left (CL) and right (CR) polarized light induced photoelecton intensities as well as K-point energy distribution curvers (EDC) of CR, CL-sum and difference. Data taken at room temperature and photon energy of 25 eV at Diamond Light source I05.

[1] M. Bauernfeind, J. Erhardt, P. Eck, P. K. Thakur, J. Gabel, T.-L. Lee, J. Schäfer, S. Moser, D. Di Sante, R. Claessen and G. Sangiovanni, *Nat. Commun*, **12**, 5396 (2021).

[2] M. Schüler, U. De Giovannini, H. Hübener, A. Rubio, M. A. Sentef and P. Werner, *Sci. Adv.*, **6**, 2730 (2020).

Reducing degradation and preferential sputtering using Ar cluster ion beam: An XPS study of some organic material and thin metal oxide films

Sari Granroth[1], Lauri Marttila[2], Juha-Pekka Lehtiö[1], and Harri Ali-Löytty[3]

1 Department of Physics and Astronomy, University of Turku, Turku, Finland

2 Department of Chemistry, University of Turku, Turku, Finland

3 Surface Science Group, Photonics Laboratory, Tampere University, Finland

**Contact: sari.granroth@utu.fi*

Keywords: Gas Cluster Ion Beam GCIB, Depth profiling, X-ray Photoelectron Spectroscopy XPS

Monoatomic Ar ion sputtering in connection to X-ray Photoelectron Spectroscopy has for a long time been one of the most versatile methods to investigate the chemical composition across the depth profile of layered structures or to reveal a contamination free surface in UHV conditions. However, especially in case of organic surfaces and thin metal oxide films, both depth profiling and cleaning with monoatomic ion beam have always been a compromise between revealing the interesting surface and damaging the surface or interface structure by causing degradation or preferential sputtering with an energetic ion beam, for example [1, 2].

In recent years, using of gas cluster ion beams (GCIB) have become an important tool to etch and depth profile materials which are known to be easily damaged by monoatomic ion sources [3, 4]. In gas cluster etching the size of clusters can vary from about 100 to 1000s of atoms in a cluster. The kinetic energy distributed to cluster atoms can be adjusted from some 100 eVs up to several thousand eVs. Larger size clusters cause clearly less damage on the sample surface still being able to remove both organic materials and metal oxides.

In this study, there are some examples of how etching with Ar clusters can be used to minimize the changes in the chemical states of surface atoms when cleaning the surface of selected organic materials like cellulose, melanin and polymethylmethacrylate (PMMA). In addition, the effect of the depth profiling across the Al_2O_3/Si interface and TiO_2 surface (Fig. 1) using Ar clusters and monoatomic Ar ion beam is demonstrated.

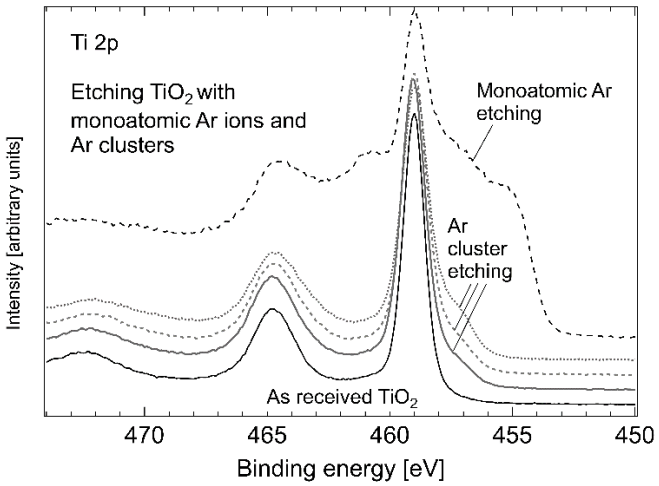

Figure 1: Effect of monoatomic Ar etching and cluster etching on TiO_2 surface. The Ar cluster etching was done using Ar_{300}^+ clusters with 4000 eV kinetic energy. The spectra were collected for as received TiO_2, after cluster etching for 30 s, 100 s and 500 s and finally after monoatomic (500 eV) Ar etching.

1. L.-S. Johansson, and J. M. Campbell, Reproducible XPS on biopolymers: cellulose studies, *Surface and Interface Analysis* **36**, 1018-1022 (2004).
2. S. Hashimoto, A. Murata, T. Sakurada, and A. Tanaka, Alteration of Ti XPS Spectrum for TiO_2 by Ar Ion Bombardment, *Journal of Surface Analysis* 9, 459-462 (2002).
3. D. W. Collinson, D. Nepal, J. Zwick, R. H. Dauskardt, Gas cluster etching for the universal preparation of polymer composites for nano chemical and mechanical analysis with AFM, *Applied Surface Science* **599**, 153954 (2022)
4. R. Simpson, R. G. White, J. F. Watts, M. A. Baker, XPS investigation of monatomic and cluster argon ion sputtering of tantalum pentoxide, *Applied Surface Science* **405**, 79-87 (2017).

NEAR-ISOTROPIC LOCAL ATTOSECOND CHARGE TRANSFER WITHIN THE ANISOTROPIC PUCKERED LAYERS OF BLACK PHOSPHORUS

Robert Haverkamp[1,2,*], Stefan Neppl[1,2] and Alexander Föhlisch[1,2]

1 Institute for Methods and Instrumentation for Synchrotron Radiation Research, Helmholtz-Zentrum Berlin für Materialien und Energie GmbH, Albert-Einstein-Straße 15, 12489 Berlin, Germany

2 Institute of Physics and Astronomy, University of Potsdam, Karl-Liebknecht-Straße 24/25, 14476 Potsdam, Germany

**Contact: Robert.Haverkamp@Helmholtz-Berlin.de*

Keywords: Black Phosphorus, Charge transfer, Anisotropy, Core-hole clock

Elemental black phosphorus is a layered 2D material with each layer possessing a naturally puckered crystal structure, distinguishing it from 2D materials with a perfectly planar conformation [1]. The corrugated pattern of phosphorus atoms leads to two inequivalent in-plane directions: zigzag (ZZ) and armchair (AC) with each distinct phosphorus 3p partial density of states. This highly anisotropic structure is distinctly reflected in the inherent long-range properties of black phosphorus [2].

We investigated to what extend this anisotropy is also pronounced on the atomic level. By means of the synchrotron-based core-hole-clock spectroscopy [3], which provides directional selectivity and sub-femtosecond capabilities, we determine the local charge transfer in black phosphorus of electrons excited into the 3p-derived conduction band in all three crystal directions: the out-of-plane direction (⊥) as well as both in-plane (∥) directions.

Surprisingly, it is found that the anisotropy prevailing in the long-range macroscopic properties of black phosphorus is not present on the scale of atomic charge transfer. Detailed analysis of bonding angles and the partial density of states derived from first principles band structure calculations clarifies the fundamental nature of this finding: Indeed, the folded nature of the quasi-2D material sheets creates the observed disparity between the macroscopic and the microscopic/atomic properties. This inherent scale-dependence is exemplified in black phosphorus for the general class of quasi-2D materials.

Thus, this work is valuable for both, experts in the fields of physics and material science as well as for scientists, curious about the latest findings in the field of nano- and functional materials linked to basic physical models.

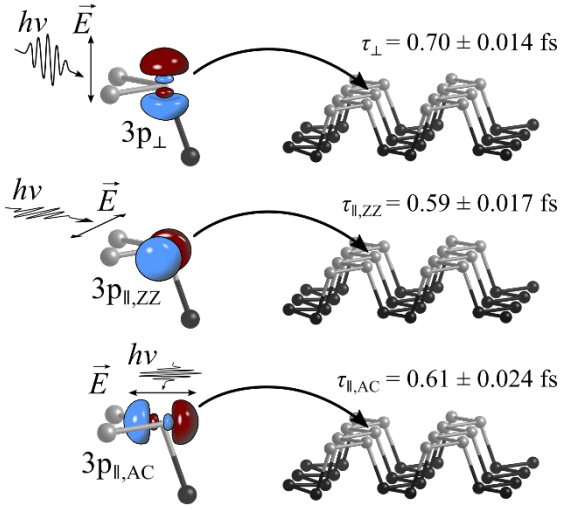

Figure 1: Directional preparation of $P3p_{\perp}$, $P3p_{\parallel,ZZ}$ and $P3p_{\parallel,AC}$ excited states within the puckered layered structure of black phosphorus, by means of linearly polarized X-rays and the resulting local sub-fs charge transfer times.

[1] Takao, Y., Asahina, H. & Morita, A. Electronic Structure of Black Phosphorus: Tight Binding Approach. *J. Phys. Soc.Jpn*. **105**, 93–98 (1981).

[2] Liu, X., Ryder, C., Wells, S., Hersam, M. Resolving the In-Plane Anisotropic Properties of Black Phosphorus *Small Methods* **1**, 1700143 (2017)

[3] Föhlisch, A., Feulner, P., Hennies, F. *et al.* Direct observation of electron dynamics in the attosecond domain *Nature* **436**, 373–376 (2005)

Hydrogen interaction with tungsten disulfide nanoparticles

Alex Laikhtman[1,*], Alla Zak[1], Jose Ignacio Martinez[2] and Julio A. Alonso[3]

[1]*Physics Department, Holon Institute of Technology (HIT), Holon, Israel*

[2]*Materials Science Factory, Institute of Material Science of Madrid (ICMM-CSIC), Madrid, Spain*

[3]*Department of Theoretical, Atomic and Optical Physics, University of Valladolid, Valladolid, Spain*

**Contact: alexl@hit.ac.il*

Keywords: nanostructures, micro-Raman spectroscopy, hydrogen, density functional theory

The chemical configuration and interaction mechanism of hydrogen adsorbed on nanoparticles of WS_2 are investigated. Our recent approaches of using hydrogen activated by microwave or radiofrequency plasma dramatically increased the efficiency of its adsorption making WS_2 a good candidate for solid state hydrogen storage media [1, 2]. The obtained results are demonstrated in Fig. 1.

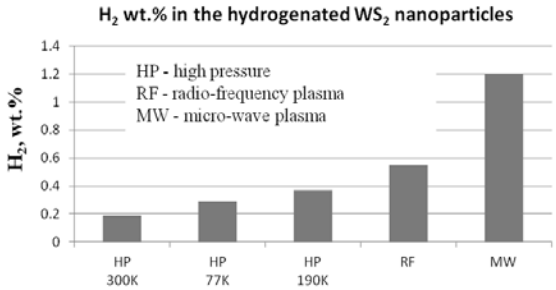

Figure 1. Hydrogen concentration in WS_2 nanoparticles following different types of hydrogenation.

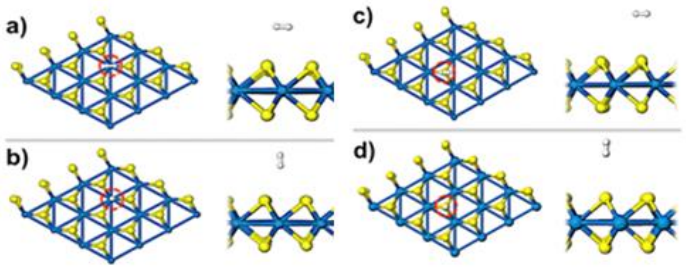

Figure 2. Top and side views of H_2 molecule adsorbed: a) on top of a W atom of a single WS_2 layer with the molecular axis parallel to the layer; b) on top of a W atom with the axis perpendicular to the layer; c) on top of a S atom with the axis parallel to the layer; d) on top of a S atom with the axis perpendicular to the layer.

To get insight on the chemical configuration, we combined the experimental analysis methods with theoretical modelling based on the density functional theory (DFT). Micro-Raman spectroscopy was used as a primary tool to elucidate chemical bonding of hydrogen and to distinguish between chemi- and physisorption. Hydrogen adsorbed in molecular form (H_2) was clearly identified in all the plasma-hydrogenated WS_2 nanoparticles samples, both experimentally and using DFT modelling. DFT provides an efficient and practical workbench to investigate the interaction of molecular and atomic hydrogen with WS_2 nanoparticles [3]. It shows that molecular H_2 physisorbs on the surface of those materials on top of W atoms, as shown in Fig. 2, while atomic H may chemisorb on top of S atoms. Diffusion of H_2 on the surface of WS_2 encounters small activation barriers and agrees with the observed dependence of H_2 concentration with temperature.

Intercalation of H_2 between adjacent WS_2 layers revealed an endothermic behavior due to interlayer expansion. A remarkable result, however, is that the presence of a full H_2 monolayer adsorbed on top of the first WS_2 layer of a WS_2 multilayer system strongly facilitates the intercalation of H_2 between WS_2 layers underneath. This phenomenon opens a new gate to implant foreign species inside the nanoparticles. The preliminary experimental results of Ga ion implantation following hydrogenation are in excellent agreement with these DFT predictions.

1. A. Laikhtman et al., *Int. J Hydrogen Energy* **39**, 9837-9841 (2014).
2. A. Laikhtman et al., *J. Phys. Chem. C* **121**, 11747-11756 (2017).
3. J. I. Martínez, A. Laikhtman, H. R. Moon, A. Zak, J. A. Alonso, *Phys. Chem. Chem. Phys.* **20**, 12061-12074 (2018).

Electronic structure of few-layer Pb on SiC

Kyungchan Lee[1,2*], Jonas Erhardt[1,2], Cedric Schmitt[1,2], Simon Moser[1,2] and Ralph Claessen[1,2]

1 Physikalisches Institut (EP4), Universitat Würzburg, Am Hubland, D-97074 Würzburg, Germany
2 Würzburg-Dresden Cluster of Excellence ct.qmat, Germany
**Contact: kyungchan.lee@physik.uni-wuerzburg.de*

Keywords: ARPES, MBE, Pb thin film, STM

Atomic monolayers with honeycomb lattice are the ultimate limit of a 2D topological insulator. Kane and Mele model predicted that spin-orbit coupling (SOC) of electrons turns graphene into a quantum spin Hall insulator (QSHI) [1]. While SOC in graphene is too weak to open an appreciable inverted band gap. Thus, monolayers of heavier group IV elements have come into focus [2-3], specifically Pb [4-7]. However, studies of mono to few-layer Pb films on large gap insulator substrates remain elusive. Here, we report the successful synthesis of thin films of Pb on 4H-SiC (0001) using molecular beam epitaxy (MBE) and a comprehensive study of Pb thin films on SiC. Our angle-resolved photoelectron spectroscopy (ARPES) reveals a metallic ground state of Pb thin films on SiC with band dispersions and Fermi surfaces in good agreement with band theory [8,9]. In addition, our scanning tunneling microscopy (STM) data show a stripe-like reconstruction of the Pb surface, forming few-nm sized domains with 1D axes following the symmetry of the SiC (0001) substrate. We discuss these observations in comparison to theoretical results.

1. Kane, C. L., & Mele, E. J. (2005). Quantum spin Hall effect in graphene. Physical review letters, *95*(22), 226801.
2. Reis, F., Li, G., Dudy, L., Bauernfeind, M., Glass, S., Hanke, W.,& Claessen, R. (2017). Bismuthene on a SiC substrate: A candidate for a high-temperature quantum spin Hall material. Science, 357(6348), 287-290.
3. Bauernfeind, M., Erhardt, J., Eck, P., Thakur, P. K., Gabel, J., Lee, T. L.,& Sangiovanni, G. (2021). Design and realization of topological Dirac fermions on a triangular lattice. Nature communications, *12*(1), 5396.
4. Adler, F., Rachel, S., Laubach, M., Maklar, J., Fleszar, A., Schäfer, J., & Claessen, R. (2019). Correlation-driven charge order in a frustrated two-dimensional atom lattice. Physical Review Letters, 123(8), 086401.
5. Yu, X. L., Huang, L., & Wu, J. (2017). From a normal insulator to a topological insulator in plumbene. Physical Review B, 95(12), 125113.
6. Matta, B., Rosenzweig, P., Bolkenbaas, O., Küster, K., & Starke, U. (2022). Momentum microscopy of Pb-intercalated graphene on SiC: Charge neutrality and electronic structure of interfacial Pb. Physical Review Research, 4(2), 023250.
7. Ghosal, C., Gruschwitz, M., Koch, J., Gemming, S., & Tegenkamp, C. (2022). Proximity-Induced Gap Opening by Twisted Plumbene in Epitaxial Graphene. Physical Review Letters, 129(11), 116802.
8. Visikovskiy, A., Hayashi, S., Kajiwara, T., Komori, F., Yaji, K., & Tanaka, S. (2018). Computational study of heavy group IV elements (Ge, Sn, Pb) triangular lattice atomic layers on SiC (0001) surface. arXiv preprint arXiv:1809.00829.
9. Vera, A., Yanez, W., Yang, K., Zheng, B., Dong, C., Wang, Y.,& Robinson, J. A. (2022). Two-Dimensional Lead at the Graphene/Silicon Carbide Interface. arXiv preprint arXiv:2205.06859.

Pattern Formation in Epitaxial Growth on a Covalent Substrate: Sb on InSb(111)A

Bing Liu[1,2]*, Tim Wagner[1,2], Stefan Enzner[2,3], Philipp Eck[2,3], Martin Kamp[1], Giorgio Sangiovanni[2,3], and Ralph Claessen[1,2]

[1] *Physikalisches Institut, Universität Würzburg, D-97074 Würzburg, Germany*

[2] *Würzburg-Dresden Cluster of Excellence ct.qmat, Universität Würzburg, D-97074 Würzburg, Germany*

[3] *Institut für Theoretische Physik und Astrophysik, Universität Würzburg, D-97074 Würzburg, Germany*

Contact: bing.liu@physik.uni-wuerzburg.de

Keywords: moi attern, Sb film, topological surface state, quasiparticle interference

Structural perstructures arising from two competing lattices may lead to unexpected electronic behavior [1,2]. Sb is predicted to show thickness-dependent topological properties [3,4], providing potential applications for low-energy-consuming electronic devices. Here we successfully synthesize ultrathin Sb films on semi-insulating InSb(111)A. Despite the covalent nature of the substrate, which has dangling bonds on the surface, we prove by scanning transmission electron microscopy that the first layer of Sb atoms grows in an unstrained manner. Rather than compensating for the lattice mismatch of −6.4% by structural modifications, the Sb films form a pronounced pattern as we evidence by scanning tunneling microscopy. Our model calculations assign the pattern to a periodic surface corrugation. In agreement with theoretical predictions, irrespective of the modulation, the topological surface state known on a thick Sb film is experimentally confirmed to persist down to small film thicknesses, and the Dirac point shifts toward lower binding energies with a decrease in Sb thickness.

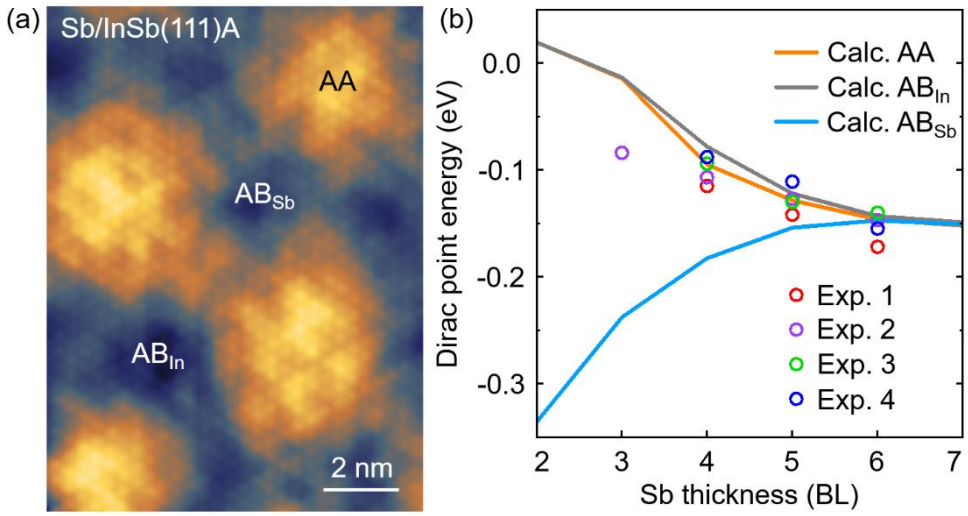

Figure 1. (a) High-resolution STM image (100 mV, 200 pA) of a 5 bilayer (BL) Sb island, showing the atomic lattice and superimposed moi pattern. The high local symmetries are marked by AA, AB_{In}, and AB_{Sb}. (b) Summarized energy of the Dirac point experimentally measured in various areas and calculated with different stackings.

1. Y. Cao, D. Rodan-Legrain *et al*., Tunable correlated states and spin-polarized phases in twisted bilayer−bilayer graphene. Nature **583**, 215−220 (2020).
2. Y. Liu, C. Zeng *et al*., Moir superlattices and related moir excitons in twisted van der Waals heterostructures. Chem. Soc. Rev. **50**, 6401−6422 (2021).
3. D. Hsieh, Y. Xia *et al*., Observation of unconventional quantum spin textures in topological insulators. Science **323**, 919 (2009).
4. P. Zhang, Z. Liu *et al*., Topological and electronic transitions in a Sb(111) nanofilm: The interplay between quantum confinement and surface effect. Phys. Rev. B **85**, 201410 (2012).

Photoelectron spectroscopy of artificially designed three-dimensional Si{111} facet surfaces on Si(110) and (001) substrates

Ni'matil Mabarroh[1,*], Juharni[1], Yuki Ida[1], Wataru Imayama[1], Yasunari Kimoto[1], Yoshihiro Kitagawa[1], Liliany N. Pamasi[1], Haobang Yang[1], Yuya Sakai[1], Tomoya Shimidzu[1], A. I. Osaka[2], Hidekazu Tanaka[2], XiaoQian Shi[3], FangZhun Guo[3], Takuji Iimori[4], Fumio Komori[4], Shin-ichiro Tanaka[2], Kiyohisa Tanaka[5], Shigemasa Suga[2], Azusa N. Hattori[2], and Ken Hattori[1,*]

1 Solid-state Information Physics Laboratory, Nara Institute of Science and Technology, Nara, Japan
2 SANKEN, Osaka University, Osaka, Japan
3 Institute of Mechanical Engineering, Dalian Jiaotong University. Dalian, China
4 Institute for Solid State Physics, The University of Tokyo, Kashiwa, Chiba 277-8581, Japan
5 UVSOR Synchrotron Facility, Institute for Molecular Science, Okazaki, Japan
**Contact: nimatil.mabarroh.nn6@ms.naist.jp, khattori@ms.naist.jp*

Keywords: lithography, three-dimensional silicon surfaces, photoelectron spectroscopy, band engineering

Highly densified device like 3D FET has been required by information society to break the limitation of miniaturizing 2D planar-type devices. Control of 3D structure surfaces is indispensable to improve the specification, such as carrier mobilities on any direction surfaces of the 3D structures. Recently, our group has successfully created 3D-Si surfaces by combining lithography and surface treatment techniques [1-5]; SEM, RHEED, LEED, or STM evaluations for lined or pyramidal structures with {111}, {110}, or {100} side/facet surfaces on (111), (110), or (001) substrates. Evaluating properties of 3D system such as electronic transport and magnetism evaluation has also been conducted [3,4]. In this study, we focus on ARPES studies for the electronic bands on 3D-Si surfaces, which will guarantee side/facet-wall channel operating 3D devices.

In this experiment, 3D-Si {111} facet-lined structures on Si(110) and (001) substrates with facet pitch of 20 μm and 4 μm, respectively, were prepared by using a photo-lithography and wet etching (Fig. 1(a)). After degassing and flashing the sample in ultra-high vacuum, {111} 7 × 7 reconstruction was confirmed by LEED (Fig. 1(b)). Valence band was measured on {111} facet surface normal to analyzer, by optimizing sample orientation (Fig. 1(c)). In 3D-Si on (110) substrate, ARPES using a lab-He source showed band dispersion assigned to projected bulk states and surface state in {111}7 × 7 [5]. **Using a syncrotron light source, {111}7 × 7 on (001) displayed much more clear band dispersion, which promises 3D surface-based band engineering toward the future functional 3D devices**.

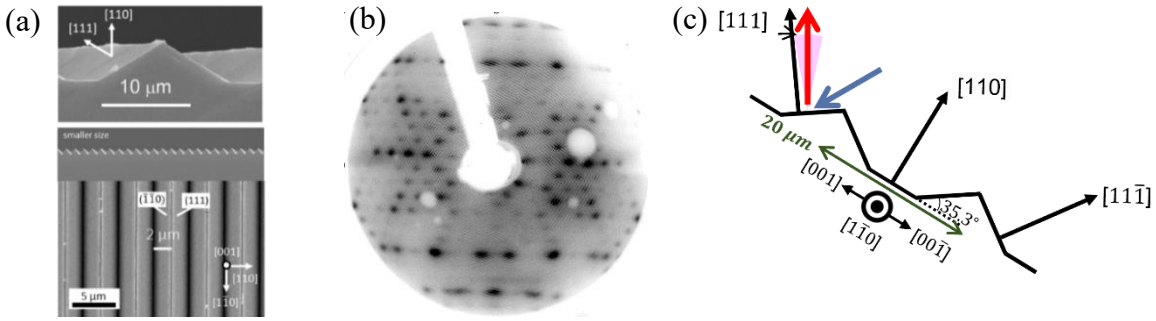

Figure 1: (a) SEM Image of 3D-Si facet-line structure (110) and (001), (b) LEED Pattern of {111}7 × 7 structure (65 eV), and (c) ARPES geometry.

1. A. N. Hattori, K. Hattori, *et al*., Creation of atomically flat Si{111}7x7 side-surfaces on a three-dimensionally-architected Si(110) substrate, *Surface Science* **644,** 86-89 (2016).
2. A. N. Hattori, S. Takemoto, K. Hattori, *et al*., Methods of creating and observing atomically reconstructed vertical Si{100}, {110}, and {111} side surface, *Appl. Phys. Express* **9,** 085501 (2016).
3. S. Takemoto, A. N. Hattori, K. Hattori, *et al*., Electric transport properties for three-dimensional angular-interconnects of Au wire crossing facet edges of atomically-flat Si{111} surface, *Jpn. J. Appl. Phys.* **57**, 090303 (2018).
4. A. Irmikimov, L. N. Pamasi, A. N. Hattori, K. Hattori, *et al*., Atomically architected silicon pyramid single-crystalline structure supporting epitaxial material growth and characteristic magnetism, *Crys. Growth* **21**, 946-953 (2021).
5. K. Hattori, A. N. Hattori, *et al*., Accessibility of ARPES for three-dimensionally architected Si{111}7×7 facet surfaces on micro-patterned Si(110), *e-J. Surf. Sci. and Nanotech.* **20**, 214-220 (2022).

In situ study of multi-phase In nanoparticles self-organized in organic thin film $CuPcF_4$

O.V. Molodtsova [1,*], D.V. Potorochin [1,2], S.V. Babenkov [1,3], S.L. Molodtsov [2,4], M. Vorokhta [5], T. Skála [5], and V.Y. Aristov [1]

1 Deutsches Elektronen-Synchrotron DESY, Hamburg, D-22607 Germany,

2 Institut für Experimentelle Physik, Freiberg, D-09596 Germany,

3 CEA-Saclay, 91190 Gif-sur-Yvette, France

4 European XFEL GmbH, Schenefeld, D-22869 Germany,

5 Charles University, Faculty of Mathematics and Physics, Prague, 18000 Czech Republic

**Contact: olga.molodtsova@desy.de*

Keywords: nanocomposite materials, In, $CuPcF_4$, dynamic XPS, HRPES, HRTEM.

The emergence and development of molecular electronics have drawn particular attention to molecular semiconductors, such as metal phthalocyanines. They have unique properties and are technologically advanced in the production of films. Using ultrathin films as a matrix, it is possible to create organometallic composites containing metal nanoparticles self-assembled in an organic matrix. The technologies for creating the described nanocomposites are quite simple and relatively cheap; therefore, such materials can take a prominent place in practical use in various electronic devices. However, despite the growing interest in hybrid systems, numerous questions about their properties and the processes that occur during their formation still remain unanswered. For example, interfacial phenomena can radically change the electronic properties of organic wide-gap matrices. It should also be noted that the processes of formation of organometallic interfaces in the manufacture of hybrid organo-inorganic systems proceed quickly. Therefore, the recording of experimental data in a dynamic mode could reveal additional properties of these materials that are important for electronics. Thus, Figure 1 shows the evolution of the spectra of core levels C 1s, N 1s, and In $3d_{5/2}$, recorded directly during the deposition of indium on the $CuPcF_4$ surface under ultrahigh vacuum conditions. A detailed description of the experiments can be found in [1, 2].

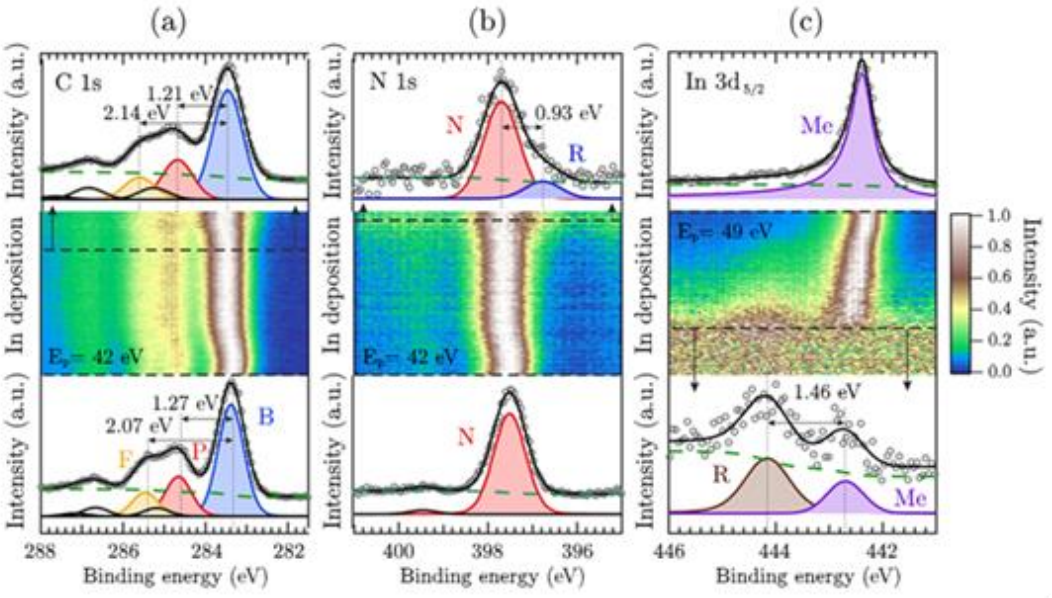

Figure 1: Evolution of the spectra of core levels (a) C1s, (b) N1s, and (c) In3d 5/2 recorded in the millisecond interval directly during the deposition of indium on the CuPcF4 surface under ultrahigh vacuum conditions.

1. O.V. Molodtsova et ai, In-situ study of multi-phase indium nanoparticle growth on/into CuPcF4 organic thin film in ultra-high vacuum conditions, *Appl. Surf. Sci*. **546**, 149136 (11) (2021).
2. V.Yu. Aristov et al, Study of formation and properties of In-CuPcF4 nanocomposite materials in the mode of millisecond recording of photoelectronic spectra, *J. Surf. Invest.: X-Ray, Synchrotron Neutron Tech.* **15** (6) 1129-1132 (2021).

Nobel metal nanoparticles self-organized in organic matrix

O.V. Molodtsova [1,*], S.V. Babenkov [1,2], D.V. Potorochin [1,3], S.L. Molodtsov [3,4], A.A. Makarova [5], D.A. Smirnov [6], and V.Y. Aristov [1]

1 Deutsches Elektronen-Synchrotron DESY, 22607 Hamburg, Germany

2 CEA-Saclay, 91190 Gif-sur-Yvette, France

3 Institut für Experimentelle Physik, TU Bergakademie Freiberg, D-09596 Freiberg, Germany

4 European XFEL GmbH, D-22869 Schenefeld, Germany

5 Institute of Chemistry and Biochemistry, Free University of Berlin, D-14195 Berlin, Germany

6 Institut für Festkörper- und Materialphysik, Technische Universität Dresden, 01062 Dresden, Germany

**Contact: olga.molodtsova@desy.de*

Keywords: metal nanoparticles, OMTF F_xCuPc, HR-TEM, HR-PES.

The aim of this work is to synthesize and study the properties of nanocomposite structures created by nanoparticles of noble metals (gold, silver), an interesting class of materials with unique properties that differ from both bulk and atomic behavior [1–3]. The nanoparticles self-assemble in/on an organic molecular thin film (OMTF) of partially fluorinated copper phthalocyanine (F_xCuPc, x=0; 4). The structure and morphology of this material, depending on the amount of deposited metal, were studied in UHV conditions using the HRTEM and HRPES methods. Metal atoms deposited on the surface of an organic substrate diffuse into the substrate, forming NPs with a narrow size distribution that correlates with the amount of deposited metal. Using HRTEM [2], the distance between the atomic planes of individual silver nanoparticles was determined (Fig. 1a) and a stable collection of individual nanoparticles into agglomerates and then into nanocrystals with intercrystallite boundaries was observed (Fig. 1b). On the whole, PES revealed a weak interaction of silver NPs with the organic matrix. However, in an organic film with small coatings of metal atoms, a strong upward bending of the band was observed. We also present the fabrication and study of the properties of nanocomposite structures consisting of two-dimensional (2D) silver nanoobjects self-organizing on the surface of an organic molecular thin-film copper tetrafluoro-phthalocyanine ($CuPcF_4$) [3]. Metal atoms deposited under ultra-high vacuum (UHV) conditions on OMFT diffuse along the surface and self-assemble into a system of two-dimensional metallic overlayers, while most of the silver atoms diffuse into the organic matrix and self-assemble into three-dimensional nanoparticles in a well-defined manner [3]

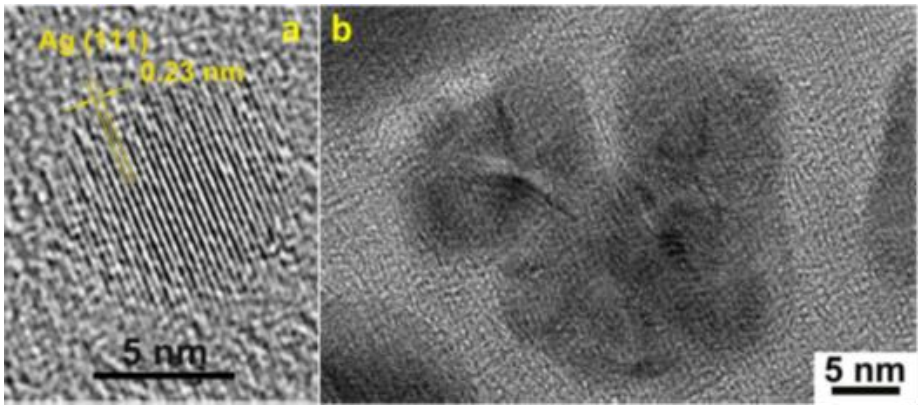

Figure 1: HRTEM image of single defect free silver NP surrounded with organic matrix and formed after nominal silver deposition of about 0.4 nm. (b) HRTEM image of silver NPs observed after nominal silver deposition of about 8.5 nm. The central NP is formed as the result of coalescence of the few ones.

1. S.V. Babenkov et al, Hybrid organic-inorganic systems formed by self-assembled gold nanoparticles in $CuPcF_4$ molecular crystal, *Organic electronics* **32**, 228 (2016).
2. O.V. Molodtsova et al, Noble metal nanoparticles in organic matrix, *Appl. Surf. Sci*. **506**, 144980 (8) (2020).
3. O.V. Molodtsova et al, 2D/3D Metallic Nano-objects Self-Organized in an Organic Molecular Thin Film, *ACS Omega* **5**, 10441 (2020).

Unveiling XPS spectra in the web browser using AiiDAlab

X. Wang[1], M. A. Hernández-Bertrán[2], P. N. O. Gillespie[2], J. Yu[1], I. Timrov[3], E. Molinari[2], D. Prezzi[2,*], N. Marzari[1, 3], and G. Pizzi[1,*]

1 Laboratory for Materials Simulations (LMS), Paul Scherrer Institut (PSI), Switzerland

2 Nanoscience Institute of the National Research Council (CNR-NANO), Italy

3 Theory and Simulation of Materials (THEOS), Ecole Polytechnique Fédérale de Lausanne (EPFL), Switzerland

**Contact: giovanni.pizzi@psi.ch; deborah.prezzi@nano.cnr.it*

Keywords: DFT, XPS, workflow, AiiDAlab

Density functional theory (DFT) represents a powerful tool for interpreting experimental core-level spectroscopies. In particular, the so-called Delta Kohn-Sham (ΔKS) approach is routinely used to rationalize X-ray photoelectron spectroscopy (XPS) data. Starting from core-hole pseudopotentials, it allows one to compute the XPS binding energies as total energy differences for the system with and without core-hole, for each given species in the target system [1].

In this work, we implement an automated, robust workflow to compute XPS spectra using the ΔKS approach and the pseudopotential-based total energy calculations in the Quantum ESPRESSO [2]. The workflow is managed by AiiDA, an open-source Python infrastructure to build and execute complex workflows [3]. The workflow handles the advanced setup for various materials (e.g., crystals and molecules), taking care of the identification of symmetry-inequivalent atoms and of the supercell generation needed to minimize the effect of the core-hole, as well as of the convolution of the results with a Voigt function to produce the final spectrum. Notably, the workflow is also integrated with the AiiDAlab web platform [4] to provide a user-friendly interface directly in the web browser, allowing researchers to perform XPS calculations and visualize results without the need to write any code.

Figure 1: Run XPS calculations using AiiDA workflow via tailored lightweight AiiDAlab web applications directly in the browser.

1. Walter, Michael, Michael Moseler, and Lars Pastewka. "Offset-corrected Δ-kohn-sham scheme for semiempirical prediction of absolute X-ray photoelectron energies in molecules and solids." *Physical Review B* 94.4 (2016): 041112.
2. Giannozzi, Paolo, et al. "Advanced capabilities for materials modelling with Quantum ESPRESSO." *Journal of physics: Condensed matter* 29.46 (2017): 465901.
3. Huber, Sebastiaan P., et al. "AiiDA 1.0, a scalable computational infrastructure for automated reproducible workflows and data provenance." *Scientific data* 7.1 (2020): 300.
4. Yakutovich, Aliaksandr V., et al. "AiiDAlab–an ecosystem for developing, executing, and sharing scientific workflows." *Computational Materials Science* 188 (2021): 110165.

Control of dipole assembly into molecular films with photoelectron spectroscopy

Alexei Nefedov[1,*], Ritesh Haldar[1], Zhiyun Xu[1], Hannes Kühner[2], Benedikt Sapotta[1], Stefan Hecht[3], Marjan Krstić[4], Carsten Rockstuhl[4], Wolfgang Wenzel[4], Stefan Bräse[2], Egbert Zojer[5] and Christof Wöll[1]

1 Institute of Functional Interfaces, Karlsruhe Institute of Technology, Eggenstein-Leopoldshafen, Germany
2 Institute of Organic Chemistry, Karlsruhe Institute of Technology, Karlsruhe, Germany
3 Institute of Technical and Macromolecular Chemistry, RWTH Aachen University, Aachen, Germany
4 Institute of Nanotechnology, Karlsruhe Institute of Technology, 76344 Eggenstein-Leopoldshafen, Germany
5 Institute of Solid State Physics, Graz University of Technology, Graz, Austria
**Contact: alexei.nefedov@kit.edu*

Keywords: dipole assembly, metal-organic frameworks, photoelectron spectroscopy

Solids with non-centrosymmetric (NC) structure (i.e., those lacking spatial inversion symmetry) exhibit a variety of interesting properties, e.g., piezoelectricity and nonlinear optical (NLO) effects including second-harmonic generation (SHG) [1]. Furthermore, the corresponding absence of inversion symmetry is a prerequisite for integrating static electric fields into a material.

Liquid-phase, quasi-epitaxial growth has been used to stack asymmetric, dipolar organic compounds on inorganic substrates, permitting porous, crystalline molecular materials which lack inversion symmetry. This allows material fabrication with built-in electric fields. We describe a new programmed assembly strategy based on metal-organic frameworks (MOFs) [2] that facilitates crystalline, non-centrosymmetric space groups for achiral compounds. Electric fields are integrated into crystalline, porous thin films with an orientation normal to the substrate. Changes in electrostatic potential are detected via core-level shifts of Br marker atoms on the MOF thin films and agree with theoretical results (Fig. 1).

The integration of built-in electric fields into molecular solids creates possibilities for band structure engineering to control the alignment of electronic levels in organic molecules and it may also be used to tune the transfer of charges from donors loaded via programmed assembly into MOF pores.

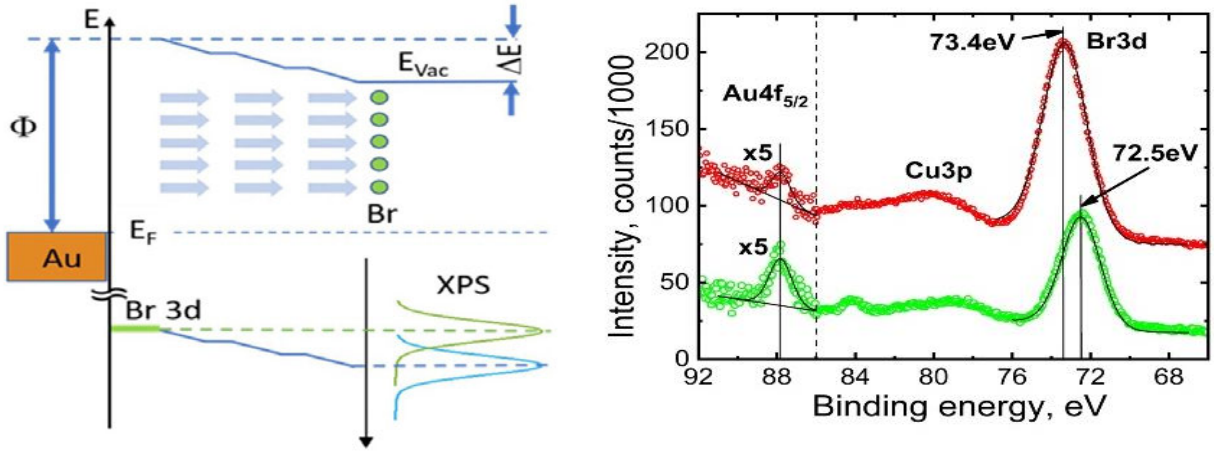

Figure 1: (left) An illustration of static electric field design using asymmetric subunits in a SURMOF and its effect on Br-core levels. (right) XPS data recorded for symmetric (green circles) and asymmetric (red circles) MOF thin films.

The integration of built-in electric fields into molecular solids creates possibilities for band structure engineering to control the alignment of electronic levels in organic molecules and it may also be used to tune the transfer of charges from donors loaded via programmed assembly into MOF pores.

1. J. Lu, X. Liu, M. Zhao, X. B. Deng, K. X. Shi, Q. R. Wu, L. Chen, L. M. Wu, Discovery of NLO Semiorganic (C5H6ON)+(H2PO4)−: Dipole Moment Modulation and Superior Synergy in Solar-Blind UV Region, *J. Am. Chem. Soc.*, **143**, 3647-3654 (2021).
2. H. Furukawa, K. E. Cordova, M. O'Keeffe, O. M. Yaghi, The chemistry and applications of metal-organic frameworks, *Science*, **341**, 1230444 (2013).

Origin of optically active color-centers in two-dimensional lead iodide perovskites revealed by photoemission

Marie Krecmarova, Jesús Rodríguez-Romero, Iván Mora-Seró, Juan P. Martínez-Pastor, Maria C. Asensio, Juan F. Sánchez-Royo*

1 Materials Science Institute, University of Valencia, 46100 Paterna, Valencia, Spain
2 institute of Advanced Materials (INAM), Universitat Jaume I, 12006 Castellón, Spain
3 ICMM-CSIC Materials Science Institute of Madrid, 28049 Cantoblanco, Madrid, Spain.
**Contact: Juan.F.Sanchez @uv.es*

Keywords: two-dimensional halide perovskites, donor-acceptor optical pairs.

Two-dimensional (2D) van der Waals nanomaterials have attracted considerable attention for potential use in photonic and optoelectronic applications on the nanoscale, due to their outstanding electrical and optical properties [1]. Currently, 2D perovskite belonging to this group of nanomaterials is widely studied for a wide range of optoelectronic applications. In particular, they are appealing since their optical emission properties can be controlled by their n value, which labels the number of inorganic monolayers building the quantum well structure (from n = 1, 2, 3 to $\sim \infty$) [2,3]. Thanks to their excitonic properties, 2D perovskites are also promising materials for photonics and nonlinear devices working at room temperature. Nevertheless, strong excitonic effects can reduce the photocurrent characteristics when using the thinner perovskites phase. There is a different carrier strategy to produce high photocurrent generation in 2D halide perovskites, which relies on the dissociation of excitons into Donor-Acceptor pairs. Our results show that the generaton of optically active Donor-Acceptor pairs is promoted in, only, n=2 2D halide perovskites. However, the chemical nature of these Donor-Acceptor pairs is not clear yet. By X-ray photoemission spectroscopy, we have found that donor-acceptor pairs are created by the displacement of lead atoms and their replacement by methylammonium, which is particularly important, as revealed also by photoemission, in n=2 2D halide perovskites.

1. J.-C. Blancon, J. Even, C.C. Stoumpos, M.G. Anatzidis, A.D. Mohite, Semiconductor physics of organic–inorganic 2D halide perovskites. *Nature Nanotechnology* **15**, 969–985 (2020).
2. A. G. Ricciardulli, S. Yang, J.H. Smet, M. Saliba. Emerging perovskite monolayers. *Nature Materials* **20**, 1325–1336 (2021).
3. K. Leng, W. Fu, Y. Liu, M. Chhowalla, K.P. Loh. From bulk to molecularly thin hybrid perovskites. Nature Reviews Materials **5**, 482–500 (2020).

Chemical and electronic structure of $Fe_xNi_{100-x}(O,OH)_y$ electrocatalysts studied by soft and hard x-ray spectroscopies

R. Sengupta[1,2], R. Daneshpour[3], D. Hauschild[1,2,4], C. Wansorra[1], R. Steininger[1], M. Janik[3,5], L. Greenlee[3,], E. L. Clark[3,], C. Heske[1,2,4], and L. Weinhardt[1,2,4]

[1] *Institute for Photon Science and Synchrotron Radiation (IPS), Karlsruhe Institute of Technology (KIT), Eggenstein-Leopoldshafen, Germany*

[2] *Institute for Chemical Technology and Polymer Chemistry (ITCP), Karlsruhe Institute of Technology (KIT), Karlsruhe, Germany*

[3] *Department of Chemical Engineering, Pennsylvania State University, Pennsylvania, USA*

[4] *Department of Chemistry and Biochemistry, University of Nevada, Las Vegas (UNLV), Las Vegas, NV, USA*

[5] *Institutes of Energy and the Environment, Pennsylvania State University, Pennsylvania, USA*

Keywords: catalysis, OER, HAXPES, XAS, synchrotron, soft and hard x-rays

The production of hydrogen-based fuels with renewable energy sources as an alternative to fossil fuel-based approach is one of the major challenges for the scientific world of today. Hydrogen production via electrolytic water splitting has emerged as a promising method in this respect. Ni-based oxides have received a lot of attention as feasible catalysts for the anodic half reaction of the process in alkaline media (also known as oxygen evolution reaction OER).[1] When alloyed with Fe, the activity of these catalysts increases, owing to the unique electronic and physical structure of the alloy.[2] This unique electronic structure and its influence on the activity of the catalyst is not fully understood, which calls for a thorough investigation.

In this contribution, we study $Fe_xNi_{100-x}(O,OH)_y$ electrocatalysts using hard x-ray photoelectron spectroscopy (HAXPES) and soft x-ray absorption spectroscopy (XAS). The data were collected at the newly-commissioned X-SPEC undulator beamline at the KIT Light Source, which covers a photon energy range of 70 to 15,000 eV. [3] The results show significant spectral changes across different chemical compositions, which will be discussed in view of the local chemical environment of the probed atoms, as well as the corresponding catalytic activity.

[1] S. I. Perez Bakovic et al, "Electrochemically active surface area controls HER activity for Fe_xNi_{100-x} films in alkaline electrolyte," *Journal of Catalysis.*, **394**, 104–112, (2021)

[2] M. W. Louie et al, "An Investigation of Thin-Film Ni–Fe Oxide Catalysts for the Electrochemical Evolution of Oxygen," *Journal of the American Chemical Society*, **135**, 12329–12337, (2013)

[3] L. Weinhardt et al, "X-SPEC: a 70 eV to 15 keV undulator beamline for X-ray and electron spectroscopies," *Journal of Synchrotron Radiation.*, **28**, 609–617, (2021)

Grazing X-ray absorption spectroscopy of 2D MoS_2-Based Memristor Device

Harishchandra Singh[1,*], Shuei-De Huang,[2] Ashok Kumar Yadav[3], Seyed Hossein Hosseini-Shokouh[2], Ekta Rani[1], Gianluca Ciatto[3], Krisztian Kordas[2], Hannu-Pekka Komsa[2]

[1]*Nano and Molecular Systems Research Unit, University of Oulu, Finland*

[2]*Microelectronics Research Unit, Faculty of Information Technology and Electrical Engineering, University of Oulu, Finland*

[3]*Synchrotron SOLEIL, Beamline SIRIUS, Saint-Aubin, F-91192, Gif sur Yvette, France*

**Contact: Harishchandra.Singh@oulu.fi*

Keywords: 2D material, XAFS, Local structure, Memristor

The potential of neuromorphic electronic synapse to revolutionize computing technology by overcoming the von Neumann bottleneck with massive parallelism, robust computation, and high energy efficiency could be realized using memristors. 2D transition metal dichalcogenides (TMDs), which have unique electronic, mechanical, and optical properties, have received dramatic attention in this regard. Among them, layered MoS2 have been shown to be promising for fabricating memristors [1,2]. MoS_2 is particularly attractive due to its large intrinsic band gap, structural stability, and the possibility of phase transitions from the 2H phase (semiconducting) to the 1T′ phase (semimetallic) or the 1T phase (metallic). The 2D layered structure of MoS_2 enables the creation of multilevel states and memory operation with significant reliability through the ion intercalation of the material.

To study the role of the electrode metal, Si-SiO_2/MoS_2/Ag or Cu/Au memristor devices with large area MoS_2 were synthesized via sulfurization of Mo film. The diffusion of metal ions (Cu or Ag) from the active electrode layer plays a crucial role in device performance, however, critical probe. Herein, Synchrotron based grazing X-ray absorption fine structure (XAFS) spectroscopy has been utilized to understand the nature of these components i.e., Cu and Ag. The XAFS measurements have been carried out at SIRIUS beamline, Synchrotron SOLEIL, France [3], and the behavior of Cu and Ag has been carefully monitored by measuring the contribution from different depths of the device sample using angle dependent XAFS measurements (see Figure 1).

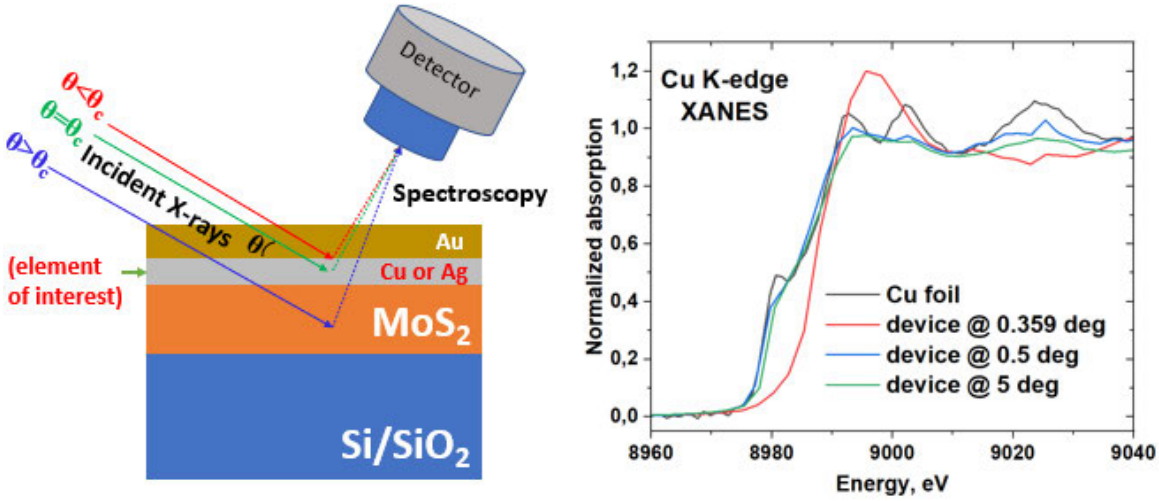

Figure 1. Representative memristor device (left) and corresponding spectroscopic data at grazing mode (right).

1. Dev, D., Krishnaprasad, A., Shawkat, M. S., He, Z., Das, S., Fan, D., ... & Roy, T., 2D MoS_2-based threshold switching memristor for artificial neuron. *IEEE Electron Device Letters*, **41**, 936-939 (2020).
2. Dev, D., Shawkat, M. S., Krishnaprasad, A., Jung, Y., & Roy, T., Artificial nociceptor using 2D MoS_2 threshold switching memristor. *IEEE Electron Device Letters*, **41**, 1440-1443 (2020).
3. G. Ciatto, M. H. Chu, P. Fontaine, N. Aubert, H. Renevier, J. L. Deschanvres, SIRIUS*:* A new beamline for in situ X-ray diffraction and spectroscopy studies of advanced materials and nanostructures at the SOLEIL Synchrotron*, Thin Solid Films* **617***, 48-54 (2016).*

Spectromicroscopy For Steel And Beyond

Harishchandra Singh

Nano and Molecular Systems Research Unit, University of Oulu, Oulu FIN-90014, Finland

Contact:harishchandra.singh@oulu.fi

Keywords: spectroscopy, steel, local structure, precipitates, non-metallic inclusions

Despite decades of study, the local structure and electronic structure of steel and its interaction with non-metallic inclusions (NMIs) remain poorly understood due to complexity of steel matrix and limitations of in-house characterizations. How the local structure of Fe in different phases of steel matrix affects the steel microstructure has remain a question. Secondly, how the known inclusions, which are regions of oxides (Al_2O_3, SiO_2, $MgAl_2O_4$), sulfides (MnS, CaS), and nitrides (AlN, BN, TiN), interact and stabilize within a steel matrix have been another focus of steel researchers. This is because, while the steel microstructure decides its strength, inclusions can have a significant effect on the mechanical properties and quality of the steel product [1-2].

Recent advancements in synchrotron-based spectroscopy in combination with microscopy have shown promise in providing answers to some of the long-standing questions about steel and its variants [2-4]. This study showcases how advanced spectroscopy has uncovered the local structure of Fe in steel matrix (Figure 1) and unknown interaction mechanisms and new findings in non-metallic inclusions (NMIs) within steel, highlighting the potential of this technique for further research in this field.

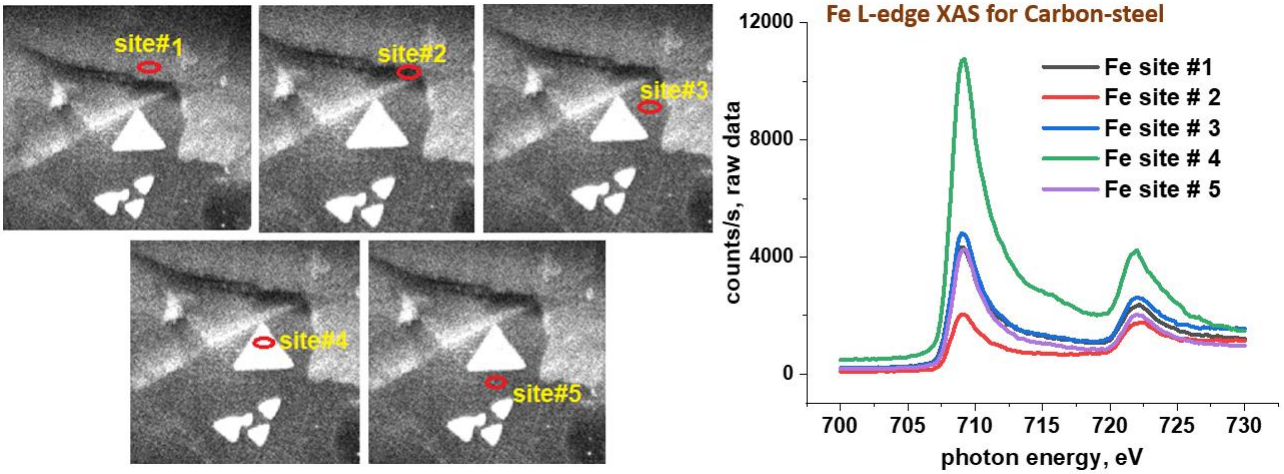

Figure 1. Steel microstructures and triangular precipitates (left) showing different spectroscopic nature around Fe (right).

Acknowledgements

HS thanks the synchrotron beamline staff from MAX IV Laboratory, Sweden and steel sample providers from process metallurgy unit and Materials and Mechanical Engineering unit, University of Oulu, Finland.

1. S. Ghosh, S. Wang, H. Singh, G. King, Y. Xiong, T. Zhou, M. Huttula, J. Kömi, W. Cao, Quantitative prediction of yield strength of highly alloyed complex steel using high energy synchrotron X-ray diffractometry, Journal of Materials Research and Technology, 20, 485-495, 2022.

2. H. Singh, T. Alatarvas, K. Andrey, SSD Assa, S. Wang, B. Sarpi, Y. Niu, A. Zakharov, F.M. de Groot, M. Huttula, W. Cao, T. Fabritius, 'Unveiling Interactions of Non-Metallic Inclusions within Advanced Ultra-High-Strength Steel: A Spectro-Microscopic Determination and First-Principles Elucidation' *Scripta Materialia*, 197, 113791, 2021.

3. E. Rani, H. Singh, T. Alatarvas, M. Kharbach, W. Cao, B. Sarpi, L. Zhu, Y. Niu, A. Zakharov, T. Fabritius, M. Huttula, Uncovering temperature-tempted coordination of inclusions within ultra-high-strength-steel via in-situ spectro-microscopy, *J. Mater. Res. Techno*, 17, 2333, 2022.

4. H. Singh, X. Xiong, E. Rani, M. Huttula S. Wang, M. Kharbach, T. Zhou, H. Yao, Y. Niu, A. Zakharav, G. King, F. Groot, J. Komi, W. Cao, unveiling nano-scaled chemical inhomogeneity impacts on corrosion of Ce-modified 2507 super-duplex stainless steels, npj Materials Degradation, 6, 54, 2022.

Momentum-selective orbital hybridization at molecule/metal interfaces

Xiaosheng Yang[1,2], Matteo Jugovac[1,3], Giovanni Zamborlini[1,4], Vitaliy Feyer[1,5], Georg Koller[6], Peter Puschnig[6], Serguei Soubatch[1,*], Michael G. Ramsey[6], F. Stefan Tautz[1,2]

1 Forschungszentrum Jülich, Jülich, Germany
2 RWTH Aachen University, Aachen, Germany
3 Elettra - Sincrotrone Trieste, Basovizza, Trieste, Italy
4 Technische Universität Dortmund, Dortmund, Germany
5 Universität Duisburg-Essen, Duisburg, Germany
6 University of Graz, NAWI Graz, Graz, Austria
**Contact: s.subach@fz-juelich.de*

Keywords: photoemission electron microscopy, hybridization, molecule/metal interfaces

In molecular orbital theory [1], chemical bonding is determined by the linear combination of atomic orbitals [2]. The valence bond picture explains bonding in terms of the overlap between hybridized atomic valence orbitals [3]. In both models, the bonding strength is determined by the degree of orbital overlap in the interaction potential [4,5]. This intuitive real-space picture of bonding is challenged if the interacting wave-functions have specific momentum distribution reflecting their symmetry. Hence one may additionally expect a momentum matching condition representing an additional selection rule for hybridization.

Here, we report photoemission electron microscopy measurements of hybrid orbitals that emerge at the interface between organic molecules and a metal, namely for *para*-quinquephenyl (5P) and *para*-sexiphenyl (6P) adsorbed on Cu(110) [6]. These new wave-functions are formed due to the hybridization of the former lowest unoccupied molecular orbitals (LUMO) of oligophenyls and the copper bulk states. Importantly, only those partial waves of the original molecular orbitals contribute to the bonding which match the metal band structure. In the distributions of the photoemission, we see no intensity at the wave-vectors that correspond to the gaps in the surface-projected bulk band structure of the metal. On the other hand, the adsorbate quenches the metal surface state at those wave-vectors, where the corresponding molecular orbital has a finite charge density. Instead, a new interface state is formed at the wave-vectors where the molecular orbitals have no sizable density. Thus, demonstrating the possibility to address the hybridization momentum-selectively, our study enables deep insights into the complicated interplay of bulk states, surface states, and molecular orbitals in the formation of the electronic structure at molecule/metal interfaces.

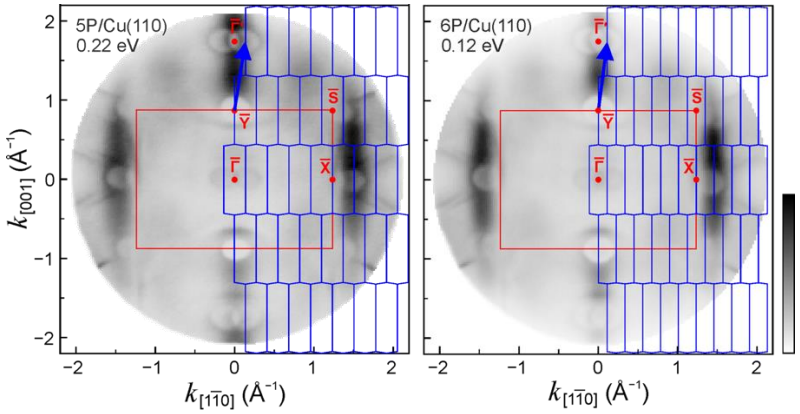

Figure 1: Maps of photoemission from the hybrid states derived from former LUMO of 5P and 6P on Cu(110) superimposed with Brillouin zones of Cu(110) (red) and nP/Cu(110) (blue).

1. J.E. Murrell, J. E. The origins and later developments of molecular orbital theory. *Int. J. Quantum Chem*. **112**, 2875–2879 (2012).
2. R.S. Mulliken, The interpretation of band spectra. *Rev. Mod. Phys*. **1**, 1–86 (1932).
3. L. Pauling, The nature of the chemical bond. *J. Am. Chem. Soc.* **53**, 1367–1400 (1931).
4. J.E. Lennard-Jones, The electronic structure of some diatomic molecules. *Trans. Faraday Soc.* **25**, 668–686 (1929).
5. W. Heitler and F. London, Wechselwirkung neutraler Atome und homöopolare Bindung nach der Quantenmechanik. *Z. Phys.* **44**, 455–472 (1927).
6. Xiaosheng Yang et al., Momentum-selective orbital hybridisation. *Nat. Commun.* **13**, 5148 (2022).

Electron Spectroscopy for Hydrogen Future as a Climate Change Solution (H2FUTURE)

Filipp Temerov, Samuli Urpelainen, Wei Cao and Marko Huttula*

Nano and Molecular Systems Research (NANOMO) Unit, University of Oulu, Oulu, 90014, Finland

**Contact: marko.huttula@oulu.fi*

Keywords: Clean hydrogen, Synchrotron spectroscopy, Sustainable energy transition

The H2FUTURE program at the University of Oulu is dedicated to finding innovative and sustainable solutions for clean hydrogen production with two unique goals: direct sunlight-driven photocatalytic water splitting for hydrogen production, and the scale-up of catalytic methane pyrolysis technology with tailored nanocarbon side stream production. In addition, the program aims to develop fossil-free hydrogen reduction methods for iron ores, focusing on creating hydrogen embrittlement-resistant tough steels that are durable for lightweight applications (**Figure 1**).

To achieve these goals, it is crucial to characterize the materials involved, including the catalysts for hydrogen production and the steel as the final hydrogen-storage product. Electron spectroscopy, particularly synchrotron-based methods, is a superior technique for this material characterization. Therefore, H2FUTURE will focus on understanding the electronic processes in materials through synchrotron-based methods, with a particular emphasis on the services and instrumentation. This will include access to advanced instrumentation provided by the Center for Material Analysis at UO. The program will also participate in national and international research infrastructures, such as the MAX IV Laboratory synchrotron radiation facility in Lund, Sweden, where UO is the coordinator of the Finnish national membership.

Moreover, the program will utilize advanced characterization methods, particularly the upcoming Hub for Hydrogen-Materials Interactions Research Infrastructure (Coordinated by UO, in collaboration with VTT Technical Research Centre and Tampere University) novel in-situ/operando methodologies, throughout the program. Specifically, Time-of-Flight Secondary Ion Mass Spectrometry (**TOF-SIMS**, VTT) with the capability to measure all elements of the periodic table from hydrogen to uranium, along with isotopes and molecular species, with superior resolution in three dimensions, **H_2 tribometer (**VTT, TUNI**)** to gain insights into the influence of hydrogen on mechanical components in relative motion against each other, and Ambient Pressure X-ray Photoelectron Spectroscopy (**APXPS**, UO) to probe materials at relevant conditions for real chemical and industrial processes, in all phases (solid-liquid-gas) and at high temperatures (up to 1200 K) and pressures (up to 100 mbar).

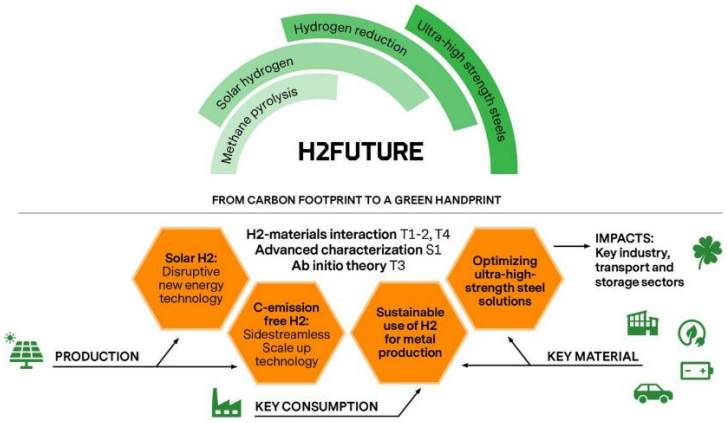

Figure 1: Roadmap of the H2FUTUTRE.

Local structural analysis of boron atoms heavily doped in diamond

Hiroto Tomita[1*], Noriyuki Kataoka[2], Takayoshi Yokoya[2], Taisuke Kageura[3], Yoshihiko Takano[4], Tomohiro Matsushita[1]

1 Division of Material Science, Nara Institute of Science and Technology, Nara, Japan
2 Research Institute for Interdisciplinary Science, Okayama University, Okayama, Japan
3 Sensing System Research Center, National Institute of Advanced Industrial Science and Technology, Ibaraki, Japan
4 Research Center for Materials Nanoarchitectonics, National Institute for Materials Science, Ibaraki, Japan
5 Faculty of Science and Engineering, Waseda University, Tokyo, Japan
**Contact: tomita.hiroto.tf7@ms.naist.jp*

Keywords: boron-doped diamond, photoelectron holography, chemical states, nanostructures

When diamond is applied to semiconductor devices, boron is generally used the acceptor. Insulator to metal transition occurs when the concentration of boron doped in diamond is above 10^{20} cm^{-3}. Furthermore, diamond with high boron concentration (10^{21} cm^{-3}) is known to exhibit superconductivity. The superconducting critical temperature of boron-doped diamond is thought to be limited by the solid solution limit of boron. Hence, as the dopant concentration increases, the ratio of boron atoms introduced into the inactive sites increases. In fact, soft x-ray PES study has shown that boron atoms in the bulk have multiple chemical states [1]. However, it is still unclear what structure of boron atom each component is derived from. This is because there was no way to observe the local structure of dopants that randomly existed in the crystal.

Our group has recently succeeded in identifying not only the chemical state, but even the energetically equivalent position of phosphorus doped in diamond [2]. This achievement was realized by photoelectron hologram (PEH) measurements using soft x-ray synchrotron radiation and a high-resolution electron analyzer at BL25SU of SPring-8, Japan.

In this study, we applied this technique to heavily boron-doped diamond, and tried to identify the chemical state and local structure. Figure 1 shows B 1*s* core-level photoelectron spectra. Experimental data were fitted using components A-G. The photoelectron emission angle dependence shows an increase in the relative intensity of components D-G. This suggests that these comonents originate from boron in the surface region. Figure 2 shows PEHs of C 1*s* and B 1*s* core-levels. The most dominant component C in B 1*s* is shown as an example. The very good agreement between the two PEHs indicated that the boron of component C was introduced into the substitution site. Interestingly, PEHs similar to C 1*s* were observed in all components except G. In the presentation, the PEH of each component of B 1s will be explained in detail.

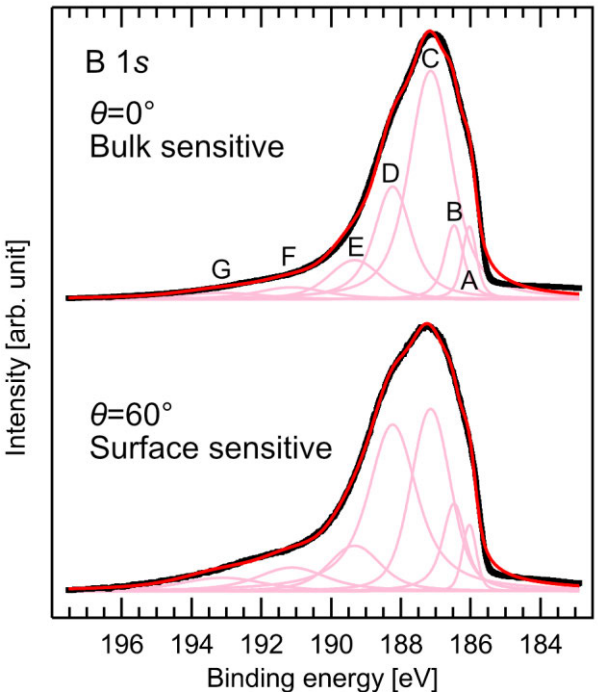

Figure 1: B 1*s* core-level photoelectron spectra from heavily boron-doped diamond (111) using $h\nu$ = 800 eV photon energy. Black lines are the experimental data, red lines are the fitting curve. Pink lines are Voigt line shapes used for fitting.

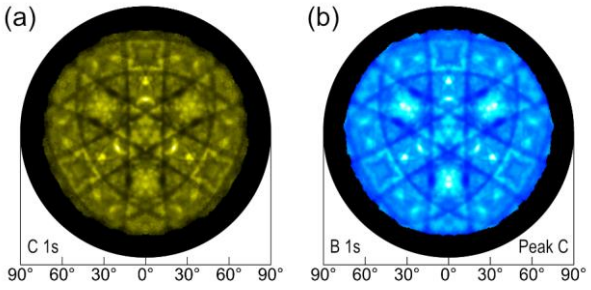

Figure 2: (a) PEH of C 1*s*. (b) PEH of component C in B 1*s* core-level. Both holograms are projected using the azimuthal equidistant projection.

1. H. Okazaki et al., *J. Phys. Soc. Jpn*. **78**, 034703 (2009)
2. T. Yokoya et al., *Nano Lett*. **19**, 5915-5919 (2019)

Valence band hybridization in sulfides

Lothar Weinhardt[1,2,3,*], Dirk Hauschild[1,2,3], Constantin Wansorra[1], Ralph Steininger[1], Monika Blum[3,4,5], Wanli Yang[4], and Clemens Heske[1,2,3]

1 Institute for Photon Science and Synchrotron Radiation (IPS), Karlsruhe Institute of Technology (KIT), Eggenstein-Leopoldshafen, Germany
2 Institute for Chemical Technology and Polymer Chemistry (ITCP), Karlsruhe Institute of Technology (KIT), Karlsruhe, Germany
3 Department of Chemistry and Biochemistry, University of Nevada, Las Vegas (UNLV), Las Vegas, USA
4 Advanced Light Source (ALS), Lawrence Berkeley National Laboratory, Berkeley, USA
5 Chemical Sciences Division, Lawrence Berkeley National Laboratory, Berkeley, USA

**Contact: Lothar.Weinhardt@kit.edu*

Keywords: x-ray emission spectroscopy, sulfides, hybridization

Understanding chemical bonding in molecules and crystalline solids is a fundamental question in chemistry and physics. When atoms are brought together, their electronic orbitals can interact by forming hybrid orbitals, chemical bonds, and, accordingly, the electronic structure of the compound. This electronic structure governs many of the material properties, and its characterization is thus in the center of fundamental and applied research. X-ray spectroscopic techniques are particularly well suited to study the electronic structure, with soft x-ray emission spectroscopy (XES) offering a local (i.e., atom-specific) probe of the valence electronic structure. In this contribution, we demonstrate that XES is ideally suited to study hybridization in the valence band of solids. In particular, we have investigated selected metal sulfides (ZnS, CdS, HgS, Ga_2S_3, and In_2S_3) as model systems to study valence band hybridization. These sulfides allow to investigate hybrid bands derived from the metal d and the S 3s and 3p states as a function of the d state energy. We have employed S $L_{2,3}$ XES to *directly* probe the degree of hybridization of these states. Our experimental spectra are compared with spectra calculations based on density functional theory and S K XES spectra from literature. Using a Hubbard U correction, the position of the metal d derived bands relative to the surrounding valence band structure can be adjusted for each compound, and a good quantitative description of the experimental spectra is achieved (see Figure 1). We find that the relative intensity of the metal d derived band features in the spectra approximately scales with the inverse square of the energy distance to the respective sulfur-derived bands. This dependency can also be derived analytically from a simple two orbital model. In addition, the studied hybrid bands allow an unambiguous speciation of the studied sulfide compounds.

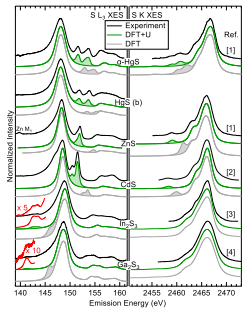

Figure 1: S L_3 (left) and S K (right) XES spectra of HgS, ZnS, CdS, In_2S_3, and Ga_2S_3. Experimental spectra are shown in black, spectra calculated by DFT and DFT+U in gray and green, respectively. The metal d derived features are shaded. Experimental S K spectra are digitized from references [1–4], as given next to the corresponding spectra.

1. R. A. Mori et al. , *Inorg. Chem.* **49**, 6468 (2010).
2. C. Sugiura, Y. Gohshi and I. Suzuki, *Phys. Rev. B* **10**, 338 (1974).
3. A. N. Gusatinskii, A. A. Lavrentyev, M. A. Blokhin, and V. Y. Slivka, *Solid State Commun.* **57**, 389 (1986).
4. C. Sugiura, H. Yorikawa, and S. Muramatsu, *J. Phys. Soc. Jpn.* **66**, 503 (1997).

Spatially resolved composition of laboratory-generated atmospheric model aerosol particles investigated with STXM-NEXAFS

Lingyu Kong,[1] Jack J. Lin,[1] Kamal R. R. Mundoli,[1] Takuji Ohigashi,[2,†] and Nønne L. Prisle[1,*]

1 Center for Atmospheric Research, University of Oulu, Oulu, Finland.

2 UVSOR Synchrotron Facility, Institute for Molecular Science, Okazaki, Japan.

[†]Now at: Photon Factory, High Energy Accelerator Research Organization (KEK), Tsukuba, Japan.

[*]nonne.prisle@oulu.fi

Keywords: Aerosol particles, spatially resolved chemical characterization, STXM-NEXAFS

Nano- and microscopic aerosol particles are found everywhere in the atmosphere and play critical roles in formation of air pollution and global climate. However, aerosol effects still constitute one of the most uncertain elements of the atmospheric system.[1] Atmospheric aerosol particles typically have complex chemical compositions, comprising mixtures of numerous organic and inorganic species.[2] Therefore, simpler model systems generated with well-established methodologies are typically used as proxies in laboratory process-level studies.[3] When interpreting the results of aerosol experiments, it is commonly assumed that these laboratory-generated particles are both internally and externally homogeneously mixed.[4,5] New chemically resolved single particle imaging methods in combination with synchrotron radiation now allow direct investigation of this assumption. We have used STXM-NEXAFS to investigate the spatial distribution maps of individual laboratory-generated particles generated with methods typically used in aerosol experiments. We focus on organic groups, in particular oxygen, chlorine, and inorganic mass fractions, using several STXM data analysis algorithms, including peak fitting, integration, and multivariate curve resolution-alternating least squares (MCR-ALS). We find a clear core-shell structure in all individual particles, demonstrating that the particles are not internally homogeneously mixed. Furthermore, the dried aerosol particles show a memory effect of formation of inverted micelle structures during the aerosol generation process. We also find significant external inhomogeneity in aerosol samples generated from a common stock solution, where the inorganic cores are enhanced in the smaller particles. These effects are likely due to complex bulk-surface partitioning effects[3–5] occurring during nebulization and drying of the aerosol samples.

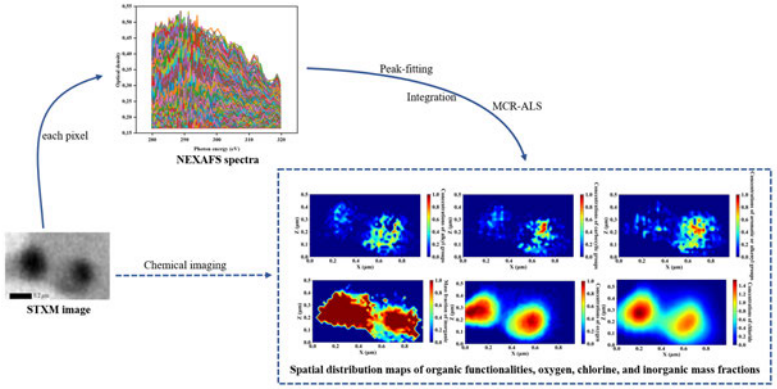

Figure 1: Chemical imaging of aerosols using STXM/NEXAFS.

[1] IPCC, *Climate Change 2021: The Physical Science Basis. Contribution of Working Group I to the Sixth Assessment Report of the Intergovernmental Panel on Climate Change*, Cambridge University Press, Cambridge, UK and New York, NY, USA, 2021.

[2] M. Hallquist, J. C. Wenger, U. Baltensperger, Y. Rudich, D. Simpson, M. Claeys, J. Dommen, N. M. Donahue, C. George, A. H. Goldstein, J. F. Hamilton, H. Herrmann, T. Hoffmann, Y. Iinuma, M. Jang, M. E. Jenkin, J. L. Jimenez, A. Kiendler-Scharr, W. Maenhaut, G. McFiggans, T. F. Mentel, A. Monod, A. S. H. Prevot, J. H. Seinfeld, J. D. Surratt, R. Szmigielski and J. Wildt, *Atmospheric Chemistry and Physics*, 2009, **9**, 5155–5236.

[3] N. L. Prisle, *Atmospheric Chemistry and Physics*, 2021, **21**, 16387–16411.

[4] N. L. Prisle, T. Raatikainen, A. Laaksonen and M. Bilde, *Atmos. Chem. Phys.*, 2010, **10**, 5663–5683.

[5] J. J. Lin, T. B. Kristensen, S. M. Calderón, J. Malila and N. L. Prisle, *Environmental Science: Processes & Impacts*, 2020, **22**, 271–284.

Construction of Ultrahigh Energy Resolution 2D-RIXS at NanoTerasu

Jun Miyawaki, Kohei Yamamoto, Kentaro Fujii, Koji Horiba, Hideaki Iwasawa, Yoshiyuki Ohtsubo, Miho Kitamura, Takashi Imazono, Tomoyuki Takeuchi, Nobuhito Inami, Takeshi Nakatani, Kento Inaba, Akane Agui, Hiroaki Kimura, and Masamitu Takahasi

Institute for Advanced Synchrotron Light Source, National Institutes for Quantum Science and Technology, Sendai, Japan

**Contact: miyawaki.jun@qst.go.jp*

Keywords: resonant inelastic X-ray scattering, RIXS

Resonant inelastic X-ray scattering (RIXS) is a powerful technique for studying the energies of electronic states and elementary excitations in materials by analyzing the energy of X-rays scattered off matter. Recent advances in energy resolution have enabled sub-50 meV energy resolution at the Cu *L* edge [1,2], making RIXS an increasingly important tool in materials science. However, to observe lower-energy excitations, even higher energy resolution is desired. Thus, efforts are underway to enhance the resolution of RIXS measurements through different approaches.

At NanoTerasu in Tohoku, Japan, we are currently constructing an ultrahigh energy resolution RIXS facility. This advanced facility consists of a dedicated beamline [3] and a 2D-RIXS spectrometer. Our goal is to achieve a total energy resolution (combined resolution of the beamline and RIXS spectrometer) of sub-10 meV below $h\nu$=1000 eV. To achieve such ultrahigh energy resolution, we employed the $h\nu^2$-concept [4,5] for our RIXS spectrometer, to compensates for the reduced measurement efficiency inherent in enhancing energy resolution.

Figure 1 shows the optical layout of the 2D-RIXS facility. The beamline and the 2D-RIXS spectrometer span ~76 m and ~12 m, respectively, and the RIXS spectrometer is planned to have a 2θ rotation range of 30–150°. The beamline has no exit slit, and vertically energy-dispersed X-ray from the beamline monochromator is directly irradiated onto a sample. The RIXS spectrometer features an imaging mirror that collects scattered X-rays from the sample and images them onto a detector while maintaining the relationship between the vertical position and the incident energy. Simultaneously, the grating in the RIXS spectrometer disperses and focuses the scattered X-rays horizontally onto the detector. Thus, the energies of the incident and scattered X-rays are "two-dimensionally" resolved on the detector, which is why we call "2D-RIXS". By integrating the intensity of the spectra along the incident energy, we can improve measurement efficiency.

In the presentation, we will provide an overview of the optical design of the 2D-RIXS facility and discuss our efficiency improvements.

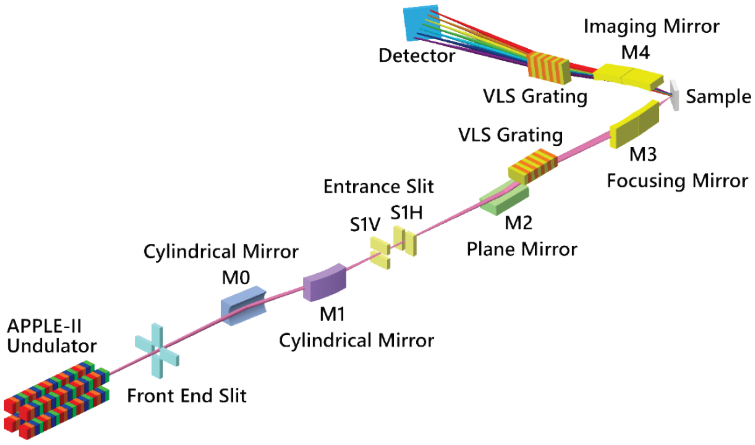

Figure 1: Schematic representation of the optical layout of ultrahigh resolution 2D-RIXS facility at NanoTerasu.

1. N. B. Brookes *et al.*, The beamline ID32 at the ESRF for soft X-ray high energy resolution resonant inelastic X-ray scattering and polarisation dependent X-ray absorption spectroscopy, Nucl. Instrum. Methods A **903**, 175 (2018).
2. K.-J. Zhou *et al.*, I21: an advanced high-resolution resonant inelastic X-ray scattering beamline at Diamond Light Source, J. Synchrotron Rad. **27**, 1235 (2020).
3. J. Miyawaki *et al.*, Design of Ultrahigh Energy Resolution RIXS Beamline at NanoTerasu, J. Phys. Conf. Ser. **2380**, 012030 (2022).
4. V. N. Strocov, Concept of a spectrometer for resonant inelastic X-ray scattering with parallel detection in incoming and outgoing photon energies, J. Synchrotron Rad. **17**, 103 (2010).
5. K.-J. Zhou *et al.*, hv2-concept breaks the photon-count limit of RIXS instrumentation, J. Synchrotron Rad. **27**, 1235 (2020).

Nano-ARPES beamline at NanoTerasu

Koji Horiba*, Takashi Imazono, Hideaki Iwasawa, Kentaro Fujii, Jun Miyawaki, Yoshiyuki Ohtsubo, Miho Kitamura, Kohei Yamamoto, Nobuhito Inami, Takeshi Nakatani, Kento Inaba, Akane Agui, Tomoyuki Takeuchi, Hiroaki Kimura and Masamitu Takahasi

Institute for Advanced Synchrotron Light Source, National Institutes for Quantum Science and Technology, Sendai, Japan

**Contact: horiba.koji@qst.go.jp*

Keywords: angle-resolved photoemission spectroscopy (ARPES), synchrotron radiation beamline

Angle-resolved photoemission spectroscopy (ARPES) is one of the most powerful experimental techniques to directly determine the band structure of a solid surface. Especially, the spatially resolved ARPES is recently attracting much attention because of the importance to resolve local band structures in exotic quantum materials, such as the helical edge states of quantum spin Hall insulators (two-dimensional topological insulators) and hinge states of higher-order topological insulators. In addition, spatially resolved ARPES is useful for studying inhomogeneous samples, hard-to-cleave samples, tiny single crystals, and the samples that contain multiple domains (ferromagnetic, ferroelectric, crystal domains etc.)

In response to the experimental requirements, we are constructing a new beamline for the nano-ARPES experiments as one of the public beamlines in 3-GeV next-generation synchrotron radiation facility “NanoTerasu” [1], which is scheduled to start operation in 2024. Figure 1 shows a 3D overview of the beamline. An APPLE-II type undulator provides brilliant soft X-rays with various polarizations (linear horizontal and vertical, and left and right circular) in the energy range of 50–1,000 eV. A collimated plane grating monochromator is adopted as a soft X-ray monochromator because we can select between the high energy-resolution (HR) mode for HR-ARPES experiments and the low divergence mode for high-flux nano-ARPES measurements. In order to achieve high photon-flux and to ensure a free environment around the sample, this beamline aims to produce the high flux nano-focused beam by using ultrahigh precision reflective mirror optics [2,3], not a Fresnel zone plate used as a focusing optics in the previous nano-ARPES station at other synchrotron facilities [4-6]. After passing the grating, the beam can be switched between the two branches. One branch is used for nano-ARPES experiments with nano-focusing mirror optics, and the other branch with a micro-focusing mirror is provided for use of versatile ARPES experiments with the spot size of a few μm. As post-focusing mirror optics, monolithic Wolter type-I mirrors are designed. In the presentation, we introduce the optical design for this nano-ARPES beamline.

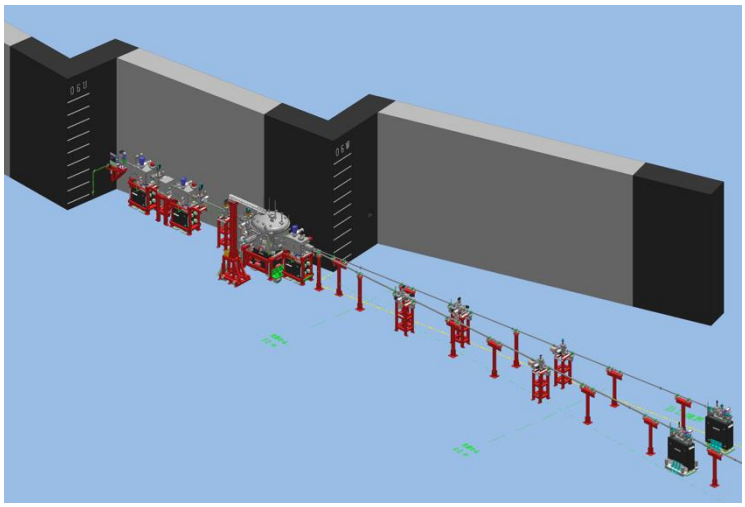

Figure 1: A 3D overview of the beamline.

1. https://www.qst.go.jp/uploaded/attachment/18596.pdf
2. Y. Senba *et al*., J. Synchrotron Rad. **27**, 1103 (2020).
3. S. Egawa *et al*., Opt. Express **27**, 33889 (2019).
4. J. Avila *et al*., J. Phys.: Conf. Ser., **425**, 192023 (2013).
5. E. Rotenberg and A. Bostwick, J. Synchrotron Rad. **21**, 1048 (2014).
6. M. Hoesch *et al*., Rev. Sci. Instrum. **88**, 013106 (2017).

Scanning Transmission X-ray Microscopy Studies of MnO_2 / Zn Ion Battery Electrodes

Haytham Eraky,[1] Chunyang Zhang,[1,2] Adam P. Hitchcock,[1*] Thomas Baker,[2] Alejandra Ibarra Espinoza[2] and Drew Higgins[2]

1 Dept. of Chemistry & Chemical Biology, McMaster University, Hamilton, ON, Canada

*2 Dept. of Chemical Engineering, McMaster University, Hamilton, ON, Canada *Contact: aph@mcmaster.ca*

Keywords: STXM, NEXAFS, ZIBs, α-MnO_2

Zn ion batteries (ZIBs) are an alternative to Li ion batteries (LIBs), with advantages of high operational voltage, low-cost and safe operation. Among different cathode materials, manganese oxides, particularly α-MnO_2, are widely used as positive electrode materials in aqueous rechargeable ZIBs because of their natural abundance, low cost, low toxicity and their relatively high reduction potentials[1]. However, due to the dissolution of the active cathode material into the electrolyte and the formation of irreversible phases, MnO_2-ZIBs are typically limited by capacity fade[2], [3]. Reversible Zn^{2+} intercalation/deintercalation combined with H^+ co-intercalation is considered the main redox mechanisms in MnO_2-ZIBs. Nevertheless, the detailed reaction mechanisms during charging and discharging, and structural stability have not been fully addressed [1], [4]. Understanding how charge is efficiently stored in MnO_2 electrodes or across the electrode/electrolyte interface is the key to develop improved MnO_2-ZIBs electrodes.

STXM provides speciation and high resolution (~30 nm) chemical mapping based on near-edge X-ray absorption fine structure (NEXAFS) contrast. *ex-situ* scanning transmission x-ray microscopy STXM stacks were measured at the Mn L_3, O 1s, Zn $L_{2,3}$ and C K edges on microtomed samples of the MnO_2 electrode of a MnO_2/Zn ZIB. The Mn L_3 and O 1s results from a 100-ctycle, discharged ZIB (**Fig. 1a, 1b**) demonstrate that MnO_2 is reduced to both Mn(III) and Mn(II) oxidation states through a reversible $Mn^{4+} \leftrightarrow Mn^{3+}/Mn^{2+}$ redox reaction. Some areas remain as MnO_2(IV), which is attributed to the redeposition of dissolved Mn species. On the other hand, Zn $L_{2,3}$ measurements showed signal in all electrode areas with 2-3 times larger amounts of Zn in the Mn(II)/Mn(III) area, than in the Mn(IV) area. This is consistent with formation of a $ZnMn_2O_4$ (Mn(III)) intermediate (**Fig.1c**). Measurements of the as-made battery, after 1 discharge and 1 charge cycle, and after 50 % capacity reduction in both charge and discharge states, will be reported. These studies are helping better understand the redox and physico-chemical processes that take place at the surface or in the bulk of α-MnO_2 ZIB electrodes

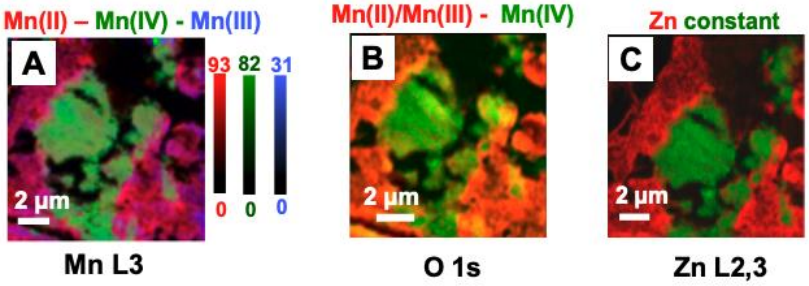

Fig 1. Quantitative chemical maps of Mn, O and Zn in a microtome sample after 100 charge discharge cycles derived from STXM stacks measured at A) Mn L_3, B) O 1s and C) Zn $L_{2,3}$ edges.

1. Tran, T.N.T., et al., *Reaction mechanisms for electrolytic manganese dioxide in rechargeable aqueous zinc-ion batteries.* Scientific Reports, 2021. **11**(1): p. 20777.
2. Rubel, O., et al., *Electrochemical stability of ZnMn2O4: Understanding Zn-ion rechargeable battery capacity and degradation.* The Journal of Physical Chemistry C, 2022. **126**(27): p. 10957-10967.
3. Alfaruqi, M.H., et al., *Structural transformation and electrochemical study of layered MnO2 in rechargeable aqueous zinc-ion battery.* Electrochimica Acta, 2018. **276**: p. 1-11.
4. Zhao, Q., et al., *Unravelling H+/Zn2+ synergistic intercalation in a novel phase of manganese oxide for high‐performance aqueous rechargeable battery.* Small, 2019. **15**(47): p. 1904545.

Scanning transmission soft X-ray spectromicroscopy of mouse liver and kidney

Tuomas Mansikkala[1,2,*], Takuji Ohigashi[3], Miia H. Salo[2,4], Anniina E. Hiltunen[4], Reetta Vuolteenaho[2], Petra Sipilä[5], Satu Kuure[6,7], Marko Huttula[1], Johanna Uusimaa[4,8], Reetta Hinttala[2,4], Ilkka Miinalainen[2], Salla Kangas[4], Minna Patanen[1,2]

1 Nano and Molecular Systems Research Unit, PO Box 3000, 90014 University of Oulu, Finland

2 Biocenter Oulu, PO Box 5000, 90014 University of Oulu, Finland

3 UVSOR Synchrotron Facility, Institute for Molecular Science, Okazaki 444-8585, Japan

4 Research Unit of Clinical Medicine and Medical Research Center, Oulu University Hospital and University of Oulu, 90014 Oulu, Finland

5 Research Centre for Integrative Physiology and Pharmacology, and Turku Center for Disease Modeling, Institute of Biomedicine, University of Turku, Turku, Finland

6 Stem Cells and Metabolism Research, Program, Faculty of Medicine, University of Helsinki, Helsinki, Finland

7 GM-Unit, Laboratory Animal Center, Helsinki Institute of Life Science, University of Helsinki, Helsinki, Finland

8 Clinic for Children and Adolescents, Oulu University Hospital, 90029 Oulu, Finland

**Contact: leo.mansikkala@oulu.fi*

Keywords: Scanning transmission X-ray microscopy, spectromicroscopy, biological specimen

Scanning transmission X-ray microscopy (STXM) is well suited to study ultrastructural features of biological specimens. Using soft X-rays we can probe the carbon, oxygen and nitrogen 1s edges. At core absorption edges the image contrast can vary drastically across the edge as different functional groups present in the tissues have differing X-ray absorption cross-sections. This allows the use of STXM to study label-free soft tissues.

Here we present a STXM imaging study of mouse kidney and liver tissue [1]. Our main focus was on ultrastructural abnormalities in genetically modified *Slc17a5* mice. *Slc17a5* modified mice were used because of our interest in studying lysosomal storage diseases from Finnish disease heritage. Salla disease is a lysosomal storage disease where the variant in *SLC17A5* gene causes the accumulation of sialic acid within lysosomes. [2] The genetically modified mice had large number of vacuolar structures in both kidney and liver tissues compared to their healthy wild type counterparts. The samples used were resin embedded thin sections of the mouse tissues and we were able to image them without using any staining agents. The best contrast was obtained at carbon 1s edge, clearly separating chromatin, the vacuoles and protein rich areas. We also compared the X-ray absorption spectra measured from different parts of the tissue samples. The spectrum inside the vacuoles resembled the pure embedding resin spectra and so did the spectrum measured from cytoplasm although in lesser extent. Spectra from chromatin and protein rich areas like nucleus and red blood cells, respectively, differed more. The best contrast for overall structural overview was obtained at energies around 287 eV or above the absorption edge, whereas energies around 288 eV emphasized protein rich regions and provided best contrast compared to the embedding material.

We concluded that the resin embedding process allows us to image the ultrastructural abnormalities, but it does not completely preserve the material within the vacuoles. The level of substitution for the resin seemed to differ between different cell structures.

1. T. Mansikkala et al. Scanning transmission soft X-ray spectromicroscopy of mouse liver and kidney, submitted to *J. Electr. Spectr. Rel. Phenom*.
2. R. Norio, The Finnish disease heritage III: The individual diseases, *Hum Genet* **112**, 470–526 (2003).

Electron transfer path in Ni-Ag-MoS_2 photocatalyst

Ekta Rani[1], V. K. Gupta[2], Md Thasfiquzzaman[1], P. Talebi[1], A. Martinelli[2], Y. Niu[3], A. Zakharov[3], M. Huttula[1], M. Patanen[1], H. Singh[1], W. Cao[1]

1 Nano and Molecular Systems Research Unit, Faculty of Science, University of Oulu FIN-90014, Finland
2 Department of Chemistry and Chemical Engineering, Chalmers University of Technology, 412 96 Gothenburg, Sweden
3 MAX IV Laboratory, Lund University, Lund 22484, Sweden

**Contact: Ekta.Rani@oulu.fi*

Keywords: Ni-Ag-MoS_2, Raman mapping, X-PEEM, interfacial interaction, photocatalyst

Photocatalysts, which are considered one of the most promising catalytic media for producing hydrogen (H_2), are essential for developing sustainable energy sources that can mitigate the impact of imminent climate change while supporting economic growth [1]. Despite the increasing catalytic response observed in 2D heterostructures through interface engineering, the fundamental understanding of interface interactions in heterostructures remains elusive. In this work, spectro-microscopic X-PEEM [2] and Raman mapping [3] were effectively used to probe the Ni-Ag-MoS_2 heterostructure, where Ni-MoS_2 interaction was evidenced using synchrotron X-PEEM, while Raman mapping was used to probe the Ag-MoS_2 interface (Figure 1). The substantial improvement in H_2 yield in the Ni-Ag-MoS_2 heterostructure (~55 µmol h^{-1} g^{-1}) compared to pristine MoS_2 and binary Ag-MoS_2 heterostructures provided evidence of successful bonding between Ni, Ag, and MoS_2. The observed small peak at the photon energy of 861 eV in XPEEM suggests a low charge transfer between the Ni NPs and the flat MoS_2 basal plane beneath and the protruding layer. The observed competition between the downshift of the MoS_2' E_{2g}^1 and A_{1g} modes due to charge carrier injection and upshift due to compressive strain during reverse laser power experiment is assigned to the non-uniform growth of Ag nanoparticles, their intimate contact with MoS_2, and Ag intercalated layered MoS_2. As per the band alignment scheme when Ni NPs and MoS_2 are joined by Ag NPs, free electrons will transfer from Ni to MoS_2 via Ag due to the work function difference. This leads to the accumulation of electrons next to the valence band of MoS_2 adjacent to the interface region and the decrease of contact resistance which is contributing to the observed higher H_2 yield by MAN. The Fermi levels of the Ni, MoS_2, and the interface region will be aligned after thermodynamic equilibrium, resulting in the band bending of MoS_2. The photoexcited electrons from the MoS_2 can thus move easily from the valence band of MoS_2 to the metal side and reduce the H^+ to $H^\cdot$.

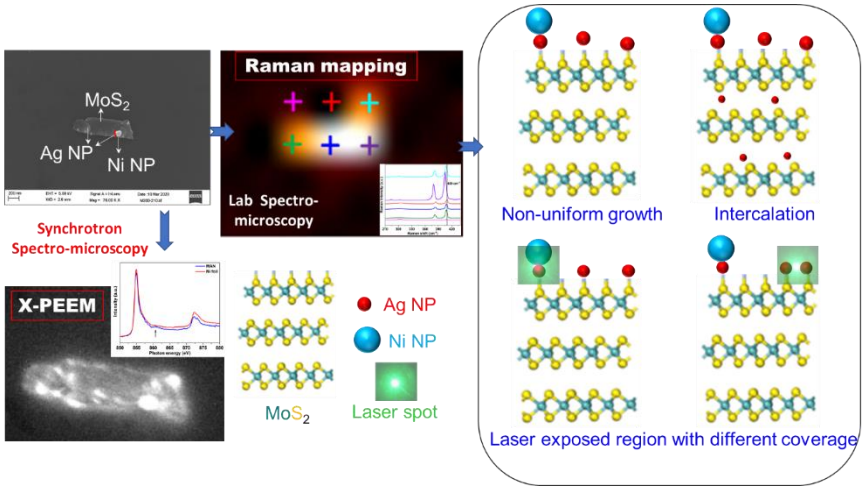

Figure 1: Schematic representation of spectro-microscopy mapping studies of Ni-Ag-MoS_2 [4].

1. X. Yang, D.Wang, Photocatalysis: From Fundamental Principles to Materials and Applications, *ACS Appl. Energy Mater.* **12**, 6657–6693 (2018).
2. X. Shi, S. Posysaev, M. Huttula, V. Pankratov, J. Hoszowska, J.C. Dousse, F. Zeeshan, Y. Niu, A. Zakharov, T. Li, O. Miroshnichenko, M. Zhang, X. Wang, Z. Huang, S. Saukko, D.L. González, S. van Dijken, M. Alatalo, W. Cao, Metallic contact between MoS_2 and Ni via Au nanoglue, *Small* **14**, 1–10 (2018).
3. E. Rani, A.A. Ingale, A. Chaturvedi, C. Kamal, D.M. Phase, M.P. Joshi, A. Chakrabarti, A. Banerjee, L.M. Kukreja, Correlation of size and oxygen bonding at the interface of Si nanocrystal in Si-SiO_2 nanocomposite: a Raman mapping study, *J. Raman Spectrosc.* **47**, 457–467 (2016).
4. E. Rani, V. K. Gupta, Md Thasfiquzzaman, P. Talebi, A. Martinelli, Y. Niu, A. Zakharov, M. Huttula, M. Patanen, H. Singh, W. Cao, Unraveling compensation between electron transfer and strain in Ni-Ag-MoS_2 photocatalyst, *J. of Catalysis* **414**, 199-208 (2022).

Analysis of Ni chemical environments in MoS_2-Ag-Ni ternary systems via spectromicroscopy

Parisa Talebi[1, *], Ekta Rani [1], Yuran Niu [2], Alexei Zakharov [2], and Wei Cao[1]

1 Nano and Molecular Systems Research Unit, Faculty of Science, University of Oulu, Oulu, Finland
2 MAX IV Laboratory, Lund University, Lund 22484, Sweden
**Contact: parisa.talebi@oulu.fi*

Keywords: MoS_2-Ag-Ni ternary system, X-PEEM, L-edge x-ray absorption, electronic structure

One approach to improve the functionalities of bulk MoS_2 (a well-known photocatalyst) is designing MoS_2-based structures. On the other hand, Nickel (Ni) as an essential element, has been taken on an attractive prospect, because of the structural stability, facile preparation of Ni-based structure, and high performance of its metallic and compositional forms in photocatalysis.[1] Although the Ni-MoS_2 composites have been constructed by using noble metals as nano-glues,[2] the effects of the Ni sizes on the electronic properties of the heterostructures remain elusive. Thanks to photoemission electron spectroscopy (PEEM)'s spectromicroscopic feature, the interfacial contact between the layered semiconductor and heterogenous sites can be studied. This is very important, especially to the determination of the chemical states of transition metals at the nanoscale. In this work, MoS_2-Ag-Ni ternary systems with two varying Ni particle sizes were prepared and the electronic structures of the Ni at microregions were spectromicroscopically determined, combining the x-ray absorption spectroscopy (XAS) near Ni L-edges and the imaging capability of the X-PEEM.[3] As shown in fig. 1(a and b), the general x-ray absorption shape in the MAN systems displays that the main structures are associated with the Ni $2p_{3/2}$ and the $2p_{1/2}$ spin-orbit splitting of ~ 17.3 eV. By more detailed analysis of the XAS spectra of MAN70 noticed that Ni in MAN70 is more in the Ni^{2+} state as a result of surface oxidization. No obvious charge transfer between S and Ni was observed spectroscopically in either of the systems. The Ni XPS data (fig. 1c), also shows the native Ni^{2+} component on top of Ni nanoparticle. Based on the X-PEEM determinations, possible electron migration channels within the system are attributed to the Ag buffer layer between the metal and layered semiconductor.

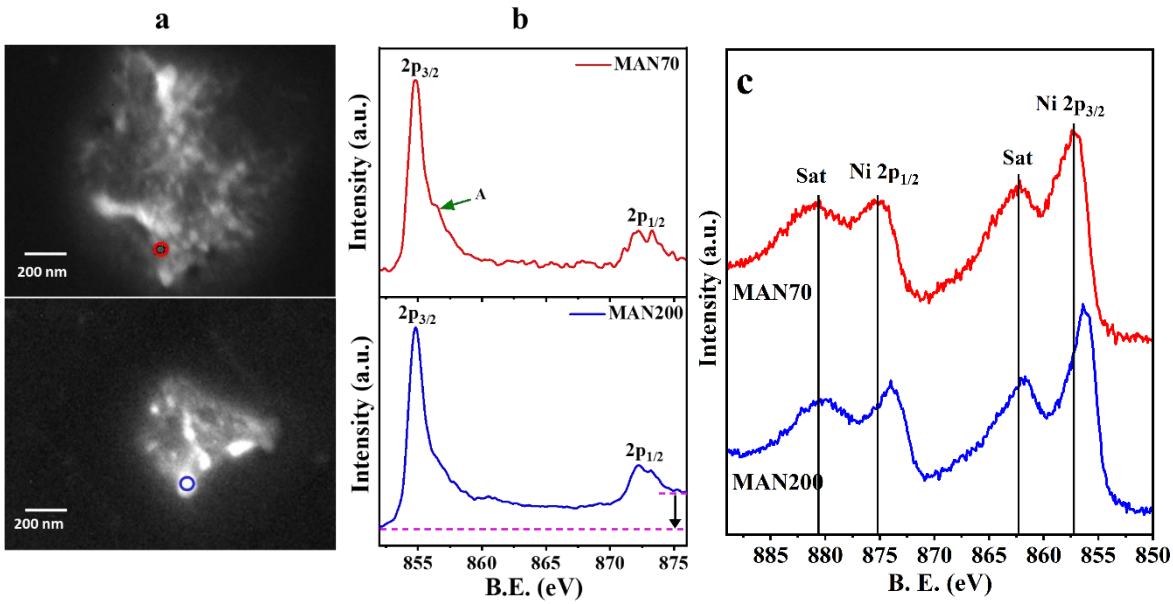

Figure 1: (a) X-PEEM images (b) XAS spectra and (c) XPS of MAN70 and MAN200.

1. Shen, Rongchen, et al. "Ni-based photocatalytic H_2-production cocatalysts2." Chinese Journal of Catalysis 40.3 (2019): 240-288.

2. Shi, Xinying, et al. "Nickel nanoparticle-activated MoS_2 for efficient visible light photocatalytic hydrogen evolution." Nanoscale 14.24 (2022): 8601-8610.

3. Talebi, Parisa, et al. "Spectromicroscopic determinations of chemical environments of Ni in MoS_2-Ag-Ni ternary systems." X-Ray Spectrometry 52.1 (2023): 38-45.

Formation of hydrated magnesium carbonate cement from brucite: A synchrotron radiation based STXM study

Md Thasfiquzzaman[1], Hoang Nguyen[2], Tuomas Mansikkala[1], Karina Thanell[3], Jörg Schwenke[3], Igor Beinik[3], Adam P. Hitchcock[4], Päivö Kinnunen[2] and Minna Patanen[1]

[1]*Nano and Molecular Research Unit, University of Oulu, Oulu, Finland*

[2]*Fibre and Particle Engineering Research Unit, University of Oulu, Oulu, Finland*

[3]*Softimax Beamline, MAX IV Laboratory, Lund University, Lund, Sweden*

[4]*Department of Chemistry, McMaster University, Hamilton, Canada*

**Contact: md.thasfiquzzaman@oulu.fi*

Keywords: Hydrated magnesium carbonate, brucite, Scanning transmission X-ray microscopy (STXM)

Cement industry has a major effect on climate, contributing 5-8 % [1] of total anthropogenic CO_2 emissions in the earth. Alternative to traditional Portland cement are therefore needed to reduce CO_2 emissions globally. Hydrated magnesium carbonate (HMC) cements may contribute significantly to this issue due to their carbon capturing ability during the hardening of cement binders [2]. Formation of HMC from magnesium hydroxides is one of the promising ways of CO_2 sequestration. In this work, HMC is formed during the reaction of $Mg(OH)_2$ (brucite) with $NaHCO_3$ in water. Mg-acetate ligands [3], are known to improve the reaction by increasing the dissolution of brucite and assisting the HMC precipitation. Also, the addition of ligand significantly affects the chemical and structural properties of HMC precipitates. The utilization of structural and advanced characterizing tool like synchrotron radiation-based scanning transmission X-ray microscopy (STXM) imaging [4] performed at MAX IV synchrotron facility helps us to get an idea about the formation and conversion of different HMC phases at different time intervals. This high brilliance X-ray radiation technique allow to obtain high-resolution chemical information from the sample bulk by raster-scanning a finely focused and monochromatized photon beam over the sample. A combination of STXM mapping and corresponding spectrum analysis differentiated HMC phase from the raw materials brucite as shown in Fig. 1. We demonstrate here that owing to simultaneous spectroscopic and microscopic observation with STXM, different HMC phases can be resolved, and their interconnections studied, making STXM a powerful tool for studies of cementitious materials.

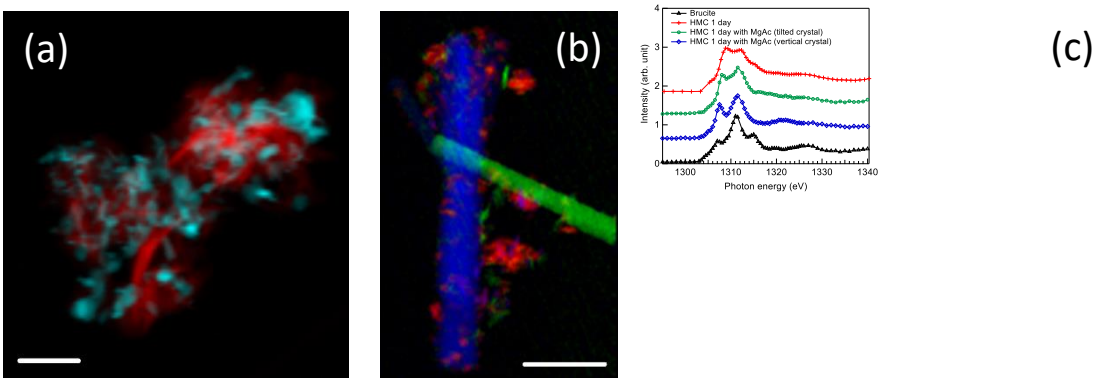

Figure 1: (a) Color composition map showing HMC precipitates (red color) formed after 1 day of reaction in water and unreacted brucite (light blue color). Scale bar 2 µm. (b) Color composition map showing HMC precipitates (blue and green colors) formed after 1 day of reaction in water with Mg-acetate and unreacted brucite (red color) as well. Scale bar 5 µm. (c) Extracted XAS spectra of HMC region from a) and HMC crystals and brucite regions from b).

References:

1. R. M. Andrew, Global CO_2 emissions from cement production, *Earth System Science Data.* **10**, 195-217 (2018).
2. H. Nguyen, H. Santos, H. Sreenivasan, W. Kunther, V. Carvelli, M. Illikainen, P. Kinnunen, On the carbonation of brucite: Effects of Mg-acetate on the precipitation of hydrated magnesium carbonates in aqueous environment, *Cement and Concrete Research.* **153**, 106696 (2022).
3. N. Dung, C. Unluer, Carbonated MgO concrete with improved performance: The influence of temperature and hydration agent on hydration, carbonation, and strength gain, *Cement and Concrete Composites.* **82,** 152–164 (2017).
4. A. P. Hitchcock, Soft X-ray spectromicroscopy and ptychography, *Journal of Electron Spectroscopy and Related Phenomena.* **200**, 49–63 (2015).

Local atomic structure analysis of F-doped layered perovskite $NaYTiO_4$ by photoelectron holography

Zexu Sun[1], Hirofumi Akamatsu[2], Koji Fujita[3], Hiroto Tomita[1], Takashi Tadamura[1], Takuya Moriki[1], Aoi Miyanishi[2], Yusuke Hashimoto[1] and Tomohito Matsushita[1]

1 Nara Institute of Science and Technology, Japan
2 Kyushu University, Japan
3 Kyoto University, Japan
**Contact: sun.zexu.rv3@ms.naist.jp*

Keywords: Perovskites, $NaYTiO_4$, fluorine dopant, photoelectron holography, atomic structure

Layered perovskites can have a number of interesting electronic properties such as piezoelectricity and ferro-electricity. In the layered perovskite $NaYTiO_4$[1], piezoelectricity is induced by the oxygen octahedral rotation and deformation. Figure 1 shows the structure of $NaYTiO_4$. As shown in the figure, there are three types of oxygen located in the Ti-O layer, Na-O layer, and Y-O layer. Researchers attempt to control the rotation of the oxygen octahedra by introducing fluorine. The change of atomic structure required to be measured. Especially local structure of fluorine dopant is important. To measure the local structure around the fluorine, we measured photoelectron holograms of two samples, $NaYTiO_4$ and $NaYTiO_{4-x}F_{2x}$. The experiment was performed at BL25SU in SPring-8, Japan, using retarding field analyzer. Figures 1(b) and (c) show holograms of Na 2s of $NaYTiO_4$ and $NaYTiO_{4-x}F_{2x}$, respectively. Red, yellow, green blue circles in the figure indicate the positions of O, Na, Y, and Ti atoms viewing from the Na atom (photoelectron emitter). Because of the forward focusing effect, bright regions in the hologram are almost located at the circles. Comparing (b) and (c), The forward focusing peak of oxygens indicated by the red arrow in Fig. 1 (b) disappears in Fig. 1(c). This implies that the oxygen atoms strongly fluctuate. We will report the analysis of the holograms of F, O, Y, and Ti to discuss the modification of the local atomic structure.

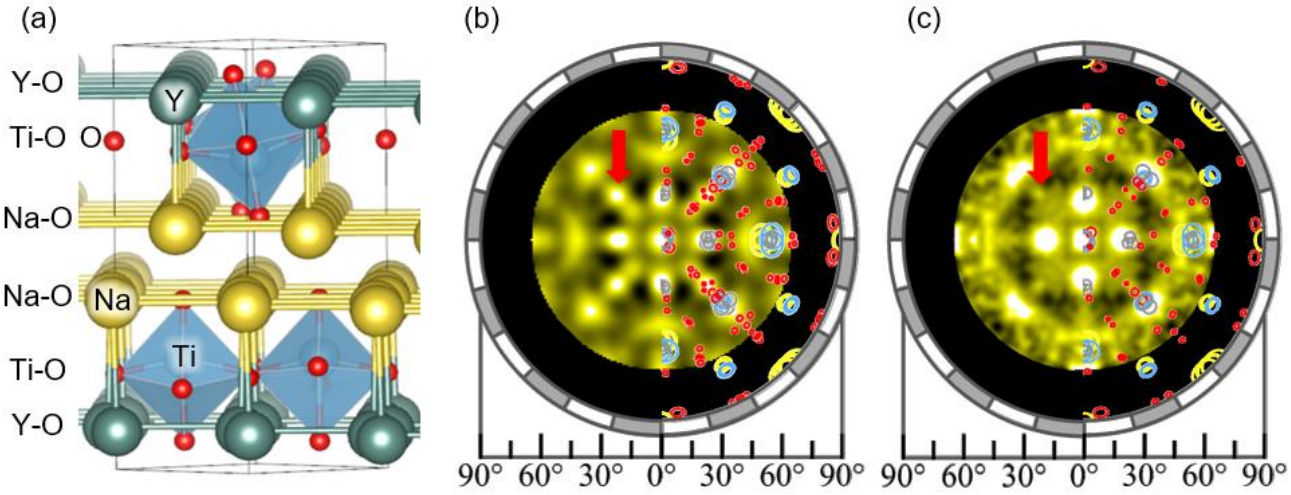

Figure 1 (a) Atomic structure of $NaYTiO_4$. (b) and (c) are Na 2s holograms of two samples, $NaYTiO_4$ and $NaYTiO_{4-x}F_{2x}$. The kinetic energy of photoelectrons is 700eV.

1. Akamatsu et al. Phys. Rev. Lett. 112,187602 (2014).

Theoretical description of X-ray experiments on magnetic materials exposed to an electric field

H. Ebert[1], A. Marmodoro[1,2], and S. Mankovskyy[1]

1 Department of Chemistry, Ludwig-Maximilians-University, Munich, Germany

2 FZU – Institute of Physics of the Czech Academy of Sciences, Prague, Czech Republic

**Contact: Hubert.Ebert@cup.uni-muenchen.de*

Keywords: magnetic X-ray dichroism, magnetic materials, electric field

Representing the electronic structure of an investigated material in terms of its electronic Green function is a well established and flexible starting point to calculate its X-ray absorption (XAS) and optical spectra [1]. With very few exceptions, this scheme was used so far only to deal with materials in their equilibrium ground state. We present extensions of this scheme that allow to account for the impact of an external electric field on the XAS of magnetic materials with a focus on the X-ray magnetic circular dichroism (XMCD).

Our computational scheme is based on the spin-polarized relativistic multiple scattering or Korringa-Kohn-Rostoker Green function (SPR-KKR-GF) method applied within the framework of spin density functional theory (SDFT). This approach allows in particular electronic structure calculations for the ground state of layered systems including surface layer systems without the use of super cells. Recent experimental XMCD investigations on the magnetism of Pt overlayers deposited on ferromagnetically ordered Co films demonstrated the possibility of controlling the induced magnetic moment in Pt by applying an external electric field applied perpendicular to the surface [2]. As in this case the electric field does not give rise to electric currents the quasi-static situation can be described by conventional electronic structure calculations that explicitly account for the electric field within the SCF cycle. This is demonstrated by results for the electronic and magnetic properties of Pt layers in Co/Pt thin surface film structures on a Pd(001) substrate [3]. Due to the Co underlayer, the surface Pt layers have induced moments that are modified by the external electric field. The field-induced changes can be explained by the modified spin-dependent orbital hybridization that varies non-linearly with the field strength. We calculate the x-ray absorption and the x-ray magnetic circular dichroism spectra for an applied external electric field and examine its impact on the spectra in the Pt layer around the L_2- and L_3-edges. We also determine the layer-dependent magneto-crystalline anisotropy, and show that the anisotropy can be tuned easily in the different layers by the external electric field.

The conventional KKR-GF approach has been extended by various authors to the steady-state out-of-equilibrium situation described by a corresponding energy dependent non-equilibrium Green function (NEGF) [4]. The NEGF has been used so far primarily to deal with transport properties. Here we demonstrate its use for the investigation of spectroscopic properties by calculating the electric field induced changes in the XAS- and XMCD-spectra of the Pd $L_{2,3}$-edges in a Co/Pd bilayer system [5]. In this case the electric field oriented perpendicular to the interface gives rise to electric and spin currents. Recent x-ray absorption experiments demonstrated the possibility to accurately monitor the magnetism in such a situation [6]. Using the first-principles NEGF scheme, we show how the measured magnetic dichroic signal for the corresponding steady-state situation can be related to the underlying electronic structure and its response to the external stimulus. Another interesting XMCD investigation on the magnetic properties of surface films use an electric field applied parallel to the surface giving rise to corresponding spin and orbital currents [7]. As this geometry implies only one-dimensional periodicity for the system we suggest a bi-linear response description that accounts simultaneously for the applied static electric field and the radiation field due to the X-rays via an appropriately extended Kubo response formalism.

1. H. Ebert, *Rep. Prog. Phys.,* **59**, 1665 (1996).
2. K. T. Yamada, *et al.*, *Phys. Rev. Lett.* **120**, 157203 (2018).
3. E. Simon, A. Marmodoro, S. Mankovsky, and H. Ebert, *Phys. Rev. B* **103**, 064406 (2021).
4. S. Achilles, *et al.*, *Phys. Rev. B* **88**, 125411 (2013); M. Ogura, H. Akai, *J. Phys. Soc. Japan* **85**, 104715 (2016).
5. R. Kukreja, *et al.*, *Phys. Rev. Letters* **115**, 096601 (2015).
6. A. Marmodoro, S. Wimmer, O. Šipr, M. Ogura, and H. Ebert, *Phys. Rev. Research,* **2**, 032067 (2020).
7. C. Stamm, *et al.*, *Phys. Rev. B* **100***,* 024426 (2019).

Interface electronic structure and anomalous magnetotransport properties of $SrIrO_3$ (111) superlattices

Ji Soo Lim[1], *Merit Spring*[1], *Martin Kamp*[1], *Louis Veyrat*[1,2], *Axel Lubk*[2], *Bernd Büchner*[2], *Michael Sing*[1], *and Ralph Claessen*[1]

1. *Physikalisches Institut and Würzburg-Dresden Cluster of Excellence ct.qmat, Universität Würzburg, Germany*
2. *Leibniz Institute for Solid State and Materials Research and Würzburg-Dresden Cluster of Excellence ct.qmat, Germany*

**Contact: ji-soo.lim@physik.uni-wuerzburg.de*

Keywords: *Spin-orbit coupling, iridates, anomalous Hall effect, face- and corner-sharing octahedra*

In 5d iridates spin-orbit coupling (0.3~0.4 eV) and short-range electron-electron interactions (~0.5 eV) are of similar magnitude, which gives rise to J_{eff}=1/2 states at the chemical potential [1] that are susceptible to Mott physics. Hence, iridates are an interesting playground for realizing novel superconductors and topological phases [2, 3, 4]. Specifically, $SrIrO_3$ (001) films have been reported to show a dimensionality-controlled metal-insulator transition at a critical thickness of 4 unit cells. Monolayer $SrIrO_3$ (001) exhibits a band structure similar to that of Sr_2IrO_4, which has been suggested to be a parent material for unconventional superconductivity [5]. Furthermore, $SrIrO_3$ films with (111) orientation have been predicted to realize a topological crystalline insulator [6].

Here we report on the epitaxial growth of $SrIrO_3$ films on $SrTiO_3$ (111) substrates that display a twinned perovskite-like superstructure with a periodicity of 3 unit cells and the observation of unusual magnetotransport properties including magnetoresistance and anomalous Hall effect. In the transmission electron microscopy (TEM) image of Fig 1b, the interfaces between the 3uc thick stacks are formed by face-sharing octahedra with a larger Ir-Ir lattice spacing than within the stacks where the octahedra share corners. The valence band from X-ray photoelectron spectroscopy (XPS) shows a different band splitting of the e_g^{π} and a_{1g} states in comparison to $SrIrO_3$ (001) films, which correspondingly is ascribed to the face-sharing octahedra within the interfaces (Fig. 1a) [7]. Corroborated by density-functional theory calculations, the modified electronic structure at the interfaces likely gives rise to ferromagnetic moments which cause a sign change of the magnetoresistance from positive to negative and the emergence of hysteresis loops in the anomalous Hall effect at about 10 K. These are unexpected results because bulk $SrIrO_3$, exhibiting a monoclinic structure with a similar atomic arrangement, is known to be paramagnetic.

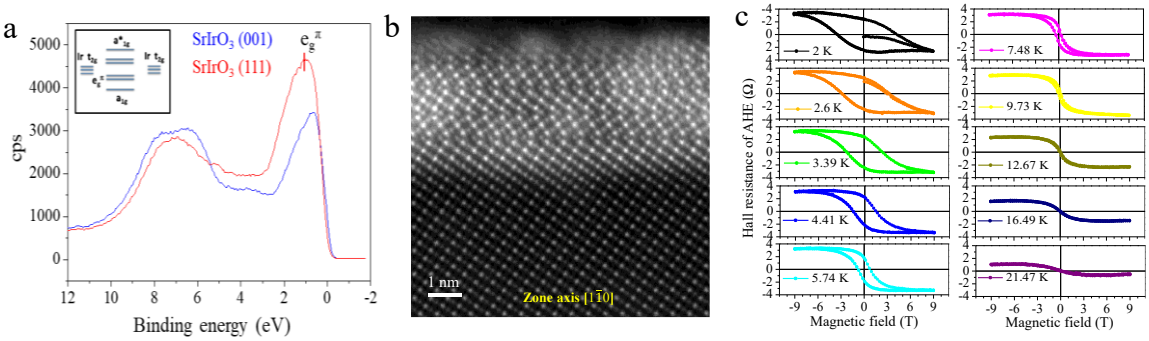

Figure 1: **a**. Valence band from XPS of $SrIrO_3$ (001) and (111) films. Inset is band splitting of face-sharing octahedral [7]. b. TEM image of a $SrIrO_3$ (111) film on a $SrTiO_3$ (111) substrate along the zone axis [1 -1 0] **c**. Anomalous Hall effect at low temperatures. Below 10 K, the magnitude of the anomalous Hall effect saturates and hysteresis loops are observed.

1. G. Jackeli and G. Khaliullin, *Phys. Rev. Lett.* **102**, 017205 (2009).
2. Y. K. Kim, *Science* **345**, 187 (2014).
3. S. J. Moon et al., *Phys. Rev. Lett.* **101**, 226402 (2008).
4. Z. Tian et al., *Nat. Phys.* **12**, 134 (2016).
5. P. Schütz et al. *Phys. Rev. Lett.* **119**, 256404 (2017).
6. P. M. Gunnink, R. L. Bouwmeester and A. Brinkman, *J. Phys: Condens. Matter* **33,** 085601 (2021).
7. S. V. Streltsov, G. Cao and D. I. Khomskii, *Phys. Rev. B* **96**, 014434 (2017).

Geometry-Induced Spin Filtering in Spin-ARPES Maps from WTe_2

Tristan Heider[1], Gustav Bihlmayer[2], Jakub Schusser[3,4], Friedrich Reinert[4], Jan Minár[3], Stefan Blügel[2], Claus M. Schneider[1], and Lukasz Plucinski[1,*]

1 Peter Grünberg Institut (PGI-6), FZ Jülich GmbH, 52428 Jülich, Germany

2 Peter Grünberg Institut (PGI-1), FZ Jülich and JARA,52428 Jülich, Germany

4 New Technologies-Research Center, University of West Bohemia, 30614 Pilsen, Czech Republic

5 Exp. Physik VII and Würzburg-Dresden Cluster of Excellence ct.qmat, Univ. Würzburg, 97070 Würzburg, Germany

**Contact: l.plucinski@fz-juelich.de*

Keywords: angle-resolved photoelectron spectroscopy (ARPES), spin-polarized ARPES

We demonstrate that an important quantum material WTe_2 exhibits a new type of geometry-induced spin-filtering effect in photoemission [1], stemming from low symmetry that is responsible for its exotic transport properties. Through the laser-driven spin-polarized angle-resolved photoemission (spin-ARPES) Fermi surface mapping, we showcase highly asymmetric spin textures of electrons photoemitted from the surface states of WTe_2. Such asymmetries are not present in the initial state spin textures, which are bound by the time-reversal and crystal lattice mirror plane symmetries. The findings are reproduced qualitatively by theoretical modeling within the one-step model photoemission formalism. The effect could be understood within the free-electron final state model as an interference due to emission from different atomic sites and is a manifestation of time-reversal symmetry breaking by the photoemission process. As such, it cannot be eliminated, but only its magnitude influenced, by special experimental geometries.

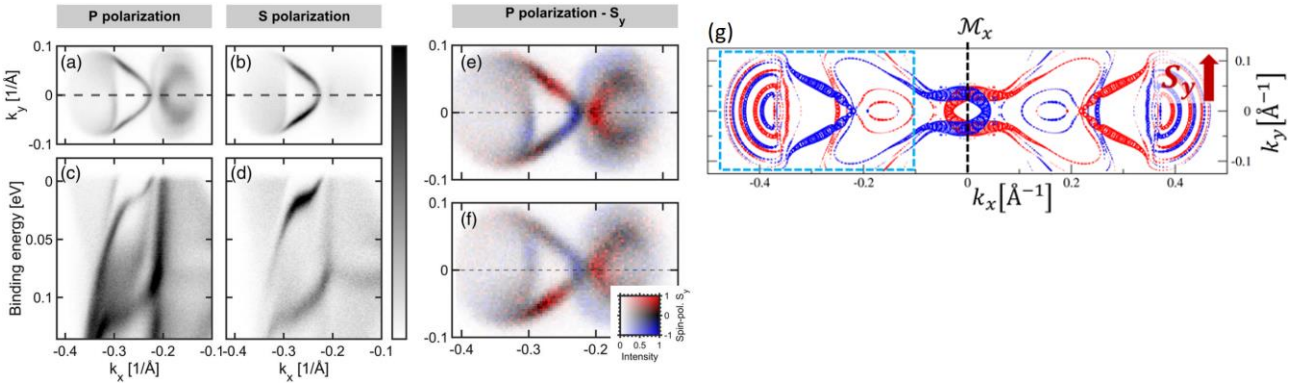

Figure 1: (a),(b) Spin-integrated laser-ARPES ($h\nu = 6$ eV) Fermi surface maps measured with *p*- and *s*-polarized light. (c-d) Corresponding energy dispersions $E(k_x)$ for $k_y = 0$ as indicated by the dashed lines in (a) and (b). (e-f) Experimental laser-spin-ARPES 57 × 89 pixel Fermi surface maps taken at two nearby spots on the same cleave using the FOCUS Ferrum spin-detector and MBS A-1 spectrometer with scanning lens. (g) DFT-LAPW surface spin texture.

WTe_2 is a low symmetry material, with polar surfaces typically denoted as a *top* and a *bottom* surface [2]. Figure 1 (a-d) presents ARPES maps from cleaved WTe_2 single crystals taken with *p*- and *s*-polarized light using cw 6 eV laser. Fig. 1(e-f) shows corresponding spin-ARPES maps taken on two different spots on the *bottom* surface corresponding to two different terrace terminations. Each of the two maps is highly asymmetric, unlike the initial state spin texture, Fig. 1(g). The adjacent terraces are connected by the M_y mirror operation (with additional in-plane sliding) which explains the relation between the two images. We will discuss a microscopic inter-site interference model, which explains the origin of the asymmetric spin-textures, and allows to predict in which cases similar effect will be present. Together with another type of inter-orbital interference [3], these phenomena provide a path to connect the initial and spin-ARPES spin-textures in an effort to provide experimental input for understanding transport properties in novel quantum materials.

1. T. Heider, G. Bihlmayer, J. Schusser, F. Reinert, J. Minár, S.Blügel, C. M. Schneider, and L. Plucinski, Geometry-induced spin-filtering in photoemission maps from WTe2 surface states, Phys. Rev. Lett. 130, 146401 (2023), https://doi.org/10.1103/PhysRevLett.130.146401
2. F. Y. Bruno, A. Tamai, Q. S. Wu, I. Cucchi, C. Barreteau, A. de la Torre, S. McKeown Walker, S. Riccò, Z. Wang, T. K. Kim, M. Hoesch, M. Shi, N. C. Plumb, E. Giannini, A. A. Soluyanov, and F. Baumberger, Observation of large topologically trivial Fermi arcs in the candidate type-II Weyl semimetal WTe2, Phys. Rev. B 94, 121112(R) (2016), https://doi.org/10.1103/PhysRevB.94.121112
3. K. Yaji, K. Kuroda, S. Toyohisa, A. Harasawa, Y. Ishida, S.Watanabe, C. Chen, K. Kobayashi, F. Komori, and S. Shin, Spin-dependent quantum interference in photoemission process from spin-orbit coupled states, Nat. Commun. 8, 14588 (2017), https://doi.org/10.1038/ncomms14588

Rashba-split image-potential state

Fabian Schöttke[1,*], Sven Schemmelmann[1], Peter Krüger[2], and Markus Donath[1]
1 Physikalisches Institut, Universität Münster, Germany
2 Institut für Festkörpertheorie, Universität Münster, Germany
[*]Contact: fabian.schoettke@uni-muenster.de

Keywords: Rashba effect, image-potential state, spin-resolved inverse photoemission

The long-range Coulomb-like surface-barrier potential at the surface of conductive materials gives rise to image-potential-induced surface states. Figure 1(a) illustrates how they form a Rydberg-like series of states outside the surface but with a finite overlap with bulk states. Therefore, image-potential states are a sensitive probe for surface properties [1]. In particular, the influence of spin-dependent interactions, exchange and spin-orbit, on these states is a topic of ongoing debate in literature.
Exchange interaction in ferromagnets causes exchange splittings in image-potential states [1]. The detected size of the exchange splitting is about a factor of ten smaller than the splitting of the magnetic bands due to the small probability density inside the material. Spin-orbit-induced Rashba-type spin splittings for image-

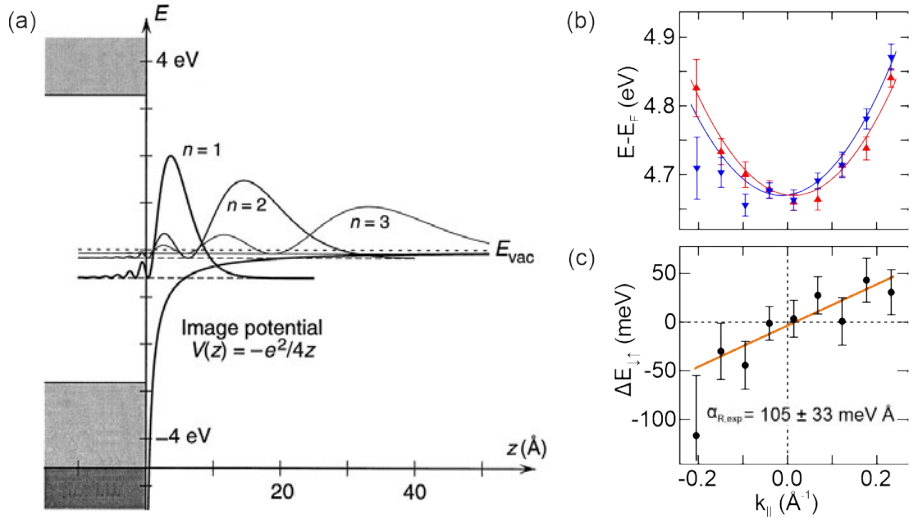

Figure 1: (a) Probability density of image-potential states (adapted from [2]). (b) Spin-resolved $E(\mathbf{k}_{||})$ dispersion of the Re(0001) image-potential state and (c) the corresponding energy splitting $\Delta E_{\downarrow\uparrow}(\mathbf{k}_{||})$ (from [5]).

potential states are predicted for surfaces of heavy elements [3]. Again, the expected size is about one order of magnitude smaller than typical Rashba splittings in crystal-induced surface states. First experimental attempts to prove this were carried out via circular dichroism two-photon photoemission. However, the results of these *indirect* measurements of spin splittings are controversially discussed in literature [4].
To resolve this issue, we apply an experimental method with *direct* access to the spin texture of unoccupied electronic states: spin-resolved inverse photoemission. In this contribution, we present measurements of the $n = 1$ image-potential state at Re(0001) [5]. The $E(\mathbf{k}_{||})$ dispersion shows separate parabolas for the two spin directions, shifted in $\mathbf{k}_{||}$ [Fig. 1(b)]. The spin-dependent energy splitting is linear in $\mathbf{k}_{||}$ [Fig. 1(c)] and results in a Rashba parameter of $\alpha_{\mathrm{R,exp}} = 105 \pm 33$ meV Å. These results provide the first direct experimental evidence of a spin-orbit-induced Rashba-type behavior of an image-potential state.

1. P.M. Echenique *et al.*, *Surf. Sci. Rep.* **52**, 219 (2004). M. Donath *et al.*, *Surf. Sci.* **601**, 5701 (2007).
2. U. Höfer *et al.*, *Science* **277**, 1480 (1997).
3. J. R. McLaughlan *et al.*, *J. Phys.: Condens. Matter* **16**, 6841 (2004). J. Braun and H. Ebert, *Phys. Status Solidi B* **258**, 2000026 (2020).
4. S. Tognolini *et al.*, *Phys. Rev. Lett.* **115**, 046801 (2015). T. Nakazawa *et al.*, *Phys. Rev. B* **94**, 115412 (2016).
5. F. Schöttke *et al.*, *Phys. Rev. B* **105**, 155419 (2022).

Bulk-sensitive spin-resolved hard X-ray photoemission spectroscopy of half-metallic Co_2MnSi

Shigenori Ueda*, Yoshio Miura, Yuichi Fujita, and Yuya Sakuraba

National Institute for Materials Science, Tsukuba, Japan

**Contact: UEDA.Shigenori@nims.go.jp*

Keywords: valence band hard X-ray photoemission, spin-polarization, half-metal, Co_2MnSi

Recently, we have developed spin-resolved hard X-ray photoemission spectroscopy (HAXPES) using an ultracompact Mott-type spin-filter, to reveal the bulk-sensitive spin-resolved electronic states of magnetic materials [1]. In this work, we focused on the temperature-dependent spin-resolved electronic states of $L2_1$-ordered Co_2MnSi as a predicted half-metal by utilizing the bulk-sensitive HAXPES. Since the strong reduction of the performance in the tunnel and giant magnetoresistance junctions, in which a predicted half-metal is used as a magnetic electrode, with increasing temperature [2] is a long-standing issue to be solved.

The spin-resolved HAXPES measurements utilizing the ultracompact Mott-type spin-filter were conducted at the undulator beamline BL15XU of SPring-8. The excitation photon energy and total energy resolution were set to 5.95 keV and ~0.65 eV, respectively [3].

Figure 1(a) shows the majority and minority spin HAXPES spectra of the valence band region for a 30-nm-thick Co_2MnSi thin film buried under a 2-nm-thick MgO layer measured at temperature (T) of 21 K [3]. A clear difference between the majority and minority spin spectra was found. The majority spin spectrum showed the Fermi edge, while the minority spin one showed a band gap across the Fermi-level. Figures 1(b) and 1(c) showed the spin-polarization curves measured at T = 21 and 300 K, respectively. One sees that the spin polarization curves at T = 21 and 300 K are similar each other. As expected from the half-metallicity of Co_2MnSi, the high spin polarization of ~0.9 at around the Fermi-level at T = 21 and 300 K was obtained. This result suggests that the spin polarization at the Fermi-level is almost temperature-independent for Co_2MnSi in the bulk region and that Co_2MnSi maintains the half-metallicity up to 300 K. Thus, the spin-resolved HAXPES method can be a powerful tool for studying bulk-derived temperature- and spin-dependent electronic states of magnetically ordered materials.

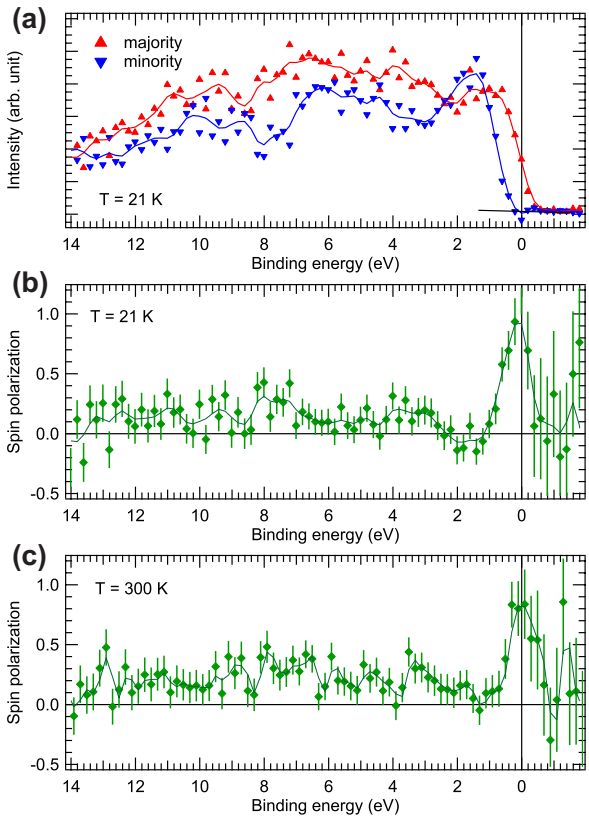

Figure 1: (a) Spin-resolved HAXPES spectra of Co_2MnSi at T = 21 K. Spin-polarization curves at (b) 21 K and (c) 300 K.

1. S. Ueda and Y. Sakuraba, Direct observation of spin-resolved valence band electronic states from a buried magnetic layer with hard X-ray photoemission, *Sci. Tech. Adv. Mater.* **22**, 317 (2021).
2. K. Elphick et al., Heusler alloys for spintronic devices: Review on recent development and future perspectives, *Sci. Tech. Adv. Mater.* **22**, 235 (2021).
3. S. Ueda, Y. Miura, Y. Fujita, and Y. Sakuraba, Direct probing of temperature-independent bulk half-metallicity in Co_2MnSi by spin-resolved hard x-ray photoemission, Phys. Rev. B **106**, 075101 (2022).

Combining XPS and Other Surface Analysis Techniques for in-situ Analysis

Christopher Deeks[1], Tim Nunney[1], Paul Mack[1], Robin Simpson[1], Hsiang-Han Tseng[1]
[1]*Thermo Fisher Scientific, Unit 24, The Birches, Imberhorne Lane, East Grinstead, RH19 1UB, UK.*

Advanced materials present ever increasing challenges to the analytical scientist. Composite materials built from nanostructures or ultra-thin films, often with complex chemistries present, are now required in a broad range of applications, and achieving full characterization is rarely managed using only one analysis method. To maintain confidence in the results from the utilization of several different methods, it is advantageous to be able to perform experiments on the same platform. Ideally, this should be without having to move the sample between several instruments, removing the need for additional registration or processing to ensure that the data is being collected from the same position.

For surface analysis, it has been common for many years to incorporate related analysis techniques onto the same instrument. For example, X-ray photoelectron spectroscopy (XPS) systems are commonly equipped with UV light sources to facilitate investigation of additional properties of materials via ultra-violet photoelectron spectroscopy (UPS). The ion source that is typically used for sample cleaning and depth profiling can also be used for low energy ion scattering (LEIS or ISS), providing more surface sensitive elemental composition information than can be delivered from XPS alone.

The latest innovation is to extend the range of offered complimentary techniques to include Raman spectroscopy. The focal points are aligned such that data can be acquired from the same point simultaneously, and that the sizes of the analysis areas are comparable in size. Chemical modifications of the material can be easily determined and quantified with XPS. Raman offers a fast way of determining the quality and conformity of the material, and direct compound identification. The greater depth of field of the Raman spectrometer also offers bulk information to complement the surface sensitive XPS data.

In this presentation we will discuss the strengths of combined, in-situ approaches to surface analysis, illustrated with examples from a range of applications.

ISBN 978-952-62-3754-1